ACTUATOR 16

15th International Conference on New Actuators
&
9th International Exhibition
on Smart Actuators and Drive Systems

13 – 15 June 2016
Bremen, Germany

Conference Proceedings

Editor
Hubert Borgmann

Published by
MESSE BREMEN
WFB Wirtschaftsförderung Bremen GmbH
Bremen, Germany

Design by Büro 7, Bremen, Germany
Typesetting by Trageser GmbH, Bremen, Germany
Printed in Germany by Wegner GmbH, Stuhr-Brinkum, Germany
ISBN 978-3-933339-26-3 (Print version)
ISBN 978-3-933339-27-0 (Digital version, USB Card)
ISBN 978-3-933339-28-7 (Double Pack, print + digital)

ACTUATOR 16

15th International Conference on New Actuators
9th International Exhibition on Smart Actuators and Drive Systems

13 – 15 June 2016
Bremen Exhibition and Congress Center
Bremen, Germany

Organised by

MESSE BREMEN

MESSE BREMEN
WFB Wirtschaftsförderung Bremen GmbH

Sponsor

- Physik Instrumente (PI) GmbH & Co. KG, Germany
  (Event Sponsor USB Cards for digital Conference Proceedings)

Endorsements

Associations / Governmental authorities / Organisations

- German Engineering Federation (VDMA), Germany
  Fluid Power Association
- The Association of German Engineers (VDI),
  Local Chapter Bremen, Germany
- The Senator of Economy Affairs, Ports and Labour /
  Ministry of the Federal State of Bremen, Germany
- VDE / VDI Society Microelectronics,
  Micro- and Precision Engineering (GMM) Germany
- VDI Technologiezentrum GmbH, Germany
- VDI / VDE Innovation + Technik GmbH, Germany

Media Partners

- MECHATRONIK / I.G.T. Informationsgesellschaft Technik, Germany
- Mikroproduktion / MIKROvent GmbH, Germany
- SENSORMAGAZIN / Magazin-Verlag Hightech Publications KG, Germany
- Commercial Micro Manufacturing / MST GLOBAL LTD, United Kingdom

Committee

- **W. Amrhein**
  Johannes Kepler Universität Linz
  Linz, Austria
- **A. Ando**
  Murata Manufacturing Co. Ltd.
  Kyoto, Japan
- **S.-B. Choi**
  INHA University
  Incheon, South Korea
- **F. Claeyssen**
  CEDRAT Technologies SA
  Meylan, France
- **J. Gołdasz**
  BWI Group
  Kraków, Poland
- **W.A. Groen**
  Delft University of Technology
  Delft, The Netherlands
- **K. Hjort**
  Uppsala University
  Uppsala, Sweden
- **P. Jänker**
  Airbus Group Innovations
  München, Germany
- **L. Kahrs**
  Leibniz Universität Hannover
  Hannover, Germany
- **H.-J. Karkosch**
  Contitech Vibration Control GmbH
  Hannover, Germany
- **R. Keller**
  Dr. Fritz Faulhaber GmbH & Co. KG
  Schönaich, Germany
- **A. Köllnberger**
  Wacker Chemie AG
  Burghausen, Germany
- **G. Kullik**
  Dräger Medical GmbH
  Lübeck, Germany
- **J.C. Lötters**
  Bronkhorst High-Tech B. V.
  Ruurlo, The Netherlands,
  and University of Twente
  Enschede, The Netherlands
- **A. Ludwig**
  Ruhr-Universität-Bochum
  Bochum, Germany
- **J. Maas**
  Hochschule Ostwestfalen-Lippe
  Lemgo, Germany
- **P. Müllner**
  Boise State University
  Boise, USA
- **E. Pagounis**
  ETO MAGNETIC GmbH
  Stockach, Germany
- **J. Perret**
  Haption GmbH
  Aachen, Germany
- **P. Pertsch**
  PI Ceramic GmbH
  Lederhose, Germany
- **A. Preumont**
  Université Libre de Bruxelles
  Brussels, Belgium
- **H.F. Schlaak**
  Technische Universität Darmstadt
  Darmstadt, Germany
- **S. Soetebier**
  ABB AG
  Brilon, Germany
- **K. Uchino**
  The Pennsylvania State University
  University Park, USA
- **E. Vander Poorten**
  Katholieke Universiteit Leuven
  Heverlee, Belgium
- **G. Vergani**
  SAES Getters S.p.A.
  Lainate, Italy

Organiser

- **H. Borgmann**
  MESSE BREMEN
  Bremen, Germany

Welcome

Welcome to ACTUATOR 2016 and another volume of the Conference Proceedings of the International Conference on New Actuators. Since 1988, this series of biennial conferences has always been held in Bremen, Germany, in the even years. And for nearly 30 years now, we have always managed to have the Conference Proceedings ready for distribution at the start of the event for the registered delegates. A full set of fourteen proceedings containing almost all the manuscripts related to the presentations – only a few of the manuscripts are missing. Thanks to all authors who supported us perfectly in this way. We feel, that's indeed a good tradition and we intend to continue this way in the future – in case the authors carry on to go along with us.

From our point of view, the manuscripts are the indispensable documentation to refer to during and after the event. About 2,000 conference presentations have been published on 9,000 pages of conference proceedings since the launch event in 1988, since 1998 also in a digital version. That's a huge fond of innovations and scientific results – and they are still available! They are available as a whole from the organiser as well as from bookshops and libraries, worldwide. Furthermore, in 2015 we started a test to publish an excerpt of the 2014 Proceedings on our event homepage for free: The first page of each manuscript is visible for everybody, the complete manuscript is available online for a fee or, if you prefer, from a public library. Thus, the first page including all the information required for citation is available gratis together with a qualified introduction.

In 2016 we are going to add quite a number of excellent new ones: in total 135 conference contributions, 86 oral presentations and 49 posters are portraying the state of the art technology and indicating future trends. Oral sessions are held in the following fields:

- Active Vibration Control / Active Noise Control
- Actuator Control
- Aerospace Applications
- MRF Actuators
- Haptic / Tactile Applications
- Low-Power Electromagnetic Actuators
- Magnetostrictive / MSM Actuators
- (Bio-) Medical Applications
- Micro Actuators / Microfluid Handling Devices
- Piezoelectric Actuators
- Piezoelectric Actuator Applications
- Polymer Actuators
- Shape Memory Actuators

Including all reviews, a 2016 conference participant has the chance to listen to as many as 39 well selected oral contributions. As usual, all the other contributions, including the posters, will be properly documented in the proceedings. We hope that the conflicts of interest will have been minimised by a well-selected placement of the sessions in the general schedule. Special thanks to all the authors who went through the additional trouble and prepared their manuscripts in time.

But ACTUATOR is not only a brilliant place to present and discuss the latest results in the area of new actuators, it also an excellent place for networking within the worldwide experts' community present at the conference venue, for creating visions for new inter-research co-operations or starting business co-operations with industrial partners.

In order to again realise such an event, we thank all the members of the Programme Committee for their excellent work and valuable assistance. We are particularly grateful to our sponsor, the endorsing institutions, the media partners and to all others who have supported our public relations work. Our special thanks go to all those participants who are actively contributing to this event by sharing the results of their research work here – as authors of papers and posters, or as exhibitors.

As every time, we look forward to interesting presentations, lively discussions and helpful new contacts, and we would be delighted to welcome you in Bremen again in two years for ACTUATOR 2018.

Enjoy your conference!

Hans Peter Schneider

Hans Peter Schneider
MESSE BREMEN
General Manager

Hubert Borgmann

Hubert Borgmann
MESSE BREMEN
Project Manager ACTUATOR 2016

Table of Contents

Detailed Table of Contents	No.	Page
Oral Contributions		
Session A		
A1 Piezoelectric Actuators	A1.0 – A1.10	8
A3 Magnetostrictive / MSM Actuators	A3.0 – A3.10	10
A6 Active Vibration Control / Active Noise Control	A6.0 – A6.5	12
Session B		
B1 Medical / Biomedical Applications	B1.0 – B1.4	13
B2 Haptic / Tactile Applications	B2.0 – B2.4	14
B3 Piezo Actuator Applications	B3.0 – B3.10	15
B6 Aerospace Applications	B6.0 – B6.4	17
Session C		
C1 Polymer Actuators	C1.0 – C1.6	18
C2 Shape Memory Actuators	C2.0 – C2.4	19
C3 Micro Actuators / Microfluid Handling Devices	C3.0 – C3.4	20
C4 MRF Actuators	C4.0 – C4.4	21
C5 Actuator Control	C5.0 – C5.3	22
C6 Low-Power Electromagnetic Actuators	C6.0 – C6.5	23
Poster Contributions		
Piezoelectric Actuators	P 1 – P 8	24
Piezo Actuator Applications	P 9 – P 17	25
Micro Actuators / Micro Fluidic Handling Devices	P 19 – P 21	26
ERF / MRF Actuators	P 23	26
Low-Power Electromagnetic Actuators	P 24 – P 27	27
Polymer Actuators	P 28 – P 32	28
Shape Memory Actuators	P 33 – P 35	29
Actuator Control	P 36 – P 38	30
Active Vibration Control / Active Noise Control	P 41	30
Aerospace Applications	P 42 – P 43	31
Fluidic / Pneumatic Actuators	P 44 – P 47	31
Haptic / Tactile Applications	P 48 – P 49	32
Magnetostrictive / MSM Actuators	P 52 – P 55	32
(Bio-)Medical Applications	P 56 – P 58	33
List of Authors		**605**
List of Exhibitors		**613**
The Crew		**619**
Announcement ACTUATOR 2018		**621**

Oral Contributions
A1 Piezoelectric Actuators

Technical Papers **No.** **Page**

Piezoelectric Actuators 2016 –
Professors' Misconceptions Top 10 (Review) · · · · · · A1.0 · · · · · · 35
K. Uchino, The Pennsylvania State University, University Park, USA

Electromechanical Properties
of the Lead-Free (1-x)Ba($Zr_{0.2}Ti_{0.8}$)O_3–x($Ba_{0.7}Ca_{0.3}$)TiO_3 System · · · · · · A1.1 · · · · · · 52
V. Rojas, J. Koruza, M. Acosta, D.R.J. Brandt,
Technische Universität Darmstadt, Darmstadt, Germany
K.G. Webber, Friedrich-Alexander-Universität Erlangen-Nürnberg, Erlangen, Germany
J. Rödel, Technische Universität Darmstadt, Darmstadt, Germany

Temperature Dependency of the Hysteresis Behaviour
of PZT Actuators Using Preisach Model · · · · · · A1.2 · · · · · · 56
C. Mangeot, Noliac A/S, Kvistgaard, Denmark
T.-G. Zsurzsan, Technical University of Denmark, Lyngby, Denmark

Should We Drive Transducers at Their Resonance Frequency? · · · · · · A1.3 · · · · · · 60
H. Shekhani, The Pennsylvania State University, University Park, USA
W. Shi, Harbin Institute of Technology, Harbin, China
M. Majzoubi, M. Choi, A. Bansal, K. Uchino
The Pennsylvania State University, University Park, USA

Single-Sided Contacting of Out-of-Plane Polarized Piezo Films
for Fluid Membrane Lenses · · · · · · A1.4 · · · · · · 65
M. Stürmer, M.C. Wapler, U. Wallrabe
Albert-Ludwigs-Universität Freiburg, Freiburg, Germany

Tailored Composite Transducers Based on Piezoceramic Fibers and Pearls · · A1.5 · · · · · · 69
K. Hohlfeld, Technische Universität Dresden, Dresden, Germany
P. Neumeister, S. Gebhardt
Fraunhofer IKTS, Dresden, Germany
A. Michaelis, Technische Universität Dresden, Dresden, Germany, and
Fraunhofer IKTS, Dresden, Germany

Dynamic Characterization of an Amplified Piezoelectric Actuator · · · · · · A1.6 · · · · · · 73
R. Lucinskis, C. Mangeot
Noliac A/S, Kvistgaard, Denmark

Oral Contributions
A1 Piezoelectric Actuators (cont.)

Technical Papers	No.	Page
Development of a Piezoelectric Micro Switch L. Seyfert, S. Zähringer, C. Müller, S. Buhr, N. Schwesinger Technische Universität München, München, Germany	A1.7	77
Characteristics of Ultrasonic Suspension Actuation Force M. Takasaki, S. Chino, R. Chida, Y. Ishino, T. Mizuno Saitama University, Saitama-shi, Japan	A1.8	82
Encapsulated Piezo Actuators for Use at High Power Levels and / or within Harsh Environmental Conditions S. Rowe, F. Barillot, A. Pages, F. Claeyssen Cedrat Technologies SA, Meylan, France	A1.9	86
Dynamic Control of the Piezoelectric Transducer's Resonant Frequency Using MOSFET Switching H. Yokozawa, The University of Tokyo, Kashiwa-shi, Japan J. Twiefel, M. Weinstein Leibniz Universität Hannover, Hannover, Germany T. Morita, The University of Tokyo, Kashiwa-shi, Japan	A1.10	91

Oral Contributions
A3 Magnetostrictive / MSM Actuators

Technical Papers	No.	Page
Magnetic Shape Memory Actuation: Trends and Design Concepts (Review) P. Müllner, Boise State University, Boise, USA E. Pagounis, ETO MAGNETIC GmbH, Stockach, Germany	A3.0	95
Fast Actuation of Magnetic Shape Memory Material Ni-Mn-Ga Using Pulsed Magnetic Field A. Saren, J. Tellinen, D. Musiienko, K. Ullakko Lappeenranta University of Technology, Savonlinna, Finland	A3.1	101
Physics of Energy Barriers for Twin Boundary Motion in Ni-Mn-Ga E. Faran, N. Zreihan, I. Benichou, S. Givli, D. Shilo Technion - Israel Institute of Technology, Haifa, Israel	A3.2	104
An Effective Method for Designing Magnetic Shape Memory Actuator Systems F. Ehle, P. Neumeister, H. Neubert Fraunhofer IKTS, Dresden, Germany	A3.3	105
Materials Design for Magnetostrictive Thin Films A. Sakai, C. Niyomwaitaya, A.A.Y Mansi, T. Washihira, Y. Matsumura Tokai University, Hiratsuka-shi, Japan	A3.4	109
Ferromagnetic Shape Memory Flapper for Remotely Actuated Propulsion Systems D. Shilo, Technion - Israel Institute of Technology, Haifa, Israel O. Kanner, Yale University, New Haven, USA J. Sheng, R. James, University of Minnesota, Minneapolis, USA Y. Ganor, Philips Health Systems, Andover, USA	A3.5	113

Oral Contributions
A3 Magnetostrictive / MSM Actuators (cont.)

Technical Papers	No.	Page
Design and Modelling of a Sensor-Integrated Actuator Using Combined Effects of Magnetostriction and Piezoelectricity M. Niu, B. Yang, G. Meng Shanghai Jiao Tong University, Shanghai, China	A3.6	114
Impulse Damping Using Magnetic Shape Memory Alloys L. Riccardi, T. Schiepp, R. Schmid, M. Maier, M. Helmer, M. Laufenberg ETO MAGNETIC GmbH, Stockach, Germany	A3.7	120
Magnetic Field Controlled Damping in MSM-Polymer Hybrids I. Aaltio, F. Nilsén, J. Lehtonen, Y. Ge, S.-P. Hannula Aalto University, Espoo, Finland	A3.8	124
Disparities in Properties (Magnetic and Structural) of Single Crystal Terfenol-D Disks V. Issindou, B. Viala CEA LETI, Grenoble, France L. Gimeno, O. Cugat Université Grenoble Alpes, Grenoble, France, and CNRS, Grenoble, France O. Geoffroy, CNRS Louis Néel, Grenoble, France F. Fillot, CEA LETI, Grenoble, France, and Université Grenoble Alpes, Grenoble, France J. Debray, Institut NEEL, Grenoble, France, and CNRS Institut Néel, Grenoble, France	A3.9	127
Study of Vibration Energy Harvester Based on the Magnetic Shape Memory Effect D. Musiienko, Lappeenranta University of Technology, Savonlinna, Finland J. Huimasalo, Elektroniikan 3K-tehdas, Savonlinna, Finland J. Tellinen, A. Saren, K. Ullakko Lappeenranta University of Technology, Savonlinna, Finland	A3.10	131

Oral Contributions
A6 Active Vibration Control / Active Noise Control

Technical Papers **No.** **Page**

Technical Papers	No.	Page
Vibration Control of Large Civil Engineering Structures (Review) A. Preumont, Université Libre de Bruxelles, Brussels, Belgium	A6.0	134
Actuator Concepts for Active Vibration Control M. Werhahn, R. Genderjahn, H.-J. Karkosch, P.M. Marienfeld ContiTech Vibration Control GmbH, Hannover, Germany	A6.1	135
An Efficient and Optimal Moving Magnet Actuator for Active Vibration Control G. Loussert, Moving Magnet Technologies SA, Besançon, France	A6.2	139
Compact, Efficient and Controllable Moving Iron Actuation Chain for Industrial Application P. Meneroud, C. Bouchet, A. Pages Cedrat Technologies SA, Meylan, France	A6.3	143
An Adaptive Negative Capacitance Shunt Network for Increasing Performance and Robustness in Terms of Noise and Vibration Attenuation M. Pohl, H.P. Monner Deutsches Zentrum für Luft- und Raumfahrt (DLR), Braunschweig, Germany	A6.4	148
Adaptive Dynamic Absorber for Wideband Micro-Vibration Control Based on Precision Self-Positioning Linear Actuator X. Wang, B. Yang Shanghai Jiao Tong University, Shanghai, China	A6.5	152

Oral Contributions
B1 (Bio-) Medical Applications

Technical Papers	No.	Page
Embedded Sensors and Actuators for Gentle Insertion of Cochlear Implants (Review) L.A. Kahrs, Leibniz Universität Hannover, Hannover, Germany	B1.0	159
Micro-Hydraulic Drives with Integrated Displacement Sensor for Medical Application L.M. Comella, K. Ayvazov, R. Kessel, T. Cuntz, A. van Poelgeest Fraunhofer IPA, Mannheim, Germany	B1.1	163
A Variable Impedance Actuator Based on Shape Memory Alloy L. Manfredi, F.L. Velsink, H. Khan, A. Cuschieri University of Dundee, Dundee, United Kingdom	B1.2	167
Piezoelectric Hydrocephalus Shunt Valve – Design and First Evaluation Results P.P. Pott, G. Allevato, M. Bartenschlager, J. Butz, P. Schmitt, H.F. Schlaak Technische Universität Darmstadt, Darmstadt, Germany	B1.3	171
A Hybrid Stimulation Device for Providing Sensory Feedback H. Huang, Berner Fachhochschule, Biel, Switzerland, and Ecole Polytechnique Fédérale de Lausanne, Neuchâtel, Switzerland T. Li, V.M. Koch Berner Fachhochschule, Biel, Switzerland	B1.4	175

Oral Contributions
B2 Haptic / Tactile Applications

Technical Papers	No.	Page
Haptic Feedback: From Force-Feedback Robots to Tactile Interfaces (Invited Review) M. Wiertlewski, Aix-Marseille Université, Marseille, France	B2.0	181
Design of Haptic Master Featuring Improved MR Brakes H.G. Gang, J.W. Sohn Kumoh National Institute of Technology, Gumi-si, South Korea	B2.1	188
Haptic Guidance in Comanipulated Laser Surgery for Fetal Disorders C. Gruijthuijsen, A. Javaux, G. Borghesan Katholieke Universiteit Leuven, Leuven, Belgium T. Vercauteren, D. Stoyanov, S. Ourselin University College London, London, United Kingdom J. Deprest, University Hospitals Leuven, Leuven, Belgium J. Perret, Haption, Lavalle, France D. Reynaerts, E. Vander Poorten Katholieke Universiteit Leuven, Leuven, Belgium	B2.2	192
Normal Force Actuator for a Tactile Display Using a Micromechanically Built Spring Element Made of Polyimide M. Rechel, Leibniz Universität Hannover, Garbsen, Germany V. Hofmann, J. Twiefel Leibniz Universität Hannover, Hannover, Germany M. Wurz, Leibniz Universität Hannover, Garbsen, Germany	B2.3	196
Investigation of Smart Materials for Haptic Feedback Applications H. Bochmann, J. Maas Hochschule Ostwestfalen-Lippe, Lemgo, Germany	B2.4	200

Oral Contributions
B3 Piezo Actuator Applications

Technical Papers	No.	Page
Miniature Piezoelectric Multilayer Actuators and their Applications (Review) W.A. Groen, Delft University of Technology, Delft, The Netherlands, and TNO Holst Centre, Eindhoven, The Netherlands P. Pertsch, PI Ceramic GmbH, Lederhose, Germany	B3.0	204
Micro Ultrasonic Motor Using One Cubic Millimeter Stator T. Mashimo, Toyohashi University of Technology, Toyohashi-shi, Japan	B3.1	210
An Ultrasonic Motor Using Side-Push of Centre-Attached Eyelets on an Octagonal Piezoelectric Plate B. Koc, Physik Instrumente (PI) GmbH & Co. KG, Karlsruhe, Germany	B3.2	214
Performance Evaluation of a Single-Stage Valve at High Temperatures Actuated by Piezoelectric Stack C. Han, W.H. Kim, S.-B. Choi Inha University, Incheon, South Korea	B3.3	218
Module Stepping Piezoelectric Actuator – A Versatile Way of Micro-Positioning Actuation F. Dubois, Cedrat Technologies SA, Meylan, France, and LaMCoS UMR 5259, Villeurbanne, France F. Barillot, V. Thiebaud, C. Belly, T. Porchez, M. Barraja Cedrat Technologies SA, Meylan, France A. Saulot, Y. Berthier LaMCoS UMR 5259, Villeurbanne, France	B3.4	221
Muscle-Like Piezohydraulic Actuators for Robotic Grippers W. Zoels, I. Vittorias, G. Bachmaier Siemens AG, München, Germany	B3.5	224
Topological In-Plane Polarized Piezo Actuation for Compact Adaptive Lenses with Aspherical Correction F. Lemke, M. Stürmer, U. Wallrabe, M.C. Wapler Albert-Ludwigs-Universität Freiburg, Freiburg, Germany	B3.6	228
Bimorph Mirrors for Adaptive Optics in Space Telescopes D. Alaluf, R. Bastaits, K. Wang Université Libre de Bruxelles, Brussels, Belgium M. Horodinca, Technical University Gheorghe Asachi, Iasi, Romania I. Burda, Babes Bolyai University, Cluj-Napoca, Romania G. Martic, Belgian Ceramic Research Centre, Mons, Belgium A. Preumont, Université Libre de Bruxelles, Brussels, Belgium	B3.7	232

Oral Contributions
B3 Piezo Actuator Applications (cont.)

Technical Papers	No.	Page
Application of Combined Ultrasonic-Levitation-Magnetic-Actuators for Machine Guideways B. Denkena, J. Reiners Leibniz Universität Hannover, Garbsen, Germany J. Wallaschek, J. Twiefel, I. Ille Leibniz Universität Hannover, Hannover, Germany	B3.8	236
High Response Proportional Flow Control Valve Using Particle Excitation D. Hirooka, T. Yamaguchi, N. Furushiro Kansai University, Suita-shi, Japan K. Suzumori, Tokyo Institute of Technology, Tokyo, Japan T. Kanda, Okayama University, Okayama-shi, Japan	B3.9	241
Performance of a Novel Small Component Conveyer Utilizing Flexural Traveling Waves T. Wielert, A. Vagapov, J. Twiefel Leibniz Universität Hannover, Hannover, Germany I. Mešan, K. Bott Afag GmbH, Amberg, Germany	B3.10	245

Oral Contributions
B6 Aerospace Applications

Technical Papers	No.	Page
Smart Structures: Recent Developments within Aeronautics Applications (Invited Review) H.P. Monner, M. Kintscher, M. Misol, J. Riemenschneider, D. Schmidt Deutsches Zentrum für Luft- und Raumfahrt (DLR), Braunschweig, Germany	B6.0	249
Design Study and Performance Evaluation of Actuator System for Subsonic GA Wind Tunnel Testing N. Kobiki, K. Saitoh, Y. Hamada JAXA, Mitaka-shi, Japan S.K. Chee, T. Yano, A. Yano Mechano Transformer Corporation, Chiyoda-ku, Japan	B6.1	255
Pulsed Air High Performances Valves Improve Aerodynamic Flow Over Airplane Wings C. Bouchet, C. Belly, M. Fournier, F. Claeyssen Cedrat Technologies SA, Meylan, France F. Ternoy, A. Choffat, J. Dandois, M. Pruvost, Q. Gallas ONERA, Lille, France	B6.2	259
Active Vortex Generator Deployed on Demand by Size Independent Actuation of Shape Memory Alloy Wires Integrated in Fiber Reinforced Polymers M. Hübler, S. Nissle, M. Gurka Institut für Verbundwerkstoffe GmbH, Kaiserslautern, Germany J. Wassenaar, DG Flugzeugbau GmbH, Bruchsal, Germany	B6.3	266
New Rating Life Calculation for Rolling Elements on Aircraft T. Münzing, H. Binz Universität Stuttgart, Stuttgart, Germany S. Seemann, M. Christmann Airbus Group Innovation, Ottobrunn, Germany S. Toro, Umbra Cuscinetti S.p.A., Foligno, Italy	B6.4	270

Oral Contributions
C1 Polymer Actuators

Technical Papers	No.	Page
Elastomers for Dielectric Electroactive Polymer Applications (Review) A. Köllnberger, Wacker Chemie AG, Burghausen, Germany H.F. Schlaak, Technische Universität Darmstadt, Darmstadt, Germany	C1.0	274
Customized Dielectric Elastomer Stack-Actuators Under Consideration of Application Specifications B. von Heckel, H. Bochmann, T. Hoffstadt, J. Maas Hochschule Ostwestfalen-Lippe, Lemgo, Germany	C1.1	278
A Compact High-Force Dielectric Elastomer Membrane Actuator S. Hau, Universität des Saarlandes, Saarbrücken, Germany A. York, Parker Hannifin Corporation, Sunnyvale, USA S. Seelecke, Universität des Saarlandes, Saarbrücken, Germany	C1.2	282
Magneto-Active Polymer Actuator A. Diermeier, D. Sindersberger, G.J. Monkman Ostbayerische Technische Hochschule Regensburg, Regensburg, Germany	C1.3	286
Haptic Actuators Based on Magnetoactive Polymers H. Böse, W. Hartmann, J. Ehrlich Fraunhofer ISC, Würzburg, Germany	C1.4	290
Magneto-Rheological Elastomer Actuators for a Reconfigurable Joystick J. Bilz, Technische Universität Darmstadt, Darmstadt, Germany H. Böse, Fraunhofer ISC, Würzburg, Germany M. Kupnik, C. Hatzfeld Technische Universität Darmstadt, Darmstadt, Germany	C1.5	294
Plasticized-Polymer Actuators with Colossal Dielectric Constant – Electro-Mechanical & Electro-Optical Functions T. Hirai, Shinshu University, Ueda-shi, Japan	C1.6	299

Oral Contributions
C2 Shape Memory Actuators

Technical Papers	No.	Page
Recent Developments in Shape Memory Alloys (Invited Review) H. Maier, Leibniz Universität Hannover, Garbsen, Germany	C2.0	303
Advances in NiTi-Based SMA for Actuators A. Coda, L. Fumagalli SAES Getters S.p.A., Lainate, Italy	C2.1	309
Industrial Safety Systems Using Shape Memory Alloy Actuators A. Czechowicz, I. Zwinscher, P. Dültgen Forschungsgemeinschaft Werkzeuge und Werkstoffe e.V., Remscheid, Germany B. Rachor, HEMA Maschinen und Apparateschutz GmbH & Co. KG, Seligenstadt, Germany	C2.2	313
Bi-Stable SMA Actuator P. Motzki, S. Seelecke ZeMA gGmbH, Saarbrücken, Germany, and Universität des Saarlandes, Saarbrücken, Germany	C2.3	317
Analysis of Performance and Energy Efficiency of Thin Shape Memory Alloy Wire-Based Actuators H. Khan, L. Manfredi, Y. Huan, F.L. Velsink, A. Cuschieri University of Dundee, Dundee, United Kingdom	C2.4	321

Oral Contributions
C3 Micro Actuators / Microfluid Handling Devices

Technical Papers	No.	Page
Integrated Systems for the Accurate Measurement and Control of Micro Liquid and Gas Flows (Review) J.C. Lötters, Bronkhorst High-Tech B.V., Ruurlo, The Netherlands, and University of Twente, Enschede, The Netherlands	C3.0	326
Resonant Three-Dimensional Electrostatic Actuator in Silicon Technology B. Goj, L. Dressler, L. Dittrich, M. Hoffmann Technische Universität Ilmenau, Ilmenau, Germany	C3.1	327
Mono-Dispersed Droplets Generation in the Flowing Ambient Liquid by Using an Ultrasonic Vibrator T. Kanda, T. Yamada, K. Mori Okayama University, Okayama-shi, Japan K. Suzumori, Tokyo Institute of Technology, Tokyo, Japan	C3.2	332
Cost-Efficient Manufacturing of a High Deflection Electrothermal Drive for Switching Applications M. El Khoury, T. Winterstein, C. Nakic, H.F. Schlaak Technische Universität Darmstadt, Darmstadt, Germany	C3.3	336
SMA Shape-Memory Microvalves for Fluidic Systems C. Megnin, Albert-Ludwigs-Universität Freiburg, Freiburg, Germany H. Ossmer, M. Gültig, T. Hanemann, M. Kohl Karlsruher Institut für Technologie, Karlsruhe, Germany	C3.4	340

Oral Contributions
C4 MRF Actuators

Technical Papers	No.	Page
Automotive MR Actuators – State of the Art (Review) J. Gołdasz, BWI Group, Krakow, Poland	C4.0	344
Controlling the Magnetorheological Effect Using Vibrations E. Leroy, P.-H. Orefice, L. Eck, M. Hafez CEA LIST, Gif-sur-Yvette, France	C4.1	349
Hybrid Magnetorheological Damper M. Jackel, J. Kloepfer, M. Matthias Fraunhofer LBF, Darmstadt, Germany	C4.2	354
Energy-Efficient MRF-Based Clutches in Hybrid Powertrains C. Hegger, J. Maas Hochschule Ostwestfalen-Lippe, Lemgo, Germany	C4.3	357
Magnetorheological Actuator for Haptic Applications M.E. Busse-Grawitz, maxon advanced robotics and systems, Giswil, Switzerland R. Pittini, maxon motor ag, Sachseln, Switzerland R. Waldvogel, D. Martin maxon advanced robotics and systems, Giswil, Switzerland	C4.4	361

Oral Contributions
C5 Actuator Control

Technical Papers	No.	Page
Combining Usability and Performance – What Smart Actuators Can Learn from Automatic Commissioning of Variable Speed Drives (Invited Review) A. Wahrburg, K.D. Listmann ABB AG, Ladenburg, Germany	C5.0	364
Control of a Compact Electrodynamic Planar Actuator M. Stock, T. Bödrich, J. Lienig Technische Universität Dresden, Dresden, Germany	C5.1	371
Vector Control of a Travelling Wave Ultrasonic Motor: Application to Efficiency Improvement by Voltage Reduction F. Giraud, Université de Lille, Villeneuve d'Ascq, France C. Giraud-Audine, Arts et Métiers Paris Tech, Lille, France M. Amberg, B. Lemaire-Semail Université de Lille, Villeneuve d'Ascq, France	C5.2	375
Power Electronics and Control Concepts for Driving Dielectric Elastomer Transducers T. Hoffstadt, J. Maas Hochschule Ostwestfalen-Lippe, Lemgo, Germany	C5.3	381

Oral Contributions
C6 Low-Power Electromagnetic Actuators

Technical Papers	No.	Page
Sensorless Control of Low-Power Electromagnetic Actuators (Invited Review) M. Nienhaus, Universität des Saarlandes, Saarbrücken, Germany	C6.0	385
A Novel Low-Power Dual-Actuator for High-Precision Magnetic Levitation Systems M. Lahdo, Technische Hochschule Mittelhessen, Friedberg, Germany T. Ströhla, Technische Universität Ilmenau, Ilmenau, Germany S. Kovalev, Technische Hochschule Mittelhessen, Friedberg, Germany	C6.1	392
Planar Magnetic Levitation in 6 DOF R. Glöß, Physik Instrumente (PI) GmbH & Co. KG, Karlsruhe, Germany	C6.2	396
Torque Measurements on an Electromagnetic Tilting Actuator M. Dörbaum, T. Winkel, S. Tappe, J. Kotlarski, T. Ortmaier, B. Ponick Leibniz Universität Hannover, Hannover, Germany	C6.3	398
An Exploratory Study of the Retardation Ability of a Thomson Coil Actuator G. Engdahl, J. Magnusson KTH Royal Institute of Technology, Stockholm, Sweden A. Bissal, ABB Corporate Research, Västerås, Sweden M. Sparr, KTH Royal Institute of Technology, Stockholm, Sweden	C6.4	402
Miniaturisation Trends in Magnetic Gears G. Puchhammer, Karl Rejlek GmbH, Wien, Austria	C6.5	406

Poster Contributions
Piezoelectric Actuators

Technical Papers	No.	Page
Longitudinal – Torsional Type Piezoelectric Actuator for the High Speed Rotational Motor Y. Yang, Nanjing University of Aeronautics and Astronautics, Nanjing, China D. Mazeika, Vilnius Gediminas Technical University, Vilnius, Lithuania P. Vasiljev, S. Borodinas Lithuanian University of Educational Sciences, Vilnius, Lithuania	P 1	410
The Investigation of Hollow Hemisphere-Shape Actuator P. Vasiljev, Lithuanian University of Educational Sciences, Vilnius, Lithuania R. Bareikis, S. Borodinas Lithuanian University of Educational Sciences, Vilnius, Lithuania, and Vilnius Gediminas Technical University, Vilnius, Lithuania A. Struckas, Lithuanian University of Educational Sciences, Vilnius, Lithuania J. Kasperoviciene, Nature Research Center, Vilnius, Lithuania	P 2	414
Piezoelectric Nonlinearity and its Temperature Dependency Under High Power Driving S. Miyake, T. Morita The University of Tokyo, Kashiwa-shi, Japan	P 3	419
Barium Titanate Thick Film Deposited by Ultrasonic-Assisted Hydrothermal Method R. Takayama, T. Morita The University of Tokyo, Kashiwa-shi, Japan	P 4	423
Full Characterisation of PZT Actuators in Quasi-Static, Large Signal Operation at Elevated Temperature C. Mangeot, B. Andersen Noliac A/S, Kvistgaard, Denmark	P 5	427
Reliability Enhancement Through the Use of Fusing Technique C. Mangeot, Noliac A/S, Kvistgaard, Denmark	P 6	431
Resonance Frequency Tracking for Piezoelectric Devices S. Safour, Y. Bernard Génie Electrique et Electronique de Paris, Gif-sur-Yvette, France	P 7	435
Nanometric Linear Piezo-Actuator with Integrated Strain Gages for High Stability Positioning T. Porchez, F. Barillot, C. Belly Cedrat Technologies SA, Meylan, France	P 8	439

Poster Contributions
Piezo Actuator Applications

Technical Papers	No.	Page
Design and Optimization of a Piezo-Actuated Flapping Wing Mechanism for Micro Air Vehicles Y. Peng, National University of Singapore, Singapore J. Cao, National University of Singapore, Singapore, and Beijing Institute of Technology, Beijing, China L. Liu, National University of Singapore, Singapore J. Wang, Zhejiang University, Hangzhou, China H. Yu, National University of Singapore, Singapore	P 9	443
Effective Vibration Mode of Ultrasonic Transducers for Low Flow Rate Spraying S. Ofuji, S. Tsuyuki, T. Kanda, S. Miyake Okayama University, Okayama-shi, Japan S.-I. Kawasaki, National Institute of Advanced Industrial Science and Technology, Sendai-shi, Japan	P 11	447
Acoustic Boosting of Battery Charging S. Tietze, G. Lindner Hochschule Coburg, Coburg, Germany	P 13	451
Design Optimization of Ultrasonic Motors Based on Power Flow Analysis T. Yuan, The Pennsylvania State University, University Park, USA, and Shanghai University, Shanghai, China K. Uchino, The Pennsylvania State University, University Park, USA C.D. Li, Shanghai University, Shanghai, China	P 14	455
Stator / Rotor Interface Analysis for Ultrasonic Motors K. Harmouch, Génie Electrique et Electronique de Paris, Gif-sur-Yvette, France Y. Bernard, Génie Electrique et Electronique de Paris, Gif-sur-Yvette, France, and Polytech Paris Sud, Paris, France L. Daniel, Génie Electrique et Electronique de Paris, Gif-sur-Yvette, France, and Université Paris Sud, Paris, France	P 15	459
Force Stepping Piezo Actuator: a Motorised Solution for High Resolution Positioning and External Forces Resistance C. Belly, F. Barillot Cedrat Technologies SA, Meylan, France	P 16	463
Dynamic Model of a PAD Actuator: Dynamic Operations and Pull-Off at High Speed C. Giraud-Audine, Arts et Métiers Paris Tech, Lille, France M. Amberg, F. Giraud Université de Lille, Villeneuve d'Ascq, France C. Mangeot, NOLIAC A/S, Kvistgaard, Denmark B. Lemaire-Semail, Université de Lille, Villeneuve d'Ascq, France	P 17	466

Poster Contributions
Micro Actuators / Microfluid Handling Devices

Technical Papers	No.	Page
Microfluidic System for Water Sample Treatment S. Gassmann, H. Schütte Jade Hochschule, Wilhelmshaven, Germany M.L. Miranda, O. Zielinski Carl von Ossietzky-Universität Oldenburg, Wilhelmshaven, Germany	P 19	471
Fabrication of Electrostatically Actuated Microshutters Arrays L. Oh, SGT Inc., Greenbelt, USA M. Li, NASA Goddard Space Flight Center, Greenbelt, USA D. Kelly, ASRC Federal Corp., Beltsville, USA A. Kutyrev, University of Maryland, College Park, USA S. Moseley, NASA Goddard Space Flight Center, Greenbelt, USA	P 20	475
Magnetoresistive Sensors for Angle, Position and Speed Measurement in Small and Micro Actuators R. Slatter, R. Buß Sensitec GmbH, Lahnau, Germany	P 21	479

Poster Contributions
ERF MRF Actuators

Technical Papers	No.	Page
New Class of Trunk-Like Robots: Structure, Control, Actuators R. Bansevicius, Kaunas University of Technology, Kaunas, Lithuania A. Drukteiniene, Siauliai University, Siauliai, Lithuania V. Jurenas, Kaunas University of Technology, Kaunas, Lithuania G. Kulvietis, Vilnius Gediminas Technical University, Vilnius, Lithuania	P 23	483

Poster Contributions
Low-Power Electromagnetic Actuators

Technical Papers | **No.** | **Page**

FlexPCB Windings, the Way Towards Very High Performance Coreless BLDC Motors · · · · · · · P 24 · · · · · · 487
F. Baudart, B. Dehez
Université Catholique de Louvain, Louvain-la-Neuve, Belgium

A High Precision Single Stage Compound Epicyclic Friction Speed Reducer · · · · · · · P 25 · · · · · · 491
J.F. Schorsch, F.F.C.T. van der Helm, D.A. Abbink
Delft University of Technology, Delft, The Netherlands

Compact Electrodynamic Planar Actuator for Automation · · · · · · · P 26 · · · · · · 495
T. Bödrich, B. Rosul, M. Stock, J. Ziske, J. Lienig
Technische Universität Dresden, Dresden, Germany

Highly Integrated Linear Direct Drive for Short Strokes · · · · · · · P 27 · · · · · · 499
J. Ziske, T. Bödrich, H. Basler, Q. Sun, J. Lienig
Technische Universität Dresden, Dresden, Germany

Poster Contributions
Polymer Actuators

Technical Papers | **No.** | **Page**

Development of an Artificial Muscle from Coiled Polymer Fibers for Humanoid Robotics Applications · · · · · P 28 · · · · · 503
A. Kalysheva, Z. Zhapar, K. Tulkibayeva, M. Folgheraiter
Nazarbayev University, Astana, Kazakhstan

Polymer-Dispersed Liquid Crystal Elastomer Thermomechanical Actuator · · P 29 · · · · · 507
A. Rešetič, J. Milavec
Jožef Stefan Institute, Ljubljana, Slovenia, and
Jožef Stefan International Postgraduate School, Ljubljana, Slovenia
B. Zupančič, Jožef Stefan Institute, Ljubljana, Slovenia
V. Domenici, Università degli Studi di Pisa, Pisa, Italy
B. Zalar, Jožef Stefan Institute, Ljubljana, Slovenia, and
Jožef Stefan International Postgraduate School, Ljubljana, Slovenia

Development and Experimental Characterization of a DE Membrane Actuated Valve · · · · · P 30 · · · · · 510
M. Hill, G. Rizzello, S. Seelecke
Universität des Saarlandes, Saarbrücken, Germany

Design and Control Strategies for a Novel Actuator System with Dielectric Electroactive Polymer and Spring · · · · · P 32 · · · · · 514
X. Zhang, A. Verhagen
Robert Bosch GmbH, Renningen, Germany
Q. Zhu, Karlsruher Institut für Technologie, Karlsruhe, Germany
S. Hau, S. Seelecke
Universität des Saarlandes, Saarbrücken, Germany

Poster Contributions
Shape Memory Actuators

Technical Papers	No.	Page
Industry 4.0 Using Shape Memory Actuators – Opportunities and Challenges R. Theiß, A. Czechowicz, P. Dültgen Forschungsgemeinschaft Werkzeuge und Werkstoffe e.V., Remscheid, Germany	P 33	518
Reconfigurable SMA End-Effector for Material Handling P. Motzki, Y. Goergen ZeMA gGmbH, Saarbrücken, Germany, and Universität des Saarlandes, Saarbrücken, Germany A. York, Universität des Saarlandes, Saarbrücken, Germany S. Seelecke, ZeMA gGmbH, Saarbrücken, Germany, and Universität des Saarlandes, Saarbrücken, Germany	P 34	522
Energy-Efficient SMA Vacuum Gripper System P. Motzki, J. Kunze ZeMA gGmbH, Saarbrücken, Germany, and Universität des Saarlandes, Saarbrücken, Germany A. York, Universität des Saarlandes, Saarbrücken, Germany S. Seelecke, ZeMA gGmbH, Saarbrücken, Germany, and Universität des Saarlandes, Saarbrücken, Germany	P 35	526

Poster Contributions
Actuator Control

Technical Papers	No.	Page
Passive Speed Control Using a Functional Clutch Driven Reversely K. Koyanagi, Toyama Prefectural University, Imizu-shi, Japan Y. Kimura, Osaka University Hospital, Suita-shi, Japan M. Koyanagi, Osaka Electro-Communication University, Shijonawate-shi, Japan A. Inoue, ER-tec Co., Minoh-shi, Japan T. Motoyoshi, H. Masuta, T. Oshima Toyama Prefectural University, Imizu-shi, Japan	P 36	530
Noise-Robust Online Parameter Identification of BLAC Machines Using Sliding Mode Differentiator N. König, E. Grasso, D. Merl, M. Nienhaus Universität des Saarlandes, Saarbrücken, Germany	P 37	534
A Direct Flux Observer for Robust to Noise Sensorless Control of PMSMs E. Grasso, M. Nienhaus Universität des Saarlandes, Saarbrücken, Germany	P 38	538

Poster Contributions
Active Vibration / Active Noise Control

Technical Papers	No.	Page
Semi-Passive Vibration Control Technique via Shunting of Amplified Piezoelectric Actuators G. Mikułowski, Institute of Fundamental Technological Research, Warsaw, Poland M. Fournier, T. Porchez, C. Belly, F. Claeyssen Cedrat Technologies SA, Meylan, France	P 41	542

Poster Contributions
Aerospace Applications

Technical Papers	No.	Page
Potentialities of APA Composite Shell Actuators and SA75D Amplifier for New Dynamic Applications M. Ragonet, J.-L. Petiniot ONERA, Lille, France M. Fournier, T. Porchez, O. Sosnicki, C. Bouchet Cedrat Technologies SA, Meylan, France	P 42	547
Embedded and Redundant Heater for Controlling of SMA-Based Rotary Actuator for Space Applications F. Stortiero, V. Visentin, S. Gualandris Technosprings Italia srl, Besnate, Italy	P 43	551

Poster Contributions
Fluidic / Pneumatic Actuators

Technical Papers	No.	Page
Hydraulic Expansion Actuators for Ball Screws – Towards Applicable Preload Adaption B. Denkena, P. Schreiber Leibniz Universität Hannover, Garbsen, Germany	P 44	552
A Multi-Functional Pneumatic Artificial Muscle – Proof of Concept T. Hassan, M. Cianchetti Scuola Superiore Sant’Anna, Pontedera, Italy B. Mazzolai, Istituto Italiano di Tecnologia, Pontedera, Italy C. Laschi, P. Dario Scuola Superiore Sant’Anna, Pontedera, Italy	P 45	557
Pneumatic Actuator Using Polyimide Film for Liquid Nitrogen Temperature D. Yamaguchi, T. Hanaki, R. Kamimura, Y. Ishino, M. Hara, M. Takasaki, T. Mizuno Saitama University, Saitama-shi, Japan	P 46	561
Surveying and Closed-Loop Control Study of Highly Elastic Bending Actuator for Biomimetic Gripping J. Isermann, S. Ulrich, R. Bruns Helmut Schmidt Universität, Hamburg, Germany	P 47	565

Poster Contributions
Haptic / Tactile Applications

Technical Papers	No.	Page
Dtact: A Tactile Device Which Changes How a Surface is Perceived F. Giraud, Université de Lille, Villeneuve d'Ascq, France C. Giraud-Audine, Arts et Métiers Paris Tech, Lille, France M. Amberg, B. Lemaire-Semail Université de Lille, Villeneuve d'Ascq, France	P 48	569
Novel Radial Locking Actuator with Magnetoactive Polymer H. Böse, T. Gerlach Fraunhofer ISC, Würzburg, Germany	P 49	573

Poster Contributions
Magnetostrictive / MSM Actuator

Technical Papers	No.	Page
Multistable Pneumatic Valve Based on Magnetic Shape Memory Alloys T. Schiepp, L. Riccardi, R. Schnetzler, M. Laufenberg ETO MAGNETIC GmbH, Stockach, Germany	P 52	577
Internal Stress Effects on Magnetostrictive Properties of Sputtered Giant Magnetostricitive Thin Films S. Sakano, R. Toyoda, A.A.Y Mansi, T. Washihira, Y. Matsumura Tokai University, Hiratsuka-shi, Japan	P 53	581
Optimization of Cutting Processes for Magnetic Shape Memory Actuator Elements A. Böhm, J. Schneider, W.-G. Drossel Fraunhofer IWU, Dresden, Germany E. Pagounis, M. Laufenberg ETO MAGNETIC GmbH, Stockach, Germany	P 54	584
Internal Stress Control for Magnetostrictive Thin Films by Substrate Bias S. Miyata, R. Toyoda, M. Hashimoto, S. Sakano, T. Iijima, A. Tonegawa, Y. Matsumura Tokai University, Hiratsuka-shi, Japan	P 55	588

Poster Contributions
(Bio-) Medical Applications

Technical Papers	No.	Page
Development of a Hand Rehabilitation Robot System for Range of Motion Exercises with Pneumatic Soft Actuators H. Taniguchi, T. Meguro, S. Yamamoto, S. Araki, R. Kobiki National Institute of Technology, Tsuyama-shi, Japan	P 56	591
Design of a Balancing Device for Small High Speed Rotors D. Pfeffer, F. Klug, H.F. Schlaak, P.P. Pott Technische Universität Darmstadt, Darmstadt, Germany	P 57	596
MRI-Compatible Piezoelectric Actuator Y. Bernard, R. Khairi, A. Razek, Université Paris Sud, Gif-sur-Yvette, France M. Poirier-Quinot, J.-C. Ginefri, R.-M. Dubuisson Université Paris Sud, Orsay, France	P 58	600

Piezoelectric Actuators 2016 – Professors' Misconceptions Top 10 (Review)

K. Uchino, The Pennsylvania State University, University Park, PA, USA

Abstract:
The "piezoelectric actuator" is really an interdisciplinary area, to which materials, applied physics, electrical and mechanical engineers are primarily approaching. Because of narrow knowledge of junior professors, they occasionally instruct the students with a sort of 'misconception', reflecting to the delay of innovative developments in the next generation. This paper reviews the top 10 among these misconceptions, which are primarily related with the misconceptions on the understanding of 'ionic displacement and strain', 'efficiency', 'energy transmission coefficient', 'constraint-dependency of piezo-material properties', 'mechanical impedance matching', 'piezoelectric damping mechanism', 'resonance & anti-resonance', 'best-selling devices', and 'system design principle'.

Keywords: Piezoelectric Actuator, Strain, Efficiency, Energy Transmission Coefficient, Mechanical Impedance Matching, Resonance / Antiresonance, Piezoelectic Energy Harvesting

I. INTRODUCTION

Actuator applications of piezoelectrics started in the late 1970s, and enormous investment was installed on practical developments during the 1980s, aiming at consumer applications such as precision positioners with high strain materials, multilayer device designing and mass-fabrication processes for portable electronic devices, ultrasonic motors for micro-robotics and smart structures. After the slump due to the worldwide economic recession in the late 1990s, we are now facing a sort of "Renaissance" of piezoelectric actuators according to the social environmental changes for sustainability (i.e., energy saving, bio-medical areas) and crisis technologies. **Figure 1** shows the piezoelectric device market estimated from multiple sources [1]. The current (2014) revenue around US$25 Billion will expand to $40 Billion by 2017. Actuator/piezo-

Figure 1. Piezoelectric device market trends. [1]

generator (energy harvesting) is the largest category, followed by transducer/sensor/accelerometer/piezo-transformer. Then, resonator/ acoustic device/ultrasonic motor category chases.

II. PROFESSOR'S MISCONCEPTIONS

The "piezoelectric actuator" is really an interdisciplinary area, to which materials, applied physics, electrical and mechanical engineers are primarily approaching. Because of narrow knowledge of junior professors, they occasionally

Table 1. Professor's misconceptions top 10 in "Piezoelectric Actuators".

1) Electrostriction is caused by a slight displacement of ions in the crystal lattice under field. This displacement will accumulate throughout the bulk and result in an overall strain along the field (cited from a famous encyclopedia).
2) When 1 J electric energy is input to a piezoelectric with an electromechanical coupling factor k, we can expect k^2 J mechanical energy converted in this piezo-material. Thus, we can conclude that the efficiency of this device is k^2 % (cited from a journal paper on Mechanical Engineering).
3) By applying 1 J electric energy on a piezoelectric with an electromechanical coupling factor k, we accumulated k^2 J mechanical energy in this piezo-material. Thus, this actuator can work mechani-cally up to k^2 J to the outside (cited from a journal paper on Mechanical Engineering).
4) Elastic compliances & sound velocity are the material's constants in a piezoelectric. Thus, the resonance frequencies are merely determined by the sample size.
5) PZT with the high electromechanical coupling factor k is the best piezoelectric material for heart beat monitoring sensors (from a conversation with an electrical engineering professor).
6) When the piezo-actuator generates unwelcomed vibration ringing in the mechanical system, the best way is to install a suitable mechanical damper in the system (from a conversation with a mechanical engineer).
7) The resonance mode is only the mechanical resonance, while the antiresonance mode is not a mechanical resonance (from a conversation with a materials professor).
8) The resonance mode is the best efficient driving condition of the piezoelectric transducer.
9) Improving the performance is the best way for seeking for the successful "Best-Selling" device (most of the professors).
10) The device developer should focus merely on the "component" development by purchasing the driving circuit from the outside for reducing the development cost and period (most of industrial engineers).

Excerpt only, page has been blanked!
A full pdf version in print quality is available here!

~

Electromechanical Properties of the Lead-Free $(1\text{-}x)Ba(Zr_{0.2}Ti_{0.8})O_3–x(Ba_{0.7}Ca_{0.3})TiO_3$ System

V. Rojas[1], J. Koruza[1], M. Acosta[1], D.R.J. Brandt[1], K.G. Webber[2], J. Rödel[1]
[1] Technische Universität Darmstadt, Darmstadt, Germany.
[2] Friedrich-Alexander Universität Erlangen-Nürnberg, Erlangen, Germany

Abstract:
The $(1\text{-}x)Ba(Zr_{0.2}Ti_{0.8})O_3–x(Ba_{0.7}Ca_{0.3})TiO_3$ piezoceramic is investigated as a possible alternative to lead-containing piezoelectrics for actuator applications. Compositions with rhombohedral, orthorhombic, and tetragonal crystal structure were prepared and the large-signal piezoelectric response and blocking stress were evaluated at different electric fields. The rhombohedral and orthorhombic compositions showed the best properties with a blocking stress of -62 MPa at 2 kV/mm and a large signal d_{33}^* of 851 pm/V at 0.5 kV/mm, which exceeds the values reported for commercial soft-type PZT. The differences observed between different compositions were attributed to the changes in the strain mechanisms that occur due to the specific crystal symmetries and their vicinity to the phase transition boundaries.

Keywords: Piezoelectrics, Lead-Free, BZT-BCT, Blocking Force

Introduction

Piezoceramics are typically used in actuator applications like fuel injectors, precision positioning devices, piezo-hydraulic pumps, ultrasonic motors, and others [1]. The traditional materials of choice for these devices over the past 60 years were lead-based piezoelectrics, such as $Pb(Zr,Ti)O_3$ (PZT), due to their excellent electromechanical properties and good thermal stability. However, the increased environmental- and health-concerns, additionally supported by governmental regulations, triggered the search for new lead-free alternatives [2]. After more than 10 years of intense scientific research, these materials are starting to attract the attention of the industry and first prototypes and products are already available [3].

The lead-free piezoceramics can be roughly divided into four main groups: alkaline niobates [4], bismuth sodium titanates [5], bismuth ferrites [6], and materials based on barium titanate [7]. The materials belonging to the last group are particularly interesting for applications in the low temperature range, whereby the most investigated compositions belong to the $(1\text{-}x)Ba(Zr_{0.2}Ti_{0.8})O_3–x(Ba_{0.7}Ca_{0.3})TiO_3$ (BZT-xBCT) system. This system has a small-signal piezoelectric coefficient d_{33} of 620 pC/N [7], which is comparable or even exceeds the properties of commercial PZT. In addition, these compositions are characterized by relatively low coercive fields. A recent study also revealed excellent fatigue resistance of these materials, whereby a decrease of the piezoelectric properties by only 7 % was observed after 10^7 bipolar electrical cycles with a frequency of 10 Hz and an amplitude of 0.45 kV/mm [8]. On the other hand, the main drawback of BZT-xBCT is the relatively low Curie temperature (60–95 °C) as compared to other lead-free systems, which currently limits their application to low temperatures. Chemical modifications with dopants, for example Y [9], have been attempted to raise the Curie temperature of the system.

The BZT-xBCT pseudo-binary phase diagram, presented in figure 1, shows three distinct ferroelectric crystallographic phases, *i.e.*, rhombohedral (R), orthorhombic (O), and tetragonal (T), while the high-temperature phase is cubic (C). The ferroelectric phases are separated by two polymorphic phase boundaries [10]. As it is known from other ferroelectric systems, the different crystal structures largely affect the strain and polarization response of the material.

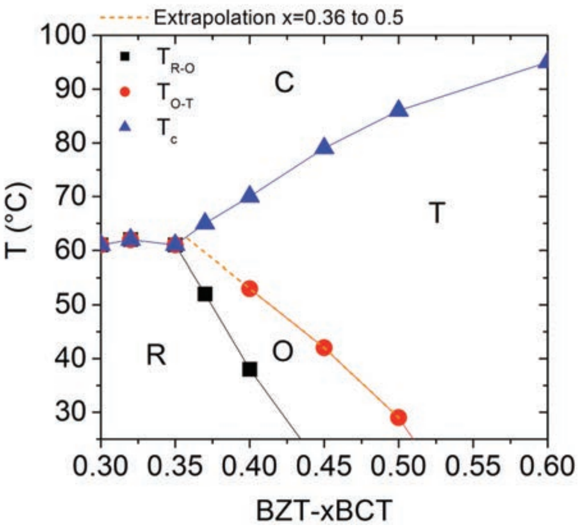

***Fig. 1:** Phase diagram of the BZT-xBCT lead-free piezoceramics system (R-rhombohedral, O-orthorhombic, T-tetragonal, C-cubic). Reprinted from Ref. 10 with kind permission from Elsevier © 2014.*

Temperature Dependency of the Hysteresis Behaviour of PZT Actuators Using Preisach Model

C. Mangeot, Noliac A/S, Kvistgaard, Denmark
T.-G. Zsurzsan, Technical University of Denmark, Kgs. Lyngby, Denmark

Abstract:
The Preisach model is a powerful tool for modelling the hysteresis phenomenon on multilayer piezo actuators under large signal excitation. In this paper, measurements at different temperatures are presented, showing the effect on the density of the Preisach matrix. An interpretation is presented, aiming at defining a temperature-dependent phenomenological model of hysteresis for a better understanding of the non-linear effects in piezo actuators.

Keywords: Piezoelectric, Multilayer, Actuator, Preisach, Model, Temperature

Introduction

Quasi-static multilayer piezoelectric actuators are generally used in quasi-static applications under large signal excitation. In these conditions, the hysteresis effect is pronounced and can become a limitation, in particular for positioning applications.
To address this, two main approaches are possible: sensor-based or model-based. In the sensor-based approach, a sensor (displacement, force…) is used to close the loop and effectively linearize the piezoelectric effect. Although it provides excellent results, this approach is not always preferred or even possible, because of cost, size or performance. In the model-based approach, the behaviour of the actuator is characterised and this model is inverted to provide open-loop control of the actuator. This approach has become very popular with the availability of powerful real-time controllers. Several models have been proposed [1, 2], among others Ishlinskii hysteresis model [3], Maxwell resistive capacitor-based lumped-parameter model [4], variable time relay hysteresis model [5] and Preisach model [6].
The Preisach model [7, 8] is a phenomenological approach that can accurately describe any hysteresis behaviour. It is often the preferred approach for piezoelectric actuators and its large number of degrees of freedom makes it possible to adjust very precisely to experimental data.

The Preisach model

In a simple Preisach model, the hysteresis effect is decomposed into an infinity of individual elements called hysterons. These elements act as relays with an activation threshold α and a de-activation threshold β.
A geometrical interpretation of the hysteron plane greatly facilitates the understanding of the Preisach model in general. In this plane, a so-called Preisach triangle T_0 is defined, which represents the region of operation of the actuator, bordered by $\alpha_{max}, \alpha_{min}, \beta_{max}$ *and* β_{min}. Only the surface above the diagonal given by $\alpha = \beta$ has any physical meaning and therefore T_0 is an upper triangular surface. The elementary hysterons have a direct correlation to the half-plane in such a way that at any point in time T_0 is divided into two surfaces S^+ and S^- representing the (α, β) pairs for which the relay elements are active or inactive, respectively.
Thereby, for a monotonic increase of an input $u(t)$, the input-output plane shows an ascending hysteresis branch, while the T_0 half-plane 'fills up' from the bottom to the horizontal line defined by $\alpha = \{\alpha_1 \mid \alpha_1 \leq u(t)\}$. Similarly, a monotonic decrease in input will then determine the surface to 'empty', but this process is orthogonal to the one for increasing input. Therefore the 'filled' space T_0 will empty starting from the right towards the vertical line defined by $\beta = \{\beta_1 \mid \beta_1 \geq u(t)\}$. Thereby, a stochastic input signal with several extrema will be represented as a combination of 'filled' and 'emptied' areas on the triangle, delimited by a boundary staircase layer, denoted L. The problem then boils down to finding the area under the obtained staircase curve. This is illustrated in Fig. 1.

The standard equation for this type of model is:

$$x(t) = \iint_{\alpha \geq \beta} \mu(\alpha, \beta) \gamma_{\alpha\beta}[u, \gamma_0](t)\, d\beta\, d\alpha$$

Where x is the model output, μ represents a weighting matrix that mathematically particularizes the model to fit different hysteresis shapes and $\gamma_{\alpha\beta}$ represents the hysteron elements that can take values from the set $\{-1, 1\}$.
Terms on the diagonal ($\alpha = \beta$) dictate the general trend of the curve without hysteresis while the density within the triangle ($\alpha > \beta$) corresponds to hysteresis effects.

Excerpt only, page has been blanked!
A full pdf version in print quality is available here!

Should We Drive Transducers at Their Resonance Frequency?

H. Shekhani , The Pennsylvania State University, University Park, USA
W. Shi, Harbin Institute of Technology, Harbin, China
M. Majzoubi, M. Choi, A. Bansal, K. Uchino
The Pennsylvania State University, University Park, USA

Abstract:
There are three losses in piezoelectric materials: dielectric, elastic, and piezoelectric, denoted by $\tan\phi'$, $\tan\delta'$, and $\tan\theta'$ for intensive losses, respectively. We discovered that the minimum total loss can be obtained at a frequency between the resonance and antiresonance frequencies, which may be the optimum drive frequency of the transducer to minimize the heat generation. This paper also presents related updated loss information, (1) new methods for characterizing losses in piezoelectrics, (2) loss anisotropy and (3) bias electric field/stress effect on the losses.

Keywords: Equivalent Circuit, Loss Mechanism, High Power, Drive Efficiency

Introduction

Piezoelectric materials are gaining increasing popularity because their aptitude for device miniaturization. Piezoelectric motors and transformers have been demonstrated to perform at the same power levels as electromagnetic devices, but at 1/10th the size [1,2]. The power density capability in piezoelectric are limited by their internal losses. In the case of ferroelectric piezoelectric materials, this loss originates primarily from domain wall motion. Losses not only limit the power conversion in the material, but also causes heat generation. High temperatures limit the operating life of a device due to gradual depoling in the material Thus, in order to advance the device miniaturization of piezoelectric materials, it is necessary to study loss mechanisms in order optimize devices and high power material compositions. which is directly related with loss and heat generation.

Losses in piezoelectric materials have three components: dielectric, elastic and piezoelectric, described using loss tangents with complex tensor notation (in ‘intensive’ loss forms):

$$\varepsilon^{X*} = \varepsilon^{X}(1 - j\tan\delta')$$

$$s^{E*} = s^{E}(1 - j\tan\phi')$$

$$d^{*} = d(1 - j\tan\theta')$$

Dielectric and elastic loss factors are standard reported values, however, piezoelectric losses have been given little attention [3]. Relatively large piezoelectric loss factors were reported in our previous study [4], which also explained the discrepancy between the mechanical quality factor at resonance and antiresonance.

In this paper, several topics with regards to loss property characterization in piezoelectric materials will be discussed. First, the method to determine the quality factor at any frequency in the resonance-antiresonance region will be discussed. Then, a method to interpret the results using an equivalent circuit explicitly accounting for piezoelectric loss will be presented. This discussion will be followed by the introduction of a new technique to measure extensive properties and losses directly in piezoelectric materials using a partial electrode configuration. Finally, both the effect of DC bias in piezoelectric materials and the dependence of effective properties on poling direction will be discussed.

Use of Electrical Power to Determine Quality Factor

Losses in piezoelectric materials operating in high power resonance conditions are usually measured using either the impedance method or the transient method. The driving parameter such as voltage, current, power, or vibration velocity is controlled while the frequency is swept across the antiresonance-resonance regime in the impedance method. Measuring the 3dB bandwidth, the quality factors for resonance and antiresonance can be determined. In the transient method, the material is excited for a number of cycles, after which a short circuit (resonance type) or open circuit condition (antiresonance type) is applied across the electrodes. The decay of current or voltage allows for the measurement of the quality factor at resonance and antiresonance, respectively. These methods are limited in their utility in that they can only measure the quality factor at two points, the resonance and

Single-Sided Contacting of Out-of-Plane Polarized Piezo Films for Fluid Membrane Lenses

M. Stürmer, M.C. Wapler, U. Wallrabe
Albert-Ludwigs-Universität Freiburg, Freiburg, Germany

Abstract:
We present an adaptive lens which tunes its focal length with a glass membrane that is deformed by an integrated piezo bending actuator. A particular challenge in the fabrication of this type of actuator is the need to contact the electrodes on both sides of the piezo element, i.e. also on the glass surface. Therefore, we show a novel contacting method where the top electrode on the piezo is segmented and the backside electrode is left at a floating potential. With this setup we achieve tuning capabilities of more than 13 m^{-1} and response times in the range of less than 4 ms at a usable aperture of 4.5 mm.

Keywords: Piezo Actuator, Bending Actuator, Contacting Method, Floating Electrode, Varifocal Lens, Adaptive Optics

Motivation and concept

Tunable fluid-membrane lenses (e.g. [1-4]) commonly use elastomer membranes like silicone as an optical surface and are filled with an optical fluid [3]. Glass membranes, however, promise a wider range of compatible filling liquids due to much greater chemical stability. Therefore, high refractive index liquids can be used, and matching to the glass promises reduced distortions and aberrations. In contrast to other varifocal lenses with glass membranes [5], our approach uses a bulk piezo material, such that larger actuators and thicker, larger membranes can be realized.
In the system design in Fig. 1, the piezo actuators are directly attached to the glass which leads to a common problem of bending actuators: The passive glass layer obstructs access to the backside-electrode of the piezo with a wire. A well-known method for contacting piezo films from one side is driving an in-plane polarized piezo with interdigitated surface electrodes in the longitudinal mode [6, 7]. The actual three-dimensional field distribution below the electrodes is, however, far from homogeneous, which leads to a drop in efficiency [7].

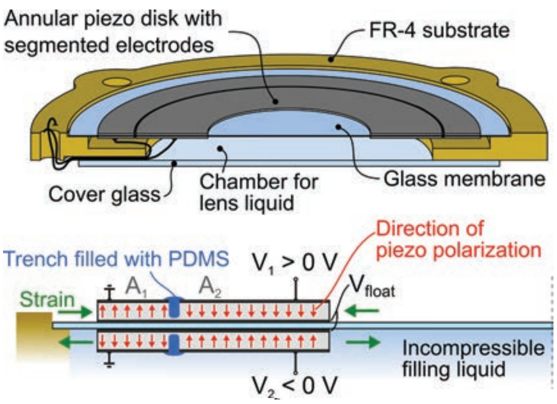

***Fig. 1: Top:** Schematic cross-section drawing of the lens. **Bottom:** Working principle.*

As an alternative, we demonstrate here a method to contact a transversely polarized piezo bending actuator with planar electrodes from one side only which leads to an almost perfectly homogeneous field distribution. We separate the electrodes on the outer side in two rings and leave the back electrode at a floating potential that is obtained from the voltage between the front-electrodes and the electrode areas by considering a series connection of capacitors: $V_{\mathrm{float},1} = V_1 \cdot A_1/(A_1 + A_2)$ (cf. quantities in Fig. 1 bottom). The resulting field is used both to re-polarize the material in the depicted directions and for the actuation.

Design

The working principle of the lens design uses the constant volume of the fluid which is encapsulated by the lens membrane. The ring-shaped actuator bends the outer part of the membrane to displace a fluid volume, and the resulting pressure causes it to bulge in the centre, shaping a lens profile.
We chose equal electrode areas, $A_1 = A_2$ to obtain a homogenous strain and maximum overall dielectric displacement over the entire piezo layer. With a simplified linear FEM simulation model we found values for the parameters shown in Fig. 2 top that maximize the achievable deflection of the membrane. We further found that a sandwich design with actuators on both sides of the glass provides a higher displacement than actuator sheets on only one side. A gap between outer support ring and piezo ($r_{\mathrm{ring}} - r_{\mathrm{outer}}$) of 500 μm provides sufficient flexibility to act as a hinge while being strong enough to resist vertical displacement from the counter pressure. Varying the inner and outer radius (r_{aperture} and r_{outer}) (Fig. 2 bottom) within their manufacturable range, we found that the maximum refractive power is achieved at an

Tailored Composite Transducers Based on Piezoceramic Fibres and Pearls

K. Hohlfeld[1], P. Neumeister[2], S. Gebhardt[2], A. Michaelis[1,2]
[1] Technische Universität Dresden, Dresden, Germany
[2] Fraunhofer IKTS, Dresden, Germany

Abstract:
The contribution reports on the fabrication of tailored piezoceramic components and composites for sensor, actuator, ultrasonic transducer, and generator applications. A slotted electrode design for fibre based patch transducers is discussed in detail, which enables significantly higher values of free displacement and blocking force compared to on top interdigitated electrode design.

Keywords: Piezoceramic, Fibres, Pearls, Piezocomposite, Transducer, Actuator, Ultrasonic Transducer

Introduction

Piezoelectric transducers based on piezoceramic polymer composites are predominantly used as sensors, actuators, ultrasonic transducers or energy harvesters applied in adaptronics, medical technology and non-destructive testing. In respect of high performance and cost-effective production, piezoceramic components as well as piezoelectric composites thereof have to be tailored to application needs.

At Fraunhofer IKTS, a fabrication technology is available, which allows for the manufacture of piezoceramic components in a broad geometrical variety [1, 2]. So far, lead zirconate titanate (PZT) fibres with diameters d = 100-800 µm as well as spherical PZT pearls with diameters d = 0.8-1.6 mm have been fabricated (see Fig. 1 and Fig. 2). For transducer manufacturing, these piezoceramic components are aligned and embedded into a polymer matrix, combining functionality of the piezoceramic with mechanical stability of the matrix material. The composite fabrication technique is referred to Arrange & Fill [3].

According to the field of application, different piezocomposite designs are preferred. Piezocomposites based on piezoceramic pearls are especially suitable for sensor or energy harvesting applications. Therefore, a monolayer of piezoceramic pearls is integrated into a polymer matrix and the surface of the spheres exposed by grinding or polishing. Then, planar electrodes can be applied. The technique is very suitable for cost-effective fabrication of large-area transducers with low power density demands.

For fabrication of ultrasonic transducers for non-destructive testing, medical and sonar applications, piezoceramic fibres are parallel aligned in bundles or with regular arrangement and infiltrated with a polymer. After curing, the piezofibre polymer block can easily be shaped into any form by dicing, CNC machining and grinding. By varying the fibre arrangement (random/regular), thickness and shape of the so-called 1-3 piezocomposite (see Fig. 3), ultrasonic transducers can be manufactured according to customs needs.

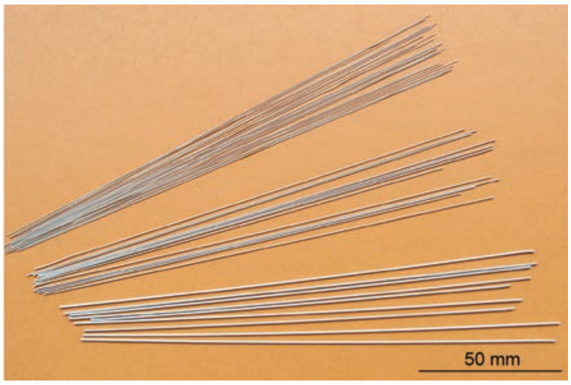

Fig. 1: *PZT-fibres with 300 µm, 500 µm and 800 µm diameter and 160 mm length; fabricated by continuous spinning process*

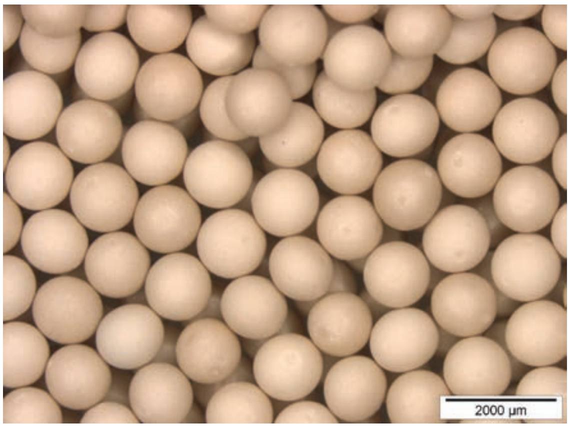

Fig. 2: *Piezoceramic pearls with 1200 µm diameter fabricated by non-continuous process*

Dynamic Characterization of an Amplified Piezoelectric Actuator

R. Lucinskis, C. Mangeot
Noliac A/S, Kvistgaard, Denmark

Abstract:
The characterisation of piezoelectric actuators in dynamic operation is critical to ensure both the functionality in the application and the survival of the actuator. Unfortunately little data is available. This paper presents a simple approach for characterisation and for the evaluation of the two main limitations of an actuator: voltage and stress. The approach is applied to an amplified piezoelectric actuator without load. The amplified actuator is based upon low voltage piezoelectric ceramic multilayer stacks for systems requiring lighter actuators with temperature stability and high resonance frequency. Experiments demonstrate that a simple first-order model approach can be used, although the parameters, in particular stiffness, are affected by non-linearity. Nevertheless, such a model can be used to evaluate the operating envelope of an actuator in a given dynamic configuration. If it should be performed in a systematic way, this approach requires additional parameters and characterisation from the suppliers.

Keywords: Amplified Actuator, Piezoelectric Actuator, Strain Limits, Dynamic Characterization

Introduction

Piezoelectric actuators are often the preferred choice for highly dynamic applications because of their low inertia and high stiffness, leading to fast response. Dynamic applications include for example fast tuning and steering of optical systems, fuel injection or active vibration control.
The static performance of piezoelectric actuators has been studied extensively [1, 2]. On the other hand, suppliers of piezoelectric devices provide only little information about dynamic characteristics of actuators. Usually a first unloaded resonance frequency is indicated, in most cases in free-free configuration which is rarely representative of how the actuator will be used. Response time is sometimes specified, however this is for very particular conditions. This makes it difficult for the designer to evaluate the limits of an actuator solution and its applicability to a given technical challenge.
The target of this paper is to analyse the dynamic characteristics of a piezoelectric actuator, applied to the example of an amplified actuator, trying to derive an approach and tools usable by designers to estimate and validate their choice. Experimental results are presented and compared to a theoretical approach.

The approach is applied to Noliac’s amplified piezoelectric actuator family NAC26xx (Fig. 1) [3]. These offer a compact solution with a high resonance frequency. The multilayer actuator features a low form factor and provides medium stroke and blocking force. The amplified piezo actuator offers push and pull with the same level of performance and it is temperature stable.

Fig. 1: *NAC26xx amplified actuator family*

Design
The amplified actuator is based upon low voltage piezoelectric ceramic multilayer stacks. The diamond construction makes the actuator mass lower and optimizes stiffness, allowing operation at higher frequency compared to other amplification solutions. The amplified actuator uses four piezoelectric stacks, connected in pairs. Each stack is hinged at its ends and maintained in place with a small angle (Fig. 2). The whole assembly is preloaded through the use of a tension member maintaining the fixed members in place.

Development of a Piezoelectric Micro Switch

L. Seyfert, S. Zähringer, C. Müller, S. Buhr, N. Schwesinger
Technische Universität München, München, Germany

Abstract:
Piezoelectric membrane actuators present a growing and dynamic sector in micromechanical applications. Fields of application are high-precision regulators, micro pumps or micro valves. In this point of view, a new actuator concept with single side electrodes was developed. As part of this concept many different electrode layouts were analysed. One of these was an actuator with a star shaped electrode layout. When actuated under forward bias and fixed clamping, this actuator shows an “upward” movement in direction of the active side of the membrane, meaning the side carrying the electrodes. Compared to common piezoelectric membrane actuators this behaviour is unique. This paper presents a practical and mobile application to prove this upward movement and to demonstrate the function of this new actuator. To prepare this actuator for other future applications such as micro valves a simple configuration in a form of a micro switch was built.

Keywords: Piezoelectric Actuator, Micro Switch, Single Side Electrodes, IDT

Introduction

New piezoelectric membrane actuators with single side electrodes were presented in [1] and [2]. These interdigitated electrodes are commonly known as interdigital transducers (IDT) and used in surface acoustic wave (SAW) devices. The use of such IDTs for micro membrane actuators is not as common. E. Hong et al. described an example with double concentric ring IDTs for thin film PZT actuators [3]. Instead of thin film PZT, we use bulk PZT with an electrode layout on just one sided. A typical interdigitated star shaped electrode layout is shown in Fig. 1.

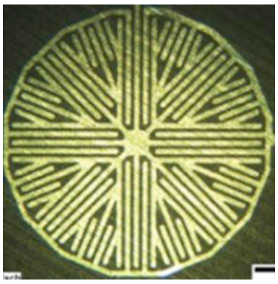

Fig. 1: *Star shaped electrode design*

When clamped along the outer radius, these actuators show a uniform deflection in direction of the active side of the membrane [2, 4], meaning the side where the electrodes are deposited. In Fig. 2 (3.) this deflection behaviour is shown and compared with traditional piezoelectric membrane transducers.
A classic unimorph (Fig. 2, 1.) uses the piezoelectric transverse effect and a piezostack (Fig. 2, 2.) uses the longitudinal effect. Both show a deflection in direction of the passive side of the actuator, when actuated under forward bias.

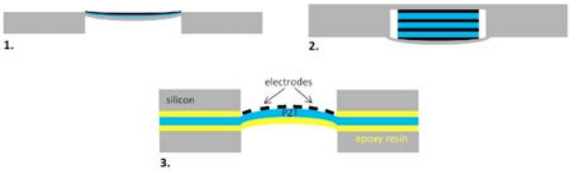

Fig. 2: *Common known and new piezoelectric micro membrane actuators*

In comparison, by using the interdigitated single side star shaped electrodes, all piezoelectric effects are enforced. The IDT driven transducers cause an inhomogeneous electric flux distribution within the material, when actuated. This flux causes inhomogeneous mechanical strain and stress distributions within the material. The result is a deformation of the transducer. To achieve a complete upward deformation the actuator is clamped at its outer radius [4].

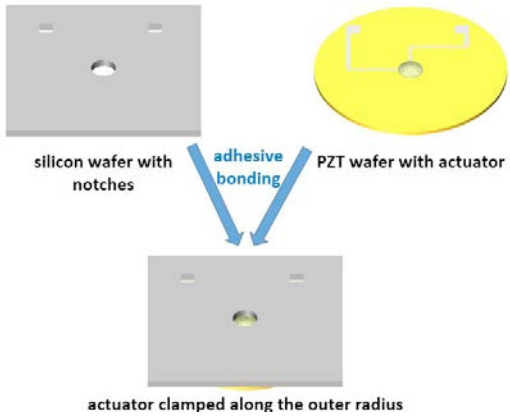

Fig. 3: *Clamping of the actuator*

The clamping was achieved through an adhesive bonding of a silicon wafer. This wafer was etched

Characteristics of Ultrasonic Suspension Actuation Force

M. Takasaki, S. Chino, R. Chida, Y. Ishino, T. Mizuno
Saitama University, Saitama-shi, Japan

Abstract:
In ultrasonic levitation, an object can be levitated vertically upward above vibrating surface of an ultrasonic transducer. On the other hand, it has been reported that an object can be suspended vertically downward under the vibrating surface in the air. We call this phenomenon ultrasonic suspension. When an object is suspended, there is restoring force, which attracts the object horizontally to the center of the vibrating surface. Characteristics of the forces acting vertically and horizontally were investigated experimentally. For this purpose, a servo type measuring mechanism was fabricated. The mechanism consisted of a base suspended by thin wires and three voice coils to stabilize the base in x axis, z axis and roll axis. The suspended object, which was a disk, was fixed on the base vertically. Ultrasonic transducer with a horn equipped with a replaceable cap to change its diameter was fixed horizontally and approached against the fixed object. While ultrasonic vibration was being excited, actuation forces acting on the object were measured as coil currents under PID control of the base. By this mechanism, relative position between the object and the cap could be arranged. Relationships between actuation forces and suspended object conditions like vibration amplitude, relative position of the object and diameters of the object / vibrating surface were investigated experimentally. Vertical attractive force can be generated if the diameter of the object and surface is smaller than 8 mm. Horizontal restoring force was obtained, but not strong as vertical one.

Keywords: Non-Contact Handling, Squeeze Film, Ultrasonic Suspension

Introduction

Recently, a non-contact handling technique that uses the ultrasonic levitation phenomenon as a means of transporting semiconductor substrates or LCD glass substrates has been considered [1-5]. In particular, the near-field levitation phenomenon has been observed. Near-field levitation is the phenomenon in which a planar object can be levitated upward from a vibrating surface with a gap of tens micrometers. Theoretical analysis considering viscosity has revealed that in near-field levitation, a force acting on a circular plate reverses from repulsive to attractive with increasing levitation distance [2].

In contrast to ultrasonic levitation, a planar object can be suspended downward under a vibrating surface without contact [6]. This phenomenon is called ultrasonic suspension and induces both vertical actuation force and horizontal actuation force. The vertical force balances gravity acting on the object. The horizontal force attracts the object to the center of the vibrating surface when there is horizontal misalignment. It acts as the restoring force.

In this manuscript, development of a mechanism for servo-type actuation force measurement is reported. The developed mechanism was applied to experimentally measure the actuation forces and their characteristics. Characterization results are also reported. In the next section, ultrasonic suspension is introduced before the main topics.

Ultrasonic suspension

An object can be levitated vertically upward above vibrating surface of an ultrasonic transducer if intensity of the vibration is strong enough, as shown in Fig. 1 (a). On the other hand, it has been reported that an object can be suspended vertically downward under the vibrating surface in the air [6] , as illustrated in Fig. 1 (b). We call this phenomenon ultrasonic suspension. To confirm this phenomenon, behavior of a planar object with diameter of 3 mm and weight of 3 mg was observed by a camera with the setup illustrated in Fig. 2. Resonance frequency of the ultrasonic transducer was 21 kHz. Vibration amplitude of the end of the ultrasonic transducer which is facing to the object was 7 $\mu m_{p\text{-}p}$. Observation result was shown in Fig. 3 as captured images. The number in left bottom of each image is relative time (ms) since the first one. Initially, there was a misalignment between the transducer end and the object. The object was pulled into the center of

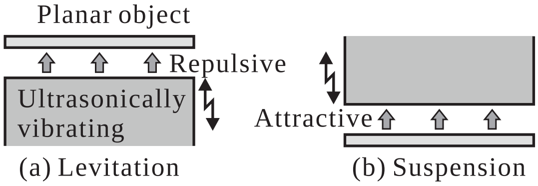

Fig. 1: *Ultrasonic levitation and ultrasonic suspension*

Encapsulated Piezo Actuators for Use at High Power Levels and / or within Harsh Environmental Conditions.

S. Rowe, F. Barillot, A. Pages, F. Claeyssen
Cedrat Technologies SA, Meylan, France

Abstract:
Traditionally piezo ceramic actuators have not been able to operate within harsh/humid environments. Furthermore, two temperature-related problems have limited the number of applications for piezo actuators. Firstly, internal heating of the ceramic from use at high frequency, for extended periods. Secondly, external environmental conditions. Encapsulation of the actuator offers an opportunity to overcome all of these problems by allowing the environment directly in contact with the ceramic to be controlled. This paper presents R&D work done on encapsulated actuators, design work, and thermal simulation calculations with an emphasis on experimental results.

Keywords: Actuator, Piezo, Encapsulation, Temperature, Cooling, Self-Heating

Introduction

In its simplest form encapsulation provides a physical barrier between the environment and the ceramic, restricting direct contact between the two. This form of encapsulation is ideal where the environmental conditions are either humid or harsh and contact between both the environment and the ceramic would limit the actuator life.

Furthermore traditionally two temperature-related problems have limited the number of applications for piezo actuators: firstly, internal heating of the ceramic from use at high frequency for extended periods; and secondly, external environmental conditions.

Self-heating is a new issue arising from the need for high power applications where actuators are expected to operate at high frequency, maximum stroke and for extended periods of continuous operation. These applications have become possible with the availability of new high power drivers.

At the same time, a range of applications are opening up where the thermal environmental conditions are elevated and above the Curie temperature of the ceramic, which requires the piezo ceramic to be protected by a physical barrier between the ceramic and the environment, however at the same time this barrier must not allow any major loss of performance of the actuator.

Encapsulation of the actuator offers an opportunity to overcome all of these problems by allowing the environment directly in contact with the ceramic to be controlled, either within a sealed actuator system, one with fluid cooling, or within a closed-loop fluid cooled system.

Some of the work presented here has been performed within the project AeroPZT, specifically funded under the Clean Sky Joint Technology Initiative (EUFP7). The project partners, Plant Integrity Ltd (UK), Cedrat Technologies (France), Noliac (Denmark) and Politecnico di Torino (Italy), are targeting the development of materials and processes for the application of piezoelectric actuators in aero engine controls, which implies harsh environmental conditions, particularly elevated temperature. Applications of such actuators could include valve control for fuel staging or clearance control.

Harsh/humid environments

As the applications for piezo actuators continue to expand especially into fields such as aerospace, oil/gas and science there is a requirement for the actuator to be immersed within increasingly harsh environmental conditions.

In the simplest form encapsulation systems, provides a single layer physical protection for the ceramic against the environmental conditions.

Dynamic Control of the Piezoelectric Transducer's Resonant Frequency using MOSFET Switching

H. Yokozawa[1], J. Twiefel [2], M. Weinstein [2] and T. Morita[1]
[1] The University of Tokyo, Tokyo, Japan
[2] Leibniz Universität Hannover, Hannover, Germany

Abstract:
For driving ultrasonic motors, it is often required to control the resonant frequency of a transducer between some mode shapes or numbers; for example, some of them are driven with combined vibration of longitudinal and bending modes, and the shift of the resonant frequency degrades their performance. As the source of this shift, the boundary condition's change and the nonlinear effect during the high power driving should be taken into account. To overcome this problem, this study proposes a dynamic control system of the resonant frequency modification by connecting FETs to the additional piezoelectric parts differently from the driving piezoelectric part. By switching on and off the FETs, the electric boundary condition for the additional piezoelectric parts changes between shorten and open conditions. Generally, the resonant frequencies under these conditions have the relationship of $f_{\text{shorten}} < f_{\text{open}}$ because of the piezoelectric effect. By switching the FETs with the same frequency as the driving frequency, the resonant frequency could be modified as a function of the duty ratio.

Keywords: Ultrasonic Transducer, Resonant Frequency Control, Dynamic Control System

Introduction

For exciting the high power ultrasonic transducers, it is often required to control the resonant frequency between some mode shapes or mode numbers [1-3]. For example, ultrasonic motors are driven with combined vibration of longitudinal and bending modes [4,5]. In these ultrasonic motors' operation, two vibration modes are excited in the synchronized frequency. R-SIDM actuators utilize the 1st and the 3rd mode of the longitudinal vibration whose frequency ratio is 1:2 [6,7]. To control the resonant frequencies of the transducer, the mechanical design and the material properties have been considered. Although, even if the design of the transducer is optimum for driving motors, the machining error is inevitable. Furthermore, the resonant frequency changes due to the nonlinear effect of the piezoelectric vibration during its high power operation [8-11] and is also shifted with the boundary condition's variation. To overcome this problem, this study proposes the dynamic control of the resonant frequency utilizing additional piezoelectric parts in the transducer. By controlling the electric boundary condition of these piezoelectric materials via the connected FETs switching, the stiffness of the additional parts can be modified according to the piezoelectric effect and the resonant frequency can be controlled.

Method

Chubachi *et al.* proposed a static control of the resonant frequency of a Langevin transducer by connecting inductors to the additional piezoelectric parts [12] as shown in the left of Fig. 1. An equivalent circuit for this transducer has two electric terminals as shown in Fig. 2. The connected inductors to the Terminal 2 in Fig. 2 (additional piezoelectric parts) corresponds to the additional equivalent mass in this equivalent circuit; therefore the resonant frequency can be controlled. Although, this control can be realized in the static situation, so it cannot compensate the resonant frequencies' shift during the operation.

In this study, the dynamic control of the resonant frequency is proposed by connecting FETs to the Terminal 2 as the right in Fig. 1. The frequency response of the admittance Y of the equivalent circuit in Fig. 2 is given by

$$Y = j\omega C_1 + \left(\frac{1}{-j\omega C_1} + \frac{j\omega L_m}{\Phi_1^2} + \frac{1}{j\omega\Phi_1^2 C_m} + \frac{R_m}{\Phi_1^2}\right)^{-1} \tag{1}$$

when the Terminal 2 is opened, where L_m, C_m, R_m are equivalent mass, compliance and loss, C_1 and Φ_1 are the damped capacitance and the force factor of the driving piezoelectric materials and C_2 and Φ_2 are those of the additional piezoelectric materials. This equation is deformed to

$$Y = j\omega C_1 + \left(\frac{1}{-j\omega C_1} + \frac{j\omega L_m}{\Phi_1^2} + \frac{1}{j\omega\Phi_1^2 C_m} + \frac{R_m}{\Phi_1^2} + \frac{\Phi_2^2}{-j\omega\Phi_1^2 C_2}\right)^{-1} \tag{2}$$

with the shorten condition of the Terminal 2. These equations mean the frequency response of the admittance and the resonant frequency change depending on the electric boundary conditions of the Terminal 2 due to the damped capacitor of the additional piezoelectric parts. By switching FETs with the same frequency as the driving voltage and changing the duty ratio of this switching, the resonant frequency can be controlled continuously.

Magnetic Shape Memory Actuation: Trends and Design Concepts (Review)

P. Müllner, Boise State University, Boise, USA
E. Pagounis, ETO MAGNETIC GmbH, Stockach, Germany

Abstract:
We review recent developments in magnetic shape memory alloy (MSMA) technology with an emphasis on actuator applications and the alloy Ni-Mn-Ga which remains the dominating MSMA regarding magnetic-field-induced deformation. Selection of suitable compositions increased the temperature range for magnetic actuation from almost zero to 350 K. Other material developments include the increase of magnetic-field-induced strain (MFIS) for 10M and 14M martensite to 7.3 and 11.2%, the stabilization of fine twin microstructures via surface coatings and surface treatments, and the study of twinning dynamics. Maximum twin boundary velocities and response times of 82.5 m/s and 2.8 μs where demonstrated implying that actuation frequencies may reach or even exceed 100 kHz. Actuator concepts may be categorized as (i) using bulk or thin film magnetic shape memory elements, (ii) actuating with a magnetic field, a combination of a magnetic field and a mechanical load, or a combination of a magnetic field and temperature field, and (iii) using homogeneous or heterogeneous fields. Examples of recently demonstrated actuators include positioning devices, clamping devices, micro-pumps, and thin-film devices. Several computational models have been proposed to simulate magneto-mechanical behavior under multi-axial loading. An increasing number of studies concern the domestication of hysteresis through advanced control mechanisms. In summary, significant progress was made in many relevant aspects for the commercialization of MSMA technology and several proof-of-concept actuators were demonstrated successfully.

Keywords: Magnetic Shape Memory, Properties, Actuators, Modeling, Control, Microfluidics

1. Introduction

2016 marks the twentieth anniversary of the seminal 1996 paper of Ullakko et al. [1] introducing magnetic-field-induced strain (MFIS) of magnetic shape memory alloys (MSMAs). The field saw rapid improvement of magneto-mechanical properties, particularly MFIS. Moving twin boundaries carry the deformation. First demonstrator actuators were already introduced over a decade ago [2]. From 2000 on, the by-annual ACTUATOR conference consistently hosted symposia on magnetic shape memory and magnetostrictive actuators. For reviews on fundamentals and applications of MSMAs, we refer to the proceedings of previous ACTUATOR conferences, of the ICFSMA conferences, and to a recent overview article [3]. The present article focuses on MSMA actuator developments of the last two years. We also present some advancement in materials properties and discoveries on twinning mechanisms since 2014.

2. Material development

Material properties relevant for actuators include the MFIS (which should be large), the twinning stress (which should be low), mechanical work output (which should be large), operating temperature range (which should be wide), and resistance against degradation (i.e. fatigue) resulting from repeated actuation (which should be high). The MFIS depends on the structure of the martensite phase. For the three most frequently reported structures, i.e. non-modulated (2M), 14M, and 10M, the MFIS values have been increased to 12% [4], 11.2% [5], and 7.1% [6].

The twinning stress is highest for 2M martensite, intermediate for 14M martensite, and lowest for 10M martensite. For 10M martensite, the twinning stress depends on crystal quality (i.e. purity and defect content), and type of twin boundaries. For type I twin boundaries, the twinning stress is less than 1 MPa directly below the martensite finish temperature and increases linearly with decreasing temperature by 0.035 MPa/K ([7]). For type II twins, the twinning stress is below 0.5 MPa independent of temperature for a wide temperature range. The twinning stress further depends on the driving force. For relatively small driving forces (i.e. static experiments), twin boundary motion is thermally activated and depends on defects correlated with the twin microstructure [8,9].

For large driving forces, twin boundary motion is athermal [8,9]and depends on temperature through the temperature dependence of the lattice parameters [10]. Very large driving forces can be achieved with pulsed magnetic fields resulting in twin boundary velocities of 82.5 m/s and twin boundary accelerations of 1.6 x 106 m/s2 and response times of 2.8 µs [11].

Fast Actuation of Magnetic Shape Memory Material Ni-Mn-Ga Using Pulsed Magnetic Field

A. Saren, J. Tellinen, D. Musiienko, K. Ullakko
Lappeenranta University of Technology, Savonlinna, Finland

Abstract:
Pulsed magnetic field-induced actuation of magnetic shape memory material Ni–Mn–Ga 5M martensite has been studied. Saturation velocities of fast-moving single type II twin boundaries in a range of 35–39 m/s were directly observed using high-speed camera technique. Corresponding actuation velocities of 2.1–2.3 m/s were acquired using laser Doppler vibrometry technique, both for elongation and contraction of the sample. In a case of multiple twin boundaries motion, actuation velocities of 4–5.5 m/s and actuation accelerations of (4-7)$\times 10^5$ m/s^2 were achieved. The actuation response time was measured to be less than 1 μs. The reported results have a potential for the development of new applications, especially in microscale devices where the working frequency can be significantly increased. Example potential applications are fast optical and electrical switches, pneumatic/hydraulic valves, microfluidic pumps and valves, micromanipulators and grippers.

Keywords: Magnetic Shape Memory, Ni-Mn-Ga, Twinning, Twin Boundary Dynamics, Magnetic Field Actuation

Introduction

Magnetic Shape Memory (MSM) alloy Ni-Mn-Ga is a promising actuating material due to the combination of a large strain ~6-10% [1, 2] and fast response to magnetic field [3]. Twin variants reorientation by twin boundary (TB) motion is the mechanism responsible for the reversible strains observed under mechanical load and magnetic field actuation [4]. Up to now, two types of TBs (type I and II) were observed in Ni-Mn-Ga 5M martensite, with substantially different stresses [5]. Recently, we observed about an order of magnitude difference in saturation velocities of TBs of these types [6]. Here we focus on the direct experimental observation of fast-moving type II single TBs under pulsed magnetic field excitation, and actuation velocity measurements for both elongation and contraction of the sample, in saturation magnetic field. The contribution of the limiting factors such as inertia and internal friction are discussed.

Experimental procedures

The MSM samples used in the study were mechanically and electrochemically polished $Ni_{50}Mn_{28}Ga_{22}$ single crystals with austenite start temperature of 42 °C. All measurements were done at RT. The samples' cross-section was ~1×1 mm^2 with a length of 8-10 mm, with faces nearly parallel to the {1 0 0} planes of the austenite. The maximum strain, ε_0, was measured to be 6%. The experimental setup is shown in Fig.1a. A Helmholtz coil, connected to a pulse generator (EMC, Transient 1000), created a magnetic field pulse providing saturation field inside the sample during ~70% of the pulse length, with rise time (to saturation level) about 5 μs. A high-speed camera (Photron FASTCAM SA5) at a frame rate of 775000 fps was used to acquire real-time images from the top surface, while a laser Doppler vibrometer (LDV) (Polytec, OFV-5000, OFV-534) was observing the left facet of the sample. Each sample was glued on its one end to a holder providing a proper alignment inside the coil frame. Prior to the pulsed excitation, the sample was set into a single variant state by placing it into a constant magnetic field of ~1 T, with subsequent introduction of a single

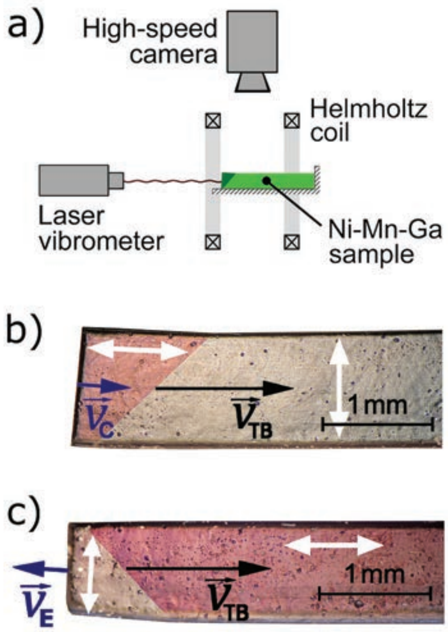

Fig. 1: *(a) Schematic of the experimental setup. (b, c) Optical side-view images of the sample with a single TB, for two twin variant arrangements. Color contrast is due to the use of polarized light. The easy axis directions are marked with white arrows. See the description of the velocity vectors in the text.*

Physics of Energy Barriers for Twin Boundary Motion in Ni-Mn-Ga

E. Faran, N. Zreihan, I. Benichou, S. Givli, D. Shilo
Technion - Israel Institute of Technology, Haifa, Israel

Abstract:
A multi scale experimental study of twinning kinetics reveals two energy barriers that dictate the motion of twin boundaries in FSMA Ni-Mn-Ga: the twinning stress barrier and the lattice potential. The former represents the minimal driving force required for boundary motion at low velocities. The latter dictates the driving force range necessary for higher boundary velocities, which enables high frequency actuation. The physical origins and characteristics of the two barriers are discussed. Using unique experimental and analysis methods we show that the extremely low twinning stress value of type II boundary in 10M Ni-Mn-Ga originates from the internal twinning micro structure in this alloy, while the contribution of the magnetic micro structure to this barrier is negligible. In addition, the temperature dependence of the lattice potential is evaluated both experimentally and theoretically, indicating the benefits in high-frequency actuation performance close to the transformation temperature.

Keywords: Ni-Mn-Ga, Twin Boundaries, Energy Barrier, Twinning Stress

Unfortunately, the final manuscript has not been received by the printing date. Please contact the author for additional information.

An Effective Method for Designing Magnetic Shape Memory Actuator Systems

F. Ehle, P. Neumeister, H. Neubert
Fraunhofer IKTS, Dresden, Germany

Abstract:
Ferromagnetic shape memory alloys (FSMA) are magneto-mechanical solid-state transducers distinguished from other actuation principles in actuation properties like high stroke, high energy density and operation frequency. However, readily usable design tools for MSM systems are still lacking. For this reason, we present a fast computing lumped element model for the design support of FMSA-based actuators in this paper. The modelling approach is based on an extended Tellinen hysteresis model for the static magneto-mechanical hysteresis. Furthermore, dynamic effects such as eddy currents and inertia are considered in form of additional lumped elements. By a rough discretization, magnetic and mechanical load contributions can be considered.

Keywords: Magnetic Shape Memory Actuators, Lumped Element Network Models, Dynamics Simulation

Introduction

Ferromagnetic shape memory alloys (FSMA) are magneto-mechanical solid-state transducers distinguished from other actuation principles in actuation properties like high stroke, high energy density and operation frequency. For this reason, they are possible alternatives to conventional actuators or enable new products. During the last years, a significant progress towards the commercialization of the technology has been achieved, primarily in the fields of material development (e.g. high temperature alloys [1]) and fabrication technology. However, readily usable design tools for FSMA-based actuator systems are still lacking. They are even more necessary because the complicated hysteretic magneto-mechanical coupling, requires a model-based design. This is especially true for the design of fast switching devices, such as circuit breakers or valves, when dynamic effects like inertia and eddy currents contribute to the mechanical and magnetic loads on the FSMA.

In our contribution, we present (i) a scalar static material model of Ni-Mn-Ga material, and (ii) the utilization of this approach for modelling dynamic effects in FSMA actuators. Both, static and dynamic models are designed to be used in network models with lumped elements.

Hysteresis Modelling Approach

Numerous modelling approaches for the strain hysteresis of FMSAs have been proposed. Most of them capture the obvious operation mode, in which a magnetic field along the short crystal-bar axis induces strain perpendicular to the field direction and the sample is reset by an external compressive force. Although recent microscopic approaches prove capable of reproducing the material behaviour accurately, macroscopic approaches are usually better suited for actuator system design. Especially lumped element modelling approaches allow for efficient coupling of different physical domains. We have proposed such an approach based on an extended Tellinen model [2,3], which takes into account the hysteresis of the uniaxial strain ε depending on magnetic flux density B and the applied compressive stress σ for the above named operation mode. The scalar nature of the model is justified by temporally constant field orientations and almost homogenous magnetic field and stress distribution inside the MSM transducer, which is basically fulfilled in most actuator designs. The advantage of the Tellinen model compared to other hysteresis models is that it requires only the limiting surfaces to be completely parametrized in the ε-σ-B-space. Good agreement between measurement and simulation has been attained with very small computational effort [3].

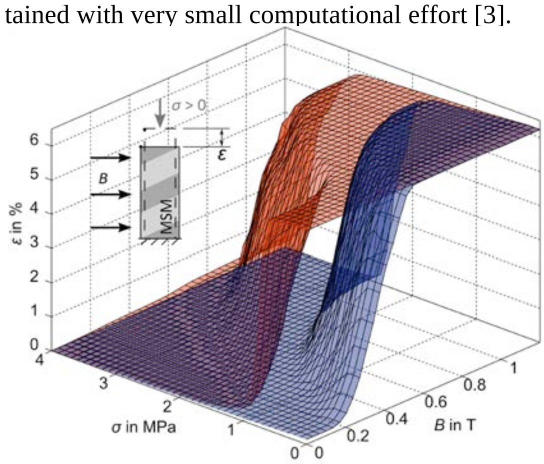

Fig. 1: *Measured limiting hysteresis surfaces (red upper, blue lower) for the depicted operation mode.*

In the present form, the Tellinen model describes the equilibrium response of the FSMA material at vanishing rates of stress and flux. However, within

Materials Design for Magnetostrictive Thin Films

A. Sakai, C. Niyomwaitaya, A.A.Y Mansi, T. Washihira, Y. Matsumura
Tokai University, Hiratsuka-shi, Japan

Abstract:
Fe alloy thin films were prepared by ion-plating process with dual vapour source and the magnetostrictive properties would be discussed. The introduced excess energy during thin film formation was analysed by plasma diagnostics. We evaluated the solid solubility of alloy thin films using Darken and Gurry plot which used the size rule and the electronegativity based on Hume–Rothery rules. In conclusion, it suggests that Darken–Gurry plot hold the potential to propose the designing of magnetostrictive alloy solid solution thin film.

Keywords: Magnetostrictive, Thin Film, Ion Plating, Excess Energy

Introduction

Magnetostriction is mostly found in the magnetic transition materials like iron, cobalt and nickel and also in the rare earth materials like lanthanum and terbium. These materials consist of numerous magnetic domains that can rotate and align under the influence of an external magnetic field. The magnetic orientation or alignment brings forth internal strain in the material, which is known as magnetostriction.

In recent years, there has been great interest in introducing magnetostrictive thin films, known as intelligent magnetostrictive materials. These materials can convert magnetic (electrical) energy into kinetic energy, or the reverse through low-voltage power source. Thus, they present several advantages in the applications by controllable without using any contactor. Magnetostrictive thin films, less than a few micrometers in thickness, are widely used to build actuators, sensors and vibration energy harvesting devices [1–6].

Clark and his co-workers at Carderock Division (Maryland) of the Naval Surface Warfare Center (NSWC) developed alloys containing Fe, Dy, and Tb. The most successful magnetostrictive material is Terfenol-D due to large magnetostriction of more than 2000 ppm in a field of 160 kA/m at room temperature. It is the most commonly used as engineering magnetostrictive material[7–9]. In addition, Rare earth-based magnetostrictive materials were known as giant magnetostricive materials for a long period of time. However, the shortage of rare-earth supplies and the brittleness of rare-earth compound inspire a new development for more sustainable magnetostrictive materials. So many researchers are attempting to find new types of material which can be easily found and provide affordable price to replace these resources.

Fortunately, Fe–based alloys recently have been concerning because of these alloys show several hundred of magnetostrictive properties. Recently, Clark et al. reported that high values of the magnetostrictive amount were found in Fe-17 at% Ga single crystals. This materials are indicating good magnetostrictive susceptibility, high resistant to corrosion and high toughness values [10–11]. However, Fe-17 at% Ga alloy exceeds the solid solubility limit at the room temperature, it must be prepared in a thermodynamic non-equilibrium state[12].

A maximum amount of solute that can be dissolved in the solvent to form a solid solution is termed as solubility limit. The addition of solute in excess of this limit results in the formation of two phase solution. Hume–Rothery et al. in very early work proposed several factors controlling the extent of solid solubility. These factors form a useful basis for discussing the formation of extensive or restricted solid solutions [14]. The first Hume–Rothery rule says about the atomic size factor which is the solid solutions should not be anticipated if the atomic sizes of solute and solvent differ by more than 15%. Provided that ‘others factors are favourable solid solutions may form if the size difference is less than 15%. And the second rule, the electronegativity difference between the two elements should not be too large, typically within a range of ±0.4.

Furthermore, Darken–Gurry made important progress in the prediction of solid solubility when they made simultaneous use of size and of electrochemical factors apply in illustrate called Darken–Gurry (DG) plot (see Fig.1). The DG plot reveals ease of the solid solubility to form a solution. The predictions regarding solubility were made by the ellipse on the plot, which is centered at the solvent (Fe) and spans a horizontal range corresponding to the atomic radius of ±15% and a vertical range corresponding to electronegativity values of ±0.4. Elements falling within the ellipse generally form extensive solid solution, while those outside do not.

A 3.5

Ferromagnetic Shape Memory Flapper for Remotely Actuated Propulsion Systems

D. Shilo, Technion - Israel Institute of Technology, Haifa, Israel
O. Kanner, Yale University, New Haven, USA
J. Sheng, R. James
University of Minnesota, Minneapolis, USA
Y. Ganor, Philips Health Systems, Andover, USA

Abstract:
Generating propulsion with small-scale devices is a major challenge due to both the domination of viscous forces at low Reynolds numbers as well as the small relative stroke length of traditional actuators. Ferromagnetic shape memory alloys are good candidates for such devices as they exhibit a unique combination of large strains and fast responses, and can be remotely activated by magnetic fields. This paper presents the design, analysis, and realization of a novel Ni-Mn-Ga shear actuation method, which is especially suitable for small-scale fluid propulsion. A fluid mechanics analysis shows that the two key parameters for powerful propulsion are the engineering shear strain and twin boundary velocity. Using high-speed photography, we directly measure both parameters under an alternating magnetic field. Reynolds numbers in the inertial flow regime (>700) are evaluated. Measurements of the transient thrust show values up to 40 mN, significantly higher than biological equivalents. This work paves the way for new remotely activated and controlled propulsion for untethered micro-scale robots.

Keywords: Ferromagnetic Shape Memory Alloy, Actuators, Active Materials, Propulsion, FSMA, NiMnGa

Unfortunately, the final manuscript has not been received by the printing date. Please contact the author for additional information.

Design and Modelling of a Sensor-Integrated Actuator Using Combined Effects of Magnetostriction and Piezoelectricity

M. Niu, B. Yang, G. Meng
Shanghai Jiao Tong University, Shanghai, China

Abstract:
This paper presents a magnetostrictive actuator integrated with a piezoelectric sensor. The output force can be detected during actuation. A nonlinear model to depict the combined effects of magnetostriction and piezoelectricity is proposed. The model for magnetostriction is based on the Jiles-Atherton model with dynamic extensions of eddy-current losses and magneto-mechanical effects, so it applies for the working conditions of high frequency and time-varying stress. A piezoelectric constitutive model is connected to the new Jiles-Atherton model with both the changing strain and the changing interaction forces. Using the combined model, the output displacement of the sensor-integrated actuator can be accurately predicted. Simulations and experiments have been conducted and compared for verification.

Keywords: Magnetostrictive Actuator, Piezoelectric Sensor, Jiles-Atherton Model

Introduction

Magnetostriction is a property of ferromagnetic materials that their shape or dimensions will change during the process of magnetization when a magnetic field is imposed on them. Possessing the property, magnetostrictive materials have large actuation strains up to 2000 ppm, huge actuation stress up to 200 MPa, short response time in the range of micro-seconds, high resolution up to 10^{-7} and wide response band. Given these superior performances, they are widely used for magnetostrictive transducers[1], linear motors, rotary motors, servo valves, precision positioning systems[2] and vibration control systems[3].
However, there are also some properties which make the material difficult to use. Nonlinearity is one of the most significant. Magnetostrictive materials show strong nonlinearity because of the hysteresis and eddy-current losses. The magnetomechanical coupling characteristics make the material more difficult for modelling. Besides, the material is sensitive to the change of temperature. And ΔE effect is also a typical property that cannot be neglected when applied in engineering. All these properties hold back the outstanding material for widely use. So a suitable model, which takes all the above mentioned factors into consideration, is necessary for the design and control based on the material. Several models have been established during the past decades.
Preisach model[4], Prandtl-Ishlinskii model[5] and Bouc-Wen model[6] are the three most representative phenomenological models. They are suitable for the control of magnetostrictive materials for their high accuracy and natural property of minor loops closure. However, the nonphysical nature of the parameters makes them difficult to construct models using physical behavior or to employ attributes of the parameters for updating models to accommodate changing operation conditions.
Physical models include Jiles-Atherton model[7], homogenized energy model[8] and Armstrong model[9]. Among them, JA model is the most classical one. It derives from the ferromagnetic magnetization theory promoted by Jiles and Atherton, which is based on micromagnetics and Weiss molecular field theory. The original JA model requires only five parameters. The construction of the model is further enhanced by the physical nature of the parameters and the fact that certain parameters can be directly specified from measured data.
Piezoelectricity is the electric charge that accumulates in certain solid materials in response to applied mechanical stress. Piezoelectric materials are widely used for energy harvesting[10], sensors, actuators and reduction of vibrations[11] and noises. Using as sensors, piezoelectric material has the advantages of ruggedness, high natural frequency and excellent linearity over a wide amplitude range.
This paper presents a magnetostrictive actuator integrated with a piezoelectric force sensor for output monitoring and accurately modelling. The structure of the actuator is introduced. A nonlinear model, which is based on JA model while taking the eddy-current losses and magneto-mechanical effects into consideration, is established. Also, a piezoelectricity model is adopted and combined with the dynamic JA model. Using the combined model, with the data of the input current into the coil and the output voltage from the sensor, the output displacement and force can be accurately predicted. The parameters of the model are identified and experiments are taken to show that introducing the

Impulse Damping Using Magnetic Shape Memory Alloys

L. Riccardi, T. Schiepp, R. Schmid, M. Maier, M. Helmer, M. Laufenberg
ETO MAGNETIC, Stockach, Germany

Abstract:
The mechanical hysteresis of magnetic shape memory alloys implies a remarkable damping capacity that can be exploited in vibration dampers and impulse dampers. This paper presents results concerning damping properties of an MSM impulse damper. The device is designed and characterized to quantify the energy absorption capabilities. Three activation strategies of the damper are discussed: a passive, a semi-active and an intelligent approach which further improves the damping.

Keywords: Magnetic Shape Memory, Damping, Hysteresis

Introduction

Damping techniques are common methods of attenuating the vibrations or impacts in a system or structure. Passive damping is usually realized using viscoelasticity, friction and material damping. Semi-active and active damping techniques are able to address a wider range of conditions. However, active damping is not always applicable due to cost, volume and power requirements.

This paper discusses the possibility to use magnetic shape memory (MSM) alloys in damping applications. MSM alloys are smart materials which can produce deformation and stress in a controlled way when excited by a magnetic field, respectively up to 6 to 12 % and 3 to 4 MPa [1]. Beyond their actuation properties, which can be exploited in innovative and energy-efficient actuators [2, 3], they have promising features that can be used in sensors, energy harvesters, and further devices such as passive, semi-active or active dampers. In fact, MSM alloys exhibit a hysteresis between stress and strain, whose area represents the energy absorbed during cycling and thus the damping capabilities of the material.

The paper is organized as follows. The first part characterizes in detail a MSM sample with respect to the damping. The second part describes a set-up for impulse damping and presents the measurements of an impact experiment where the MSM sample is compared to Aluminum and Iron. The final section closes the paper with concluding remarks.

Damping properties of MSM alloys

The energy absorption of MSM alloys is described by the area delimited by the stress-strain hysteresis. The hysteresis in MSM alloys originates from the presence of an internal stress in the material called *twinning stress*, which is strain dependent. The stress value which produces 3% strain at zero field is usually considered as an average, representative value of twinning stress. Two qualitative stress-strain curves are shown in Fig. 1, where stress is applied along *x*, parallel to the strain, and field along *y*. Refer to the blue curve at zero field. At the beginning of the compression test, the MSM element exhibits an elastic behavior (from A to B0). When the stress is close to the average twinning stress σ_{TW}, the so called *twinning region* starts (from B0 to C0), which describes the large deformation of MSM alloys. At the end, another elastic region follows (from C0 to D0). For elongation, the alloy should be subjected to a tensile stress or to a magnetic field along *y*, i.e. perpendicular to the stress. The red curve shows the case in which a non-zero field is applied. The elastic region increases (from A to B1) because the stress must now overcome the sum of twinning stress and magnetically induced stress; between B1 and C1 lies the twinning region for $H = H_1 > 0$. The area enclosed by the stress-strain curve is the energy absorbed during the mechanical cycling. The bigger the twinning stress, the bigger the area.

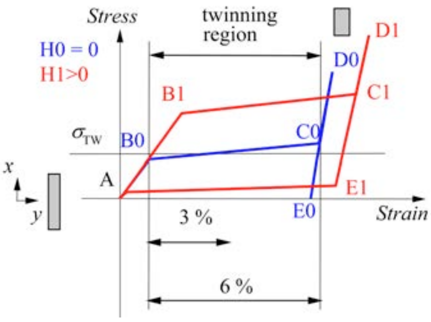

Fig. 1: *Qualitative stress-strain curves of MSM alloys, at field strengths H0 = 0 (blue curve) and H1 > 0*

The damping capabilities of a MSM sample measuring 3 mm × 5 mm × 20 mm are characterized in a setup where both magnetic field and mechanical

Magnetic Field Controlled Damping in MSM-Polymer Hybrids

I. Aaltio, F. Nilsén, J. Lehtonen, Y. Ge, S.-P. Hannula
Aalto University, Espoo, Finland

Abstract:
In addition to the well-known actuation property Magnetic Shape Memory (MSM) alloys have been found to have good vibration damping properties in particular in the low to moderate frequency range. The high vibration damping capability in MSMAs is based primarily on the hysteretic motion of martensite twin boundaries or on the reversible stress-induced-intermartensitic transformation. Both of these mechanisms enable several percent mechanical shape change of MSM material. Single crystal Ni-Mn-Ga MSM materials have been widely studied and used for their high capability of relative shape change. However, the size and shape of these single crystal is limited, e.g., due to the complex manufacturing process and the need of special methods for their cutting. In addition the material price is rather high for many damping applications. These limitations may be overcome by an alternative approach: the MSM-polymer hybrids.

We studied the vibration damping properties of MSM-polymer hybrid composites and the effect of external magnetic field on damping. The Ni-Mn-Ga MSM material was produced by gas-atomization method and the resulting powder consisted of spherical particles of approximately 100 μm diameter. The MSM powder was mixed with epoxy and oriented by external magnetic field at the curing stage of the polymer matrix. The resulting hybrid material consisted of chains of MSM particles aligned with the magnetic field direction, which results to anisotropic mechanical and damping properties of the hybrid. Vibration damping properties of the hybrids were characterized. The properties of the hybrid depend on the filling ratio as well as the matrix material used. Application of the MSM-polymer hybrids to magnetically controllable vibration dampers is also briefly discussed.

Keywords: MSM, Hybrid, Polymer Composite, Damping

Introduction

High damping MSM-polymer hybrids utilize the mechanical elasticity and adequate bonding properties of the epoxy matrix and the special properties of the Ni-Mn-Ga MSM powder. An important feature of the MSM powder is the hysteretic twin boundary motion, which is induced by the external stress. Actuating MSM-epoxy composites have been prepared earlier using EDM-cut single crystal Ni-Mn-Ga pieces [1]. Instead of the actuation, the present paper focuses on the damping properties of the composites and uses gas-atomization for producing the MSM particles. Unlike the process based on the EDM cut pieces, gas atomization is a well-known industrial method to produce metallic powders with a large batch size and low costs. Therefore, it is interesting to apply it to MSM alloy. A drawback is that the gas atomized particles are not single crystals and their twinning stress is expected to be high. Thus, it is not likely that they as such will be capable of producing direct actuation in an applied magnetic field. However, mechanical damping properties are possible to obtain, even if the twinning stress is higher.

Experimental

The Ni-Mn-Ga powder was produced by gas atomization from elemental Ni, Mn and Ga raw materials. The resulting powder consisted of highly spherical particles. The particles were sieved to a selected particle size and then heat treated in a protective atmosphere and sieved to a selected particle size. The chemical composition was determined by scanning electron microscopy (SEM) and energy dispersive x-ray analysis (EDS) and the phase transformation temperatures were obtained by the low-field *ac* susceptibility method. The phase structure of the powder was determined by x-ray diffraction (XRD).

A magneto-mechanical training treatment was applied to the MSM powder before the hybrid processing. The aim of the training was to enhance the motion of the twin boundaries. The training included magnetization by 1 T applied field and subsequent compression by 10-20 MPa stress. The training cycle was repeated 3 times for the powder.

Disparities in Radial Properties (Magnetic and Structural) of Single Crystal Terfenol-D Disks

V. Issindou[1], B. Viala[1], L. Gimeno[2,3], O. Cugat[2,3], O. Geoffroy[4], F. Fillot[1,5], J. Debray[4,5]
[1] CEA LETI, Grenoble, France
[2] G2Elab, Université Grenoble Alpes, Grenoble, France
[3] CNRS, Université Grenoble Alpes, Grenoble, France
[4] CNRS, Institut NEEL, Grenoble, France
[5] Université Grenoble Alpes, Grenoble, France

Abstract:
Disparities in magnetic properties of disks of <112>-oriented single-crystal Terfenol-D are reported, in relation to their crystallographic structure. A sampling of 11 disks was used (from two rods). The in-plane saturation magnetostriction of disks ($\lambda_s^{//}$- $\lambda_s^{\perp}$) was measured by the capacitance method. The differences between disks are significant (~ 35%). Polar plots (0°-360°C) of the equivalent squareness ratio (SQR) at 0.2T are shown for the two series of disks. It is a simple, fast and accurate method based on standard vibrating sample magnetometer (VSM) which is well suited to large sampling of miniature disks. They reveal typical shamrock-shaped plots with four leaves with two maxima at 0° and 90° and two minima at 49° and 131°. Some disks exhibit a degraded shape. They are the same that have a lower magnetostriction. θ-2θ X-Ray diffractions, metallographic observations and Laue method have determined that crystal twinning and equiaxed grain germination are responsible of these degradations.

Keywords: Terfenol-D, Magnetostriction, Anisotropy, Twins

Introduction

Terfenol-D is a high performance single crystal magnetostrictive material which naturally grows in a <112> direction [1]. It has been fabricated for decades in form of elongated rods of approximately one centimetre in diameter. Historical applications have used whole rods being deformed in length, such as cylindrical actuators and transducers [2]. Recently, smart composites have appeared coupling magnetostrictive and piezoelectric elements. They enable new applications like broadband transducers [3] and magnetoelectric sensors [4]. Composites are more and more miniaturized and require smaller and thinner magnetostrictive elements. This leads to use today miniature disks of Terfenol-D cut from rods. Therefore, properties of disks are crucial, yet remain rarely investigated. Disks are prone to process variations, which can be linked to their growth and structure. The aim of this work is to evaluate finely these disparities on a disks sampling from two rods.

Experiment

The sampling is realized on 11 miniature disks (6 mm-diameter, 1 mm-thick) cut perpendicularly to the growth axis from two commercial rods (13 mm-diameter and 350 mm-long). The two series are labelled A1 to F1 for rod 1 and A2 to E2 for rod 2. Samples were cut by electrical discharge machining (EDM), and diamond saw.
The saturation magnetostriction ($\lambda_s^{//}$- $\lambda_s^{\perp}$) of disks was measured by the capacitance method [5]. The disks were rotated (180°) about their axis with a constant magnetic field of 2T applied in the disk plane. No pre-stress was used.
In-plane hysteresis loops were measured by vibrating sample magnetometer (VSM) at different azimuthal angles (up to 360°).
Crystallographic orientations normal to the disk were determined with θ-2θ X-ray (Cu-α) diffraction (XRD). The structural characterization was completed with detailed metallographic examinations and Laue diffractions on the disks surface after polishing and etching (Vilella reagent).

Results

Table 1 highlights the disks sampling based on the maximum values of measured saturation magnetostriction. The results are very scattered with a variation up to ~ 35%. Such disparities may be unacceptable for the mass production of miniature devices. Therefore, a detailed understanding of the origin of this disparity is necessary. This was undertaken on a selection of representative samples (B1, F1 and C2).

***Table 1:** Saturation magnetostriction of series of disks (in ppm)*

Sample	A1	B1	C1	D1	E1	F1
λ//- $\lambda\perp$	2371	2340	2300	2232	2157	1996

Sample	A2	B2	C2	D2	E2
λ//- $\lambda\perp$	2251	1776	1773	1617	1552

Study of Vibration Energy Harvester Based on the Magnetic Shape Memory Effect

D. Musiienko, Lappeenranta University of Technology, Savonlinna, Finland
J. Huimasalo, Elektroniikan 3K-tehdas, Savonlinna, Finland
J. Tellinen, A. Saren, K. Ullakko
Lappeenranta University of Technology, Savonlinna, Finland

Abstract:
In present study theoretical model of MSM energy harvester is discussed and stand-alone energy harvesting device is developed and characterized in the frequency range from 10 to 200 Hz at vibration conditions that are close to real applications. The device utilizes 4 MSM elements (1*2.5*10 mm each) actuated by external mechanical stress that leads to magnetic flux modulation. With external oscillation mechanism the MSM material showed V_{RMS} over 2 V (at 3% stroke, with no resistive electrical load), which is enough for DC rectification. To model real vibration conditions harvester prototype was mounted onto shaking platform with adjustable frequency and amplitude of oscillation. It was found that harvesting productivity strictly depends on mechanical resonance of the oscillating part of the device. Mechanical system improvements allowed achieving maximum power output of more than 38 mW (1 mW • cm^{-3}) at 101 ± 1 Hz.

Introduction

Power generation from ambient environmental energy becomes a growing field of interest [1]. Mechanical vibrations in particular have attracted attention due to its prevalence [2]. Several technologies have been developed to harvest this energy such as magnetostrictive, piezoelectric, electrostatic and electromagnetic technologies. An emerging technology combines the principles of electromagnetism with the magnetic shape memory (MSM) effect to create an energy harvester using Ni-Mn-Ga as the actuating material [3-7]. Due to magnetic anisotropy of martensitic crystal lattice, the longer *a*-axis has a magnetic permeability that is over 20 times greater than that of the shorter *c*-axis [8]. If a sufficient mechanical stress is applied a single crystalline element of martensitic Ni-Mn-Ga reorients from one twin variant to another. This crystallographic reorientation induces the corresponding change to the easy direction of magnetization within the sample. As such, the flux of an applied magnetic field changes according to the twin variant ratio of the MSM element. The MSM energy harvester is realized when the electromotive force within a pick-up coil appears according to this magnetic flux modulation, therefore generating an alternating electric current.

See full review of literature in our recent study [9], in which experimental energy harvesting setup was built and theoretical model was developed. The model allows construction of energy harvester (EH) with preliminary defined characteristics. Experimental setup utilized external DC power supply to bias magnetic field in the system, while harvested AC power was measured over the adjustable load in the parallel line with capacitor, which was simultaneously used to achieve electric resonance conditions. It was found that material itself is capable to produce 0.33 mW • mm^{-3} and 1.37 mW • mm^{-3} when electric resonance system is used. Developed model was used to build stand-alone energy harvester prototype with a permanent magnet as a magnetic field source.

Results and discussion

Figure 1 shows the energy-harvesting device containing 4 parallelepipedal MSM elements (1*2.5*10 mm). To maximize the performance and lifetime stabilized fine twin structure was created in MSM elements [10]. Stress-strain characterization of MSM elements inside the assembled energy harvester prototype was performed prior to harvesting tests and is shown on Figure 2.

Vibration Control of Large Civil Engineering Structures (Review)

A. Preumont, Université Libre de Bruxelles, Brussels, Belgium

Abstract:
Large civil engineering structures are sensitive to vibrations due to various excitations sources such as earthquakes, wind, traffic or pedestrians. These vibrations may induce a catastrophic failure of the structure as in the case of earthquake or flutter instability (e.g. Takoma bridge), or they can affect the comfort of the occupants (e.g. wind induced sway of high rise buildings). They may result from a fairly complicated interaction between the structural motion and its environment which necessitates multiphysics tools for their analysis (e.g. in flutter, the structural vibration is the source of unsteady aerodynamic forces). In other cases, they result from the nonlinear behaviour of the structure itself (e.g. parametric excitation of stay cables due to the deck motion of cable-stayed bridges). In some circumstances, pedestrian bridges may be subjected to the phenomenon of synchronization according to which the bridge motion induces the crowd marching on the bridge to synchronize their steps (it was the case in the Millenium bridge in London on the inauguration day). Large bridges are often more sensitive during the construction phase. As the structures tend to become ever larger with time and metallic structures have very little damping, vibration phenomena tend to become more and more important and necessitate special engineering devices to mitigate them and reduce the resonance peaks. Because of their size and the requirements in terms of reliability and serviceability, the actuators play a critical role in the active control loop. This paper reviews various vibration mechanisms and various vibration control devices which have been used successfully (mostly in the Far-East), and explores some new applications where vibration control could be applied successfully.

Keywords:

Unfortunately, the final manuscript has not been received by the printing date. Please contact the author for additional information.

Actuator Concepts for Active Vibration Control

M. Werhahn, R. Genderjahn, H.-J. Karkosch, P.M. Marienfeld
ContiTech Vibration Control GmbH, Hannover, Germany

Abstract:
Even though active vibration control systems can especially offer a wide range of benefits for passenger cars, they are not yet widespread in the automotive industry. With this in mind, an overview of commonly used actuator types is given and specific requirements of the automotive industry are discussed. It then goes on with the introduction of a newly designed, linear electromagnetic actuator, which is particularly suited for the use in active engine mounts. To demonstrate the effectiveness of an implemented solution vehicle test results are presented.

Keywords: Active Vibration Control, Linear Reluctance Actuator, High Frequency Applications, Active Engine Mounts, LINAK

Introduction

Consumers are becoming more environmentally aware, global reserves of raw materials are dwindling, and the legislature is intensifying pressure on automotive manufacturers to reduce fleet emissions. OEMs are amplifying their efforts to develop efficient, low-emission engines accordingly. These include high compression gasoline or diesel engines in combination with hybrid drives, engines with cylinder deactivation, or engines with only two or three cylinders. As a matter of principle, all of these approaches lead to an overall increased level of vibration and/or a wider excitation frequency range. At the same time, lightweight vehicle design is being advanced in order to reduce consumption and, for example, to compensate for the weight of the growing number of assistance and comfort systems. However, lightweight constructions tend to increase vehicles' susceptibility to vibrations and thus have a negative effect on the NVH behavior in the vehicle interior. Seeing as, over the years, customers' comfort requirements have steadily increased, there is a pressing need to resolve the growing tensions between comfort, efficiency, and lightweight design [1].

Systems for active vibration control (AVC) can intervene and resolve these conflicts of objectives. Active engine mounts or absorbers, which work across a wide frequency range and can therefore be effective across almost the entire speed range of the engine, are particularly suitable. They are used to minimize and/or selectively influence the transmission characteristics of structure-borne noise between engine and chassis.

This article will focus on the actuator technology for active hydromounts and its effects on the design process of the AVC-system. The demands on active hydromounts will be explained and, with the help of a simplified mathematical replacement model, the conflict between active and passive mount performance will be illustrated. An actuator optimized in this way and measurement results used to demonstrate the effectiveness of a system with broadband capabilities will be presented.

How an active engine mount works

Alongside road and airflow excitations, vibrations caused by the engine represent a main source of air-borne and structure-borne noise in the vehicle interior. This noise is generally experienced as disruptive by passengers and contributes significantly to the perception of worth. Seeing as the engine mount is the primary transmission path from the engine to the interior, the active regulation of this interface creates huge potential for improving the driving experience [2].

In a conventional engine mount, the main rubber spring bears the engine's static load. Here, the elasticity of the rubber results in the partial isolation of the high-frequency engine excitations from the chassis, while the low-frequency engine vibrations are damped by the flow of fluid in the hydraulic channel. Both effects are influenced by the mainspring stiffness in contradictory ways and lead to a conflict of objectives. Thanks to the principle of the active engine mounting system, the structure-borne noise fed from the engine into the chassis can be reduced to a minimum, while the passive mount characteristics are largely retained. On the one hand, active absorbers near the engine mount can be used to generate counterforces to the engine excitations. On the other hand, actuator technology can be integrated in the engine mount in order to tune the engine mount to a lower dynamic stiffness rate for particular frequency ranges and operating states, and thus to isolate the engine excitation from the chassis. This article concentrates on the latter method. This consists of one or two active mounts, each with a sensor on the chassis side and an electronic control unit (ECU) with an integrated amplifier. The engine

An Efficient and Optimal Moving Magnet Actuator for Active Vibration Control

G. Loussert, Moving Magnet Technologies S.A, Besançon, France

Abstract:
The need for fuel economy and emission restriction has led OEMs to put emphasis on different strategies which allow effective improvements in that field (engine downsizing, cylinder deactivation …). These new applications imply significant vibration increase, created by the engine and transmitted to the chassis and the vehicle interior, such that their cancellation is a key topic for the automotive industry. The use of active engine mounts, acting directly on the fluid of the hydromount, or active absorber, acting as an inertial mass-spring system, are very effective solutions, particularly when using actuators working on electromagnetic principles. Nevertheless, when it comes to concrete solutions, the choice of such actuators must be considered, taking into account the full performances and overall cost of the solutions. This paper deals with the presentation of an electromagnetic actuator, up to a realistic demonstration stage, showing that it can be considered as the most convenient solution, particularly by saving several tens of grams of magnets compared to the electrodynamic ones currently proposed by automotive suppliers.

Keywords: NVH, Vibration Cancellation, Electromagnetic Actuator, Demonstrator, Transfer Function

Introduction

The need for fuel economy and emission restriction have led OEMs to put emphasis on different strategies which allow effective improvements in that field, such as engine downsizing, cylinder deactivation, start/stop system or hybridization (Fig.1). As a consequence, these new applications imply significant changes on noise, vibration and harshness (NVH) occurrences. Particularly, several unwanted vibrations appear, created by the engine and transmitted to the chassis and the vehicle interior, such that their cancellation has been a key topic for the automotive industry [1].

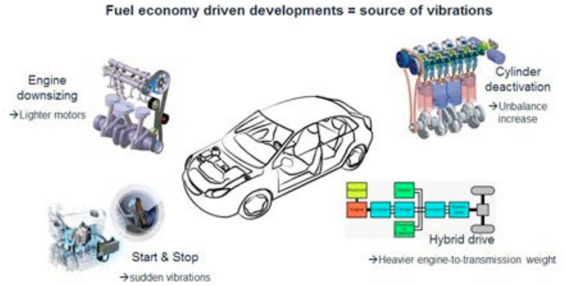

Fig. 1: *Fuel economy driven developments are sources of NVH*

As it was relevantly studied in the recent past [2], the use of active engine mounts [3], acting directly on the fluid of the hydromount, or active absorber, acting as an inertial mass-spring system, are very effective solutions, particularly when using actuators working on general electromagnetic principles.
Nevertheless, when it comes to concrete solutions, the choice of such actuators must be considered, taking into account the full performances and overall cost of the solutions.

This paper deals with the presentation of an electromagnetic actuator, showing that it can be considered as the most convenient solution, particularly by saving several tens of grams of magnets compared to the electrodynamic ones currently proposed by some automotive market leaders [4], [5].

Comparison between moving magnet and moving coil actuators

Because of their intrinsic principle, electrodynamic and electromagnetic actuators, even though working on the same magnetic equations, have different magnetic flux paths (Fig. 2) that lead to various designs with inherent benefits. As for example, the first cited depicts better dynamics ability thanks to a low inductance and a low electrical time constant, while the second cited implies a better coil thermal dissipation and a generally higher force constant per magnet mass.
In the particular application of active vibration control, and although high current dynamic is requested, it can be shown that electromagnetic actuators with moving magnet can be considered as a best solution in order to save tens of grams of magnet, keeping high dynamic ability within realistic specifications.

Compact, Efficient and Controllable Moving Iron Actuation Chain for Industrial Application

P. Meneroud, C. Bouchet, A. Pages
Cedrat Technologies SA, Meylan, France

Abstract:

In the field of aeronautics, some parts of aircraft engines are tricky and costly to manufacture. In the low pressure turbine very thin pieces obtained by turning require a complex support. The R&D work performed here aims at improving the manufacturing process through the reduction of vibrations and active modification of the clamping conditions. For that purpose, Cedrat Technologies has designed a new innovative **M**oving **I**ron **C**ontrollable **A**ctuator (MICA), which is embedded on the work-piece support. In the first part, the application goals and the main particularities of the developed MICA200M magnetic actuator are presented. To be easily driven in closed loop, the force is designed to be linear with the current and independent from the interface position. The MICA200M stroke is ±2.5mm and its force constant reaches 11.6N/A for a current range of ±15A in steady state. The nominal force of 174N for only 1 dm^3 size and 3.2kg facilitates the integration and allows acceleration up to 132G in transient operation thanks to reduced 0.25kg mobile mass. In the second part, results of complete experimental characterisation are detailed. Finally, a comparison analysis is done with COTS voice coil actuators and the article concludes with the benefits of the MICA200M.

Keywords: Actuator, Magnetic, MICA, Moving Iron, High Bandwidth, Current Switching Amplifier

Introduction

The ICT FP7 European project INTEFIX requires a high dynamics linear actuator suitable for anti-vibration applications like chatter reduction for the turning of thin work-pieces [1] for example the turbine casing. In the frame of this project, Cedrat Technologies has designed a new innovative Moving Iron Controllable Actuator (MICA). This paper presents in the first part the application goals and the main particularities of MICA200M magnetic actuator. Then, results of complete experimental characterisation are detailed. Finally, a comparison analysis is done with existing voice coil actuators and the article concludes on the benefits of the MICA200M.

Intefix project and actuation needs

The INTEFIX project aims at improving the machining of thin work-pieces thanks to the use of INTElligent FIXtures which includes the reduction of vibration, the compensation of constraints relaxation and the accurate positioning of work-pieces. The study case described here concerns the turning of the low pressure turbine casing (see Fig. 1). The objective is to improve the manufacturing process during finish turning, through the reduction of vibrations and active modification of the clamping conditions. Modifications performed on the current fixture include the integration of active vibration damping to reduce the vibrations during machining and the integration of active actuators to produce an active controlled deformation on the work-piece in order to improve the clamping conditions (see Fig. 2).
The requirements of both types of actuation are different. Vibration reduction requires large bandwidth actuation whereas the production of active controlled deformations requires significant stroke. Additionally, both need large forces and a compact profile as they are embedded actuations. Both functionalities are fulfilled with the MICA200M actuator.

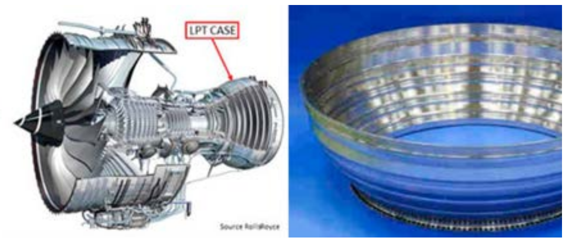

Fig. 1: *Turbine casing work-piece*

Fig. 2: *MICA integrated in turning support*

Principle of MICA actuator

MICA actuator, which is a patented technology of linear magnetic actuator, whose particular characteristic is its high and controllable force on an iron mobile part. The actuator force is proportional

An Adaptive Negative Capacitance Shunt Network for Increasing Performance and Robustness in Terms of Noise and Vibration Attenuation

M. Pohl, H.P. Monner
Deutsches Zentrum für Luft- und Raumfahrt (DLR), Braunschweig, Germany

Abstract:
Due to its broadband performance, the negative capacitance shunt can be used for damping multimode systems with varying eigenfrequencies. They are usually built with operational amplifiers and passive components. This setup is sufficient for laboratory tests, but in real applications, this rather simple setup cannot be used, due to a tradeoff between efficient damping and the risk of instability. Therefore an adaptive negative capacitance circuit is presented in this paper, which is developed for automatically tuning the capacitance ratio to the appropriate value. Tests at a beam structure show, that both better damping and the avoidance of saturation effects and instabilities are achieved.

Keywords: Negative Capacitance, Piezoelectric Shunt Damping, Noise and Vibration Attenuation

Introduction

For ecologic sustainability and decreasing reserves of fossil energy sources, fuel efficiency is a major concern especially for passenger aircraft. Therefore, lightweight structures made from carbon fiber reinforced plastics offer a great potential. But when used for panel-like structures, they have the disadvantage of a lower damping and a lower coincidence frequency compared to conventional differential metal constructions. Both aspects lead to an increased vibration level and by this to a higher sound radiation. Because of this, special noise and vibration treatments are needed to ensure passenger cabin comfort. Besides passive damping and active structural acoustics control (ASAC), piezoelectric shunt damping is investigated.

Piezoelectric shunt damping

Piezoelectric shunt damping subsumes all concepts, where an oscillating structure is damped with applied piezoelectric actuators connected to electric shunt networks. The basic principle can be seen in *Fig. 1*, in which the external electrical impedance Z_1 is connected to the electrodes of the piezoelectric transducer. In order to ensure proper damping, the shunt network has to fulfil two tasks. Firstly it has to dissipate the vibration energy and secondly it has to match the impedances between the electric system, the piezoelectric transducer and the mechanical structure to maximize the energy flow from the mechanical to the electrical system. Therefore, several concepts are known from the literature, such as passive resonant shunts [1], [2], [3] for one or multiple modes, switching shunts [4], [5] or the semi-active negative capacitance circuit. Due to its broadband performance, the negative capacitance shunt can be used for multimode systems with varying eigenfrequencies [6], [7].

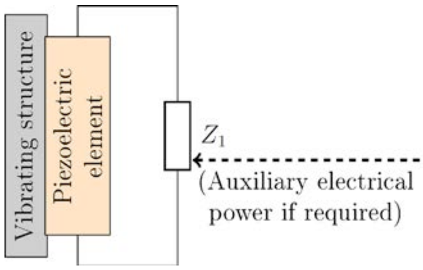

Fig. 1: *Working principle of shunt damping*

The basic concept of the negative capacitance can be seen in *Fig. 2*. An external impedance C_{neg} is used in this case, which acts like a capacitance, but with opposite sign, so that the inherent capacitance of the piezoelectric transducer C_{PZT} is compensated.

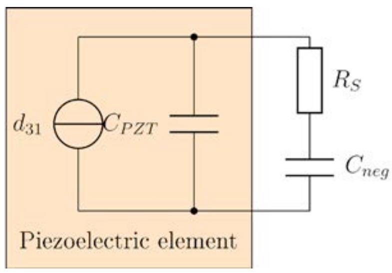

Fig. 2: *Serial negative capacitance shunt*

Hereby, the power transfer from the mechanical system is increased. This transferred energy is then dissipated at the resistor R_S shown in *Fig. 2*.

Negative capacitances can only be created by active circuits. Therefore, usually negative impedance converters are used as shown in [8]. The basic circuit of a negative capacitance shunt with all currents and voltages can be seen in *Fig. 3*. There

Adaptive Dynamic Absorber for Wideband Micro-Vibration Control Based on Precision Self-Positioning Linear Actuator

X. Wang, B. Yang
Shanghai Jiao Tong University, Shanghai, China

Abstract:
Micro-vibration suppression for variable excited frequency in wideband is a tough challenge in vibration control field. This paper presents an adaptive vibration dynamic absorber (ADVA) based on precision self-positioning via driving linear actuators to meet the challenge. This ADVA is applied to suppress micro-vibration in a wideband range. When a harmonic external force with variable frequency is detected, the ADVA can adjust its natural frequency to create an anti-resonance for vibration suppression of primary system. In order to achieve the wideband micro-vibration control, a precision self-positioning inchworm linear actuator combined with a beam are presented, with the self-positioning and driving motion of the actuator, the stiffness of ADVA can be tuned on-line to match the absorber natural frequency with the frequency of external excitations. An inchworm linear actuator/linear motor is designed to realize the scheme of tunable stiffness. Theoretically, when the beam is long and thick enough, the ADVA can achieve the vibration suppression in arbitrary range. Based on this point, the AVDA is proposed in this paper.

1. Introduction

Dynamic vibration absorber (DVA) is widely used to suppress the vibration of a system excited by harmonic disturbance. Theoretically, when the natural frequency of the DVA is tuned properly to equal to the exciting frequency, the vibration of the primary system can be completely neutralized. But the vibration may increase significantly with the variation of the exciting frequency. In order to broaden the effective frequency range, the adaptive dynamic vibration absorber (ADVA) is developed to make the DVA’s natural frequency tunable online. The ADVA belongs to semi-active vibration control, it means less power is consumed when ADVA works. No power is consumed after the tuning progress, in other words, the ADVA is more reliable.
The methods of vibration control can be classified as passive, active and semi-active [1]. DVA is a typical passive device used to suppress the vibration excited by harmonic disturbance, however the vibration of the primary system may increase when the exciting frequency shifts [2]. Active control method can adapt characteristics and parameters of the absorber with the variation of exciting force, the active vibration absorber is mathematically equivalent to DVA, and its stiffness, interia and damping coefficient are tunable online [3], but this active control method it not reliable because it works and consumes power all the time. Semi-active method is easily to achieve the adjustment of stiffness or damping value by get the feedback signal from the response. A flexible cantilever beam attached with a mass is used to develop the ADVA, the stiffness of the beam varies with the effective length of the beam changes [4]. Similar to the cantilever beam ADVA in [4], an absorber with circular cross-section beam is used to compare two tuning algrithms [5]. An electromagnetic ADVA is presented in [6], it consists of a clamped-clamped beam and a permanent magnet which embedded in the center of the beam, the electromagnet force produced between the C-shaped electromagnetic coil and permanent magnet, the stiffness changes when the current in the coil is adjusted. Vibration absorber that uses piezoelectric element combined with a resonant electrical circuit can be tuned to the required frequency, the stiffness of the absorber is adjusted electrically, another feature of the piezoelectric material is the ability to use the piezoelectric elements as sensors in DVA [7-10]. Shape memory alloy can be used as a variable stiffness element, the Young’s modulus of the element is changed by adjusting the temperature of the alloy by passing an electrical current through it, thus it results in the changing of the natural frequency [11-13]. Magneto-rheological fluid is used to achieve stiffness changing, and the shear stiffness of the fluid is adjusted by changing permanent magnets or electromagnet to change the magnetic field applied to the fluid [14-17].
This paper presents an ADVA based on inchworm linear motor, the natural frequency of the ADVA varies when the inchworm actuator moves on the beam, the vibration of the primary system will be suppressed when the natural frequency of ADVA equals to the exciting frequency. To tune the natural frequency precisely, the analytical model of the variable natural frequency of the ADVA is proposed. Optimal design based on the analytical model is

Review on Embedded Sensors and Actuators for Gentle Insertion of Cochlear Implants (Review)

L.A. Kahrs, Leibniz Universität Hannover, Hannover, Germany

Abstract:
Cochlear implants are the actual treatment of choice for severe hearing loss and profound deafness. One part of the surgical procedure is the insertion of the electrode array into the cochlea; more precise into one of its compartments: the scala tympani. The sheath of the electrodes is made from silicone rubber, has a diameter of approx. one millimeter and an inserted length of approx. 25 mm. Insertion of this array is done by pushing gently until roughly one or one and a half turn (360°-540°) of the cochlea is reached. To monitor the insertion procedure and to avoid potential failures during this process (e.g. buckling, tip fold over, rupture of the basilar membrane) research is undertaken. This contribution gives an overview of actual developments towards embedded sensors and actuators into the electrode array.

Keywords: Wires, SMA, Hydrogel, Fluidic, Magnetic Actuation, Proximity, Contact, Optical Sensing

Introduction

For electrode arrays of cochlear implants, neither embedded sensors nor advanced embedded (mechanical) actuators are used in clinical routine to support a gentle and non-invasive insertion. The so-called stylet is a common basic actuator: A platinum wire is used to initially straighten the pre-bent shape of the silicone-based electrode array. By pulling out the wire, the electrode array curls around the modiolus. The actuation is achieved by linear motion, releasing the strain energy and causing the electrode return into its curled shape. During the procedure, the surgeon performs the insertion of the electrode array into the cochlea manually by simultaneously pulling the stylet and pushing the electrode array into the cochlea. Several research groups are performing investigations on insertion tools to support this push-pull-process by means of external actuation, either mechanically or by mechatronic systems [1,2]. Another mean to control the insertion of the electrode array is intraoperative medical imaging, which has been proposed clinically by applying fluoroscopy [3]. However, the aforementioned means are exclusively external. In this review, the focus lies on embedded sensors and actuators supporting the insertion process. Here, the term ‘embedded’ refers to utilization of existing structures of the electrode array as well as integration of parts inside the silicone sheath.
The cochlea with its small sized shape and even smaller inner lumen is an extremely delicate structure which makes it challenging to perform non-traumatic surgery (see Fig. 1). Only expert surgeons have high success rates in gentle and non-invasive insertion of the electrode array into the cochlea. The (simplified) two-chamber compartment of the inner lumen which curls around the modiolus is divided by a membrane, which should stay intact during insertion to guarantee the best outcome for patients with residual hearing. This so-called basilar membrane is reported to be

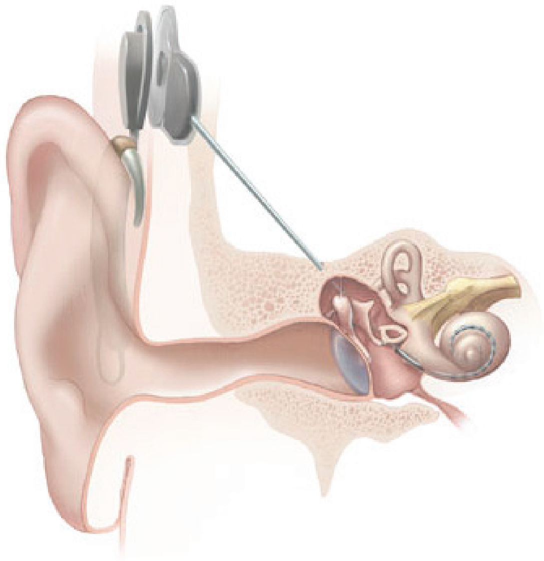

Fig. 1: *Cochlear implant. Sound signals from a microphone are transmitted to an array of electrodes placed within the cochlea to stimulate the acoustic nerve and thus restore the sense of sound.*

ruptured in most of the cases when problems during the insertion of the electrode occur. Furthermore, other failures like buckling and tip fold over, that may arise from friction inside the cochlea, often result in rupturing the membrane. The literature reports on rupture forces of the basilar membrane between 42 mN and 122 mN, depending on analysed specimen [4]. Insertion forces (as accumulated friction force) during insertion of the electrode array inside the cochlea were determined as well [5]. Thus, the overall aim of incorporating sensors and actuators into the electrode array is to control the insertion process by keeping forces under those critical thresh-

Micro-Hydraulic Drives with Integrated Displacement Sensor for Medical Application

L.M. Comella, K. Ayvazov, R. Kessel, T. Cuntz, A. van Poelgeest
Fraunhofer IPA, Mannheim, Germany

Abstract:
Laparoscopic procedures are becoming increasingly popular in modern medicine, because of the advantages that they provide to the patient. However, this type of procedures are more complicated for the surgeons, who have to operate in small spaces losing dexterity. In order to overcome these difficulties, new and more performant instruments have been developed, actuated with hydraulic force transmission.
Their success in this field is due to their high force and power density. However, they are often subject to leakage, which can lead to undesired movement of the instrument tip. Unwanted movements of the tip represent a danger for the patient, and therefore must be avoided.
The patient safety can be guaranteed by continuously monitoring the instrument's tip position, but because of the drives small dimensions this is not feasible with an off-the-shelf sensor. For this reason, a compact sensor has been developed which uses the actuator itself as a sensor, using it as a two cylindrical parallel plate capacitor, the plates of which are the rod and the barrel.

Keywords: Actuators, Capacitive Sensing, Displacement Measurement, Electro-Hydraulics

Introduction

High force and power density make piston-cylinder fluidic actuators ideal for integration into micro robots [1] and medical instruments.
An example of their application is instruments for minimally invasive surgery, such as laparoscopy [2] and also more advanced techniques: Single-Port-Surgery [3] and Natural Orifice Transluminal Endoscopic Surgery (NOTES) [4].
The reasons for the success of these techniques are the benefits that they provide to the patient: short recovery time, and less pain and haemorrhaging. These benefits are mainly due to the small incisions necessary for the procedures.
Although, the patients benefit from these surgical techniques, the surgeons do not. They lose dexterity, working volume as the procedures often require more time to complete.
Technology is the solution to overcome those difficulties [3] and to continue the development of minimally invasive surgery techniques, which in return improves and speeds up the patient recovery.
Minimally invasive surgical instruments are improved by the use of hydraulic drives. Equipped with these actuators, the instruments can be handled more precisely and can apply higher forces [5] [6]. Force which is even higher as, because of their small size, these drives can be integrated directly on the tip of the instruments.
The main disadvantage of this technology is its tendency to leak, which results in unwanted movement of the instrument, dangerous for the patient. The precise control on the instrument tip position is of great importance for medical applications as the patients' safety is essential. Therefore the actuators must be equipped with an appropriate position sensing system.
Given the typical instrument design and the actuator dimensions, an off-the-shelf linear displacement sensor cannot be used. Hence, a sensor had to be developed which is accurate and compact enough to be used with actuators where the size is a critical parameter. The proposed solution uses the parallel cylindrical plate capacitance principle to measure the actuators displacement. The hydraulic cylinder itself acts as a cylindrical capacitor, the electrodes of which are the barrel and the rod. The measurement principle is based on the fact that the capacitive value in parallel cylindrical plate capacitor is proportional to the length of the inner electrode overlapped by the external one. Thus a variation of this length can be measured in terms of changes in the capacitance value. The movement of the piston results in variation of the rod length inside the barrel and consequently the measurement of the capacitance can be interpreted as the piston's position.
The result is that the integration of an external sensor is not required to measure the displacement. The sensor is part of the drive itself and a position change of the piston can be measured in terms of capacitance variation.
Compared to already existing sensor solutions [7] [8] the proposed sensing method is more easily integrable and does not require additional external components to be added to the hydraulic cylinder design.

A Variable Impedance Actuator Based on Shape Memory Alloy

L. Manfredi, F.L. Velsink, H. Khan, A. Cuschieri
University of Dundee, Dundee, United Kingdom

Abstract:
Surgical robotic design is challenging mostly because of the restricted working space of the platform necessitating miniaturized actuators and sensors. Compliance is a fundamental requirement of an actuator design for safe atraumatic clinical interaction of the robot with organs and tissues [1]. In the present paper, the authors describe a variable impedance miniaturised rotary actuator (VIMRA) using shape memory alloy (SMA) wires in antagonist configuration, to achieve a high force to weight ratio. The two SMA wires are connected to a pulley providing two forces, which can be independently controlled to adjust the joint stiffness.

Keywords: Smart Materials, Variable Stiffness Actuator, Robotic

Introduction

Several designs have been proposed for surgical robots [2]-[3]. Most however, employ cable transmission with location of the actuators outside of the robot [7]-[9]. The advantage of this approach is to reduce the size of the robot, keeping both weight and inertia low. The disadvantage of this design is that the number of cables needed increases with the number of joints, which limits the degree of freedoms (DoFs) of the robot. An alternative design solution consists of using actuators embedded in the body of the robot, but this requires use of small and light actuators. Shape memory alloys (SMAs) are materials that can provide a solution to this miniaturization issue in view of their light weight and high force to weight ratio. The main disadvantage of SMAs is their low energy efficiency, which ranges from 5 to 7% [10]. SMA shaped as a wire, can only be contracted and extended by 7% of their total length. This imposes a limitation for the length of the joint in order to achieve a wide range of motion. Several reports have proposed control the output torque by use of SMA wires in antagonistic configuration using different design solutions [11]. Force sensors connected in series to the SMA have been used to control the output torque [12], as this can limit the overall size and weight of a miniaturised actuator.
Another challenge in robotic surgery is a soft interaction with the environment, which can be satisfied by appropriately compliant actuators, where the required position can be changed by applying an external force. In a variable impedance actuator (VIA), the compliance can be adjusted. Compliance is crucial for safety, to ensure that the robot does not harm adjacent tissues and organs. At the same time, the manipulator must be stiff enough to perform the component tasks of surgical operations. VIAs provide a solution for these conflicting requirements [13].

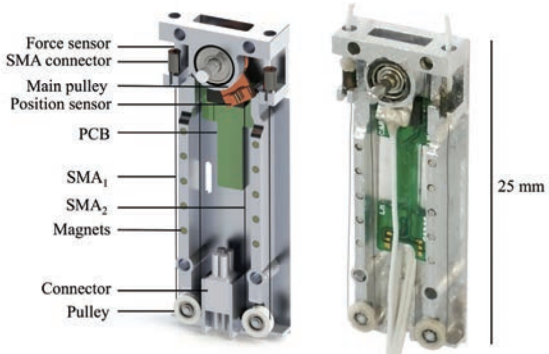

Fig. 1: *Actuator design using SMA wires in antagonistic configuration. Force and position sensors are used to control the stiffness of the actuator and an electronic on-board electronics to measure the main pulley's angle. The overall size is 25 x 9 x 3.5mm*

To achieve both a compliant behaviour and a compact design, we propose a miniaturised variable impedance rotary actuator (VIMRA) based on SMA wire in antagonistic configuration by using miniaturised pulleys to reduce the overall length (Figure 1). The adopted antagonistic configuration, SMA wire vs. SMA wire, reduced the energy consumption needed to achieve a high maximal output torque. The two SMA wires are controlled independently, thereby achieving a compliant behaviour with changing the actuator stiffness by regulating the force provided by the opposing SMA wires.

Methods

The proposed design (Figure 1) consists of three parts: a) a frame, b) a sensory system which includes an analogue position sensor and two force sensors, c) an electronic system to control both the position and the stiffness of the joint. To reduce the friction of the system, each pulley has a miniaturized ball bearing. The frame itself was designed to work as a force sensor by incorporating

Piezoelectric Hydrocephalus Shunt Valve – Design and First Evaluation Results

P.P. Pott, G. Allevato, M. Bartenschlager, J. Butz, P. Schmitt, H.F. Schlaak
Technische Universität Darmstadt, Darmstadt, Germany

Abstract:
Excess production and / or impeded drain of *Liquor Cerebrospinalis* can lead to increased intracranial pressure (ICP) resulting in pain and severe damage to the brain. A possible therapy is the use of shunt valves that control the drain of the liquor to the abdominal cavity. Conventional valves distinguish between supine and standing position and use pre-defined default pressure values. In advanced systems, the pressure can be defined from outside the cranium using external programming devices. However, default pressure changes during daytime activity cannot be considered eventually leading to headache and dizziness. A user-programmable mechatronic valve would be advantageous to overcome these limitations.
Requirements concerning size, pressure range, electromagnetic compatibility, robustness against external acceleration, and power consumption have to be met. Above all, safety has to be ensured at all times by providing a fail-safe state in case of malfunction and power shortage.
To meet these requirements, a system consisting of a conventional spring-loaded ball-in-cone valve and a piezoelectric bending actuator is proposed. Here, the actuator is used to raise the preload of the spring above the fail safe level. To maintain a certain preload with the piezoelectric actuator, only charge losses have to be delivered by the energy source. The internal electronics are based on a new integrated circuit charge pump to alter the battery voltage to meet the voltage requirements of the piezo element while avoiding any inductance.
First evaluation shows that the opening pressure can be controlled with 6 bit. Biocompatibility as well as compatibility with an MR environment can be derived by making the housing from PEEK and by using glass for the valve ball and PEEK springs.

Keywords: Shunt Valve, Piezoelectric Actuation, MR Compatibility

Introduction

Intracranial pressure (ICP) is the pressure of the cerebral fluid (*Liquor Cerebrospinalis*) surrounding the brain and the spinal cord. This fluid is built up and resorbed constantly. In supine position the pressure is normally within a range of 7 to 15 mmHg (930-2000 Pa) [1]. Intracranial hypertension can be caused by excess production or impeded drain of the *Liquor Cerebrospinalis*. In case the pressure is constantly above 20 mmHg (2.7 kPa) medical treatment is indicated [2]. Increased ICP leads to headache, nausea, loss of consciousness, back pain, papilledema, and ocular palsies. One possible treatment is the implantation of a shunt system consisting of a catheter leading from a ventricle to the abdomen while the flow and pressure in the catheter are controlled by a shunt valve (*Fig. 1*). The valve is implanted below the skin and cannot be accessed directly. Modern systems thus can be adjusted using external programming devices and magnetic forces (e.g. [3, 4]). As the actual set point of the ICP changes within the range of a few mmHg during daytime activity, an adjustable valve would be desirable. However, the static pressure difference between standing and supine position (refer to *Fig. 1*) sums up to ~50 cm water column (~4.9 kPa) has to be accounted for to avoid excess drainage in standing position. This is usually achieved by a so-called gravity unit or valve that determines the orientation of the patient within earth's gravitational field.

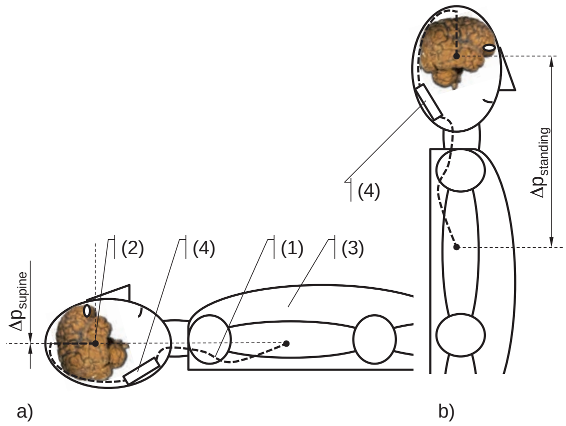

Fig. 1: *Intracranial Pressure (ICP) is the pressure of the cerebral fluid. In case of dysfunctional drainage or excess production, the pressure can rise above a healthy level. To regulate drainage, a catheter (1) leading from the ventricle (2) to the abdomen (3) and incorporating an shunt valve (4) can be implanted that controls ICP and considers different static pressure in supine (a) and standing (b) position.*

A Hybrid Stimulation Device for Providing Sensory Feedback

H. Huang, Berner Fachhochschule, Biel, Switzerland, and
Ecole Polytechnique Fédérale de Lausanne, Neuchâtel, Switzerland
T. Li, V.M. Koch
Berner Fachhochschule, Biel, Switzerland

Abstract:
Providing sensory feedback is important for active upper limb prosthesis users. It cannot only improve the functionality of the prosthesis, but also introduce an embodiment feeling to the amputee, thus increasing the acceptance of the active prosthesis. One of the major challenges of providing sensory feedback is to increase the haptic vocabulary and improve the localization and intensity identification performance. To address the two points, a hybrid stimulation device is designed incorporating mechanotactile and vibrotactile modalities into a single device. A stimulation array of 5 designed hybrid devices was tested on two amputee subjects. The results have shown that in most cases, the hybrid stimulation device could improve both the localization and intensity identification performance at the same time could also reduce mental load.

Keywords: Sensory Feedback, Mechanotactile, Vibrotactile

Introduction

Hand amputation is a traumatic event that brings a lot of inconvenience in everyday life. There are around three million hand amputees all over the world. During the last decades, the dexterity of active prosthesis has made significant progress. However, there is still no or only limited sensory feedback in the commercial prosthesis. To our knowledge, the only commercial prosthesis equipped with sensory feedback is the Vincent Hand Evolution (Vincent System GmbH, Germany). But it has only one vibrator, providing limited information. A survey done by Biddiss *et al.* has shown the importance of providing sensory feedback for active prosthesis users, because providing sensory feedback can not only provide more information regarding the grasping force, but also introduce embodiment feeling to the prosthetic users [1].

During the last decades, some research has focused on providing sensory feedback to active prosthetic users. There are mainly two methods: the invasive one and the non-invasive one. The invasive methods directly stimulate the central [2] or peripheral nerve system [3-5] using cortical electrodes. Non-invasive sensory feedbacks apply stimulation on the skin surface. The three commonly used non-invasive sensory feedback modalities are mechanotactile (static pressure or low-frequency tapping) [6, 7], vibrotactile (high frequency vertical or horizontal vibration) [8, 9], and electrotactile (electrical current) [10, 11]. The invasive sensory feedback method involves implants, thus it is neither widely accepted nor available. Most of previous research on non-invasive sensory feedback has used only one modality and/or one actuator per finger, providing mainly only the grasping force information [12].

Electrotactile was used by many researchers for sensory feedback because of their lightweight and small sizes [13-16]. However, electrotactile can invoke uncomfortable even painful feelings. Its interference with electromyographic (EMG) signal is also a major drawback.

Mechanotactile stimulation applies a normal force to the skin. Previous researchers have applied mechanotactile stimulation both on healthy subjects (on the forearm [17] and the toes [18]) and amputees (reinnervated chest area [19] or residual limb [20]). The commonly used devices include motor-driven pushers, voice coil DC linear actuator, DC motor, and servo motors.

Vibrotactile stimulation normally involves stimulation frequency between 10 to 500 Hz [12]. This stimulation modality has been used for providing grasp force feedback by many researchers [21-23]. The two commonly used ones are linear resonant actuators (LRA) and eccentric rotating mass (ERM). For LRAs, the frequency is normally fixed. ERM can

There are four types of mechanoreceptors in human skin: Pacinian corpuscles, Meissner's corpuscles, Merkel's discs, and Ruffini endings [24]. Among the four, Meissner's corpuscles are responsible for static force. Its response frequency ranges from 0 to 10 Hz. Pacinian corpuscles are responsible for high frequency vibration perception. Its frequency response ranges from 100 to 300 Hz. Some research

Haptic Feedback: From Force-Reflecting Robots to Tactile Interfaces (Invited Review)

M. Wiertlewski
Aix-Marseille Université, CNRS, ISM UMR 7287, Marseille, France

Abstract:
During the last century, technical means of broadcasting sounds and pictures came into existence. And today, many scientific and industrial efforts are being made to develop means of broadcasting tactile and haptic sensations. This review covers the latest technological systems and smart actuators used to stimulate the sense of touch and deliver programmable haptic sensations.

Keywords: Haptics, Tactile Feedback, Vibrotactile, Actuators, Surface Haptics

Introduction

More than a decade ago, Hayward et al. observed that before computers became a common workplace fixture, most human tasks used to involve fine sensory-motor skills, whereas little use has been made so far of the sense of touch in human-computer interactions [1]. Haptic interfaces restore the tangibility of the interface with a computer and are beginning to transit from the laboratory to the industrial world in the context of concrete applications such as virtual reality, gaming and wearable electronics.

However, most human-computer interfaces are still devoid of tactile and haptic feedback and their performances therefore fall far short of our exquisitely complex human sensorimotor skills. Whenever we use a keyboard, mouse, or touchscreen to interact with a machine, the mechanical cues that we perceive are not in the least interactive. The resistance of a click will be identical, whether or not the virtual button has been disabled, and the frictional drag of the user's finger on the touchscreen will not reflect the shapes conveyed by a visual display.

Haptic interfaces bridge this gap by providing bi-directional interactions in which the user can touch the artificial environment and the computer will respond by providing tactile and/or kinesthetic feedback. The force levels fed back to the user can be correlated with the displacement, velocity and acceleration of a limb and generate realistic dynamic environments that have elastic, viscous or inertial properties.

Human sensory-motor abilities

Haptic interfaces strive to mimick the mechanical interactions occurring in the real world. Actions such as pushing an object, sensing the texture of a fabric and handling a cup generate forces that vary in time and space. The effects of these forces on the muscles contribute to our kinesthetic perception of the environment and the deformation of the skin, which also occurs in the vicinity of the contact between the body, and an object constitutes the basis of tactile (cutaneous) perception.

The somatosensory system combines these mechanical stimuli along with the motor commands to create a haptic representation of the surroundings, Perception of friction, stiffness, curvature and other attributes of held objects play a central role in planning fine motor actions. Because the properties of the contact often cannot be assessed visually –for instance because vision is occluded by the hand– tactile cues are absolutely necessary for guiding movement.

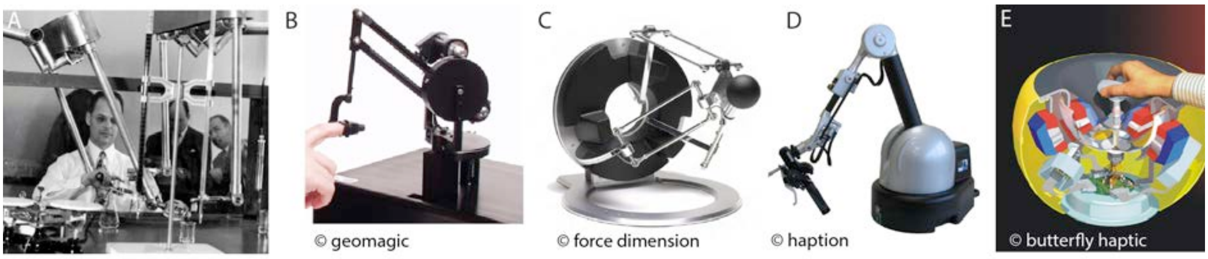

Fig. 1: *A. First teleoperation apparatus [5]. B. The PHANToM, one of the first commercial haptic interfaces to be developed [7]. C. Parallel robots with greater stiffness and a wider frequency bandwidth. D. Serial implementation for larger workspaces. E. Magnetic levitation replaces linkages and effectively removes friction.*

Design of Haptic Master Featuring Improved MR Brakes

H.G. Gang, J.W. Sohn
Kumoh National Institute of Technology, Gumi-si, South Korea

Abstract:
In this paper, a new design of haptic master featuring lightweight and low inertia configuration is proposed and its performance is evaluated experimentally. To reduce the weight and inertia of the master device, aluminium frame is designed and four haptic actuators for 3-DOF rotational motion and 1-DOF gripper motion are installed to the frame. Magneto-rheological (MR) brake, which has large braking torque with small size and lightweight, is suggested as an actuator to generate haptic feedback force. For the MR brake, dual magnetic core type is adopted to obtain large braking torque under limited size and weight. The braking torque of the proposed MR brake is evaluated experimentally according to applied input currents. After designing control algorithm, torque tracking control performance of the actuator is also investigated for desired sinusoidal input. By constructing the proposed haptic master device, the suitability of practical workspace is also evaluated by compared with that of free human wrist motion.

Keywords: Haptic Master, Magneto-Rheological Fluid, MR Brake, Tracking Control

Introduction

Recently, since the robot assisted surgery system has many advantages, such as small invasion, reduced infection rate, and fast recovery, the number of application in surgical operation has been greatly enlarged. But, because the limited visual data is only provided for the operator in surgery system, the immersion and reality are restricted and performance of surgery can be affected. Due to this reason, many research works have been carried out about master mechanism with haptic effect for the robot assisted surgery system. However, most of the developed haptic system has a bulky package with mechanical components and cannot be implemented to real medical systems.
Magneto-rheological (MR) fluid is a kind of smart fluid and its rheological properties can be changed by applied external magnetic field. Then the yield stress can be controlled accurately according to applied magnetic field intensity. The advantages of MR fluid application are simply listed as follow; extremely fast response time, small power consumption, and simple mechanism. Among the mechanical applications of MR fluid, MR brake is widely studied mechanism which can generate controllable large braking torque with simple structural configuration [1, 2]. The application methods of MR brake can be classified into three types as disk type, drum type and hybrid type by considering the position and direction of generated MR effect. For drum type MR brake, the MR effect take place at the radial gap between rotor and stator. Imaduddin et al. reviewed the previous researches for the design and modelling of MR brakes [3]. In these days, many research works for MR clutch and brake have been conducted to apply as a haptic actuator. Liu et al. reported design, modelling of disk type MR brake and suggested its application in haptic device [4]. An and Kwon proposed five-bar linkage haptic device featuring DC motors and MR brakes [5]. Senka and Rurocak developed spherical MR brake for multi degree of freedom actuator and applied to joystick type haptic device [6]. Nguyen et al. developed optimally designed MR brake-based 3D haptic gripper for tele-operation [7]. However, the structural configuration of the haptic master becomes complex and the number of degree of freedom is also increased. This means that the required feedback force is also increased to provide precise haptic effect.
In this paper, a new type of mechanism for haptic master device is proposed and its performance is evaluated experimentally. To increase haptic effect for master device, the master device is designed with lightweight and low inertia configuration. Then, a dual magnetic core type of MR brake is designed for large actuating force under limited small size and lightweight. The braking torque of the proposed MR brake is evaluated through experiment and it is demonstrated that enough braking torque can be obtained. After designing and implementing of control algorithm, tracking control performance of the manufactured MR brake is evaluated according to desired input. Then master device is designed with lightweight aluminium frame structure and four actuators. Available workspace for rotational motion is measured by gyro sensor and its effectiveness is verified by compared with workspace of free hand motion.

Haptic Guidance in Comanipulated Laser Surgery for Fetal Disorders

C. Gruijthuijsen, A. Javaux, G. Borghesan
Katholieke Universiteit Leuven, Leuven, Belgium
T. Vercauteren, D. Stoyanov, S. Ourselin
University College London, London, United Kingdom
J. Deprest, University Hospitals Leuven, Leuven, Belgium
J. Perret, Haption, Lavalle, France
D. Reynaerts, E. Vander Poorten
Katholieke Universiteit Leuven, Leuven, Belgium

Abstract:
The current techniques in minimally invasive surgery allow treating fetal disorders. Treatment in an earlier stage increases the chance or level of recovery. However, fetal interventions require precise instrument manipulation from the surgeon. For instance, in the treatment of the twin-to-twin transfusion syndrome (TTTS) the surgeon needs to bring a laser in close vicinity to the placenta. It is crucial that the surgeon maintains a specific distance between the tip of the employed instrument and the placenta, while lasering target sites on the placental surface. To facilitate this procedure, we suggest a new approach where the surgeon comanipulates the instruments together with a robotic stabilizer arm. The stabilizer arm provides haptic guidance to the surgeon, augmenting the surgeon's precision and helping him maintain a desired lasering distance. The benefit of this approach is demonstrated experimentally.

Keywords: Comanipulation, Haptic Guidance, Fetal Surgery, Twin-To-Twin Transfusion Syndrome

Introduction

Current surgical techniques allow treatment of fetal disorders in a minimally invasive surgical (MIS) manner. In such procedures, the surgeon enters the uterus with a small diameter – typically 3mm – endoscope through a small incision in the patient’s womb in order to perform the necessary diagnostic and therapeutic steps. Most endoscope manipulations require a considerable amount of dexterity and high precision from the surgeon, as the surrounding structures are very delicate. As such, this type of surgery requires highly skilled surgeons [1].
One particularly challenging intervention aims to treat the twin-to-twin-transfusion syndrome (TTTS), a pathology where unwanted blood vessel connections, anastomoses, in the placenta of monochorionic twins cause an unbalanced blood flow [2]. If left untreated, this condition can be lethal for both fetuses. The treatment of TTTS is a non-contact laser-coagulation procedure. The surgeon manoeuvres the endoscope, equipped with a laser fibre, over the placenta to coagulate all anastomoses. Alternatively or additionally he/she will laser a continuous coagulation line over the vascular equator of the placenta, in order to separate the blood circulation of both twins [3].
During the lasering, it is essential to maintain a minimum distance between the placental surface and the laser, i.e. the tip of the fetoscope. A larger distance would render the laser process ineffective, while a smaller distance introduces the risk of undesired and dangerous contact.
TTTS treatment is a highly demanding task for the surgeon, not only due to this distance criterion, but also because of the scale, the required precision and the fulcrum effect, typical to MIS [4]. To facilitate this task, we suggest an approach where a robotic stabilizer arm provides haptic guidance to the surgeon. A comanipulation approach, where both the surgeon and the stabilizer arm hold the instrument and jointly determine the instrument pose, was preferred over a teleoperation approach, as comanipulation can be more readily integrated into the current surgical practice and it allows the surgeon to remain in close vicinity to the patient.
In this paper we investigate to what extent a robotic stabilizer arm can improve safety and precision during a lasering task.

Method

For the proposed application the requirements for the robotic stabilizer arm are that it is highly back-drivable, has a very large workspace and can display fairly large levels of stiffness throughout its workspace. The back-drivability of the stabilizer is crucial as the surgeon must be able to move the instruments in an unhindered fashion. The workspace of the stabilizer has to be sufficiently large to be able to cope with the variability in the location of the incision point on the patient’s womb. The reachable stiffness (Z-width) is important for comanipulation as it allows providing effective

Normal Force Actuator for a Tactile Display Using a Micromechanically Built Spring Element Made of Polyimide

M. Rechel, Leibniz Universität Hannover, Garbsen, Germany
V. Hofmann, J. Twiefel
Leibniz Universität Hannover, Hannover, Germany
M. Wurz, Leibniz Universität Hannover, Garbsen, Germany

Abstract:
We present a tactile display able to induce normal and shear forces into the human fingertip within the same pin. This is realised by combining an electromagnetically driven normal force actuator with a piezoelectrical driven bending actuator to induce shearing forces. To design a normal force actuator with high performance and low energy dissipation in heat a hybrid solution of micro and precision mechanics is employed. This innovative approach leads to an actuator with small dimensions in the planar level with a pin to pin distance of 2.4 mm, combined with high flux densities resulting in high forces at low applied currents. Dimensioning of the system includes geometric, mechanic, electromagnetic and thermal aspects of the normal force actuator. Characterization is done by measuring the amplitudes over a specific frequency band with a Laser Doppler Vibrometer and by determining the blocking forces with a prestressed resistance strain gauge. The results are compared to the requirements of such a system.

Keywords: Tactile Display, Precision- and Micromechanics, Hybrid Actuator

Introduction

The interest in tactile perception and tactile displays is rising since the past decades [1]. To design a tactile actuator that is able to induce a wide range of tactile sensations, special care regarding the neurophysiological considerations has to be taken.
Three of the four types of mechanoreceptors within the human skin are identified to be responsible for vibro-tactile sensations. As shown in table 1, the Merkel (SA1), Meissner (RA) and Pacinian (PC) receptors show strong distinctions regarding their sensitivity to frequency and activation threshold [2]. The forth type of mechanoreceptors, the Ruffini corpuscles (SA 2), is known to be responsible for detecting slow skin stretch, so it can be neglected. Designing an actuator capable of producing vibrations of at least 30 µm amplitude, the contact force exerted on the actuator pin becomes a crucial aspect for the mechanical specification.

Table 1: *Properties of afferent systems [2]*

Afferent type	SA 1	RA	PC
Sensory function	Form and texture perception	Motion detect-ion	Vibrations of distant events
Range [Hz]	0-100	1-300	5-1000
Peak sensitivity	5 Hz	50 Hz	200 Hz
Mean activation threshold	30µm	6µm	0.08µm

Measurements of the finger pads' impedance, which is strongly dependent on the vibration frequency can be found in literature [3]. At low frequencies of 1-2 Hz, the impedance magnitude of the finger pad is about 0.09 N/mm, whereas at frequencies greater than 56 Hz the impedance reaches values of about 0.24 N/mm. If the tactile display should be enabled to reach an amplitude of 30 µm, a total force of 7.2 mN needs to be applied. It must be noted, however, this value neither includes the pressure force applied by the finger itself nor the influence of this pressure on the impedance.

Concept

To face the challenge of high actuator density with a distance between two pin centers of 2.4 mm in the X-Y plane and a force requirement of at least 7.2 mN per pin in normal direction a hybrid concept combining precision- and micromechanic production techniques is created. This way the restriction concerning the effective work per volume of electromagnetic driven actuators, due to small dimensions in the microcosm is avoided because the volume can be extended by increasing the dimensions in the Z-axis.
The combined actuator can be divided into three components: The bending actuator, the coupling element and the normal force actuator (Fig 1). The normal force actuator is guided by two slide bearings. In this way moments induced by the bending actuator can be absorbed.

Investigation of Smart Materials for Haptic Feedback Applications

H. Bochmann, J. Maas
Hochschule Ostwestfalen-Lippe, Lemgo, Germany

Abstract:
Haptic feedback is an important feature when a user distraction due to the interaction with a touch-sensitive display should be avoided. For this purpose, an introduction into human haptics and development objectives of haptic devices is given. Furthermore, novel and existing concepts providing haptic feedback are introduced and evaluated with respect to the defined objectives. Finally, smart materials such as electroactive polymers (EAP), magnetorheological fluids (MRF) and magneto active elastomers (MAE) are investigated considering their suitability for haptic feedback applications.

Keywords: Haptik Feedback, Smart Materials, Electroactive Polymers

Introduction

Due to their versatile possible applications, touch-sensitive visual displays became a popular user interface. In many use cases they gradually replace mechanical buttons, providing a haptic feedback when pressed. Consequently, the user has to rely solely on the visual feedback if there is no possibility to utilize sound. However, there are circumstances where the user must be aware of the environment and must not be distracted by the display. Thus, a haptic feedback is necessary and additionally increasing the customer's convenience [1]. This publication presents initial investigations on the utilization of smart materials such as electroactive polymers (EAP), magnetorheological fluids (MRF) and magnetoactive elastomers (MAE) for haptic feedback applications. A haptic feedback device mainly has to fulfil two tasks. On the one hand it has to sense the user input and on the other hand it has to actuate the user interface to provide a feedback. In the following these two tasks are called force sense and force feedback.
The aim is to develop a device which is able to emulate the "click" feeling provided by pressing a typical mechanical button. Additionally, the sensing of the force exerted by the user creates new possibilities of input methods. Thus, different tasks can be executed depending on the pressure on the screen. This, for example, is utilized by Apple in their current generation of MacBooks and IPhones and is named Force Touch.

Human sense of touch

The design of haptic feedback devices requires a basic understanding of the sense of touch. Therefore, a brief introduction into the function of human haptic perception is given.
Mechanical stimuli are perceived by various kinds of receptors in the different layers of the skin. Their distribution and density vary with the area of the body. Four different kinds of mechanoreceptors are located in the hand's glabrous skin [2]. They mainly differ in the speed of their adaptation to a change in applied external pressure. Thus, they are classified as slow adapting (SA) and fast adapting (FA) receptors. Further important characteristics such as frequency range and threshold of skin deformation are summarized in Table 1 [2, 3].

Table 1: *Summary of the skin's mechanoreceptors* [3].

Receptor	Class	Frequency range (most sensitive)	Threshold skin deformation (median)
Pacinian corpuscle	FA-II	40-800 Hz (200-300 Hz)	3-20 µm (9.2 µm)
Meissner's corpuscle	FA-I	10-200 Hz (20-40 Hz)	4-500 µm (13.8 µm)
Ruffini ending	SA-II	7 Hz	40-1500 µm (331 µm)
Merkel's cells	SA-I	0,4-100 Hz (7 Hz)	7-600 µm (56.5 µm)

Requirements of the actuation and sensing

In order to develop haptic feedback systems, requirements of the actuator and sensor system can be derived from Table 1. To achieve an optimized perception of the feedback, preferably all kinds of receptors should respond. For this reason, the actuators and sensors should operate within a frequency range from DC to approximately 300 Hz. Furthermore, the deformation of the skin and therefore the stroke of the actuation has to exceed the threshold of the receptors. Since the threshold varies a lot between the receptor classes, a feasible value of 300 µm has been chosen as reference value. Both, fre-

Miniature Piezoelectric Multilayer Actuators and their Applications (Review)

W.A. Groen, Delft University of Technology, Delft, and TNO Holst Centre, Eindhoven, The Netherlands
P. Pertsch, PI Ceramic GmbH, Lederhose, Germany

Abstract:
Piezoelectric multilayer actuators are well suited driving elements for miniaturized electro mechanical systems with geometrical dimensions in the lower millimeter range. They have properties like high electromechanical energy conversion rate at small volume, low driving voltages, high displacement resolution as well as large bandwidth for very dynamic mechanical signals.
The manufacturing process of miniaturized co-fired piezoelectric multilayer actuators is described in the first part of the paper. It addresses technological challenges like small grain size piezoceramic materials, layer thicknesses smaller than 20 µm, low lateral manufacturing tolerances as well as appropriate termination electrode technologies.
The second part of the paper gives a survey on recent applications of such miniaturized actuators in acoustical and optical systems, in hard disc drives, in ultrasonic motors as well as in micro fluidic assemblies like micro pumps and ink jet devices.

Keywords: Piezoelectric Ceramics, Multilayer Actuators, Layer Thickness, Grain Size, Applications, Ultrasonic Motors, Micro Fluidics, Acoustics, Optics

Introduction

Piezoelectric actuators became the primary technology for electromechanical solid state actuators during the last 25 years [1,2,3]. Their main advantages are ultrahigh displacement resolution, very dynamic mechanical response and high induced forces. Although there are several technological routes to manufacture and assemble piezo actuators, multilayer co-firing is the most important for industrial applications [4]. The fundamental technologies tape casting and screen printing allow for low driving voltages and efficient parallel batch manufacturing. Furthermore this is an appropriate technological approach to produce miniature devices in the mm-dimensional range which can be assembled by conventional methods like gluing and soldering [5].
Even smaller components, i.e. microactuators, can be made by thin film technology. They usually exhibit very low forces and request higher manufacturing quantities because of higher initial efforts [6].
Miniaturization is also a major trend for multilayer ceramic capacitors (MLCCs). These components are produced by similar technologies to multilayer actuators in very high quantities of some trillion pieces per year. Applications in smart phones, wireless and wearable devices put an extreme pressure on downsizing these capacitors. Smallest MLCC's have an envelope of 0.250 x 0.125 x 0.125 mm³ and a layer thickness below 1 µm including the screen printed electrodes [7,8]. Core shell type materials [9] as well as base metal electrodes – mostly nickel – together with special sintering conditions to prevent oxidation in the electrodes as well as oxygen vacancies in the ceramic are state of the art [10].

Although similar, MLCC technologies can't be applied to co-fired actuators on a one-to-one basis. Actuators will need a minimum height because displacement is related to the length. Passive electrodes are compressed by the lateral contraction of the stack and therefore hinder the longitudinal displacement. Hence, layer thickness should be finite to get a good relation between active and passive material in the stack.
Finally tight contact is needed between the stack and the mechanical environment to transfer the mechanical signals. This implies a minimum size of the device to allow for conventional assembly techniques and proper manual handling at smaller quantities.
Nevertheless, there is a miniaturization trend for piezo actuators too (Fig. 1). A few micrometer or even some hundred nanometer displacement are sufficient for a lot of applications in optics, semiconductor manufacturing, acoustics and ultra-precision engineering.
The following paper describes the design and the technological challenges of miniature actuators in the first part as well as typical applications of such small actuators in the second part.

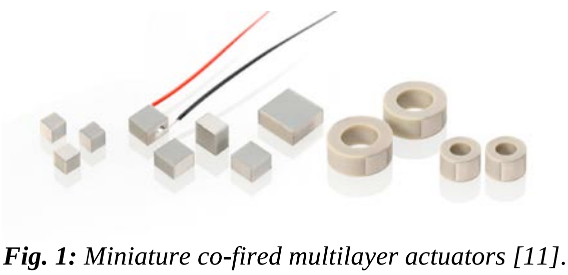

Fig. 1: *Miniature co-fired multilayer actuators [11].*

Micro Ultrasonic Motor Using One Cubic Millimeter Stator

T. Mashimo, Toyohashi University of Technology, Toyohashi-shi, Japan

Abstract:
We propose a miniature ultrasonic motor using a cubic stator with a side length of one millimeter. The proposed motor uses a three-wave mode generated at the circumference of its hole, unlike bending vibration modes that is often used in existing micro ultrasonic motors. In this paper, we built an experimental setup and study how to improve of the torque by changing the thickness of the piezoelectric elements and the preload between the stator and rotor.

Introduction

Ultrasonic motors have been expected as the micro actuator to be used for future medical devices such as catheters and endoscopes. They have two advantages for miniaturization: (1) high energy density, which is a high ratio of output to volume, and (2) a simple structure comprising of a simple stator and rotor [1-3]. In fact, an ultrasonic motor with diameter less than 5 mm has been implemented for rotating calendar rings in watches [4]. For further miniaturization, several researchers have built micro ultrasonic motors that use a bending vibration mode of the cylindrical stator as the driving principle. These micro motors are constructed of a stator with a diameter of approximately 1.5 mm and about 5 mm length [5-7]. A similar–sized linear ultrasonic motor are commercially available [8]. The linear motor uses the same bending vibration mode and translates its rotary motion to linear motion by a screw mechanism. The smallest ultrasonic motor uses coupling of axial and torsional vibration modes of the coil stator as the driving principle [9, 10]: A stator with 0.25 mm diameter and 1 mm length is excited by a piezoelectric element and generates the rotation of a sphere. However, total size including magnets for preload is over a few millimeters.

We have built a micro ultrasonic motor using a vibration mode that generates three waves inside the hole of a stator [11]. Fig. 1 shows the prototype micro ultrasonic motor comprising of a single metallic cube with a side length of 1 mm and a through-hole of 0.7 mm. Four piezoelectric elements are bonded to the four sides of the stator and generate vibration. This simplicity of the stator makes the manufacturing easy and makes the size small. An output shaft, which is inserted to the through-hole as a rotor, generates rotation when voltages are applied to the piezoelectric elements and the vibration mode is excited. We have reported that the micro ultrasonic motor could generate large torque when some weights are applied as the preload [12, 13]. However, the size of the preload mechanism using weights is too large in comparison with that of the micro ultrasonic motor.

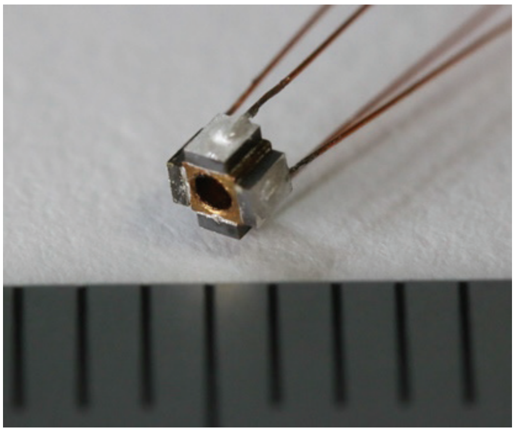

Fig. 1: *Prototype micro ultrasonic motor*

Next step is the miniaturization of the preload mechanism attached to micro ultrasonic motors. In this report, we propose a new miniature preload mechanism using a coil spring and clarify the motor output experimentally.

Driving principle

The stator uses a vibration mode that excites three waves along the circumference of the through-hole

An Ultrasonic Motor Using Side-Push of Centre-Attached Eyelets on an Octagonal Piezoelectric Plate

B. Koc, Physik Instrumente (PI) GmbH & Co. KG, Karlsruhe, Germany

Abstract:
An octagonal piezoelectric plate, on which two alumina eyelets are attached symmetrically at the center of the two main surfaces, was used as the vibrator of a piezoelectric resonance motor. The electrodes that are dividing the two main surfaces into two regions are arranged at 90 degrees to each other. Two alumina rods are attached at both ends of a U-shaped slider, which is used as the sliding element. A hula-hoop motion is generated when two signals (one driving the top and the other driving the bottom electrodes) with 90 degrees out of phase drive the vibrator. The hula-hoop motion is transferred to the slider through frictional coupling as the side surfaces of the both eyelets are contacted tangentially to the alumina rods on the U-shaped slider.

When the test motor was driven by 160 Vp-p square waveform signal at its first in plane mode that is about 68 kHz, it can supply a force of 20 N. Independent driving method also improves speed-control voltage nonlinearity significantly at low speed region.

Keywords: Octagonal Piezoelectric Plate, Ultrasonic Motor, Hula-Hoop Motion

Introduction

Precise positioners in the order of several tens of nanometer resolutions are in demand for medical and biological research such as in microscope stages and micro assembly units. Requirements from these positioners are not only obtaining a motion at high precisions but also very wide range of moving speeds from 100 nanometers per second to one meter per second. The obvious solution is to use a hybrid motion using two types of positioners; one is to obtain fast and coarse motions and the other is slow and precise motions. However, availability of space and requirement of many wires for electrical driving of actuators in moving stages make the system to be complex and costly. A linear motor with a wide range of moving speed and a capability to make motion steps in the order of several tens of nanometers could be useful for industrial and assembly technologies.

Resonance piezoelectric motors have the feature of low speed at high torque without a need of gear mechanisms. These motors also have the advantages of wider operating speed compared to inertia and piezo-walk drive type piezoelectric motors [1-2]. In a resonance type piezoelectric motor, a continuous motion is generated because a small vibratory microscopic elliptical or oblique motion is transferred to a moving element through frictional coupling. However, the “driving voltage-speed” nonlinearity causes some limitations when using a resonance piezoelectric motor for nano-positioning applications [3-4].

In general, normal component of this microscopic motion with pre-stressing force define generated force and tangential component defines the motor speed [5-7]. Controlling microscopic displacement in normal and tangential directions at the vibrator-slider interface independently could improve speed-driving voltage nonlinearity. Several researchers [8-9] tried to solve this speed-driving voltage nonlinearity by redesigning surface electrodes on various piezoelectric vibrating elements and control displacement in normal and tangential direction independently. However, after installing a vibrating element into a motor unit, holding and pre-stressing force could change two orthogonal resonance mode frequencies. In addition, temperature dependency of the two orthogonal modes could be different, which could also create a frequency shift of corresponding resonance modes differently after the motor operated for some time. As a result, an efficiency decrease could be observed.
In order to minimize the frequency changes of the two resonance modes, a symmetric structure was selected so that the excited two resonance modes are identical in orthogonal direction.

The octagonal piezoelectric plate with surface electrodes configuration and attached eyelets was modified from one of our previous work, where a square plate with identical electrodes was used in a rotary motor [10].

Performance Evaluation of a Single-Stage Valve at High Temperatures Actuated by Piezoelectric Stack

C. Han, W.H. Kim, S.-B. Choi
Inha University, Incheon, South Korea

Abstract:
This paper propose a single-stage valve system actuated by a piezostack actuator and control performance is experimentally evaluated from room temperature to high temperature(150℃). In order to achieve this goal, a design of a piezostack driven single-stage valve system is proposed and an experimental apparatus is manufactured to evaluate the valve performance with high temperature conditions. The experimental apparatus consists of a heat chamber, pneumatic-hydraulic cylinders, a hydraulic circuit, a pneumatic circuit, thermal insulator, and electronic devices such as computer, Data acquisition (DAQ) board, sensors, and a high voltage amplifier. The displacement control performance of the valve system is evaluated via experiment. In order to evaluate of performance with high temperature, the piezostack valve system is heated and controlled at the inside of heat chamber. The experiment results are compared between room temperature condition and high temperature condition. Control of displacement tracking is evaluated and compared between room temperature and high temperature.

Keywords: Piezostack Actuator, High Temperature, Single-Stage Valve, Displacement Control

Introduction

The piezoelectric actuator are widely used for various control applications because of their salient features such as fast frequency response, high actuating force and infinite control resolution. The lead-zirconate-titanate (PZT) type of piezoelectric material are widely used for actuators because the PZT type has good performance to convert electronic to mechanical energy. However, the PZT piezoelectric material has low Curie temperature which materials lose their permanent piezoelectric properties. Usually, the guarantied temperature of PZT material actuator is up to 80℃. In many industrial fields, however, working temperature is over then 100℃. Therefore, the behaviour of the piezoelectric actuator needs to be researched under various temperature conditions. Li *et al.*, Schranz *et al.*, and Senousy *et al.* studied the actuating properties of the piezostack actuators under the temperature range from 25 to 125℃ [1-4]. Furthermore, Chio *et al.* researched the dynamic properties and control capability of a piezostack actuator at various temperature conditions up to 190℃ [5]. They proved that the piezoelectric actuators are dependable under its accessible working temperature conditions.

The hydraulic-mechanical system is widely used because the system has high power density and can convert from hydraulic power to mechanical power. Many mechanical systems is controlled using hydraulic control valves to control mechanical motions. In hydraulic-mechanical systems, the performance of mechanical system is decided from performance of a valve system. Almost valve systems are actuated using an electric hydraulic, a pneumatic, and a solenoid actuator. A valve system has low limit performance ability because the actuators has low limit performance [6,7]. Kitching *et al.* proposed semi-active suspension based on hydraulic oil. The suspension is controlled by a solenoid actuator [8]. However, the damper has slow response time more than 30 ms because a solenoid actuator has slow respose time.

Consequently, a valve system is proposed actuated piezostack actuator and evaluated at various temperature conditions including up to 150℃. After briefly explaining the piezostack valve system, the experimental apparatuses at various temperature conditions are described. The temperature of valve system is controlled by a heat chamber and the performance of valve system is measured using a gap sensor and flow rate meter. The output results are displayed and discussed.

Proposed Piezostack Based Single-Stage Valve

Figure 1 shows schematic diagram of proposed valve system based on piezostack actuator. The proposed valve system is consist of a piezostack actuator, a housing, displacement amplifier, a spool valve system, and aerogel. The commercial piezostack actuator (pst150/20/80/V25, PIEZOMECHANIK) is considered to control of a valve system. The guarantied working temperature of the piezostack is 80℃ because the actuator bases on PZT piezoelectric material. The lever-hinge type displacement amplifier is adopted to magnify the displacement from the actuator. A spool valve system is used for control flow rate and a gap sensor is placed on the end of spool for detecting the position of spool. Because the gap sensor use eddy

Module Stepping Piezoelectric Actuator
- A Versatile Way of Micro-Positioning Actuation -

F. Dubois[1,2], F. Barillot[1], V. Thiebaud[1], C. Belly[1], T. Porchez[1], M. Barraja[1], A. Saulot[2], Y. Berthier[2].
[1]Cedrat Technologies SA, Meylan, France
[2]LaMCoS UMR 5259, Université de Lyon, INSA-Lyon, Villeurbanne, France

Abstract:
Stepping Piezoelectric Actuators (SPA's) – based on the Piezoelectric Friction-Inertial Actuation (PFIA) principle – are made from Cedrat Technologies Amplified Piezoelectric Actuators (APA). They use the stick-slip principle to couple high resolution positioning (<µm), long stroke (>cm) and low volume (<15cm^3). These motors are used in optronic, medical and military applications. However, current rubbing contact between the shaft and clamp limits the potential evolution of SPA's. In this paper, a new concept: called Module SPA (MSPA) – offering long stroke capabilities (>10cm), allowing easier multi-DoF mechanism developments and miniaturization possibilities – is presented. Results obtained on three innovative engineering models – linear long stroke, rotary and three-DoF actuators – are presented, giving the reader actual benefits of this concept and allow addressing new applications such as consumer goods and medical devices.

Keywords: Piezoelectric Motor, Micro-Positioning, Multi-DoF Actuation.

Introduction

Piezoelectric Friction-Inertial [1] SPA's use the stick-slip principle to have high resolution positioning (<µm), long stroke (>cm) and small size (<15cm^3) [2]. These motors are composed of four main elements: an APA, an inertial mass, a shaft and a clamp [3]. In this paper, firstly, current rubbing shaft/clamp configuration' limitations are highlighted. Then, the MSPA concept is detailed with its differentiating factors. Finally, three engineering models – linear long stroke, rotary and three-DoF actuators – are introduced to highlight the benefits of this concept and to prove a miniaturization capability.

Scientific context

PFIA principle
PFIA principle of SPA relies on the stick-slip effect. ***Fig. 1***.A-B illustrates the two phases needed to produce steps; from slow-fast alternation voltage order to friction drived step-by-step moving mass displacement. By repeating this operation, a stroke of several millimeters can be reached. The opposite motion is done by inversing the slow-fast voltage sequences. SPA's are suitable to offer a high blocking force at rest, micron and submicron positioning capabilities, high miniaturization potential and nonmagnetic properties.

Shaft-Clamp SPA configuration' limitations
In former Linear SPA motors, a shaft was enclosed in a clamp. The clamp was moved by friction at a variable distance from the APA. This introduced limits in stroke of the motor, and a reduction of force with the distance. Additionally, when integrated in a stage, hyperstatism appeared with the guidance. Additionally, noise and parasitic vibrations are amplified by the different casing parts of the stage.

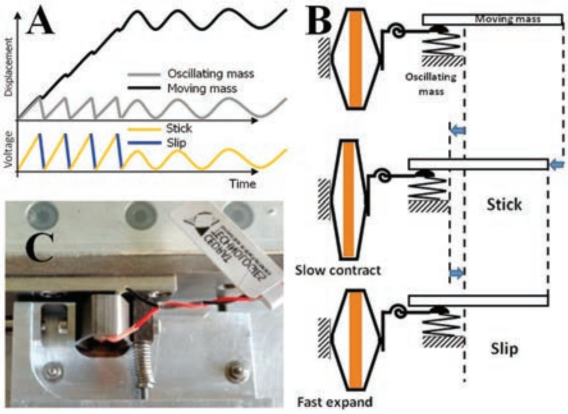

Fig. 1: *MSPA motor: A- Stick-Slip principle, B-scheme and C- preliminary breadboard.*

MSPA Concept

In comparison, MSPA frees the rubbing contact and distance between the friction force and the APA electromechanical force remains co-localized (see ***Fig. 1***.B-C). So, the payload can be driven by friction in a linear or rotary motion depending on the guiding. This configuration allows removing the limitations of the first generation of SPA's with largely extended stroke and higher versatility.
In addition, as in the shaft-clamp configuration, the main MSPA characteristics such as high force at rest, nonmagnetic properties, micron and submicron positioning are retained.

Muscle-Like Piezohydraulic Actuators for Robotic Grippers

W. Zoels, I. Vittorias, G. Bachmaier
Siemens AG, München, Germany

Abstract:
Industrial robotic grippers nowadays do not present the required flexibility against changing or individual workpieces. As a result, tools and gripping systems have to be changed often. The human-hand, on the other side, with a huge degree of dexterity can handle many workpieces with a wide variety of dynamic properties ranging from precise positioning up to applying high forces. The goal of this contribution is to demonstrate the usage of the piezohydraulic actuation principle as a muscle-like actuator in the realization of a versatile robotic hand. By combining a human-like multi-fingered robot hand with this flexible actuation principle, a dexterous gripping mechanism can be realized. Fifteen such actuators are integrated in the fore-arm of a 6-DoF robotic arm and drive the tendons of the human-like robotic end-effector. This enables a broader range of objects that can be grasped with such a gripper than with typical grippers, being able to grasp both delicate objects using soft dynamics as well as to realize high forces required in many industrial applications.

Keywords: Human-Like Robot Hand, Piezohydraulic Actuator, Dexterous Manipulation, Variable Impedance

Introduction

Today's automation customers call for more flexibility from robotic solutions. Versatile and flexible robots are required to avoid re-designing and re-engineering the system as long as the problem to be solved changes. Use cases such as *lot size 1*, envisioned in Industry 4.0 settings can then be much easier realized. The ability of a robot to handle objects like a human - dexterously - is with nowadays actuators still challenging and has been a wide research field for the past years. Classical stiff electric drives cannot respond to the aforementioned problem settings, as it is recognized in [1]. Secondly, in terms of safety, human-friendliness of the robotic actuators has been already criticized in [2]. This highlights the large need for modern, safe, and in parallel high-performing actuators. Further, Robotics - VO, a NSF sponsored organization in the U.S., presented in [3] a roadmap for the robotics field in the next 15 years. Amongst other key drivers of robotics they identify the need for human-like capabilities, similar to the ones of a hand, in terms of dynamic performance, force, and intrinsic safety. There is, therefore, a strong need on actuators and robotic gripping technologies with human-like characteristics and safety to enable collaboration with the human.

In the required actuator power range of less than 30W, the efficiency of electromagnetic devices drops sharply. In contrast, piezo actuators have a constant efficiency even in this low power range. Additionally, piezo actuators have several advantages such as high force density and high dynamics. However, the limited stroke is a big drawback. Combining the piezo with a micro-hydraulic transformer, the limited stroke of the piezo can be compensated by a hydraulic stroke integrator as shown in [4]. Furthermore, the flexibility and versatility of hydraulic circuits makes it easy to built additional functionality like variable impedance or back-drivability directly into the actuator hardware. In contrast to traditional approaches utilizing closed control loops for the same purpose, the hardware-only approach offers advantages in regard to safety, reliability and certification. The abilities of such a muscle-type actuator were demonstrated in a first laboratory sample presented in [5].

In this contribution this muscle-like piezohydraulic actuator is further developed, miniaturized and integrated on the fore-arm of a 6-DoF robotic manipulator. The kinematics of a human-like robotic hand, that of the Shadow Robot Company [6], are combined in one system with 15 of the developed piezohydraulic actuators to realize a versatile human-like robot hand.

The paper is organized as follows. First, a background on the piezohydraulic actuation is provided. Next, the actuator integration in a tendon-driven structure is demonstrated. Experimental results of the actuator conclude the paper.

Muscle-like piezohydraulic actuation

As described in [5], the muscle-like piezohydraulic actuator works basically like a hydraulic pump by using a PWM voltage signal. During the rising edge of the PWM-signal, the piezo actuator in Fig. 1 compresses the fluid of the input volume so that it flows over check valve 1 (cv1) into the output. At the falling edge, the piezo actuator contracts and induces low-pressure so that the fluid is sucked from

Topological In-Plane Polarized Piezo Actuation for Compact Adaptive Lenses with Aspherical Correction

F. Lemke, M. Stürmer, U. Wallrabe, M.C. Wapler
Albert-Ludwigs-Universität, Freiburg, Germany

Abstract:
In this contribution, we investigate the effects of using in-plane polarized piezo actuators with topological buckling displacement to drive glass-piezo composite membranes for adaptive lenses with aspherical control. We find that the effects on the focal power and aspherical tuning range are relatively small, whereas the tuning speed is improved significantly with a first resonance of 1 kHz for a 13 mm aperture lens.

Keywords: Adaptive Lens, Aspherical Correction, In-Plane Polarization, Buckling

Introduction

Adaptive lenses usually have a large outer diameter compared to their aperture and are limited to tens of ms response time (e.g. [1]). In [2, 3] we demonstrated piezo actuated ultra-compact lenses with aspherical correction and ms-scale response. These consist of an ultra-thin glass membrane sandwiched between two out-of-plane polarized ("d_{31}") piezo rings (Fig. 1a) that cover a flexible oil-filled fluid chamber made out of polyurethane as shown in Fig. 2 (with the new piezo design). The supporting ring in the fluid chamber acts both as a hinge for the membrane and as a soft spring to give way to the volume displacement.

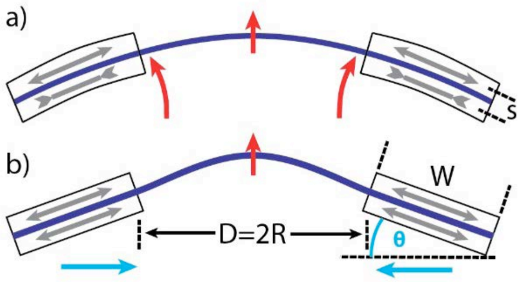

__Fig. 1:__ Cross-section of glass (blue) and piezo rings (black) and their actuation principle: bending mode (a) and buckling mode (b)

In our new approach we replace the d_{31}-piezo actuators by in-plane polarized films with ring-shaped finger electrodes, both with single-sided and with double-sided electrodes. This leads to the overall lens structure shown in figure 2. On the one hand, it allows for single-sided contacting that may simplify the fabrication. On the other hand, these actuators have an intrinsic buckling effect and potentially larger, anisotropic strains.

We will investigate whether the topological buckling effect [4] of the piezos does influence the deflection and aspherical control. We further investigate the difference between single-sided electrodes with easier fabrication and double-sided electrodes with potentially larger deflection [4, 5]. Furthermore, we analyse the resonance behaviour of the lens.

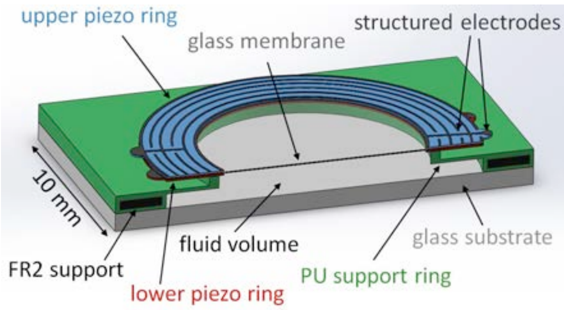

__Fig. 2:__ Cross-section (schematic layout) of new lens with in-plane polarized piezo rings

Theory

When applying an effective radial electric field E to the rings along the radial polarization, they contract tangentially and hence also overall radially with

$$\Delta R = R d_{31} E \,, \qquad (1)$$

which is the same as for the conventional actuators. The width of the rings however expands with

$$\Delta W = W d_{33} E \,. \qquad (2)$$

By taking into account the finite width of the rings, we can apply the results of [4] that they will tilt conically with

$$\theta_{ring} = \pm\sqrt{2(d_{33} - d_{31})E} \,. \qquad (3)$$

While this result was derived for a closed disk, the mathematical locality of the derivation in [4] means that it applies also for an open ring.

In [2,3], we found that the active membrane has two actuation principles: The buckling and the bending mode. In the buckling mode, both piezo actuators contract with electric fields E_{upper} and E_{lower}, such

Bimorph Mirrors for Adaptive Optics in Space Telescopes

D. Alaluf, R. Bastaits, K. Wang
Université Libre de Bruxelles, Brussels, Belgium
M. Horodinca, Technical University Gheorghe Asachi, Iasi, Romania
I. Burda, Babes Bolyai University, Cluj-Napoca, Romania
G. Martic, Belgian Ceramic Research Centre, Mons, Belgium
A. Preumont, Université Libre de Bruxelles, Brussels, Belgium

Abstract:
This paper discusses a concept of bimorph deformable mirror used in adaptive optics to compensate for manufacturing errors, gravity release and thermal distortion affecting large lightweight mirrors in space telescopes. The mirror consists of a single-crystal Silicon wafer (D=75 mm t=500µm) covered with an optical coating on the front side and an array of 25 independent PZT actuators acting in d_{31} mode on the back side. The mirror is mounted on an isostatic support with three linear PZT actuators controlling the rigid-body motion. The paper presents the experimental results obtained with this design and a new, more compact alternative.

Keywords: Adaptive Optics, Deformable Mirror, Bimorph Actuator, Piezoelectric Actuator.

Introduction

Adaptive Optics (AO) has been used very successfully to improve the image quality of terrestrial telescopes. AO systems use a small deformable mirror (DM) located in the optical train, deformed mechanically with a set of actuators, to produce a wavefront correction opposing the wavefront error produced by the atmospheric turbulence and the residual error of the active optics. The main parameters of a DM are: the number of actuators (number of independent degrees of freedom); the stroke (typically a few microns); the size (from microsystems up to more than one meter for the future E-ELT; the size of the DM is related to the field of view); the temporal bandwidth (typically 50-100 Hz, which brings a lower limit to the first natural frequency of the mirror). The linearity and hysteresis have only a second order impact on performance in closed-loop.

More recently, the space telescope community has been interested in using deformable mirrors to compensate for manufacturing errors, gravity release and thermal distortion affecting large lightweight mirrors in space telescopes (D>0.5m). This paper describes the outcome of the ESA project BIALOM [1].
The main goals of this project were as follows: RMS wavefront error λ/10 at 633nm; long term stability (open loop): 24 h; voltage range for active control: 20% of V_{max}; reflectivity at test wavelength >95%; surface roughness < 2nm; lowest eigen-frequency > 140Hz; design load: 20 g. The minimum clear aperture should be 30 mm.
The deformation amplitude of the various Zernike modes Z4 to Z11 should be:
Z4, Z7, Z8: 1 µm ; Z5, Z6 : 2 µm
Z9, Z10 (trefoil): 500 nm
Z11 (spherical) : 750 nm
with an accuracy of 30 nm RMS.

Design and manufacturing

The mirror consists of a single-crystal Si wafer (D=75 mm t=500µm) covered with an optical coating on the front side and an array of PZT actuators acting in d_{31} mode on the back side (d=50 mm, t=200 µm) with 25 independent electrodes. The mirror is mounted on isostatic support with linear PZT actuators.

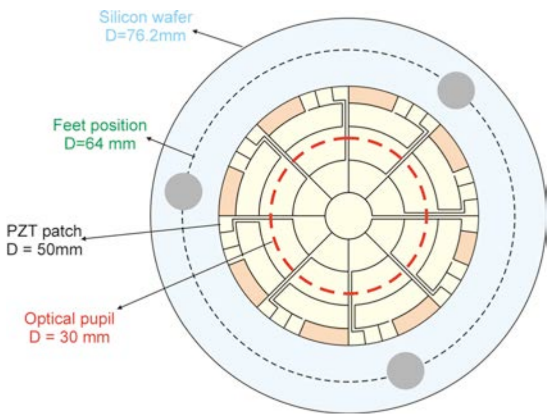

***Fig. 1:** Geometry of the deformable mirror (isostatic support,* keystone *electrode design, electric tracks and optical pupil).*

Application of Combined Ultrasonic-Levitation-Magnetic-Actuators for Machine Guideways

B. Denkena, J. Reiners, B. Wallaschek, J. Twiefel, I. Ille
Leibniz Universität Hannover, Hannover, Germany

Abstract

A machine tool's manufacturing accuracy depends significantly on its structural dynamics. By integrating active guiding systems into the machine structure, the structural dynamics can be adapted during the machining process. In this publication a novel class of contactless guiding systems is presented. The guiding concept is based on ultrasonic levitation and reluctance forces. This combination enables the development of compact, fluid- and contactless guiding systems which supersede a mechanical wrap around. This article presents two variants of the novel actuator concept. The first one is suitable for non-controlled, self-stabilizing systems, the second one allows controlled high performance active damping and fine positioning guiding systems. Finally the development of a position controlled three degrees of freedom (3 DOF) planar-guide is shown. First measurements proves the concept by a stationary exact positioning step response.

Keywords: Ultrasonic Levitation, Reluctance Force, Magnet Actuator, Contactless Guiding System

Introduction

Contactless guiding systems are common in applications that require precise positioning within a range of a few micrometres or below. Known systems, such as air-lubricated and magnetic guides offer the advantage of very low friction losses as well as the absence of the stick-slip-effect and wear [1][2][3][4]. These systems are characterized by unidirectional force generation of each guiding element. Consequently, conventional contactless guiding systems require a mechanical wrap around. This results in complex and large machine structures. In addition to that, air lubricated bearings provide its characteristic low compliancy for air gaps less than 10µm [1]. Already small heating effects results in a few µm thermal growing of the structure. In worst case, air bearings mounted in a wraparound will get jammed and loose its guiding capabilities.

This work develops a novel guiding system based on bidirectional actuators which we presented in [5] and [6]. These actuators use ultrasonic levitation to generate repellent forces and magnetic actuators to generate attracting forces. Both technologies are implemented in a combined, bidirectional actuator. These allows compact machine designs without a mechanical wrap around. The actuator principle allows non-controlled, self-stabilizing systems as well as controlled, high performance active damping and fine positioning guiding rails. For both alternatives an actuator design is presented. Finally the development of a position controlled 3 DOF planar-guide is shown.

Actuator Principles

In this application the ultrasonic levitation works like a static controllable air lubricated bearing. By applying additional magnetic reluctance forces, the air gap of the air lubricated bearing can be adjusted.

Ultrasonic squeeze film levitation occurs between two planar surfaces when one of the surfaces oscillates at a frequency usually above 20 kHz. The principle of the squeeze film levitation is shown in Fig. 1 (left). Typically, the gap between the surfaces is within a range of 10 to 50 µm. Due to the high frequencies there is nearly no exchange of the medium inside the gap and the ambience. Therefore, the gap can be considered as a closed cylinder and the fluid film is rapidly compressed and expanded within a vibration period [7].

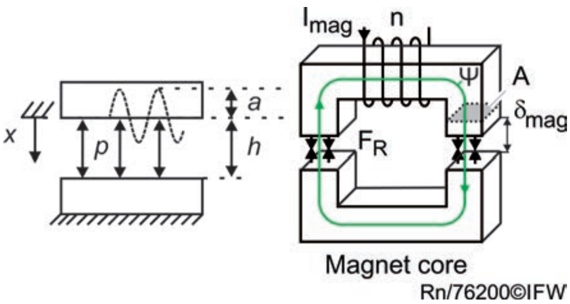

Fig. 1: *Actuator principles ultrasonic squeeze film levitation and reluctance forces*

Due to thermodynamic effects the time-averaged mean pressure inside the gap is higher than the ambient pressure. This kind of levitation is called squeeze film levitation or near field levitation and is the base of the functional principle of the ultrasonic levitation actuators. In Fig. 1 (left), *a* is the vibration

High Response Proportional Flow Control Valve Using Particle Excitation

D. Hirooka, T. Yamaguchi, N. Furushiro
Kansai University, Suita-shi, Japan
K. Suzumori, Tokyo Institute of Technology, Tokyo, Japan
T. Kanda, Okayama University, Okayama-shi, Japan

Abstract:
This paper reports a new proportional flow control valve for pneumatic actuators. We have researched valves that use particle excitation with a piezoelectric transducer. The valves have high flow rate/weight and high controllability. In this report, we introduce a new proportional flow control valve using particle excitation by piezoelectric transducer. The valve is composed bolt-clamped Langevin-type transducer (BLT) and the flow rate is proportion to the applied voltage at the transducer. We have designed a prototype of the valve using finite element method (FEM) and measured flow rate characteristics by experiments. In the results of the experiments, we have confirmed that the control flow rate is proportionate to the applied voltage at the transducer and maximum flow rate is about 70 L/min under 0.5 MPa.

Keywords: Pneumatic, PZT, BLT, Proportional Flow Control Valve

Introduction

Pneumatic actuators have light weight and a high power/weight ratio compared to electromagnetic actuators and hydraulic actuators. However, because pneumatic actuators are nonlinear and their control is very complex, highly controllable devices are in great demand. In general, highly controllable devices like proportional flow control valves have large volume, heavy weight and low response. Several new pneumatic control devices have been developed, including proportional valves [1] and small control valves [2] using PZT elements. We designed a control valve using particle excitation by PZT devices, and this device can control air flow smoothly with small weight.
Here, we report the design of a proportional flow control using particle excitation. This control valve uses resonance mode by PZT vibration and is driven by a bolt-clamped Langevin transducer (BLT). In this paper, we first show the basic mechanism of the particle excitation valve and explain how the valve proportionally controls flow rate.
Second, we demonstrate the prototype using BLT.
Next, we describe the prototype's basic characteristics. Finally, we provide the results of our flow rate change experiment and explain the flow rate characteristics.

Working principle and Configuration

First, we explain the working principle and the basic structure of the particle-excitation flow control valve we previously proposed [1]. The particle excitation valve consists of an orifice plate, a PZT vibrator, and iron particles. This valve controls the air flow rate to change the orifice plate vibration amplitude. Fig. 1 shows a cross-sectional image of the flow control valve. Fig. 1(a) shows the valve's closed state. Because the particles seal the air flow by supplying air pressure, this valve is closed without driving voltage. Fig. 1(b) shows the valve's opened state. In this state, the excitation of the orifice plate by the PZT vibrator moves the particles away from the orifice plate, generating space between them and the orifices so that air flows through them. The excitation intensity controls the flow rate. The flow control valve is designed through calculation and analysis.

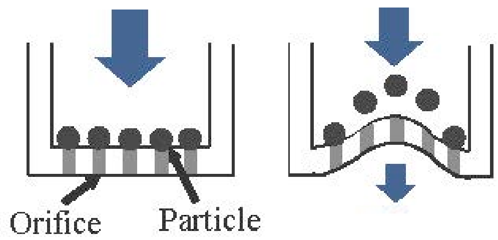

(a) (b)

***Fig. 1**: Basic working principle of particle excitation flow control valve*

Its drive condition is decided by acceleration in the orifice part. The condition for making the particles move away from the plate is derived as follows from the dynamic balance of forces acting on the particle:

$$a > \frac{\pi r^2 P \pm mg}{m} \qquad (1)$$

where a represents the acceleration at the particle on the orifices, P is the air-flow pressure inner control valve, r is the radius of the orifice, m is the particle mass, and g is the acceleration of gravity. In this

Performance of a Novel Small Component Conveyor Utilizing Flexural Travelling Waves

T. Wielert, A. Vagapov, J. Twiefel
Leibniz Universität Hannover, Hannover, Germany
I. Mešan, K. Bott
Afag GmbH, Amberg, Germany

Abstract:
The linear transport of small components on long distances is an important part of the automation technology. This paper presents a novel conveyor system for this task. The ambition for developing the conveyor was to improve the overall system performance compared to conventional linear conveyors, especially in terms of a dynamic start and stop behavior, the reduction of wearing processes and audible noise emission. The developed system utilizes structural vibrations in a bar shaped conveying body for the transport of small objects. Ultrasonic travelling waves are generated in the conveying body by a piezoelectric transducer. Thus, complex contact processes, namely stick, slip and separation, between the vibrating conveying body and the objects placed atop of it take place. As a result, the objects are driven forward. This contribution describes the new transport system, its working principle and characteristics. The main focus is the performance of the new device compared to the conventional technique. Experimental studies are carried out attesting an overall performance on pair or above typically used vibration conveyors.

Keywords: Ultrasonic, Travelling Wave, Conveyor, Piezoelectric, Object Transport

Introduction

Small components for mechatronic and microsystem devices set high standards on reliable and efficient feeding systems in production environments. Sensitive parts must be transported gently to reduce mechanical damage. At the same time the industry claims for more and more dynamic feeding characteristics. Thus, high performance conveyor systems are needed that ensure an adequate supply of the components.

This contribution presents a novel conveyor system utilizing ultrasonic vibrations to realize the linear transport of small components. This technique offers several advantages compared to conventional vibration conveyors [1]. The operating frequency is above the audible frequency range and results in a very low hearable noise emission. Simultaneously, the high operating frequency leads to very dynamic conveying characteristics with a very fast start and stop behaviour. The maximum normal force in the contact interface between the transported objects and the conveyor is lower throughout the transport process and ensures a gentle conveying characteristic. The compact system allows the transport of a broad range of objects up to a weight of 0.015 kg. Thus, it is variable applicable and allows an easy integration in existing production processes.

In the following, the working principle of the new conveyor system is described in detail. Experimental studies of a prototype system are carried out investigating the conveyor characteristics. The overall performance is compared to a reference system based on the conventional vibratory conveyor technique.

Travelling wave conveyor

The transport of small components utilizing travelling waves is based on the function principle of ultrasonic travelling wave motors. The fundamentals of these motors are described in detail by e.g. Wallaschek [2], Ueha und Tomikawa [3], and Sashida and Kenjo [4]. However, instead of driving a motor shaft the principle is used to move small objects. Fig. 1 shows the basic structure of the novel travelling wave conveyor. A piezoelectric Langevin transducer driven in the second longitudinal vibration

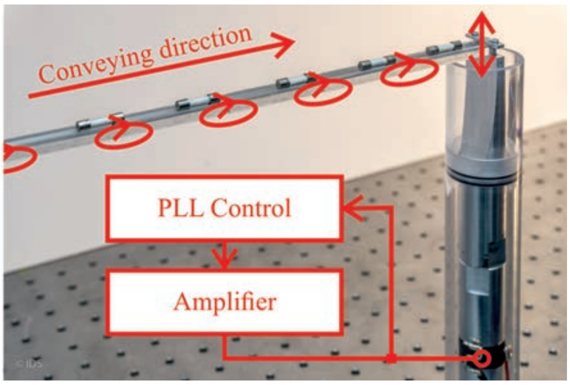

Fig. 1: Function principle of the small component travelling wave conveyor.

mode is utilized to generate the ultrasonic travelling waves. It is attached to the end of a bar shaped conveying body made of polycarbonate (PC). Considering the mounted conveying body, the transducer resonance frequency is in the range of

Smart Structures: Recent Developments within Aeronautics Applications (Invited Review)

H.P. Monner, M. Kintscher, M. Misol, J. Riemenschneider, D. Schmidt
Deutsches Zentrum für Luft- und Raumfahrt (DLR), Braunschweig, Germany

Abstract:
Smart structures influence the elastomechanical behaviour in a wanted way by optimally integrated actuators and sensors to realize morphing, active vibration reduction, active structural acoustic control and structural health monitoring. Especially in aeronautics large progress can be observed, meaning that the lab stage has been passed and high TRL levels are reached. Challenges for harsh environmental conditions involving lightning strike, bird impact and icing, just to name a few, have to be overcome. Also integrational aspects of actuators and sensors play a major role to realize lightweight and producible smart structure like morphing droop noses, actively twisted rotor blades, smart linings or CFRP fuselages with integrated structural health monitoring. This review gives an overview of some recent applications within aeronautics which involve full-scale demonstration and wind tunnel testing of smart structures as well as an outlook for further developments.

Keywords: Morphing, Adaptive Wing, Smart Droop Nose, Active Twist, ASAC, Active Structural Acoustic Control, Smart Lining, SHM, Structural Health Monitoring, Smart Structures

Introduction

The challenging long-term targets formulated in the ACARE research agendas (75% reduction in CO2 emissions, 90% reduction in NOx emissions and 65% reduction of the perceived noise in reference to narrow body engine performance of year 2000 are envisaged up to 2050) have motivated the introduction of new technologies like smart structures into aeronautics applications in the past 10 years [1], [2]. National and European funding has strongly supported this development. Smart structures have great potential in aeronautics since they allow a structure to actively influence its elastomechanical behaviour. This way morphing, active vibration reduction, active structural acoustic control and structural health monitoring can be realised. Morphing structures have especially been boosted by the European projects SADE, CHANGE, NOVEMOR, Clean Sky I-SFWA and SARISTU. The *smart morphing droop nose* is one major result of these efforts and illustrates the development from basic research to an industrial level of maturity in an impressive way. Highly dynamic morphing for helicopter rotor blades has intensively been investigated within the European projects FRIENDCOPTER and Clean Sky I-GRC. *Actively twisted rotor blades* with integrated piezoceramic actuators have proven to master this challenging task both structurally and aerodynamically. Strategies for active structural acoustic control, better known as ASAC, could be demonstrated within the national projects SYLVIA and DIANA. A *smart lining* based on a lining structure of an aircraft's interior from the shelf could be demonstrated to reduce broadband and multi tonal noise but also in parallel to be used as replacement for loudspeakers. Finally for *structural health monitoring* systems the level of maturity was lifted to another step within the European Project SARISTU. A full scale CFRP fuselage structure with integrated actuators and sensors proved the feasibility of the Lamb wave based approach. These are some outstanding examples for recent developments of smart structures within aeronautics which will be illustrated in the following sections.

Actively twisted rotor blades

The complex unsteady aerodynamic conditions on helicopter main rotors cause vibration and noise in and around rotary wing aircrafts. One way of working against those is the use of individual blade control to increase the miss distance between vortexes and blades – a major reason for most of the noise. Most prominent technologies to support individual blade control are blade flaps, and active pitch links to introduce control inputs. An effective way, which does not generate additional vortexes, is active blade twist. The basic principle to derive tip twist (φ) on a blade of the length l is the implementation of piezoceramic actuators in a way that a twist momentum (M_t) is being generated, which is working against the torsional rigidity (GI) of the blade.

$$\frac{\varphi}{l} = \frac{M_t}{GI} \qquad (1)$$

Several different methods that introduce such twist into a blade can be found in literature [3] and [4]. The reason for the use of piezoelectric actuators is their quick response which allows actuation even at

Design Study and Performance Evaluation of Actuator System for Subsonic GA Wind Tunnel Testing

N. Kobiki, K. Saitoh, Y. Hamada
JAXA, Mitaka-shi, Japan
S.K. Chee, T. Yano, A. Yano
Mechano Transformer Corporation, Chiyoda-ku, Japan

Abstract:
JAXA has been conducting research and development of the on-board safety avionics technology to prevent turbulence-induced aircraft accidents (Safe Avio) that uses Doppler light detection and ranging (LIDAR) to detect the turbulence in advance and the preview controller to utilize the turbulent velocity information measured by LIDAR to attenuate the aircraft acceleration in turbulence. The preview controller should be validated by a subsonic GA (Gust Alleviation) wind tunnel testing as the first step. The high performance actuator system, which drives the control surfaces to alleviate the gust influence on the aircraft, is required to realize the wind tunnel testing. A design study, prototyping and performance evaluation of the piezoelectric actuator system installed in a model wing for the subsonic GA wind tunnel testing are carried out. The results show that the actuator system demonstrates the sufficient dynamic and endurance performances to satisfy the requirements including the +/-10deg wide range of the output deflection.

Keywords: GA (Gust Alleviation), Preview Controller, Piezo Actuator, Wind Tunnel Test

Introduction

To improve the safety of passengers and crew on the aircraft, JAXA has been conducting research and development of the on-board safety avionics technology to prevent the turbulence-induced aircraft accidents (Safe Avio) that uses Doppler light detection and ranging (LIDAR) to detect the turbulence in advance and automatically control and suppress the lurching of the aircraft [1]. In order to demonstrate one of the prime technological targets comprising of Safe Avio, a gust response and mitigation algorithm utilizing the preview controller [2] should be validated by a GA (Gust Alleviation) wind tunnel testing [3, 4]. The key components of the wind tunnel testing such as a gust generator, a dynamic supporting system, an aircraft model and an actuator system are under studying and developing to perform the subsonic GA wind tunnel testing as the first step as shown in Fig.1.

The gust generator set on the upstream side of the wing of the half model aircraft oscillates the cascade to generate specified types of the gust, then the wing model supported by the dynamic supporting system heaves and pitches responding to the gust. The control surface, the aileron, is driven by the actuator system to suppress the wing model movement controlled by the algorithm utilizing the preview controller.

A design study of the actuator system is carried out to satisfy the requirements based on the assuming wind tunnel test conditions and model wing geometry.

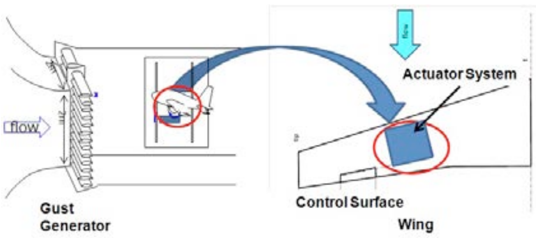

Fig. 1: *Schematic view of GA wind tunnel testing*

This paper describes the design study process and the results of the performance evaluation which contains the dynamic performance and durability of the actuator system.

Requirements for Actuator System

Based on the assuming wind tunnel test conditions, the requirements for the actuator system are set up as follows.

Operating performance:

Output deflection	+/-10deg
Frequency	22Hz
Gain	-3dB
Phase	90deg

Applied loads (under which the operating performances should be satisfied.):

Static airload	0.1Nm
Dynamic load	0.01Nm/deg
Inertia of the control surface	5.6*10^-5kgm^2

Pulsed Air High Performances Valves Improve Aerodynamic Flow Over Airplane Wings

C. Bouchet, C. Belly, M. Fournier, F. Claeyssen
Cedrat Technologies SA, Meylan, France
F. Ternoy, A. Choffat, J. Dandois, M. Pruvost, Q. Gallas
ONERA, Lille, France

Abstract:
The objective of the European Cleansky project is to develop new technologies for future aircraft enabling a 20-30% fuel burn reduction and related CO2 emissions and a similar reduction in noise levels compared to current aircraft. One of the ways to reach this goal is to improve the aerodynamic performances of current high lift devices. Active flow control is unanimously seen as the best mean to reach this objective. By suppressing flow separation and/or delaying stall, active flow control will increase wing aerodynamic performances. The partnership between CTEC and ONERA in the framework of the VIPER project has led to the design, manufacturing and test of an innovative pulsed jet actuator based on a CTEC amplified piezo-actuator (APA). Its aim is to provide a pulsed sonic jet up to 500Hz with a mass flow around 34 g/s through a slot 1mm wide and 80mm long. Coupled with CTEC SA75D switching power amplifier this actuator produces the expected sonic jet with an electrical consumption around 40W thanks to energy recovery. The results of the actuator characterisation (mechanical, fluidic) are presented in this paper.

Keywords: Pulsed Blowing Actuator, Piezoelectric Actuator, Fast Piezo Valve, Active Flow Control, Switching Power Amplifier.

Introduction

The main objective of European research in aeronautics is to reduce the fuel burn and environmental impact of current aircrafts by improving their aerodynamic performances. One of the means to fulfil this target is to control the airflow around the wings, rudders, etc. At high angle of attack, the apparition of flow separation decreases the aerodynamic performances on two aspects: the lift is reduced and the drag is increased. Therefore, the main objective of active flow control is to keep the flow attached on the largest part of the wing.
Several techniques are investigated to control the flow. In the framework of the VIPER project, a pulsed blowing jet is studied (see Fig. 1). This kind of actuator uses the engine bleed air and blows it along the span which allows a delay or a suppression of flow separation. The air which is blown through the actuators adds energy to the boundary layer and prevents it from separating from the wing.

Fig. 1: *Concept of blowing to suppress flow separation.*

VIPER actuator features

Many pulsed jets actuators have been designed and tested in the past. VIPER actuator is innovative because:

- The mass flow rate reached is the highest one obtained on an actuator within this volume (more than 420g/s per meter span at 500Hz);
- The improved efficiency when the actuator is coupled with CTEC switching amplifier SA75D;
- The high power density of the actuator;
- The enduring lifetime.

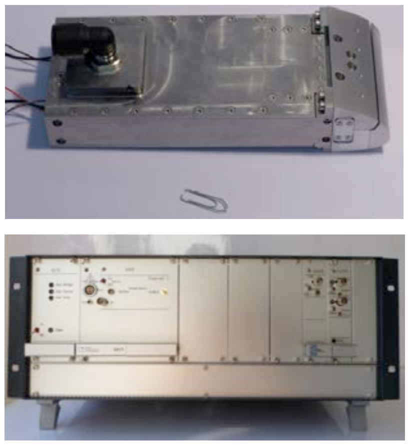

Fig. 2: *VIPER pulsed jet fluidic actuator and its driving electronic SA75D (lab version).*

The fact that the motion is created with piezo ceramics makes it very interesting in terms of bandwidth, compacity and weight.

In parallel to the actuator development, CTEC has designed a specific switching power amplifier called SA75D. This power amplifier is very efficient. Its

Active Vortex Generator Deployed On Demand by Size Independent Actuation of Shape Memory Alloy Wires Integrated in Fiber Reinforced Polymers

M. Hübler, S. Nissle, M. Gurka
Institute für Verbundwerkstoffe GmbH, Kaiserslautern, Germany
J. Wassenaar, DG Flugzeugbau GmbH, Bruchsal, Germany

Abstract:
Flow control functions are often required in areas where construction space as well as weight is premium. Furthermore, there is a huge range of control surface sizes, beginning with large-scale rudders like ailerons with some meters of length down to small-scale control surfaces like trimming tabs or vortex generators with some centimeters of size. An actuation principle covering all these applications needs to be highly scalable. However the current state of the art actuator-mechanical system solution is strongly limited. Active hybrid structures, combining the actuation of shape memory alloys (SMA) with fiber reinforced polymers (FRP) on the materials level, provide a scalable actuation principle with high lightweight potential. Also the compact design requires less construction space and makes the integration in the aircraft system simple. Being one of the first applications of active hybrid structures from SMA and FRP, the presented active vortex generators help to demonstrate the advantages of this new technology. Commonly used high performance airfoils show minimum drag and maximum lift, but tend to suddenly stall due to flow separation at low air speed. New active vortex generators, deployed only on demand at low speed, can help to overcome this contradiction without any drawback for cruise flight.

Keywords: Shape Memory Alloy, Fiber Reinforced Polymer, Vortex Generator, Aircraft, Adaptive Structures, Active Flow Control

Introduction

A high number of control surfaces are used to adjust and optimize the aerodynamics of aircraft, especially with fixed-wing aircrafts. These control surfaces are commonly rotated and/or moved by a mechanical system. Most often these complex systems require space and add weight. Due to the localized load transfer between a dedicated actuator and the entire control surface, additional effort is significant. This strongly limits the implementation of control surfaces, and thus a high number of aerodynamic important surfaces are realized in a static manner. The static design therefore represents only the optimum aerodynamic shape for a certain flight situation, for all other situations a worse performance is the consequence. Examples for static design elements which could increase the performance by a situational adaption are e.g. winglets, vortex generators, the wing profile, engine air in- and outlets. [1-7]

A new and innovative actuation principle, based on integrated solid state actuation elements enables the implementation of new functions such as the above mentioned situation adapted aerodynamics. With so-called active hybrid structures the mechanical system is simplified and the required construction space as well as the additional weight is strongly reduced. There is no need for mechanical couplings and hinges with the integrated approach. Furthermore, scalability is given, as the size of the control surface can be increased and reduced arbitrarily without paying attention to performance limits of a certain actuator, coupling and/or hinge. However, only the complete integration of the actuating element on a material level enables the full potential of weight and space saving.

Vortex generators (VGs) are not widely used in aircraft systems today as the static design leads to significant disadvantages. VGs are responsible for stabilization of the flow at high angles of attack and low air speed. Therefore, the application of static VGs as well as their omission is always a compromise, not able to give the optimal performance on all flight states (e.g. cruise – take-off and landing). VGs are small elements about the size of a stamp (2x2 cm^2), commonly installed on the wing surface in a large number. They protrude the laminar boundary layer and generate a stabilized air flow. Therefore, airflow separation is suppressed and the aircraft is controllable even at lower air speeds and higher angles of attack. Without them, the aircraft tends to stall more suddenly, while the minimum possible speed e.g. for take-off and landing is increased. However, additional drag is the consequence of the use of VGs, challenging the efficiency of cruise flight. An adaptive solution able to deploy the VGs on demand can optimize the aerodynamic performance for all flight states: maximum performance for cruise flight with minimum drag – maximum safety and reduced noise at take-off and landing at minimum

New Rating Life Calculation for Rolling Elements on Aircraft

T. Münzing, H. Binz
Universität Stuttgart, Stuttgart, Germany
S. Seemann, M. Christmann
Airbus Group Innovation, Ottobrunn, Germany
S. Toro, Umbra Cuscinetti S.p.A., Foligno, Italy

Abstract:
An innovative sizing method for rolling contact drivetrain elements addresses the adverse combination of very little angular motion and dynamic loads or vibrations. This is a typical challenge for aeronautical ball screws for which conventional bearing standards are not fully valid and no other method exists. Conservative sizing is to the detriment of weight and operating cost. The new method takes small oscillation angles into account and has substantial weight saving potential. Validation testing is currently being performed with promising results.

Keywords: Ball Screw, Aircraft, Life Rating, Wear, Fatigue, False Brinelling, Validation

Introduction

An innovative sizing method for Rolling Contact Drivetrain Elements (RCDE) in aircraft mounted transmission components, e.g. ball bearings and ball screws, has been developed. Work has been carried out by University of Stuttgart, Umbra Cuscinetti and Airbus Group Innovations in the perimeter of the Clean Sky SGO HEMAS Project and the associated Partner Project DREADS.

On today's certified rotary and fixed-wing aircraft a large variety of RCDEs is in use. This encompasses subsystems such as engine, primary and secondary flight controls, doors and landing gears, among others [1]. Positioning profiles, exerted loads and failure modes vary among the applications.

The commonly applied standard sizing is based on the theories of Palmgren and Lundberg [2]. This is based on the assumption of a continuous rotary motion generating a stable lubricant layer. This lubrication prevents wear mechanism such that the critical failure mechanism to be regarded is fatigue.

There are several aircraft applications where this assumption is not fully valid. Especially actuation systems show motion profiles with intermitting motions or even standstill and superposed dynamic load affections. In this context, a critical application is the primary flight control system of a helicopter, typically positioned by means of swashplate actuation – as introduced for instance in [3].

Technical Motivation

For many rolling elements operating on aircraft vibrating loads coupled with no or very small angular displacements are the most challenging condition. Particularly electromechanical actuators (EMA) are typically subject to significant levels of dynamic load and speed reversals at very little angular motion. This is in contradiction to the conventional life calculation according to commonly applied standards, e.g. ISO 3408 for ball screws, assuming constant load distribution and sufficient lubrication through continuous rotary motion [4]. Therefore the conventional sizing method is only valid for a limited range of environmental and operating conditions.

As a consequence, aviation industry applies commonly accepted safety factors established thanks to empirical data. Moreover, substantial maintenance is carried out to ensure early in-service detection of component wear mechanisms prior to failure. This may over-fulfil safety targets whilst limiting design options and leads to a detrimental impact on weight and operating cost.

Reference Application

The application in scope is an EMA for swashplate actuation. It is equipped with a commercial off-the-shelf (COTS) aeronautical ball screw assembly. The sub-assembly is characterized by highly wear and corrosion resistant steel screw shaft and nut, standard steel balls and typical aerospace grease lubrication.

Fig. 1: *Aeronautical ball screw assembly*

Elastomers for Dielectric Electroactive Polymer Applications (Review)

A. Köllnberger, Wacker Chemie AG, Burghausen, Germany
H.F. Schlaak, Technische Universität Darmstadt, Darmstadt, Germany

Abstract:
After more than 15 years of research and industrial development, Electroactive Polymers (EAP) show a large variety of materials and functional principles. They are commonly classified in two major families: ionic EAPs, activated by an electrically-induced transport of ions, and electronic EAPs, activated by electrostatic forces. Electronic EAPs consist of piezoelectric polymers, electrostrictive polymers, dielectric elastomers, liquid crystal elastomers. In the field of Dielectric Elastomers (DE) large progress in materiel, fabrication technologies and devices has been demonstrated. Dielectric Elastomer Transducers (DET) are applicable in three modes of operation as sensors, actuators and generators. For all of them, the dielectric layer plays a decisive role. This overview describes the path from research to industrial applicability. The chemistry, physical molecular networks and properties of elastomers as well as industrial aspects of manufacturing play a key role in the future success of this technology.

Keywords: Dielectric Elastomers, Electroactive Polymers, Silicone

Introduction

Polymers that change their shape under the stimulus of electricity (voltage or current) are defined to be electroactive polymers. Wilhelm Conrad Röntgen was the first to show the effect by applying spray-on electrodes on a natural rubber band which was fixed on the top end and pre-stretched by a weight on the other end [1] [2]. The research activities in that field increased in the 1990s and many researchers worked on the basis, the materials and the possible applications [3]. A categorization into two major groups - ionic and electronic EAPs – can be made by the different mechanism that drive actuation. The transport of ions and/or molecules in the ionic EAPs or electrostatic forces in the electronic EAPs can be used to transform electrical into mechanical energy [4]. *Fig. 1* illustrates the classification of EAPs including subcategories.

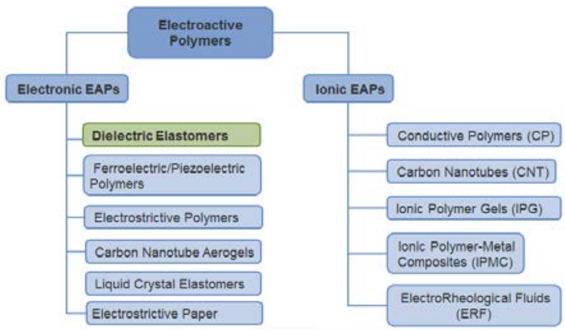

Fig. 1: *Classification of EAPs*

A detailed description of each subcategory can be found in various literature including [5]. Electronic EAPs are generally driven by an electric field and the mechanical response of those systems depends dominantly on the field strength squared. For this reason, the devices built have to be operated at an electric field as high as possible. The driving voltages behind are typically in the range of 500 V to 10 kV [6] [7] [8]. The focus of this paper will be on dielectric elastomers, which are classified by actuation stress and actuation strain in *Fig. 2* [9].

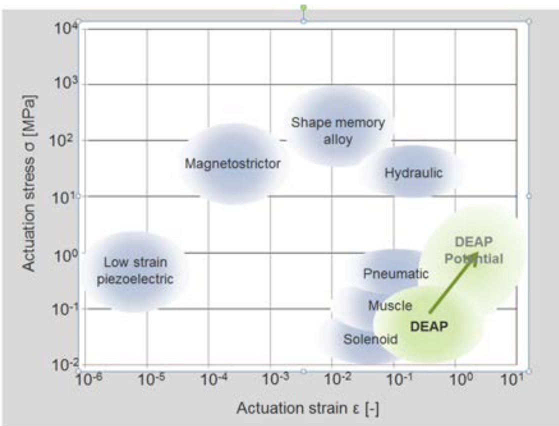

Fig. 2: *Classification of actuators*

Dielectric elastomers

The advantages of that promising class of materials are:

- Large stroke
- High energy density
- Elastic, flexible
- High actuation speed
- Proportional mode
- Lightweight
- Silent
- All environmental conditions
- No rare earth

Customized Dielectric Elastomer Stack-Actuators Under Consideration of Application Specifications

B. von Heckel, H. Bochmann, T. Hoffstadt, J. Maas
Hochschule Ostwestfalen-Lippe, Lemgo, Germany

Abstract:
Multilayer stack-actuators based on dielectric elastomers offer a considerable amount of deformation and force generation with a comparatively high energy density. In order to design such an actuator in accordance with the specifications of a certain application, a design tool is proposed. This tool considers constraints for the design of a DE stack-actuator, e.g. due to inactive areas or the influence of mechanical interfaces required for the integration into an application. The Design tool is validated via FEA and experimental tests. Finally, the characteristics of prototype actuators produced with different materials are rated in terms of static and dynamic characteristics.

Keywords: Dielectric Elastomer, Multilayer Stack-Actuator, Electroactive Polymers

Introduction

Dielectric elastomers (DE) consist of thin elastic films coated with stretchable conductive electrodes on their opposing sides. They offer a considerable amount of deformation and force generation. Thus, they have high potential for sensor [1], generator [2] and actuator [3] applications. The actuation principle is based on the electrostatic pressure σ_{el} that deforms the elastomer when a voltage v_p is applied and is given by

$$\sigma_{el} = \varepsilon_0 \cdot \varepsilon_r \cdot \frac{v_p^2}{d^2} = \varepsilon_0 \cdot \varepsilon_r \cdot E^2, \qquad (1)$$

where ε_r is the relative permittivity and d the layer thickness of the DE. Currently available elastomers allow operating electrical fields E around 50 V/µm. Thus, for 50 µm thick layers the operating voltage amounts to 2.5 kV. In order to increase the total contraction, many DE films are laminated to multilayer stack-actuators. Due to the operation principle such actuators contract themselves when a voltage is applied. Thus, in order to transmit tensile forces mechanical interfaces have to be applied on both ends of the actuator. However, these mechanical endcaps impede the planar expansion of the actuator and thus, decreases the total deformation. Therefore it is not useful to mount two mechanical interfaces by default. If the actuator is precompressed only one respectively none mechanical interface is enough to use the actuation of the actuator. Within this publication the design of customized actuators for specific applications is dealt with. For this purpose, the automated fabrication process and the model-based design via FEA and analytical methods are described. For validation the theoretical models are compared with experimental test results.

Actuator Design and Manufacturing Process

DE multilayer stack-actuators consist of several DE films with stretchable electrodes applied in the centre, see Fig. 1c [4] ,while the surrounding insulating area prevents arcing during actuation. The DE films are stacked to the intended height, alternating the direction of the contact tab by a rotation of 180°. Thus, the contact tabs of the electrodes are available on two opposing sides and are contacted with an elastic contact stripe, see Fig. 1b. The transmission to a stiff wiring can be realised by rolling in a wire in the contacting film and fixing the compound at the bottom of the actuator (if possible in a mechanical interface). Depending on the application specification mechanical connections can be applied on both ends of the stack compound. Finally, the actuator is encapsulated with an elastomer film, to protect it against environmental influences and touching, see Fig. 1d. In order to produce the DE stack-actuators with reproducible

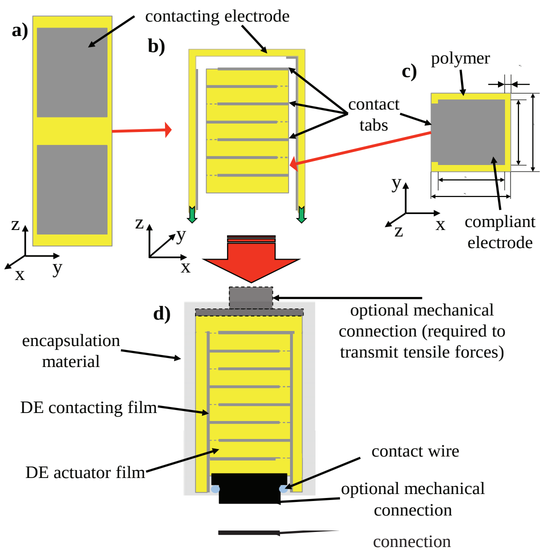

Fig. 1: Multilayer actuator consisting of DE films c) that are stacked on each other b) and contacted with a contact stripe a). Finally, optional mechanical connections are applied and the actuator is encapsulated by an elastomer d).

A Compact High-Force Dielectric Elastomer Membrane Actuator

S. Hau, Universität des Saarlandes, Saarbrücken, Germany
A. York, Parker Hannifin Corporation, Sunnyvale, USA
S. Seelecke, Universität des Saarlandes, Saarbrücken, Germany

Abstract:
Dielectric Elastomer actuators (DEA) show high potential for lightweight, energy efficient and scalable systems. Dielectric elastomer (DE) stack actuators are known to provide high forces and low strokes while compared to DE membrane actuators, which combined with an appropriate biasing mechanism provide relatively lower forces but higher strokes. This work combines the advantages of both concepts by stacking layers of DE membrane actuators. To maintain a compact overall size the biasing mechanism is embedded in the inactive center of the DE membrane actuator stack. Two actuator systems are built. One lifts 7.5 kg while the second one is able to generate 66 N of force at a stroke of 2.25 mm, respectively. These advances enables DE actuators to compete with solenoid actuators in performance and have the advantage of consuming significantly less energy during typical operation.

Keywords: Dielectric Electroactive Elastomer (DEAP), Dielectric Elastomer (DE), Actuator, High Force Actuator, Manufacturing, Membrane Actuator, Cone Actuator, Diaphragm Actuator

Introduction

In principal dielectric elastomer transducers (DET) are flexible capacitors. They consist of an elastomer film sandwiched between two compliant electrodes. Applying a mechanical load onto them leads to a compression of the elastomer which results in a capacitance change. Utilizing this effect, DETs can be used as a sensors. Conversely, DETs can be also used as actuators. When high voltage is applied to the electrodes, the elastomer is squeezed together by electrostatic forces called Maxwell pressure (Fig. 1).

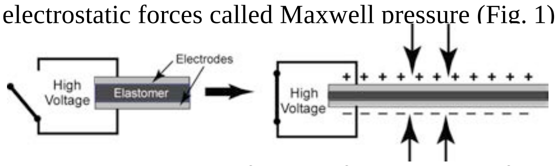

Fig. 1: *Dielectric EAP before and after application of high voltage. Applying a voltage squeezes the elastomer with electrostatic forces which leads to an increase in area.*

Several different concepts have been proposed to utilize such changes in shape for manufacturing actuators. One type are stack actuators, consisting of several layers stacked on top of each other. An applied voltage compresses each layer and thus contracts the entire stack. Kovacs et al. [1] presented such an actuator capable lifting 2.6 kg approx. 1.5 mm. Another type are roll actuators, at which the elastomer film is wrapped up into a roll. Applying a voltage to this kind of actuator leads to a radial stress within the film, thus an axial elongation. For this actuator type, Pei et al. [2] reported a performance of up to 21 N with a stroke of approximately 10 mm. A third DEA type are membrane actuators. In their basic concept, they are using only a single layer of elastomer which is clamped at its ends. Actuating with a voltage causes a lateral expansion of the membrane. This concept separates into two subsets. First, in-plane motion actuators like the one presented by Kofod et al. [3], which lifts a maximum mass of 670g. Secondly, Wang et al. [4] presented a three layer out-of-plane (also called cone or diaphragm) actuator with a stroke of up to 17 mm or a maximum blocking force of 5 N.

This paper deals with circular membrane actuators similar to the ones previously mentioned, and also investigated in the work of Hodgins et al. [5]. Studies of the influence of the geometry on the actuator performance (stroke and force output) [6] and simulation results using the model proposed by Rizzello et al. [7] have shown the potential to push the force output of these actuators up to high double-digit newton range and beyond when combining them with an appropriate biasing mechanism. An overall concept, starting with the DE manufacturing and ending with a complete integrated actuator, is presented. Finally, the actuator is tested in terms of force and stroke output.

Actuator Design and Manufacturing

The DE membrane actuators investigated in this paper consist of a silicone membrane sandwiched between compliant electrodes and a rigid frame material with an annular opening (Fig. 2). When an appropriate biasing mechanism is pushing on the rigid frame center, these actuators generate an out-of-plane motion.

Hau et al. [6] have shown that it is possible to influence the stroke and force output by varying the inner and outer radius of the annular electrode ring. A bigger ring width leads to a higher stroke while the force output is reduced, and vice versa when reducing

Magneto-Active Polymer Actuator

A. Diermeier, D. Sindersberger, G.J. Monkman
Ostbayerische Technische Hochschule Regensburg, Regensburg, Germany

Abstract:
Magneto-active Polymers (MAP) are closely related to magneto-rheological fluids in that they contain magnetic micro-particles. However, instead of being freely suspended in a carrier fluid they are physically bound within a highly elastic polymer-matrix. The application of an external magnetic field allows changes in the mechanical properties, such as elastic and shear moduli, of the composite material to be achieved. The colossal magneto-rheological effect has been shown to demonstrate changes in Young's modulus by over 1E6 %.
Current research concentrates on controllable compliance and the resulting shape memory properties of MAP. This paper deals with recent advancements in this respect, including tubular magneto-active devices with potential applications in medical and other technology.

Keywords: Magneto-Active Polymer, Magnetorheology, Magnetodeformation

Introduction

Magneto-active Polymers (MAP) are rapidly becoming an established class of hybrid smart materials. Homogeneity of particle distribution and specific elastic properties of the matrix are achieved by special fabrication processes [1].

The influence of an external magnetic field can produce changes in Young's modulus of over 1E6 % (colossal magneto-rheological effect) [2]. In addition to dramatic changes in mechanical storage and loss moduli, changes in electrical properties are also measurable. In addition to various additives, MAP can be made using both soft and hard magnetic particles where pre and post cure magnetization is possible [3,4].

Hitherto, the main focus of research has been on improving MAP fabrication processes, particularly in terms of reproducibility and macro-, meso- and micro surface structuring [5]. Rheological characterization of MAP is achieved through oscillating rheological measurement techniques while confirmation of magnetic particle distribution homogeneity can be achieved through three-dimensional computed X-ray tomography [6].

Current research concentrates on controllable compliance of MAP volumes. Depending on the degree of magnetic field homogeneity, together with the colossal magneto-rheological effect, contributions from both magnetostriction and magnetodeformation are observed [7].

This paper deals with recent advances in MAP applications in many fields including bio-medical, automation and controllable geometry.

Prior Art

Magnetorheological fluids (MRF) have been used in actuators for many years. Typical applications include damper systems [8], clutches for torque transfer [9,10] or braking systems [11].

In contrast to MRF, the magnetic particles in MAP are embedded into an elastic matrix structure which avoids sedimentation problems associated with MRFs, whilst maintaining homogenous particle distribution. This offers new actuation possibilities such as the retention of complex shape geometries. Nevertheless, MAP damping characteristics remain of interest in field concerning controlled viscoelastic behaviour [12].

The combination of piezoelectric devices with MAP allows a high energy conversion rate by adjusting the MAP load through a controlled magnetic field [13]. MAP also finds applications in pneumatic valve systems for air flow control. In this invention an annular shaped magnetoactive elastomer (MAE) body expands radially through the influence of an applied magnetic field thus closing the gap between MAE and the valve body [14]. In a similar manner, the aim of this research is to establish and control hydraulic flow by MAP driven systems.

Material

MAP is a composite material essentially comprising two components: a polymer matrix and a suspension of magnetically susceptible micro-particles. Many different polysiloxanes, also commonly known as silicone, may be used for the matrix. Silicones are available with different hardnesses and viscosities. Modification and handling of silicone is simple and inexpensive. However, other polymers/elastomers, such as polyurethane [15] may also be utilised. In this work, the industrial two component silicones “Sylgard” (Dow Corning), Elastosil RT60 (Wacker), SF00 and SF13 (Silikonfabrik.de) are used. Commercially available products offer the advantage of stable reproducibility when using

Haptic Actuator Based on Magnetoactive Polymers

H. Böse, W. Hartmann, J. Ehrlich
Fraunhofer ISC, Würzburg, Germany

Abstract:
A new haptic actuator based on magnetoactive polymers (MAP) and hydraulic force transmission is described. It consists of a magnetic circuit with inner and outer yokes having cylindrical symmetry and a coil which generates the magnetic field. The haptic actuation effect is caused by a disk of MAP material which is attracted by the inner yoke of the magnetic circuit when the electromagnet is activated. The deformation of the MAP disk pushes a hydraulic liquid through a channel in the inner yoke and bulges a passive elastomer membrane at the other side of the actuator, which can be perceived with a finger touching the membrane. A demonstrator of the haptic MAP device was designed, the magnetic circuit was simulated and the device was manufactured and tested. The maximum displacement of the passive membrane in the activated state was measured as nearly 1,5 mm. The response time of the activation and deactivation of the actuator was determined as about 10 ms.

Keywords: Magnetorheological Elastomer (MRE), Magnetoactive Polymer (MAP), Haptic Actuator

Introduction

With the progress of existing and the introduction of new human-machine interfaces, haptic feedback becomes more and more important. If a user controls a technical function on a flat panel with his hand, he wishes to feel a tactile response on the finger which touches the panel, in order to get the confirmation that his intended action was executed.
Various technologies already exist or are being developed, which are capable to supply haptic or tactile feedback. In most cases, electromagnetic drives accelerate a movable mass. This motion causes an impact on the panel, which the user can feel on his finger. It was demonstrated that such haptic feedback can also be generated by dielectric elastomer actuators (DEA) in connection with a smartphone. However, this kind of haptic feedback is generally very unspecific, because it excites the whole display or panel mechanically.
In some applications, it would be more advantageous, if haptic feedback could be locally generated. In this case, the haptic sensation is triggered only at the location of the finger. Approaches for localized haptic feedback have also already been demonstrated with DEA. Mößinger et al. described a tactile feedback device with local resolution using specially shaped DEA [1]. Carpi et al. presented another device, in which a thin film DEA causes a deformation at the backside of a panel. This deformation is transmitted with a hydraulic medium to the front side of the panel, where the user can feel the deformation of a passive membrane [2]. An advantage of this approach is the location of the active DEA film with high voltage, which is remote to the touchable front surface.
Comparable deformations of soft membranes can also be generated with another class of smart elastomers, named magnetorheological elastomers (MRE) [3]. They consist of magnetic particles which are embedded in an elastomeric matrix [4, 5]. By applying a magnetic field, the composite material reversibly changes its mechanical properties like the Young’s and shear modulus.
If the elastomer matrix of the composite is sufficiently soft and the applied magnetic field is strong enough and inhomogeneous, the MRE material is also capable to actuate [6]. In an inhomogeneous magnetic field, the material is deformed and changes its shape or geometrical dimensions. Therefore, MRE composites which reveal such an actuation effect are also named magnetoactice polymers (MAP), in analogy to electroactive polymers (EAP, which are driven by an electric field. A MAP body can be strongly deformed in the magnetic field. It was demonstrated, that deformations of ca. 10 % can be achieved [6].
Flexible magnetoactive polymers are also capable to perform more complex motions in a magnetic field than it is possible with rigid bodies. In contrast to a voice coil, in which a magnetic body moves linearly with respect to the coil, driven by a magnetic force, a ring-shaped MAP body can radially be deformed by a magnetic field, which is applied between concentrically arranged inner and an outer yokes.
This radial deformation of MAP materials has already been shown to be useful for various applications. In [7] a valve mechanism was introduced, where the radial deformation of a MAP ring in a magnetic field controls the flow rate of an air flow. The clamping effect of MAP rings can even be used to realize an inchworm actuator which moves a rod over principally unlimited distance [8]
The objective of this work is to demonstrate that MAP materials can also perform linear motions and are very useful for haptic applications. After a short explanation of the work principle of the haptic actuator, the magnetic circuit with the magnetic field distribution is described, followed by the actuator design, the construction and the results of

Magneto-Rheological Elastomer Actuators for a Reconfigurable Joystick

J. Bilz, Technische Universität Darmstadt, Darmstadt, Germany
H. Böse, Fraunhofer ISC, Würzburg, Germany
M. Kupnik, C. Hatzfeld
Technische Universität Darmstadt, Darmstadt, Germany

Abstract:
Reconfigurable interfaces offer new prospects for intuitive human-machine-interfaces. In this paper, we investigate the design and application of magneto-rheological elastomer (MRE) based actuators for the use in a reconfigurable joystick. MREs consist of magnetisable particles, embedded in an elastomer matrix. Thus they provide a base elasticity. By using external magnetic fields, the storage and loss modulus can be manipulated. We developed two actuators, one with prominent elastic and one with damping characteristics. The development is based on a simplified material model, measurements and simulation. The actuators achieve forces up to 60 N, resulting in a reaction torque of up to 0.4 Nm. The damping actuator achieves a loss modulus increase of 82 kPa.

Keywords: Magneto-Rheological Elastomer (MRE), Reconfigurable Joystick, Material Model, Elasticity and Damper

Introduction

Reconfigurable joysticks are used in human-machine-interfaces to achieve better intuitive feeling in operation [1].
State-of-the-art systems often use conventional actuators or springs combined with brakes. The springs generate restoring torques towards the null position. Brakes allow higher reaction torques opposing the user's movement. Latter improves the haptic quality of contact with hard objects. Examples for actuator combinations include pneumatic actuators and magneto-rheological fluid (MRF) brakes [2], DC motors and particle brakes [3], as well as springs and MRF brakes [4]. Magneto- and electro-rheological fluids offer a short reaction time, but are prone to sedimentation. Pneumatic actuators and DC motors can generate high reaction torques, regardless of the current angle of the joystick, but are quite costly.
We use magneto-rheological elastomer (MRE) actuators, integrated in the commercial joystick J2 by Co. elobau (elobau, Leutkirch i.A., Germany), to obtain spring and brake characteristics and to avoid these drawbacks. MRE consist of a magnetisable filler material (mostly iron particles), embedded in an elastomer matrix and are therefore not prone to sedimentation while the advantages, such as fast response time and large reaction forces, remain. Furthermore the manufacturing process of MRE is cost-effective.
The particle arrangement in the MRE can be controlled by applying an external magnetic field during the curing time of the elastomer. The embedded particles will form chains and align themselves in an anisotropic order. Curing without an external field leads to an isotropic particle distribution.
In a field-free state, the resulting composite material shows a domination of the polymer properties. When exposed to an external magnetic field, the properties of the embedded magnetic particles prevail. Therefore, physical properties can be tuned via the flux density.

Functionality of MRE and requirements for the actuators

The properties of the flexible matrix (mostly silicon rubber) lead to a composite material with an always existing elasticity and internal friction. In [5] the characteristics of MRE are described as a change in the complex shear modulus, where the storage modulus G' (proportional to the Young's modulus) as the real component describes the stored deformation energy. The loss modulus G'', as the imaginary component, describes the viscous friction. This representation is commonly used to describe hyper-elastic materials such as elastomers and MRE. When exposed to external magnetic fields, both storage and loss modulus increase, resulting in a stiffer material with increased inner friction.
In order to achieve an intrinsic safe design as it is specified in [9] with good haptic quality, MRE actuators with tuneable stiffness and friction are required. A separation and individual tuning of these characteristics using only the strength of the field as the manipulated variable is not possible. Applications with individual control of stiffness and friction could not be found in the state of the art.

According to [5] and [6], changes in composition and manufacturing of the MRE alter the physical properties in terms of elasticity and damping when

Plasticized-Polymer Actuators with Colossal Dielectric Constant – Electro-Mechanical & Electro-Optical Functions

T. Hirai, Shinshu University, Ueda-shi, Japan

Abstract:
Conventional polymers, such as polyvinyl alcohol, poly vinyl chloride (PVC), etc., used in textile industries have been considered electrically inactive. However, they can be very efficient electrically active actuators with huge strain and swift motion by softening with dielectric solvents or plasticizers. In these soft matter, the deformations are not induced by swelling and deswelling. The concept can be applied to not only elastomers but also stiff crystalline polymers. Deformation has varieties such as contraction, creeping, and folding. Particularly, plasticized PVC turned out to be highly potential actuator material. It shows colossal value of dielectric constant in low frequency range. The value reaches 1000 times larger than those of the component materials. The colossal value is suggested to be originated from the cooperative interaction between PVC and plasticizers. The function is not limited only to electro-mechanical, but also be extended to electro-optical function.

Keywords: Plasticizer, Soft Actuator, Gel, Elastomer, Colossal Dielectric Constant, Dielectric Polymer

Introduction

Conventional polymers, such as poly(vinyl alcohol) (PVA), poly(vinyl chloride) etc. are known to be electrically inactive and considered insulating polymers. We, however, found these polymers can be converted into efficient electrically active actuators. Of course, in the form of highly swollen polymer gels, they can be actuator through swelling and deswelling. But actuators with swelling or deswelling processes can not be practical conventional use, since they can only be actuated under the presence of solvent, and cannot be actuated without the presence of solvent. On the other hand, non-solvent nonionic polymers are usually, stiff and difficult to be deformed by applying a dc electric field. They are usually good electrical insulator with low dielectric constant. These polymers are usually dielectric and are miscible to dielectric solvents and plasticizers, and are also electrically inactive. What we found is that these dielectric gels and soft plasticized-polymers can be deformed by applying a dc electric field with huge deformation and swift response time, quick enough for conventional use.[1] Not only the electro-mechanical functions but also electro-optical function was observed in the soft dielectric materials.[2] We propose these functions based on the colossal dielectric constant observed in the low frequency range. These findings might lead novel application field for conventional soft dielectric polymer materials, such as actuators.

Experimental

Materials

PVA gels: Poly(vinyl alcohol) gels were prepared by chemical crosslinking with glutaraldehyde. The reaction was catalyzed by HCl. The degree of crosslinking was controlled by reaction time. This was also possible by controlling the concentration of gutaraldehyde. Delicate condition was necessary for attaining the desirable crosslinks. The reaction is carried out in aqueous solution. After the reaction the gels were subjected in the solvent exchange from water to dimethyl sulphoxide (DMSO). After the several time of the solvent exchange process, the samples were served for measurements. The gels were not durable in air for long time. Solvent leakage is observed, and actuator performance is observed usually for several hours, but can be recovered in soaking in the solvent for a couple of hours.
PVA gel actuator: For contractile actuator, metal electrodes, such as aluminum, stainless steel, etc., can be used. We usually use aluminum plates. For bending actuator, we employed thin gold sheets as electrodes. The thickness of the sheet is 200 nm.
For crawling actuator, the gel was placed on a glass plate on which thin stripes of aluminum sheets were aligned, and the gels were placed on the alignment.
PVC gels: In this paper plasticized PVC is denoted as PVC gel, since the plasticizer content is mostly larger than 60 % by weight. Plasticizers employed were mainly phthalates and adipates. The gels were not plastic under the experimental conditions, and can hold their shape under the operations. PVC was dissolved in tetrahydrofran (THF) solution with the plasticizers, and casted in a Petri dishes of Teflon. After removing THF by evaporation, the transparent gels were obtained. PVC gels were stable in air for a couple of years depending on the plasticizer and its content. PVC gels are plausible for practical use at a moment.
PVC gel actuator: For observing creep deformation and folding deformation, the electrodes are metal plates. We mainly employed aluminum plates. Effect

Recent Developments in Shape Memory Alloys (Invited Review)

H.J. Maier, Leibniz Universität Hannover, Garbsen, Germany

Abstract:
Shape memory alloys (SMAs) feature unique properties, which make them attractive for various applications. Yet, there are certain drawbacks such as difficult processing or expensive constituents, which hinder their widespread use. A case in point is NiTi-based SMAs, which are widely employed in the biomedical field, but are rarely used outside this niche.

Lately, however, the extensive research conducted by various groups has resulted in substantial progress and new effects can now be exploited. This overview will address some of the recent developments in this exciting field. One area of research is Fe-based SMAs, which have attracted a lot of recent attention due to their better workability and lower processing costs as compared to NiTi. On the other hand, ferromagnetic Ni- and Co-based SMAs feature additional functional behavior that may be exploited for new applications. Finally, high-temperature SMAs are of great interest as new alloys have become available that do not rely on substantial amounts of noble elements.

It appears that processing issues and microstructural instability are the major roadblocks that need to be overcome in all these alloys. Specifically, data from detailed electron optical characterization combined with mechanical tests revealed that the dominant functional degradation mechanism can vary substantially in the different SMAs. The ramifications of these findings with respect to applications will be discussed and directions for future research will be pointed out.

Keywords: Shape Memory Alloys, Martensite Stabilization, Magnetocaloric Effect, Elevated Temperature, Functional And Structural Degradation

Introduction

Phase transformations in shape memory alloys (SMAs) have been studied extensively over the last decades as these materials display unique mechanical properties. Moreover, their specific energy density, i.e. the work output, outperforms most conventional actuators. Consequently, much effort has been put into developing new SMA applications. In fact, as pointed out in a recent review by Jani et al. the number of publications and patents in this field has drastically increased in recent years and the global market for smart actuators has been forecast to reach USD 25.4 billion by 2016 [1]. There are, however, certain drawbacks such as difficult processing, insufficient microstructural stability or expensive constituents, which hinder the widespread use of these alloys. The current paper will highlight some more recent developments in metallic SMAs from a materials perspective. For more extensive overviews that also include other matrices, see Refs. [1-6].

Fe-based SMAs

Early on, Fe-based SMAs such as Fe-Mn-Si have been viewed as promising candidate materials for the mass market as these feature better workability and lower processing costs as compared to NiTi, e.g. [7]. Unfortunately, experimental data revealed that most of the Fe-based SMAs that feature an fcc to bct phase transformation display only very low transformation strains. However, in a more recent study, very high recoverable superelastic strains of up to 13% under tensile loading were demonstrated for a FeNiCoAlTa SMA in single cycle tests [8]. In this system, the matrix was hardened by nano-sized, coherent γ’-precipitates, which curtail dislocation slip, and transformation strains reported approach the theoretical limit. To further strengthen the matrix against functional degradation upon cyclic loading, higher volume fractions of the γ’-precipitates are needed. These non-transforming particles will, however, substantially reduce the macroscopic transformation strain [9].

Clearly, minimum functional degradation upon cyclic loading is a key issue in most applications. This in turn calls for a microstructure that provides for minimum dislocation activity and ease of crystallographic reversibility of the martensitic transformation. In the FeNiCoAlTa system, the nano-sized precipitates can be easily tailored by heat treatment. As shown in Fig. *1* for single crystals, shorter aging times, i.e. finer particles, result in substantially improved cyclic stability. As best demonstrated by the sample aged at 700 °C/7h, most of the residual strain is accumulated early on (Fig. *1*a). By contrast, the sample heat treated at

Advances in NiTi-based SMA for Actuators

A. Coda, L. Fumagalli
SAES Getters S.p.A., Lainate, Italy

Abstract:
Shape memory alloys (SMA) are known to be multifunctional materials which can be naturally considered as sensor-actuator elements, demonstrating large possibilities for applications in high-tech smart systems. The fascinating property of shape recovery allows generating large work outputs particularly in small dimensions. Upon miniaturization, intrinsic advantages of these materials are maximized. Thus, SMAs are virtually predestined for applications in microsystems technology, which is rapidly evolving and it is not surprising that the most successful SMA products are nowadays in that field.
However, there are still a few limiting factors to a widespread diffusion of SMAs in some technological fields. The probably most debated aspect around NiTi alloys is microcleanliness considered as the main factor affecting functional and structural fatigue. This concept is becoming increasingly important as the industrial market moves to smaller, lower profile devices with thinner structures.
In this work a comprehensive microstructural and functional characterization of NiTi-based shape memory wires with diameter below 100µm is presented. Considerations about the effects of their nanocrystalline microstructure, as well as enhanced microcleanliness on the functional properties and fatigue behaviour are spent and discussed.

Keywords: Shape Memory, Functional Properties, Fatigue, Thin Wires

Introduction

Shape memory alloys (SMA) are functional materials with a multitude of properties interesting for technological applications. These properties depend on the peculiar deformation mechanisms, accounting for the shape memory effect, the superelastic behaviour and the damping capacity of these materials [1]. SMAs are used in different fields, like thermo-mechanical devices [2], anti-loosening systems [3], biomedical applications [4], mechanical damping systems, and in some cases employed for large scale civil engineering structures [5]. Over 90% of all shape memory applications make use of the binary NiTi alloy system. NiTi shows a very good combination of properties, especially in terms of energy density and the large amount of recoverable strain compared to other actuator principles. The obvious simplicity of mechanical design and minimum number of moving parts is amazing for an actuator and make SMAs particularly attractive for microsystems applications. Considerable progress was made thanks to integration and miniaturization of sensors, control electronics and implementation of intelligence by using integrated microcontrollers and specific software.
However, there are several design criteria that must be controlled to guarantee a widespread diffusion of SMAs to technological fields. For instance, SMAs display a narrow dependence of the shape-memory related properties, like transition temperatures, on their actual composition. For this reason, a great care in the production steps, mainly based on casting processes, is required. Another design criteria is the strong influence of thermo-mechanical history on their properties. This may disclose interesting perspectives of application to smart devices in which different aspects of the shape memory phenomenology, like one and two way shape memory effect, pseudoelasticity, damping capacity, etc., are used.
Currently, studies are mainly devoted to some aspects related to the material quality and behaviour enhancement. Among these, the improvement of thermo-mechanical fatigue represents with no doubts the most important one [6].
Fatigue of SMA is related to microcleanliness. The size and distribution of inclusions can play a critical role in affecting the fatigue behaviour and the quality of NiTi alloys used in components or products [7]. The Industry is investing lots of efforts to achieve the benefits of low-inclusions, while preserving strength and integrity of the material. This is becoming increasingly important as the medical and industrial markets move to smaller, lower profile devices with thinner structures.
In this work the outstanding fatigue behaviour of NiTi trained thin shape memory wires produced by a hard review of melting and thermo-mechanical processes will be presented and discussed.

Experimental

SmartFlex^{R} trained wires (Ti 51.0 ±0.05 at.%) with diameter of 25µm, 76µm, and 100µm were prepared with standard VIM-VAR approach and with a new combination of melting and thermo-mechanical process, modified to have smaller inclusions size.

Industrial Safety Systems Using Shape Memory Alloy Actuators

A. Czechowicz, I. Zwinscher, P. Dültgen
Forschungsgemeinschaft Werkzeuge und Werkstoffe e.V., Remscheid, Germany
B. Rachor, HEMA Maschinen und Apparateschutz GmbH & Co. KG, Seligenstadt, Germany

Abstract:
Shape memory alloy actuators (SMA) have the ability to change into an imprinted shape after a defined mechanical deformation by use of thermal fields or electrical current. In this presentation the focus is laid on the development of a safety system in machining application. Today pneumatic solutions are used to stop a linear movement of an axis within less than 100 ms. The presentation focuses the development of an alternate SMA element which is used a high speed and high force actuator implemented in a brake unit.

Keywords: Shape Memory Alloys, Actuators, Safety, Fast Actuation

Introduction

Todays machining industry demands high standards concerning safety and precision during the production and maintain processes. Hence a wide range of safety components for nearly every production machine is used as an automated device for controlling the machine's and user's state and react in case of malfunctions and endagenerments of the user itself. Among the automated safety components, today's linear break systems have to meet three major requirements:

1. enabling short breaking times (often under 50 ms),
2. generating high breaking forces (often in a field between 1 and 10 kN)
3. generating breaking displacements of more than 0,3 mm, reaching even up to 1 mm.

A state of the art system as showed in figure 1 uses a pneumatic drive principle in order to break the movement of a slider on a linear axis. The main carrier is elastic and can move the breakshoes towards the linear axis. If the chamber between the two spring steel diaphragms is deformed by compressed air, the springlike chamber (consisting of the diaphragm elements) is short in the horizontal direction. The main carrier is thereby unaffected. In

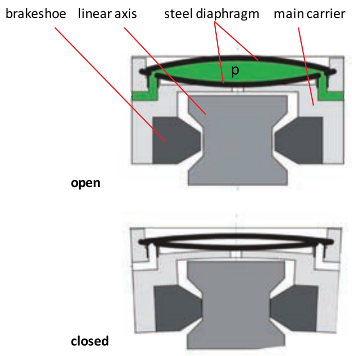

__Fig. 1:__ state of the art linear clamp system [1]

this state, the brakeshoes do not touch the linear axis [1]. If the air pressure is switched off, the diaphragm elements are not deformed by the air pressure causing an expansion in the horizontal direction. Due to their mechanical elasticity, they transmit the potential energy into the deformation of the main carrier causing its sheering resulting in clamping of the breakshoes against the linear axis.

This construction utilizes the pneumatic principle to fulfill the three major requirements with a focus on the high force factor. Due to simplification and cost reduction of machines, a general trend in omitting pneumatic drives can be noticed in the machining industry [2]. Hence, a fourth demand of future requirements can be added for sub systems, especially for industrial safety systems:

4. usage of electrical actuators

Shape Memory Alloy Actuators

Referring to different comparisons of actuator principles and the energy-volume ration, shape memory alloys (SMA) stand out as smallest and most powerful actuators with energy density up to 10 J/dm^3 [3, 4]. Among different functional materials, SMA provide the possibility to imprint a specific shape and to trigger this shape after a pseudoplastic deformation. SMA revert to their imprinted shape as a result of a phase transformation between the low temperature phase (martensite) and the high temperature phase (austenite). The characteristic transformation temperatures, martensite start (M_s), martensite finish (M_f), austenite start (A_s) and austenite finish temperature (A_f) represent the start and finish points of this phase transformation as presented in figure 2. The phase change between the two solid phases leads not only to a shape change causing a mechanical movement, but also to a significant change of the specific electrical resistance

Bi-Stable SMA Actuator

P. Motzki, S. Seelecke
ZeMA gGmbH, Saarbrücken, Germany, and Universität des Saarlandes, Saarbrücken, Germany

Abstract:
Shape Memory Alloy (SMA) actuators like SMA wires are already present in a few commercially available products, like valves or locking mechanisms. In these actuator systems, the SMA wires are always coupled with an additional biasing mechanism, such as a restoring coil spring. Other possible restoring forces are, for example, the gravitational force of a mass or the pulling force of a second SMA actuator. One drawback of an SMA actuator wire system, such as when coupled with a coil spring, is the continuous energy needed to remain in the contracted position. In this paper, a new SMA actuator design is presented that addresses and solves this drawback. In this actuator, a bi-stable snap mechanism is combined with a protagonist-antagonist SMA wire configuration. In this way, the actuator has two defined stable and energy-free positions. The SMA wires are only activated to switch between these two positions.

Keywords: SMA, Shape Memory Alloy, Bi-Stable, Protagonist-Antagonist, Snapping

Introduction

Shape Memory Alloy (SMA) actuators like SMA wires are already present in a few commercially available products. The company Actuator Solutions GmbH, for example, offers a variety of different gas and fluid valves with SMA wires [1]. SMA actuator wires will contract when heated, typically via an applied current, as a consequence of a phase transformation (Fig. 1) between Martensite (cooled wire) and Austenite (heated wire) [2, 3]. In order to return to the extended length, the wires are coupled with an additional biasing mechanism, such as a restoring coil spring, the gravitational force of a mass (Fig. 2) or the pulling force of a second SMA actuator. One drawback of an SMA actuator wire system, such as when coupled with a coil spring, is the continuous energy needed to remain in the contracted position [4-6]. The spring force keeps the not-activated SMA wire in a defined initial position. Activation and contraction of the SMA wire causes the SMA actuator to reach a second position. To remain in this second position, the SMA wire has to be constantly heated, resulting in a continuous energy consumption. Also, a complex position control is necessary to keep the actuator in that defined second position, independently of environmental influences like temperature changes or increased convective cooling through higher air flow rates [7]. The stroke of the actuator is dependent on the SMA wire's length (typically 4 % [8, 9]). To produce large strokes, SMA actuators often need large construction space. The pulling force, as well as actuation cycling speed, is directly dictated by the diameter of the SMA wire [2, 3].

To address these drawbacks mentioned above, a new SMA actuator design is presented. In this actuator, a bi-stable snapping mechanism is combined with a protagonist-antagonist SMA wire configuration. In this way, the actuator has two defined stable and energy-free positions. The SMA wires are only activated to switch between these two positions. The force output and the stroke of this actuator are only dependent on the snap design, rather than being directly linked to the SMA wires' lengths and diameters. This allows for the construction and the design of very compact and energy-efficient actuators. Additionally, the actuation frequencies are increased, because the protagonist-antagonist configuration provides active actuation in both directions, unlike in a SMA-spring combination.

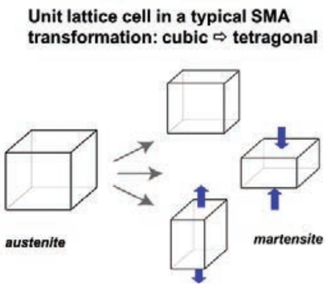

Fig. 1: *Phase transformation in SMA material*

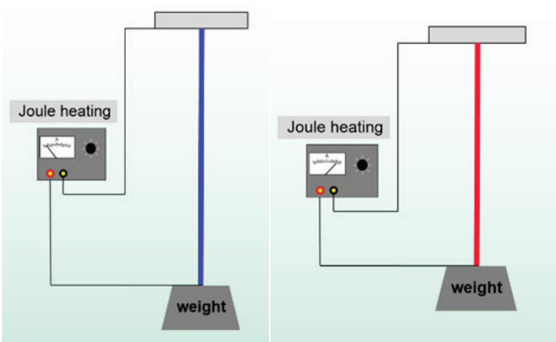

Fig. 2: *SMA actuator wire in operation*

Analysis of Performance and Energy Efficiency of Thin Shape Memory Alloy Wire-Based Actuators

H. Khan, L. Manfredi, Y. Huan, F.L. Velsink, A. Cuschieri
University of Dundee, Dundee, United Kingdom

Abstract:
Recently actuators based on smart materials have attracted considerable interest in the field of Micro-electromechanical systems (MEMS), due to their potential to provide high power-to-weight ratio. Shape memory alloy (SMA) s are effective these material for actuation because of their lightweight, low power consumption, and heating actuated and superelastic properties. The objective of the current study concerns the selection of the appropriate design configuration for thin SMA wire-based actuators. We proposed two compact SMA-wire based rotary actuators, which use thin SMA wires or extension spring in antagonist configuration. The main contributions of this paper are the study of position tracking performance of the proposed actuators on a purpose designed reconfigurable experimental test bed as a proof-of-concept together with evaluation of their energy efficiency.

Keywords: Smart Materials, SMA Actuators, SMA Wires

Introduction

In recent years, the active materials [4,7, 9] have provided an effective solution for the design compact and high performance actuators for the miniaturized robotic applications. Shape memory alloys (SMAs) are uniquely suited to miniaturization with the added benefit of low power consumption. SMAs as straight-wires are most commonly used in SMA actuator systems [15], these wires contract when it is heated, and revert to their original length on cooling it [10, 16]. The heating of SMA wires is easily achieved by changing their electrical resistance. However, one of the main challenges of SMA actuators concerns achieving a high bandwidth. Thus, a maximum bandwidth of 0.033-2 Hz is reported in the published literature [13]. Moreover, the maximum achievable bandwidth of SMA based actuators is highly dependent on the efficiency of the method used for cooling the wires [3]. The actuation frequency can be increased by rapid cooling of the SMA wire, usually by forced heat convection. *Wet SMA actuators* [8, 12, and 14] are characterized by an SMA wire embedded within a compliant electrolyte fluid-filled tube, an arrangement that allows electricity to be used for heating the wire, causing its contraction. In this arrangement, cold fluid is pumped through the tube for fast cooling of the wire, resulting in relaxation (extension). However, this arrangement increases the overall mass of the system and requires more heat to contract the SMA. The wet SMA actuators power-to-weight ratio is typically smaller. Another important factor in the achieving the desired bandwidth with SMA wire is its thickness. Currently, the thinnest SMA wires readily available in the market are 25 μm diameter. These SMA wires have low cooling time (up to 0.15 Sec) [1] with faster cooling at room temperature. The higher bandwidth comes at the expense of a lower output force. For the SMA wire to return to its original state after cooling, a bias force is needed. The application of this bias force and pre-stress on the wires also influence the bandwidth of the actuator. The bias force can be passive, by a spring or mass. An antagonistic configuration of SMA wires can also be used, in which arrangement; the other SMA wire undergoes the reverse transformation. As the bias force is not constant, it influences the bandwidth. [13].

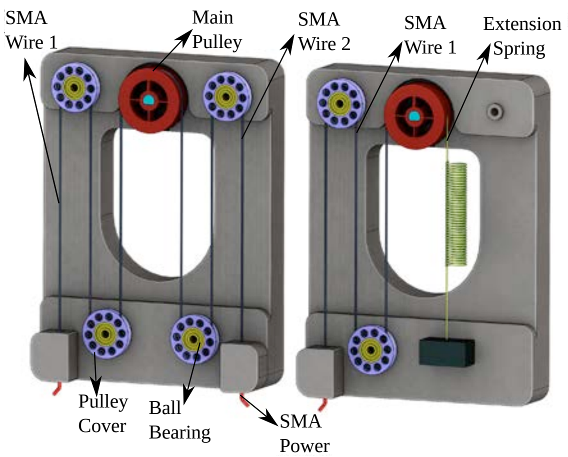

Fig. 1: *The proposed SMA-wire based actuators design, these actuators provide rotary actuation through an output shaft attached with a main pulley (in red);* ***Left:*** *SMA wire Vs SMA wire.* ***Right:*** *SMA wire Vs linear spring.*

Recent advancements in thin SMA wires have enabled their use for compact and high performance actuators for the low actuation force applications. Novel actuators have been developed, using many different configurations of SMA wires, such as miniature rotational actuators. [17], [11] Practical

Integrated Systems for the Accurate Measurement and Control of Micro Liquid and Gas Flows (Review)

J.C. Lötters, Bronkhorst High-Tech B.V., Ruurlo, The Netherlands, and
University of Twente, Enschede, The Netherlands

Abstract:
Worldwide, accurate measurement and control of small and extremely small mass flow rates of both gases and liquids is becoming more and more important, driven by numerous economically important applications in for instance semiconductor industry, analytical instrumentation, food, medical, pharmacy, energy, and micro reaction systems. Necessary components for these integrated microfluidic handling systems are for instance flow and pressure sensors, proportional control valves, pumps, passive and active mixers and droplet generators. The individual components may exist, but they have not yet been designed from the system and industrial end-user point of view. In this presentation, we propose to realise integrated microfluidic handling systems, composed of building blocks that are designed to fit within the system.
Particular attention will be paid to multiparameter sensing and actuation principles, first to be able to measure and control micro and nanoflows very stably over a very large dynamic flow range, and second to get more information from the system than "just" the flow rate, such as e.g. the composition, energy content, density, viscosity, thermal conductivity and heat capacity. Examples of societally relevant applications are e.g. improvement of medical infusion pump systems, increasing the efficiency of processes that extract oil from oil wells (enhanced oil recovery), systems that measure the energy content (calorific value or Wobbe Index) of natural gas and biogas, monitoring of ground water pollution and the production of pharmaceuticals by means of flow chemistry. An insight will be given in commonly used technologies and technologies to come, as well as technological challenges for which a solution is needed.

Keywords:

Unfortunately, the final manuscript has not been received by the printing date. Please contact the author for additional information.

Resonant Three-Dimensional Electrostatic Actuator in Silicon Technology

B. Goj, L. Dressler, L. Dittrich, M. Hoffmann
Technische Universität Ilmenau, Ilmenau, Germany

Abstract:
We introduce a controlled triaxial electrostatic actuator which is suitable for multiple applications such as force sensing, microprobing, nanoindenting and cell manipulation. The system comprises an arrangement of serpentine springs, three independently controlled electrostatic actuators, one for each Cartesian direction, and a stylus featuring a ruby ball that is utilised as force transducer. The design, the calculation and the characterisation of the triaxial electrostatic actuator are presented. Crucial features of the actuator are the multiple application scenarios, the compact design, the low actuation voltage and the independent motion in three Cartesian directions even though a shared suspension is employed.

Keywords: Triaxial Electrostatic Actuator, Microprobe, Nanoindentation, Cell Manipulation, Transducer, Force Measurement, Tactile Profilometry

Introduction

Triaxial miniaturised actuators are utilised in numerous microdevices such as positioning systems in AFM, SEM and micro assembling systems [1]. The small movements are generated by piezo actuators in most cases which are very accurate. However, piezo actuators are quite expensive and occupy large space compared to the desired travel. Their fabrication cannot be easily integrated into standard MEMS process flows, rather their employment entails time-consuming and expensive assembly steps. Electrostatic microactuators are an advantageous alternative which are fabricated utilising silicon micromachining [2]. These systems are compact and inexpensive to fabricate due to the parallel processing of many devices in batches. Nevertheless, micromachining of truly three-dimensional structures is challenging since typical fabrication methods such as reactive ion etching (RIE) of silicon or sputtering of aluminium are capable for so-called "2 ½D structures", only [2]. These restrictions lead to complex triaxial microsystems as state of the art which comprise stacked spring arrangements and more than three transducers to uncouple all movement directions [3,4].

We present a controlled triaxial electrostatic actuator that is suitable for multiple applications such as force measurement, microprobing, nanoindenting and cell manipulating. (cf. Fig. 1).

Applications of the triaxial actuator can make use of two actuation modes: (1) static actuation and (2) dynamic actuation. A static actuation is suitable for force sensors which base on the deflection of a microspring, an AFM cantilever or a cell membrane.

A broader range of applications arises if the dynamic actuation mode is utilised. One crucial application is the measurement of surface topographies utilising semi-contact measurements (comparable to AFM) [5,6] that avoid sticking. Additionally, a material characterisation on surfaces (nanoindentation) is possible. If the oscillating ruby ball gets in contact with a surface, the amplitude and the phase shift of the oscillations are changed. An evaluation of the magnitude and the direction of the phase shift yield the contact stiffness and thus young's modulus of the contact partners. Beside the classical applications the triaxial actuator can be utilized for cell manipulation by systematically deflecting cell membranes and thus induce cell growth or inducing biological differentiation mechanisms.

In the next chapters we present the design of the triaxial microprobe as well as first experiments referring to different possible applications.

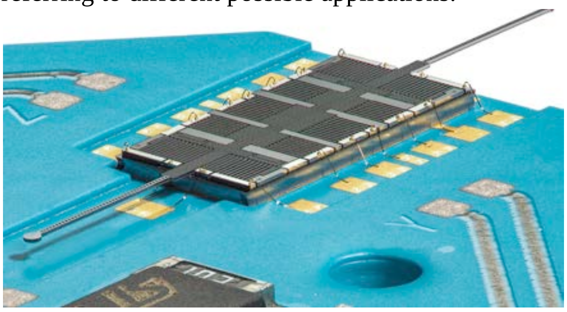

Fig. 1: *Triaxial electrostatic actuator on an LTCC adapter [5]*

Design of the triaxial actuator

The triaxial electrostatic actuator comprises one shared serpentine spring, three independently controlled actuators, one for each Cartesian direction, and a stylus featuring a ruby ball that is utilised as force transducer (cf. Fig. 2). All components of the triaxial electrostatic actuator (excluding the ruby ball) are integrated in one shared silicon-on-insulator substrate. Thus, expensive (manual) as-

Mono-Dispersed Droplets Generation in the Flowing Ambient Liquid by Using an Ultrasonic Vibrator

T. Kanda, T. Yamada, K. Mori
Okayama University, Okayama-shi, Japan
K. Suzumori, Tokyo Institute of Technology, Tokyo, Japan

Abstract:
In this study, we have generated mono-dispersed droplets in the flowing ambient liquid by using an ultrasonic vibrator. By using a torsional vibration of the bolt-clamped Langevin type vibrator and a micropore, small droplets were generated in the continuous phase. To generate the mono-dispersed droplets, we have observed the relationship between the droplets' ejection speed and the droplets generating state. By estimating the viscous resistance to the droplet, we have discussed the relationship between the viscous resistance and generated droplets' stability. As a result, we have succeeded in generating mono-dispersed droplets by estimating the droplet condition.

Keywords: Droplet, Ultrasonic Transducer, Micro Fluidic System, Piezoelectric Transducer

Introduction

Generation of small and mono-dispersed droplets has attracted attentions in many industrial and scientific fields. In this study, to generate mono-dispersed droplets in the flowing ambient liquid, we have used an ultrasonic actuator. The actuator is bolt-clamped Langevin type transducer oscillated in torsional direction. Droplets can be generated by using the torsional vibration and a micropore plate on the tip of the transducer. To generate mono-dispersed droplets, we have investigated the conditions of vibration and liquids. As a result, we have succeeded in generating micro droplets which have diameter of a few tens of micro meters. By generating droplets in flowing ambient liquids, we can apply this droplets generating system to the continuous flow process.

In previous studies, to generate micro droplets for a chemical manufacturing process, we designed and fabricated a system using a bolt-clamped Langevin type torsional vibrator and a micropore plate in order to generate micro droplets [1-4]. We succeeded in generating micro droplets of water or oil in air [1-2]. Those droplets have diameter of a few tens of micro meters. Additionally, we generated such droplet as dispersed phase in the continuous phase [3]. However, the generating condition for mono-dispersed phase was not obtained precisely. In this study, we have observed the relationship between droplets' discharge speed and droplets generating state.

Principle and device structure

Figure 1 shows a cross-sectional view of a bolt-clamped Langevin-type transducer for the droplet generation. The transducer is a torsional vibrating type and a micropore plate is attached on the tip of the transducer [1-4]. A fabricated transducer is shown in Fig. 2. The body of the transducer is made of stainless steel. Piezoelectric elements are used to oscillate the transducer. By the poling directions of the piezoelectric elements, the transducer can generate torsional vibration.

SEM photos of the micropore are shown in Fig. 3. The micropore plate is also made of stainless steel. As shown in the close up photo, the micropore has a tapered structure. This structure is effective to generate stable state for the droplet generation [4].

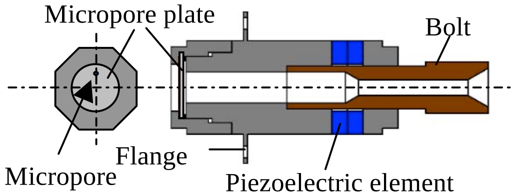

***Fig. 1:** Cross-sectional view of bolt-clamped Langevin-type transducer for droplet generation*

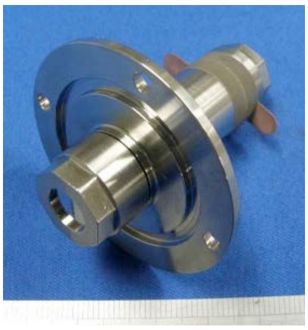

***Fig. 2:** Fabricated bolt-clamped type torsional ultrasonic vibrator for droplet generation*

Cost-Efficient Manufacturing of a High Deflection Electrothermal Drive for Switching Applications

M. El Khoury, T. Winterstein, C. Nakic, H.F. Schlaak
Technische Universität Darmstadt, Darmstadt, Germany

Abstract:
We present a cost-efficient method for manufacturing of electrothermal actuators. For concept validation, a bidirectional out-of-plane actuator is fabricated using two Polyether Ether Ketone (PEEK) layers which are milled and assembled using rivets. The actuator generates a high open loop deflection of 4.4 mm, 21.5 mN blocking force and has a footprint of 35 x 13 mm². The presented device can be mass produced using manufacturing methods available for flexible printed circuit boards. It can be used to drive micro fluid valves and electrical switches which require relatively high deflection and driving forces.

Keywords: Electrothermal Actuator, Switching Applications, Cost-Efficient Manufacturing.

Introduction

Polymer electrothermal actuators (ETA) are under research at the Institute for Electromechanical Design (EMK) of the Technische Universität Darmstadt.
Polymer cantilevers elongate due to local thermal expansion. Joule heating on polymer surface is achieved by metallic heating elements. ETAs generate force and deflection when the cantilever elongation is transformed by compliant mechanisms (see Fig. 1).

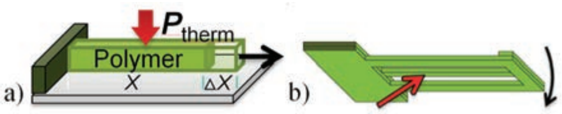

Fig. 1: *ETA working principle; a) elongation of a heated cantilever; b) cantilever combined with a compliant amplification mechanism deflected in out-of-plane direction.*

ETAs are mainly fabricated using the methods of surface micromachining like deep lithography and micro-milling. A transfer to mass-production requires low material prices and high throughput technologies. This work presents an improved fabrication method for ETA, which allows the transfer to available cost-efficient mass-production methods for flexible printed circuit boards (flex-PCB). As a proof-of-concept an ETA for switching applications with high deflection is designed, fabricated and characterised.

Switching applications

In literature, ETAs are developed for applications such as micro positioning stages [1], micro relays [2] and Braille displays [3], where deflections up to 500 µm and maximum forces of 11 mN are required. In this work, we focus on mass-produced applications such as locks, electrical switches and micro valves.
These applications require high deflections and therefore are still not actuated by ETAs.

For this study, a model substituting the presented mechanisms is designed (see Fig. 2). It consists of a shaft positioned in a counter bearing. The shaft is 51 mm long and has a diameter of 3 mm. A minimum force of 12 mN and a minimum deflection of 2 mm are required to operate the mechanism and overcome friction occurring between bearing and shaft.

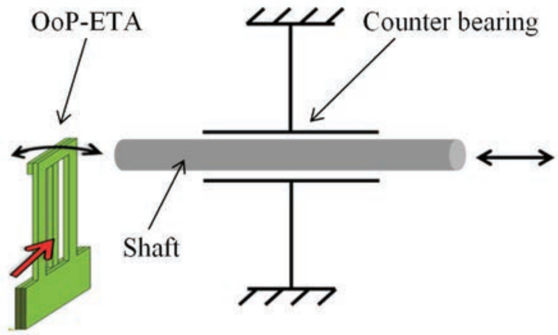

Fig. 2: *Model of switching applications with a shaft actuated by an OoP-ETA.*

Electrothermal actuator

The presented switching model is actuated by an out-of-plane (OoP) ETA based on the mechanism presented by Chen [4]. It consists of three cantilevers positioned in two functional layers (see Fig.3).
Polymer OoP-ETAs are mainly unidirectional. They deflect in one direction only. To open and close the switch, the actuator is designed bidirectionally. By heating the inner cantilever, the actuator tip deflects downward. The actuator tip deflects upward, once heat is applied to the outer cantilevers.
This bidirectional OoP-actuator has separately controlled heating elements for each functional layer. A doubled total deflection can be reached without increasing the actuator length by using up and down strokes combined.

SMA Shape-Memory Microvalves for Fluidic Systems

C. Megnin[1], H. Ossmer[2], M. Gueltig[2], T. Hanemann[1,2], M. Kohl[2]
[1]Albert-Ludwigs-Universität Freiburg, Freiburg, Germany
[2]Karlsruher Institut für Technologie, Karlsruhe, Germany

Abstract:
We report on the design, fabrication, and performance of microvalves based on micromachined shape memory alloy (SMA) film actuators. The microvalves are based on an academic research program on the topic of SMA films and corresponding SMA microactuators starting in the '90s. Within this framework, normally open (NO), normally closed (NC), proportional, and bistable microvalves were developed. This paper presents a review on these activities focussing on the development of NO and NC microvalves. Major performance specifications are described in detail, such as SMA material parameters, mechanical output of the SMA microactuators as well as fluidic performance characteristics including pressure range, flow rate, time constants and required heating power. Furthermore, the integration of the SMA microvalves to fluidic backplanes is described. Currently, the presented microvalve technology is transferred to an industrial fabrication process within a spin-off at Karlsruhe Institute of Technology (KIT).

Keywords: Shape Memory Alloy (SMA), Microvalve, Microfluidic, Industrial Fabrication

Introduction

One of the first microvalves was presented in academic research in 1990 [1]. Since this date, many research groups and industrial companies developed microvalves for various applications ranging from lab-on-chip, chemical analytics, pneumatics, or chromatography [2]. Several actuation principles have been explored, including magnetic, electric, piezoelectric, thermal, electrochemical, phase change or rheological principles [3]. Thus, microvalves differ considerably with respect to their dimensions, fabrication technology, and fluidic performance. Major thermal actuation principles are based either on bimetallic, thermopneumatic, or shape memory effect.

The shape memory effect was depicted by the "Naval ordnance laboratories" in the material system consisting of titanium and nickel (TiNi) [4]. Due to the giant energy density of 10^7 J/m^3 and the good scaling behaviour of work output upon miniaturization, SMA materials are predestined for microactuation [5]. The first microvalve based on SMA film technology has already been presented in 1991 [6]. Still, most research and development of SMA valves focuses on SMA wire actuators until now [7,8]. This is due to various reasons including material issues (nonlinear characteristics, hysteresis, fatigue, temperature range), technology barriers (limited compatibility to MEMS fabrication processes), as well as cost factors (material processing, integration costs). In recent years, however, considerable progress has been made in SMA materials research [9-11], SMA microtechnology [12] and integration technology at low-cost [13], paving the way for this exciting technology to reach readiness for marketing.

In the following, we present a review on the development and performance of NO and NC SMA microvalves using state-of-the-art integration of SMA microactuators and novel rapid prototyping technologies of 3D printing and laser ablation.

SMA- Material

The actuator material is a cold rolled TiNi foil with a thickness of 17 µm. The one-way shape memory effect is adjusted by a final heat treatment at 550 °C for 30 min in flat condition. The transition temperatures are measured by differential scanning calorimetry (DSC) and temperature dependent electrical resistivity measurements. The measurements are performed in a thermal cycle between -90 to 120 °C and a second ranging from 25 to 120 °C. Upon cooling from the austenitic state (A_s = 43 °C, A_f = 52 °C), the material exhibits a rhombohedral (R-) phase transition starting at R_s = 52 °C and ending at R_f = 39 °C. For the small temperature cycle the martensitic transition (M_s = -11 °C, M_f = 8 °C) is suppressed and only the R-phase is used. Therefore, the thermal hysteresis is 5 K smaller and the energy consumption for heating is reduced by 70 %. This small hysteresis of the R-phase offers advantages with regard to switching performance and time constants [5]. By energy dispersive x-ray spectroscopy, the composition is determined to be $Ti_{49.35}Ni_{50.65}$, which corresponds well to literature and measured transition temperatures [14].

Automotive MR Actuators – State of Art (Review)

J. Gołdasz[1], BWI Group, Kraków, Poland

Abstract:
Magnetically responsive fluids have been designed to undergo a transition from a fluid to a pseudo-solid material in the presence of magnetic field. So far the controllable property of magnetorheological (MR) fluids has been utilized by the automotive industry in the form of semi-active vehicle dampers and powertrain mounts. Since the introduction in 2002 in the North American market the technology has been proven on many vehicle platforms from compact sedans to sport-utility-vehicles and supercars. The most recent incarnation of this technology has revealed major progress in controllability and dynamics. In the review paper the author discusses the recent developments and provides and in-depth overview of the state-of-the-art of MR actuator technologies in several key areas related to performance range, authority and dynamics.

Keywords: Magnetorheological Actuator, MR Damper, Automotive Suspension, Review

Introduction

Magnetorheological (MR) fluids are a suspension of fine, non-colloidal, low-coercivity ferromagnetic particles in a carrier fluid. The material is a representative of the class of fluids whose physical properties can be programmed to achieve particular goals. Specifically, MR fluids have shown the ability to transition from a liquid to a semi-solid with a yield stress when subjected to external magnetic fields [1]. When exposed to magnetic fields the material develops a yield stress resulting in an increased resistance-to-flow and force build-up. The individual characteristics have made them suitable for use in semi-active applications and vehicle suspension platforms in particular. By using the technology real-time benefits in vibration damping and isolation were already recognized in the 1990s [2, 3]. The inventors of the technology claimed a method of controlling the characteristics of an MR device through an on-board electronic control unit (ECU). In the 1990s the progress that has been made in the smart fluid formulation, hardware, control algorithms and power electronics has resulted in the world's first MR damper-based vehicle suspension system [2]. The MagneRide™ technology has remained the first and only high-volume produced semi-active suspension system that is based on smart fluids. In 2009 BWI Group expanded its MR product line with controlled powertrain mounts. To begin with, the MR damper system required four position sensors, yaw sensor and lateral acceleration sensor as well as the information on vehicle speed and steering, four controlled MR dampers and an ECU (Electronic Control Unit). Connecting the system to on-board CAN network ensured the flawless exchange of information between the MR system and the others present on the car, namely, traction control, air suspension and ABS. Since the introduction on the North American Cadillac Seville STS 2002 vehicle platform the system has undergone three major series of improvements (generations). In the actuator area they were focused on improving the dynamic range, low-speed response and dynamics.

The automotive MR actuators are unique devices in several aspects. Alternative semi-active vehicle suspension systems are valve-based. In other words, they require the action of continuously variable electromechanical actuators to vary the damping force level. For comparison, valveless MR dampers have the ability to influence the damping force by modifying the apparent viscosity of smart fluids exposed to magnetic fields of sufficient magnitude. From the engineering perspective, benefits over other competitive systems are numerous. The control valve is rid of moving mechanical parts (simplicity). The high range of damping forces results in a major turn-up ratio advantage in the low and medium speed regimes of damper operation. The system is fast and noiseless (no moving parts in the control valve), and it draws less than 30 W of electrical power per damper under most driving conditions. For example, MR system total power consumption on a high performance car was found to be 10-15 W (typical road conditions) and average 38 W (the Nürburgring Nordschleife loop). Moreover, damper measurements of the recent generation have shown the response time of the system to be below 10 milliseconds, and its durability equals that which is required for the semi-active valve-based dampers.

Since its introduction, significant performance improvements have been achieved due to better fluid formulations, control algorithm development and the hardware evolution. In sections that follow below the author discusses the advances in the damper hardware which gave rise to improved dynamics and performance gains. Control algorithm,

[1] Faculty of Electrical Engineering and Computer Science, Cracow University of Technology, ul. Warszawska 24, 31-155 Kraków, Poland

Controlling the Magnetorheological Effect Using Vibrations

E. Leroy, P.-H. Orefice, L. Eck, M. Hafez
CEA LIST, Gif-Sur-Yvette, France

Abstract:
Magnetorheological fluids (MRF) are interesting for building devices that require high strength without a need for active actuation such as dampers, brakes or clutches. Usually, the use of MRF requires an electromagnetic coil that makes them difficult to apply to compact, miniature devices. In this work, we present a new technology to operate magnetorheological fluids, it is based on the use of mechanical vibrations. Experiments conducted on a cylindrical brake showed that the braking torque can be reduced when vibrations are applied to the shearing element. The effect depends on multiple parameters such as the frequency and the amplitude of the vibration and a drop of the total torque up to 40 % has been observed in a constant magnetic field. The combination of vibrations and permanent magnets could be interesting for building miniature MRF-based device. These could be used in various applications such as haptic interfaces, reconfigurable articulations, etc.

Keywords: Magnetorheological Fluids, Vibrations, Brake, Actuator, Piezoelectric

Introduction

Magnetorheological fluids are fluids in which the viscosity can be controlled by an external magnetic field. Therefore, it is possible to use these fluids to design intelligent systems such as adaptive damping systems, controllable brakes or electrically controlled clutches. Numerous applications are found in literature in areas such as haptic systems [1], automotive dampers [2], prosthetics…

The most common way to use these fluids is to combine an electric coil to a magnetic circuit with a small cavity filled with fluid. As a moving part shears the fluid, a variable braking force is exerted on this part. This force depends on the magnetic field.

In this paper, we present a new effect that has been observed in magnetorheological fluids. A prototype has been built to evaluate how vibrations affect the braking torque of a magnetorheological brake. We show that it is possible to reduce the braking torque using vibrations. This effect is interesting and may lead to new design possibilities for adaptive brakes, clutches and dampers.

The paper is divided into two parts: the first one describes the experimental setup and procedure and the second one presents and discusses the results.

Experimental setup and procedure

Design of the shearing interface

The objective of the designed experiment is to observe whether the generation of vibrations in a magnetorheological fluid affects the braking capability of the fluid. Although numerous configurations are possible for the design of a magnetorheological brake [3], we chose a brake geometry based on a hollow cylinder as similar devices have been designed in our laboratory [1], [4]. Furthermore the geometry is well suited for the integration of vibratory actuators such as piezo stack actuators.

The actuator used to generate vibrations is a parallel pre-stressed actuator from Cedrat technologies [5]. Its characteristics are shown in table 1.

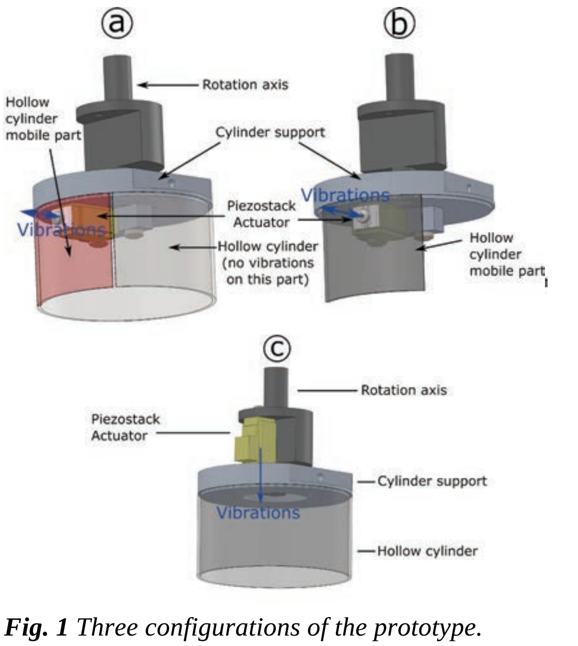

***Fig. 1** Three configurations of the prototype. Configuration "a": part (about 20% of the total surface) of the hollow cylinder is cut and a Piezostack actuator is used to generate radial vibrations. Configuration "b": same as configuration "a", but without the passive hollow cylinder surface. Configuration "c": the Piezostack actuator is used to excite vertical vibration in a complete hollow cylinder.*

Hybrid Magnetorheological Damper

M. Jackel, J. Kloepfer, M. Matthias
Fraunhofer LBF, Darmstadt, Germany

Abstract:
Fraunhofer LBF developed an energy efficient magnetorheological damper called hybrid magnetorheological damper. An adjustable field generated by a physically moveable permanent magnet is superposed by a second field generated by a solenoid coil. This concept was realized in hardware and characterized. Furthermore the damper together with control and power electronics was integrated in a quarter vehicle demonstrator that is used as a development platform, too.

Keywords: Magnetorheological Damper, MR Damper, Permanent Magnet, Adaptive Damper

Introduction

Within the Fraunhofer System Research for electromobility [1] in the technological cluster “drive train and chassis” an air-cooled electrified drivetrain was developed. The Fraunhofer institutes IISB, IFAM and LBF worked together on this task. The drivetrain consists of an air-cooled wheel hub motor, an air-cooled drive inverter, a multi-level DC-DC converter, a special designed rim for promoting cooling air and an adaptive damper based on a magnetorheological fluid.

The development of this adaptive damper was motivated by the rised unsprung masses that come along with a wheel hub motor. They result in an exacerbated conflict between drive safety and comfort [2] and an increase of transient dynamic loads [3]. These effects can be minimized with an adaptive damper.

In comparison to magnetorheological dampers already on the market, Fraunhofer LBF has developed a novel energy efficient design, which results from a superposition of an adjustable field generated by a physically moveable permanent magnet and a second field generated by a solenoid coil.

Principle of the hybrid magnetorheological damper

Magnetorheological fluids (mr-fluids) are suspensions of ferromagnetic particles in a non-magnetic carrier fluid. If subjected to a magnetic field, the transferable shear stress correlates with the applied magnetic flux. Magnetorheological dampers use this effect to modify the damper stiffness. The stronger the magnetic flied, the higher the damping force. The dampers available on the market generate the needed magnetic field by a solenoid coil. Integrated into a control circuit they are capable to adapt the stiffness to the actual boundary conditions. Especially in electric vehicles where electrical energy is limited by the accumulator capacity, such semi-active systems like adaptive dampers need to be very energy efficient. Therefore this new hybrid design of a magnetorheological damper was developed at the Fraunhofer LBF (see figure 1) [4]. The magnetic field in the fluid gap is adjustable by current of a solenoid coil as well as the position of a permanent magnet. At slow changing boundary conditions (e.g. loading condition or driver’s selection) the moveable permanent magnet can be used to adjust the damping characteristic. For fast changing boundary conditions (e.g. at quick evasion manoeuvres) the solenoid coil ca be used.

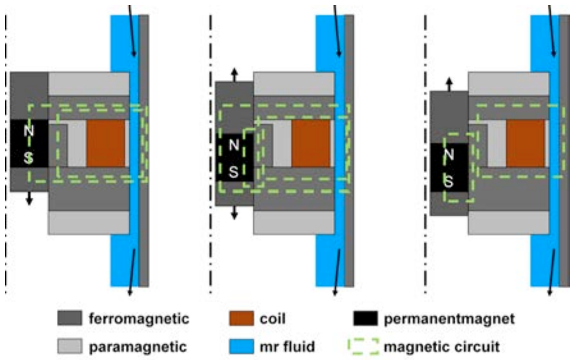

Fig. 1: Principle of the hybrid magnetorheological damper [4]

Functional demonstrator

After the magnetic field simulations presented on ACTUATOR 14 [4] a first functional demonstrator was manufactured. Figure 2 shows a cross section view of the demonstrator and figure 3 shows it partly assembled.

Energy-Efficient MRF-Based Clutches in Hybrid Powertrains

C. Hegger, J. Maas
Hochschule Ostwestfalen-Lippe, Lemgo, Germany

Abstract:
This contribution deals with the theoretical and experimental investigation of a special clutch based on magnetorheological fluids (MR-fluid). The MR-fluid based clutch can be equipped with three different varieties of the magnetically induced MR-fluid movement control. This feature enables a drag torque-free operation for the design of an energy-efficient powertrain and provides additional safety behaviors. The investigation is focused on the dynamically response behaviour, the transmission behaviour for different speed ranges up to n = 6000 min^{-1} and the fail-safe behaviours.

Keywords: Magnetorheological Fluids, Reduced Viscous Induced Drag Torque, MRF-Based Coupling Elements

Introduction

The main challenge for a further establishment of hybrid or electrical vehicles is the increase of the driving range to a competitive level compared to combustion driven vehicles. To achieve the balance between the technologies progresses are necessary at different levels, one of them is the design of a maximized energy-efficient powertrain. Hence, this contribution deals with the investigation of energy-efficient clutches based on magnetorheological fluids (MRF). Magnetorheological fluids consist out of a carrier fluid (synthetic-oil) with suspended carbonyl iron powder particles and additives reducing e.g. the sedimentation. If the MR-fluid is placed between two shearing surfaces and exposed to a magnetic field an adjustable force can be transmitted depending on the magnetic flux density. This functional principle is utilized in the design of MR-fluid actuators like brakes and clutches [1, 2]. In [3] a MR-fluid clutch was also utilized directly in the powertrain as a differential between the front and the real axle. Thereby, a large number of different shear gaps are realized resulting in a high torque capability of up to T = 700 Nm. Due to narrow shear gaps, high differential speeds induce high viscous losses even in idle mode. Hence, this clutch design is not predestinated as a starting or shifting clutch in vehicles. Main disadvantages of the conventional coupling elements like wet multi-plate clutches are the drag losses in the disengaged mode causing dissipation [4]. However, coupling elements based on the MRF can be modified by the MR-fluid movement control to reduce the parasitic viscous drag torque to zero. The MR-fluid movement control [5, 6] is based on a partially filled shear gap and on several volume forces for the movement of the MRF. The shear gap is divided into an active and inactive region, whereby the active region permits the contact of the two shear surfaces through the MRF and the inactive region avoids the contact. Through various combinations of electro- and permanentmagnets (PM) different types of the MR-fluid movement control can be realized, each having a typical coupling characteristic and fail-safe behaviour [5].

In this contribution three variants of the MR-fluid movement control will be investigated considering the feasibility utilizing MR-fluid actuators in hybrid powertrains. A test-actuator will be designed based on derived models considering the MR-fluid movement control concepts. The transient behaviour will be analyzed and compared considering different rotational speeds and degrees of MRF filling.

Model based design of the MR-fluid clutch

In the following chapters a MRF-based clutch is designed by a multiphysical finite element analysis considering three different MR-fluid movement control concepts in a comparable scope. A detailed design of one magnetic circuit for each different MR-fluid movement control is shown in Fig. 1.

The conditional stable MR-fluid movement concept consists out of one electromagnet to ensure the torque transmission. The idle mode without drag losses can be only ensured by radial accelerations. The bistable MR-fluid movement control concept comprises one permanentmagnet and one electromagnet on the opposing shear surface sides. The magnetically induced forces by the electromagnet are utilized to move the MR-fluid into the active or inactive region, whereby the magnetic fields of the permanent magnet can sustain the current state. The monostable MR-fluid control concept consists of two permanentmagnets. The polarization of the permanentmagnets is crucial responsible for the transition mode while the electromagnet is deactivated. In the shown case the polarization of the permanent magnet is equal and

Magnetorheological Actuator for Haptic Applications

M.E. Busse-Grawitz, maxon advanced robotics and systems, Giswil, Switzerland
R. Pittini, maxon motor ag, Sachseln, Switzerland
R. Waldvogel, D. Martin,
maxon advanced robotics and systems, Giswil, Switzerland

Abstract:
Most present magnetorheological (MR) actuators suffer from two main drawbacks if applied to haptic drives: bulkiness and lacking speed of response. We present a novel actuator which overcomes these disadvantages, achieving response times of 3 ms at a torque of 9 Nm. Additionally, it offers virtually play free operation, extremely low active inertia and very graceful reaction to overload conditions.
Achieving peak speeds above 300 rpm, this drive is well suited for parallel and serial robot architectures as well as for single axis actuators.

Keywords: Magnetorheological Actuators, Haptics, Collaborative Robotics

Introduction

If faced with the task of designing an actuator for haptic purposes or for robotics in general, one is immediately confronted with a basic dilemma: that the delivered torque and the rotor moment of inertia are closely linked together. All else being equal, the rotor moment of inertia is a little less than the torque squared. Only a change in technology can help here, and today, the best technologies are found in specially designed inner rotor machines. One key figure of merit is the mechanical time constant which links torque related copper losses with the rotor moment of inertia, the lower, the better:

$$\tau_m = \frac{I_{rotor}}{k_M^2} = I_{rotor}\frac{P_{Cu}}{T^2} \quad (1)$$

where τ_m is the mechanical time constant, k_M the motor constant, I_{rotor} the rotor moment of inertia, P_{Cu} the copper losses generated when the motor delivers the torque T.
While machines with iron-less windings boast very good (i.e. low) mechanical time constants, they are about three times heavier than slotted motors. The latter suffer from iron core losses and cogging torque.
This leads to another dilemma: good, haptic devices are very transparent, in the sense that the delivered torque is very much related to the intended torque which might be set by the motor current. Good robotics devices are not too heavy. Light machines use iron cores and gears, and both destroy the actuator transparency.

The Haptic Drive

This is where the Haptic Drive kicks in:
It is characterized by the following treats:

- Extremely low rotor moment of inertia, about one hundred times less than that of an equivalent motor with ironless windings.
- Very easily controllable output torque
- Virtually play free operation
- Low response time for torque control, well below 5 ms.
- Very graceful behavior under overload conditions.

Hence, the Haptic Drive has the properties of a direct drive while maintaining lower weight and lower inertia. The only drawback is that it is limited to about 400 rpm output speed, but this is sufficient for most robotic applications.

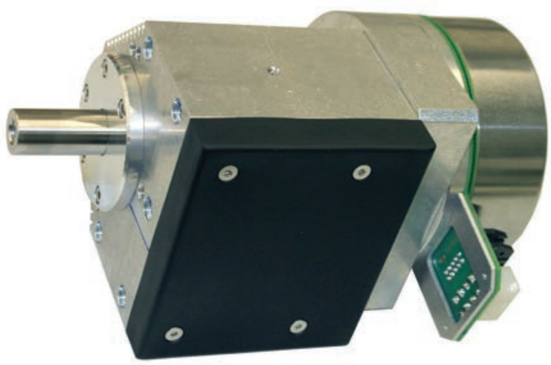

Fig. 1: *Prototype of the maxon Haptic Drive.*

Combining Usability and Performance – What Smart Actuators Can Learn from Automatic Commissioning of Variable Speed Drives (Invited Review)

A. Wahrburg, K.D. Listmann
ABB AG, Ladenburg, Germany

Abstract:
The required steps for an automatic commissioning system for variable speed drives are summarized and an overview of existing approaches to the individual steps is provided. Furthermore, new results are presented on automatic design of plant identification experiments and the simultaneous parameterization of all relevant filters in the control loop based on the quality of available measurement signals. This results in a complete toolchain for commissioning speed control loops and allows to get the best possible performance out of the available hardware without requiring expert knowledge. It is discussed which steps will be necessary to establish a similar combination of performance and usability for smart actuators such as e.g. SMA or EAP.

Keywords: Automatic Commissioning, Plant Identification, Variable Speed Drives, Controller Design

Introduction

Variable speed drives (VSDs) are state-of-the-art in modern automation applications due to their energy efficiency and flexibility. Typical tasks include tracking of speed set-points and maintaining desired speed despite external disturbances. This is why drives are operated under closed-loop feedback as shown in Fig. *1*.
Productivity is key in such applications and can directly be related to the tuning of the parameters of the feedback-loop. As a consequence, poorly tuned parameters may have negative effects, ranging from degraded performance to instability and mechanical damage. But tuning requires expert know-how, from both a controls and application perspective. This is the major reason why the majority of VSDs are operated with very defensive default parameters in practice, resulting in poor overall performance of the application.
In order to change this situation and lift the full potential of VSDs in such applications, this paper presents methods for automatic parameterization of the control loops during the commissioning phase. While this in itself is not new, this paper focuses on incorporating two disregarded aspects: i) In order to develop a truly automatic commissioning system, the experiments for gathering measurement data for plant identification have to be carefully designed. Particularly, identification experiments without operator input are needed.
ii) The quality of the speed signal available for feedback plays a crucial role for the achievable control performance, since any measurement implies the introduction of noise into the control loop as depicted in Fig. *1*.
While it is intuitive that a clean signal obtained from a high-quality encoder allows for higher control performance, compared to the noisy speed signal measured by a low-cost device, an automatic commissioning system has to take into account the quality of the speed measurement.
To this end, not only the speed PI controller but also additional filters in the control loop have to be considered simultaneously.
Many of these consequences should be carefully taken into account when designing controllers for systems containing smart actuators as well. Thus, the latter can still learn a lot from classical drives.
The remainder of the paper is organized as follows: In the next Section we will present the basic models used inside drive commissioning and introduce the plant identification experiment performed together with the plant identification itself. After that the fundamentals of the combined controller/filter tuning are explained before we highlight the major learning possibilities for smart actuators. Lastly, a conclusion is provided.

Automatic Speed Control Commissioning in Variable Speed Drives

As an example for automatic commissioning, we consider the parameterization of the speed control loop of variable speed drives connected to a mechanical load. The control loop with its relevant dynamic elements is sketched in Fig. *1*.

Control of a Compact Electrodynamic Planar Actuator

M. Stock, T. Bödrich, J. Lienig
Technische Universität Dresden, Dresden, Germany

Abstract:
Planar motions for future small machine tools and for automation with strokes up to approximately 20×20 mm² can advantageously be realised with electrodynamic planar direct drives. Integration of the position control and power electronics thereby results in particularly compact devices. In this contribution, the design and characteristic of a built demonstrator of such a novel drive unit are shortly described in the beginning. It features a medium precision, low-cost position sensor system. A mathematical model for the planar direct drive is shown. A flatness based state space controller for transition between desired rest positions has been developed. Finally the achieved dynamics and accuracy are shown.

Keywords: Planar Direct Drive, 3 DOF Position Control, Flatness-Based Control, Feedback Control

Introduction

Planar direct drives for two (x, y) or three (x, y, φ) DOF enable dynamic positioning of work elements or workpieces in handling, machining, assembling and additional fields of applications. With proper design, those direct drives can be compact, simple in structure, easy to manufacture and low-cost. In contrast to widespread x-y planar stages with serial arrangement of two stiff lead screw linear actuators however, the mover position must be actively controlled due to missing stiffness in de-energized state.

Within a research program on components for future small machine tools [1], a novel electrodynamic planar direct drive has been developed at Technische Universität Dresden (Fig. 1). It has a travel area of 20 × 20 mm², a maximum rotation of ± 11° and peak forces of ± 72 N. The aimed position accuracy is about 10 µm. It consists of four independent windings with iron core in a stator and permanent magnets with back iron in a mover. Low-cost linear position sensors for measurement of the positions x and y and the orientation φ of the mover are integrated into the actuator. Integration of a microcontroller board for embedded position control is work in progress. The overall design and the subsystems of that planar actuator are described in [2]. The following sections will focus on position control of the developed actuator.

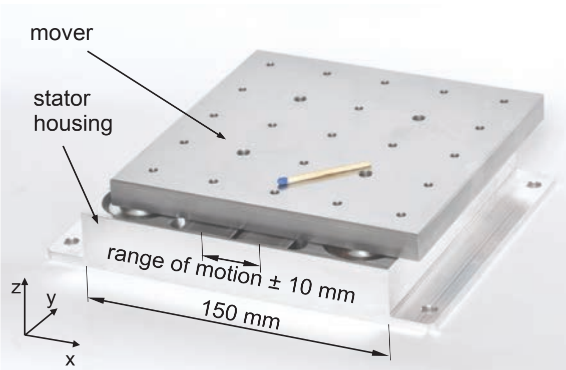

__Fig. 1:__ Prototype of a novel electrodynamic planar drive (maximum rotation of mover ± 11°)

Actuator Setup

Basically, the planar actuator consists of four independent single-phase moving-magnet actuators. Each of the four windings comprises a U-shaped iron core with two poles that interact with the belonging rare-earth permanent magnet in the mover [2]. This magnetic design enables for high thrust forces at little ohmic losses due to small air gaps and large winding cross-section areas. Nonlinearities in the force-position-current characteristic of each individual actuator are moderate (Fig. 2).

In most planar direct drives described in the literature [3-6], the mover is either guided by air bearings or magnetically levitated. In contrast to this, the first prototype of the novel planar drive has a simple, small and low-cost planar ball guide. It is biased by the permanent magnetic attraction forces between stator and mover.

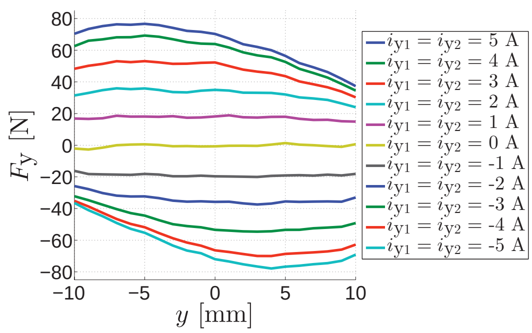

__Fig. 2:__ Measured force-position-current characteristic of the planar direct drive in y-direction at lateral mid position (x = 0 mm)

Vector Control of a Travelling Wave Ultrasonic Motor: Application to Efficiency Improvement by Voltage Reduction

F. Giraud, Université de Lille, Villeneuve d'Ascq, France
C. Giraud-Audine, Arts et Métiers Paris Tech, Lille, France
M. Amberg, B. Lemaire-Semail
Université de Lille, Villeneuve d'Ascq, France

Abstract:
Traveling Wave Ultrasonic Motors (TWUM) use piezoelectric material to produce an ultrasonic bending wave in a ring shaped stator. A rotor firmly pressed on it is driven by the travelling wave. The TWUM is characterized by a high torque to mass ratio, and can be built up with non-magnetic material. Hence, they are commonly used into MRI environment. However, they suffer from a low efficiency. In the paper, we propose a control method which supplies the minimum voltage level to the motor which is necessary to ensure a stable operation. By this way, during a no-load operation, we can cut off the apparent power to the motor by 75%, with a voltage from 200V peak to 60V peak. The proposed control has been implemented into a low cost and small in size microcontroller of ARM-core type.

Keywords: Piezoelectricity, Ultrasonic Motor, Vector Control, Power Efficiency

Introduction

Travelling Wave Ultrasonic Motors (TWUM) exhibit large torque to mass ratio and low rotational speed. Therefore, they are suitable for servo-mechanisms where weight and bulk size are critical issues. Moreover, they can be built up with non magnetic materials, this is why they are often used in medical applications, in particular in medical imaging instruments where magnetic interferences have to be avoided. Several papers use them in MRI environment. For example, [1] and [2] both demonstrate that a TWUM can stand close to a MRI device, without producing interferences.
Unfortunately, these motors also have numerous disadvantages which limit their use, like the non linearity of the torque / speed characteristics, the pull-out phenomena which makes the motor stall. Several papers show how to deal with these issues with an appropriate control scheme.
However, due to the manufacturing process which leads to bonding a layer of piezoelectric material, those motors are very sensitive to temperature rise, which increases because of the power losses. The global efficiency of a piezoelectric motor is hardly over 30%. Most of the power is dissipated into heat, mostly at the stator/rotor interface, where friction occurs, but also in the piezoelectric material, where conversion losses as well as dielectric losses appear.
One key issue is to operate the motor with the maximum vibration amplitude per volt, i.e. at the resonance of the stator, in order to decrease the conversion and dielectric power losses. However, reducing the voltage also increases the risk of the pull-out phenomena, and this is why, the classical control schemes operate at constant voltage and variable frequency.
This paper presents a vector control of the vibration amplitude of a TWUM which helps to operate at the lowest voltage possible, which avoid the pull-out phenomena. We first presents the theoretical background of the proposed method, and then experimental validation on a commercial motor.

Vector Control of the Vibration Amplitude

The torque produced by a TWUM depends on the vibration amplitude of the stator, which is called w in the paper. Many methods to control w directly or indirectly have been proposed in the literature. For example [3] uses a neural network to adjust voltages' frequency and phase, in order attain a reference speed. To avoid the pull-out phenomena, the authors used a constant voltage amplitude, and they do not consider efficiency as an issue. In [4], the authors propose a control based on a specific modelling. They adjust the voltage in frequency, amplitude and phase in order to operate close to stator's resonance, hence achieving optimal efficiency operations. However, their control is based on an online identification of stator's parameters, and is then difficult to implement in a light DSP.
In the paper, we use the control into the rotating reference frame of the travelling wave. This control is an extension to TWUM of the vector control generally applied to synchronous motor. However, with TWUM, we control the amplitudes of the stator's standing waves instead of motor's current,

Power Electronics and Control Concepts for Driving Dielectric Elastomer Transducers

T. Hoffstadt, J. Maas
Hochschule Ostwestfalen-Lippe, Lemgo, Germany

Abstract:
While the general transducer design is important to emphasize the unique and outstanding properties of smart materials like dielectric elastomers (DE), the driving power electronics have to take into account their electrical properties, too. For this purpose, a tailored bidirectional DC/DC flyback-converter for supplying capacitive loads with voltages in the kilo-voltage range has been developed. Under consideration of the electrical DE properties a smart cascaded sensor-less current control with superimposed voltage control loop is presented. This control can be used as an interface by further application oriented controls. The proposed control schemes are finally validated by measurements with a prototype converter.

Keywords: Bidirectional Flyback-Converter, Sensor-Less Control, Dielectric Elastomer Transducer

Introduction

Transducers based on dielectric elastomers (DE) consist of a thin elastomeric dielectric, e.g. silicone, polyurethane or acrylic that is coated with compliant and conductive electrodes on its surfaces. Thus, from an electrical point of view DE transducers are shape varying capacitors. Since these materials offer a large amount of deformation they are predestined for actuator, sensor and generator applications, [1]. However, especially in case of actuator and generator applications high electric fields (around 50 V/µm) are required to obtain sufficient effects. This yields to voltages in the lower kilo-voltage range in case the thickness *d* of the utilized polymer is in the range of several 10 µm.

Thus, in order to realize an accurate control of a DE transducer a precise and dynamic high-voltage power converter is necessary to adjust the electric field *E*. Furthermore, the utilized power electronics must provide a continuously adjustable output voltage, e.g. to adjust the electrostatic pressure

$$\sigma_{el} = \varepsilon_0 \cdot \varepsilon_r \cdot E^2 = \varepsilon_0 \cdot \varepsilon_r \cdot \frac{v_p^2}{d^2} \qquad (1)$$

depending on the materials permittivity ε_r for a continuous actuation of a DE actuator.

Due to the capacitive behaviour with electrical parasitics modelled by the electrode resistance R_e and high polymer resistance R_p, a controlled current source has to be realized supplying the feeding current i_{DE}. This allows a control of the voltage v_{DE} according to the differential equation $i_{DE} \approx i = d(C_p \cdot v_p)/dt$, where v_p is the voltage across the DE capacitance C_p, see Fig. 1.

Amongst other, the flyback-converter represents one advantageous topology fulfilling these specifications with a comparable low amount of components resulting in comparatively simple control schemes, too, [2]-[4]. For the continuous adjustment of the output voltage either a unidirectional flyback-converter has to be used for charging combined with an active discharging circuit for discharging, or a bidirectional flyback-converter can be realised for this purpose, [4]. The latter also ensures the higher energy efficiency what becomes even more important in case of higher operating frequencies of the DE transducer.

In the following different variants of the flyback-converter are summarized and the control scheme for the bidirectional converter is presented and validated by measurements with a prototype converter.

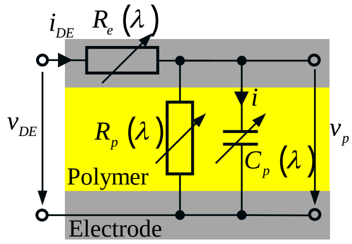

Fig. 1: Equivalent circuit diagram of a planar DE transducer.

Flyback-Converter for feeding DE Transducer

As can be seen in Fig. 2a) a unidirectional flyback-converter only consists of a switch S_1 on the primary side, a diode D_2 on the secondary side and the flyback transformer T_1 with a winding ratio *w*. In this case the magnetising inductance L_m of the flyback transformer, different from conventional high frequency transformers, is used as an energy storage element analog to the inductor in a buck-boost converter and provides additionally galvanic isolation between primary and secondary side, [5].

Sensorless Control of Low-Power Electromagnetic Actuators (Invited Review)

M. Nienhaus, Universität des Saarlandes, Saarbrücken, Germany

Abstract:
Over the years many sensorless control methods have been developed but only a few are well suited for low-power electromagnetic actuators. This review will give a systematic overview of sensorless control methods available today and reflect on their suitability to be applied in miniaturized drive systems. The second part of the review will focus especially on sensorless control methods for low-power electromagnetic actuators including aspects of integration as well as additional functionalities such as parameter identification and condition monitoring of the drive systems.

Keywords: Sensorless Control, Low-Power Drive Systems, Condition Monitoring

Introduction

"Sensorless" driven electromagnetic actuators are controlled without employing any speed and/or shaft position sensor. As a rule here and at the same time perhaps misleading, "sensorless" does not mean that no sensors are used such as for temperature or current measurements, etc. "Sensorless" particularly addresses the field of electronically commutated electromagnetic motors such as brushless DC motors (BLDC) and brushless AC motors including asynchronous induction motors, reluctance motors and – especially well suited for small sized driving systems – permanent magnet synchronous motors (PMSM, see Fig. 1). In contrast to mechanically commutated DC motors, electronically commutated ones require a separate position signal, which can be delivered by a discrete angle encoder typically mounted on the rotor shaft or, as addressed in this article, delivered by a chosen type of sensorless method.

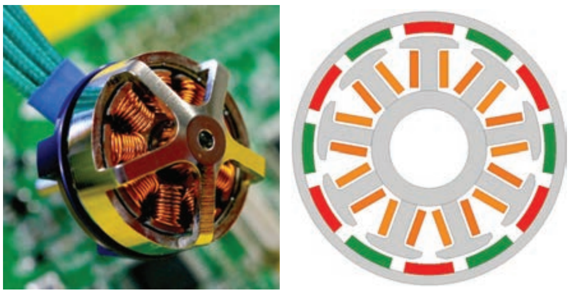

***Fig. 1:** Low-power PMSM as photo (left) and model for FEM simulation (right) with rotating permanent magnet ring, 12 poles, concentrated windings, three strands with 120 degree offset, star connection*

Why is it of interest to use electronically commutated motors when DC motors are still available und utilized today in a wide range of applications in extremely high numbers and at very low cost? Because mechanical commutators show many disadvantages, e.g lower efficiency, high electromagnetic emission, strongly load-dependent wear and, as a consequence, a considerable need for maintenance. Furthermore, modern applications are more and more based on digital control and communication. Especially low-power electromagnetic actuators are predestined for integration as an embedded subsystem in superordinate systems such as different types of devices, machine tools or automobiles. Electronically commutated motors which are originally equipped with a microcontroller are therefore preferred.

Why should sensorless methods be employed when precise, fast, miniature and inexpensive speed and/or shaft position sensors are available and moreover the subject of strong developments? Because any additional sensor increases the system's complexity, needs space not at least for cable and connectors, can fail and generates additional cost. Admittedly, sensorless methods in the sense of this article and depending on their concrete realization could also demand a significant amount of effort, e.g by using low-noise current sensors with a large bandwith and by employing high performance microcontroller technology for required fast calculations. Low-power electromagnetic actuators, which are especially addressed within this article, have some boundary conditions such as space, costs and limited computational power which significantly influence the range of suitable sensorless methods.

Overview - Sensorless position detection methods

The today's widespread use of field oriented control (FOC) for brushless AC motors implies the necessity of rotor position detection. The number of sensorless control methods has been continuously increasing over the past decades with the rising computational performance of available microcontrollers in combination with suitable sensors especially for current and voltage measurement. An impressive yet only rough overview of today's huge number of

A Novel Low-Power Dual-Actuator For High Precision Magnetic Levitation Systems

M. Lahdo, Technische Hochschule Mittelhessen, Friedberg, Germany
T. Ströhla, Technische Universität Ilmenau, Ilmenau, Germany
S. Kovalev, Technische Hochschule Mittelhessen, Friedberg, Germany

Abstract:
This paper presents a Lorentz force dual-actuator, which generates repulsive and propulsion forces. The advantages of repulsive and attractive magnetic levitation systems are combined and the drawbacks of both are eliminated. It provides a compact and cost-effective solution for vacuum compatible high precision magnetic levitation positioning systems. Two possible positioning systems based on this actuation scheme will be presented. The calculation of the repulsive magnetic guidance force of this actuator and the verification by finite element method (*FEM*) will be presented in this paper as well.

Keywords: Active Magnetic Bearing, Halbach Array, High Precision Positioning System, Linear Lorentz-Actuator, Magnetic Levitation

Introduction

In recent years, high precision positioning systems up to the nanometre-range (*nm*) in combination with long planar strokes and vacuum compatibility have been demanded for many industrial applications, such as semiconductor manufacturing or nanotechnology. Magnet levitation systems as high precision positioning drives are of great interest for such applications due to their positive properties: The propulsion actuators in these systems generate the forces directly to the moving element (*mover*), omitting the necessity of mechanical transmission elements. The latter causes, through backlash and friction, restrictions concerning precision and dynamics. The magnetic guidance in these systems can act simultaneously as a contactless guiding element and as a high precision positioning element in the vertical direction with strokes in the range of several hundred micrometres [1]. Consequently, due to the non-contact propulsion and guiding of the mover, which means an absolute friction-free operation, these systems can also operate without any restrictions in a high vacuum environment or clean-room. Furthermore, a proper position measurement and closed-loop control in six degrees-of-freedom (*6-DoF*) allow for a position accuracy, which would not be possible with mechanical guidance.

Halbach arrays for 6-DoF Positioning Systems

Typically, the top side of the magnetically levitated *mover* should be freely accessible from above to enable easy loading and unloading of objects for various applications. For this reason, usually reluctance actuators (*RA*) are not satisfactory, since they have to be positioned above the mover [2]. Nevertheless, to overcome this drawback, some topologies with *RA*s are known in the literature, where a freely accessible *mover* from above can be realised. However, these concepts are also not satisfactory, since the footprint of the whole system as well as the mass of the *mover* increases too. As a result, compact constructions are not possible [3]. Therefore, most existing high precision positioning systems based on magnetic levitation are realised by moving Halbach arrays (*HA*) and stationary electrodynamic linear actuators (*LA*). This is mainly because of two reasons:

- A freely accessible *mover* from above;
- A arbitrary scalability of the stroke without a dramatic increase of suspended mass.

Through the working principle of these systems, the *mover* is repulsed from the stator. This allows the placement of the sensors and actuators below the mover. Fig. 1 shows one Halbach actuator unit (*HAU*) for high precision magnetic levitation systems, where the *HA* is placed in the *mover* and the *LA* in the stator.

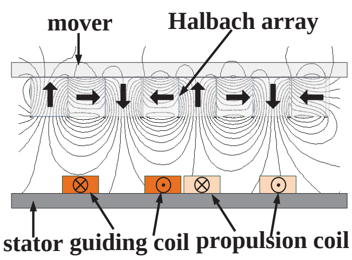

Fig. 1: *Halbach actuator unit (HAU)*

As a result of the field distribution, this *HAU* can generate simultaneously levitation and propulsion forces and need no iron-yoke, which is also beneficial. By using at least three of such *HAU*s in a

Planar Magnetic Levitation in 6 DOF

R. Glöß, Physik Instrumente (PI) GmbH & Co. KG, Karlsruhe, Germany

Abstract:
The paper describes a new magnetic levitation system for 6 DOF with nanometer resolution. The system consists of a movable stage with 8 Halbach arrays and a grid for 4 optical incremental sensors, and 8 analog hall sensors. The electromagnetic forces to lift and move the stage in all directions, are generated in a 12-layer PCB board by a 144-coil design. Pulse-width modulated (PWM) drivers with 350 kHz frequency are directly coupled at the main board. A new multi-core controller connects the 48 PWM drivers, the optical and magnetic reference sensors with the main processor unit with hardware and firmware real-time synchronization for force and momentum calculations.

Keywords: Magnetic Levitation, Nanometer Resolution, Halbach Array, PCB Coil Structure, Multi Cluster

Introduction

Maglev systems with PCB coils are already familiar in the literature, but all these systems need displacement sensors for vertical position and tip/tilt angles which span over the upper working surface of the movable stage. Some systems use cist expensive laser interferometers. In that case, the stage can't be used in industrial applications where the upper surface has to be free for the customer scanning application or the costs of the system does not match the low budget requirements. [1] [3]

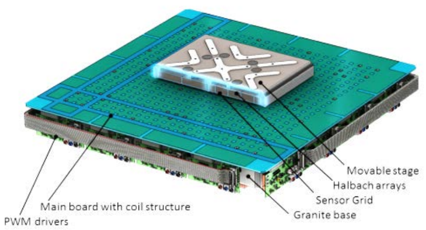

***Fig. 1:** Planar magnetic levitation stage with 6 degrees of freedom (schematic cross section)*

In our new design, the platform surface is free. The coils inside the PCB are placed at gaps of 5mm. Some of the gaps have rectangular holes through the PCB to open the light path for the incremental optical sensor heads. The stage design is optimized for high electromagnetic forces. The static lifting force (Z-direction) is more than 4 times the weight of the stage and can overcome 6 times this value for dynamic operations. This is much higher than in our former design with the six coil structure. [2]

The force calculation is done with a combination of FEM magnet field methods, a Lua script based on Python, and a newly designed fully graphical software interface. Fig.2 shows the good correspondence of the calculated magnetic field components to the measured field distribution. The 3D field magnetic measuring technology based on a 3D magnet field sensor, a high precision positioning technology synchronized with PI's hexapod controllers.

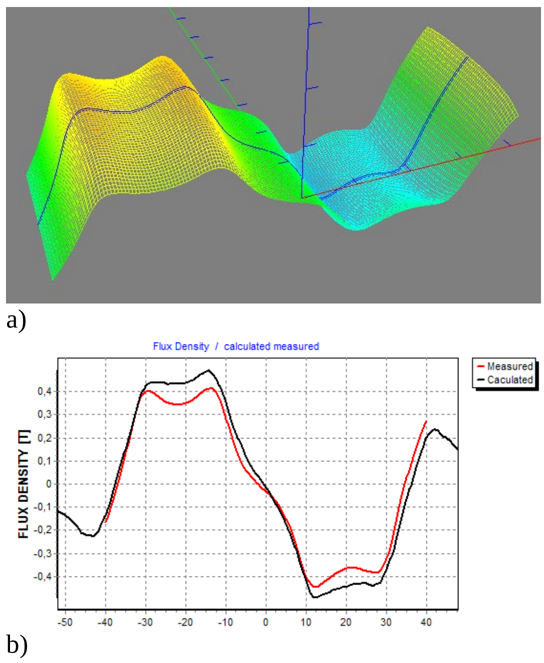

***Fig. 2:** a) 3D - measured magnetic flux density in horizontal direction (X); the blue line shows the cross section for 2D*
b) 2D - verification between measurement and simulation shows acceptable conformity

With a moderate current of only 1.5A in the clusters of coil assembly, the stage can be driven by more than 40N in a vertical and horizontal direction. The coil structure (in 12 layers on a PCB) does not need additional wiring and is connected with highly efficient PWM drivers, placed directly on the main board. 48 full bridge drivers are used, the design is very cost efficient and it reduces the risk of EMI distortions because of the short connection to the

Torque Measurements on an Electromagnetic Tilting Actuator

M. Dörbaum, T. Winkel, S. Tappe, J. Kotlarski, T. Ortmaier, B. Ponick
Leibniz Universität Hannover, Hannover, Germany

Abstract
This article presents the measurement and simulation results for a novel electromagnetic tilting actuator concept with special focus on its holding torque. The superior aim of this concept is to overcome restrictions of common endoscopes considering the ratio of flexibility to shaft stiffness. Therefore, the prediction and increase of the holding torque is essential. For the prediction of torque, 3D Finite Element Analysis is used and compared with measurement results. To increase the holding torque or rather reduce the necessary holding currents and losses, a material variation from St37 steel to Vacoflux 50 is investigated.

Keywords: Electromagnetic Tilting Actuator, 3D Finite Element Analysis, Vacoflux, Endoscope

Introduction

The use of endoscopes has become more and more standard in the field of medical and industrial applications. Common endoscopes are struggling with being either flexible or rigid, but not both at the same time. Most flexible endoscopes use Bowden wires to interact at their ends with the surrounding environment. But their flexible shafts tend to form loops while moving through hollow spaces and may stress the surroundings and cause the patient pain in the case of medical applications.
The approaches to overcome this discrepancy described in literature can be classified into actuation units using Bowden wires, concentric tubes or serial actuators with varied actuation concepts (see [1]–[3]). Nevertheless, many concepts described are restricted due to several aspects, such as low flexibility, low resistance against external forces, complex setup or high reaction time.
In this article, the approach presented uses a chain of binary electromagnetic tilting actuators (ETA) to achieve the aim of being flexible and stable with the same platform. Concerning the system stiffness in a sequential actuator chain, the applicable holding torque of each individual ETA is important. The holding torque is provided by a thermally permitted DC current in both coils of the closed ETA side [4]. It was simulated with ANSYS Maxwell 3D in static simulations with a fully parameterized model.

Actuator Design

The ETA acts similar to common electromagnets but shows significant differences to the functional principles of solenoids [5]. Two similarly built halves represent one actuator element (*Fig. 1* (a)). Each half consists of a kidney-shaped coil which is inside a bevelled iron core. The sides of one half are electromagnetically segregated through paramagnetic joints (*Fig. 1* (c)). Several actuators are joined in a line, composing an actuator chain, *Fig. 1* (b).

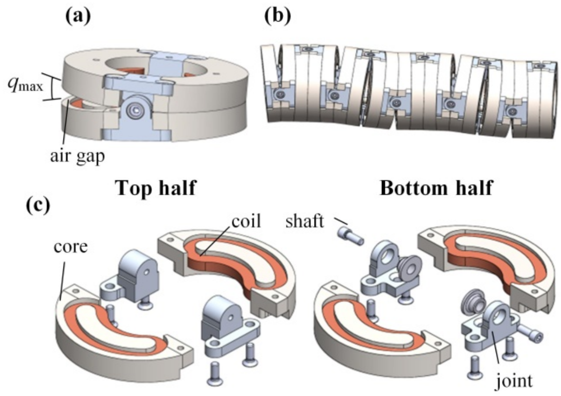

Fig. 1. *(a) CAD model of one ETA, (b) fully actuated shaft with twisted actuators (c) exploded view of its components,[4]*

Different actuator types were designed, simulated, and measured (see [4] and [6]). The characteristics of the ETA used in this paper are given in *Table 1*.

Table 1: *Data of the prototype ETA*

Parameter		*Value*	*Unit*
Outer ETA diameter	d_a	45	mm
Inner ETA diameter	d_i	22.5	mm
Height of one ETA half	h_A	8	mm
Height of slot	h_S	5	mm
Tilting angle	q_{max}	± 6	°
Number of turns per coil	w	50	

Simulation Setup

The electromagnetic simulation of the ETA and the prediction of its torque was carried out using finite element analysis (FEA) with ANSYS Maxwell 3D and a fully parameterized ETA model. The resulting torque is mainly influenced by the air gap. As the actuator rotates, the air gap width δ is not even but V-shaped and, therefore, a function of areal position (x, y) and tilting angle q.

An Exploratory Study of the Retardation Ability of a Thomson Coil Actuator

G. Engdahl, J. Magnusson
KTH Royal Institute of Technology, Stockholm, Sweden
A. Bissal, ABB Corporate Research, Västerås, Sweden
M. Sparr, KTH Royal Institute of Technology, Stockholm, Sweden

Abstract
In mechanical switching devices for HVDC, a feasible actuator concept for maneuvering the galvanic contacts is the so-called Thomson coil actuator. By this concept, hundreds of km/s^2 can be attained. To ensure reliability and operational endurance, an effective retardation mechanism is required. In this work, an exploration of the feasibility to also use the Thomson concept for the retardation of the contact movement was performed. A conclusion is that it is possible to attain a complete retardation down to a velocity in the vicinity of stand still. This, however, only is possible if the amplitude of the excitation of the retardation coil is matched appropriately to the velocity and position of the incoming moving mass. The work performed has been to numerically explore within which ranges of the excitation voltage and separation distance a feasible retardation can be obtained for a specific configuration of a Thomson coil actuator system.

Keywords: Thomson Coil, Actuator, Retardation, Electromechanical, Contact, Electromagnetic

Introduction

Thomson coil actuators have shown to be feasible for actuation of galvanic contacts in ultra-fast electromechanical electrical switches [1-2]. The option to use this actuator concept also for contact retardation has recently been proposed [3]. In this paper a more comprehensive study has been performed that investigates under which conditions an appropriate retardation of the contact system can be obtained.

The concept

A Thomson coil (TC) actuator comprises two parts, a primary coil and an armature. The coil is wound with a wire like a flat spiral. The armature in shape of a conducting disc is attached concentrically in near vicinity of the primary coil. A surge current in the coil induces, according to Lenz' law, eddy currents in the opposite direction in the armature disc. The resulting current force according to Biot and Savart's law then generates a huge repulsive force between the coil and the armature. The principle idea is to locate an armature between two coils designated as the acceleration coil and the retardation coil. This armature is mechanically connected via a push or pull rod to current carrying contacts. Once the incoming armature reaches the vicinity of the retardation coil, the retardation coil is excited to smoothly damp the velocity enabling a smooth landing. A smooth damping greatly extends the lifetime and reliability of such devices since large stresses due to collisions are avoided.

The model

The exploration was performed with the use of a Finite Element Method (FEM) model with a movable geometry. A detailed description of the model can be found in [4]. The resulting volume force $\mathbf{F}_{em}=\mathbf{j}\times\mathbf{B}$ is integrated over the armature and inserted in Eq. 1 and Eq. 2.

$$\iiint \boldsymbol{F}_{em} \cdot \boldsymbol{n}_z \, r dr d\theta dz = m_{arm} \frac{d\boldsymbol{v}}{dt} \qquad (1)$$

$$z = \int \boldsymbol{v} dt \qquad (2)$$

, where m_{arm} is the mass of the movable contact including the armature.
This FEM-model constitutes a part of the electric excitation circuit according to Fig. 1.

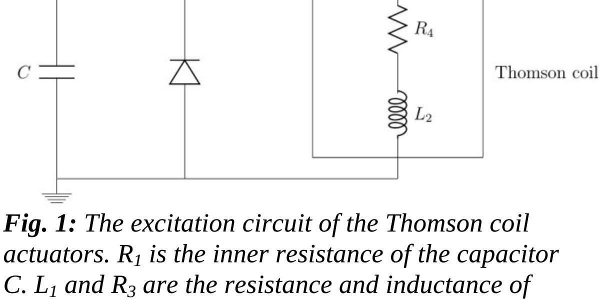

Fig. 1: *The excitation circuit of the Thomson coil actuators. R_1 is the inner resistance of the capacitor C. L_1 and R_3 are the resistance and inductance of the connection cables. The components within the box are modelled by the FEM-model.*

Miniaturisation Trends in Magnetic Gears

G. Puchhammer, Karl Rejlek GmbH, Wien, Austria

Abstract:
Many mechatronic applications in industry could profit from the outstanding properties of magnetic gear boxes. Currently, there are few commercially available magnetic gear boxes for very small dimensions. Generally, two problems arise when miniaturising magnetic systems. The first is directly related to miniaturised magnets. There is a natural limit for downsizing them, which is affected by the physical size. The second problem relates to excessive loss in system torque when minimizing the dimensions of magnetic systems. In this paper, two ways to overcome these problems of miniaturisation are addressed. In both cases, Magnetic Wobbling Gears in Type-C mode can make valuable contributions in overcoming these problems. High reduction ratios can be realized in one single gear stage, thereby using magnets that are big enough for handling and assembling purposes. New methods of torque-enhancing technology can allow for the generation of additional torque.

Keywords: Magnetic Gear, Gear Box, Magnets, Magnetic Wobbling Gear, Torque Enhancing, Torque Density, Robustness, High Reduction Ratio

Introduction

Most of performance needs in applications for which actuators are needed are sufficiently covered by previously existing actuation principles. So, it is in actuators powered by motors in direct drive mode, or by motor-gearbox assemblies if higher output torque is required. These represent state-of-the-art solutions.
Nevertheless, in cases where exceptional purposes are required, these well-established solutions can fail. Extreme robustness in electric powertrains for linear axes, extremely lightweight motor-gear units with ultra-high motor speeds, lubricant-free motor-gear units operating in a vacuum, extremely precise positioning ability resulting from backlash-free motor-gear units, and many other cases for magnetic gears may allow challenging projects to be solved in industry. It is known that magnetic gearing is superior to all of these special purpose applications listed above. For magnetic gearing, the process of industrialisation only recently started.

General Effects Induced by Miniaturization

Miniaturizing a magnetic system usually entails miniaturization of all individual components within this system. Linear miniaturization can proceed with over-proportional nonlinear degradation of magnetic properties. This also applies to magnetic gears. Thus, each magnetic effect follows its own law.
The manufacturing method of producing small strong magnets consisting of NdFeB or SmCo depends upon the required shape of these magnets. Because of the hardness of sintered magnetic material, special techniques such as wire cutting, grinding, or sawing with diamond-studded circular saw blades are commonly used techniques. Insufficient cooling during these processes can result in local heat generated defects, which may result in the degradation of the magnetic properties of these magnets. In the case of a defective magnet, new magnetization is recommended.
The thickness of the surface coating of a magnets is driven by anti-corrosion requirements and the coating layer structure. Therefore, the coating thickness is independent of the magnet size and has a fixed height. The layer dimensions are very small compared with the magnet dimensions. Hence, the influence of coating in reducing the magnetic flux can be neglected. However, this does not hold if the physical dimensions of the magnets become smaller and smaller. The influence of the non-magnetic coating material that is applied on magnets with physical dimensions <1 mm can become an impediment. For example, the coating thickness for the most frequently used Ni-Cu-Ni coat measures ~12 microns. When applied on a cubical shaped magnet with an edge length of 1 mm, a volume loss of magnetic material of 7% will result. Because the coating material is non-magnetic, it behaves like a magnetically non-conductive material, so it has the same magnetic flux generating poverty as an air gap. Reduction of the air gap dimension appears to have a positive contribution that enhances magnetic flux. Nevertheless, a contactless motion of all rotating parts that form the magnetic system needs to be guaranteed by the surrounding mechanical system. The maximum amount of radial tolerance of all single system components, such as bearings, magnets, and back iron, shall be less than the designed air gap. In electric machine design, the typical air gap dimension is taken considered to be the thousandth part of the diameter of the magnetic system. For small system dimensions, this well-established recommendation appears to be far too low. In special cases in which manufacturing costs are of secondary importance, expensive manufac-turing procedures can help to realize this small air

Longitudinal - Torsional Type Piezoelectric Actuator for the High Speed Rotational Motor

Y. Yang, Nanjing University of Aeronautics and Astronautics, Nanjing, China
D. Mazeika, Vilnius Gediminas Technical University, Vilnius, Lithuania
P.Vasiljev, S. Borodinas
Lithuanian University of Educational Sciences, Vilnius, Lithuania

Abstract:
A new ultrasonic compound type piezoelectric actuator for high speed unidirectional rotational type motor has been developed. Longitudinal-torsional hybrid vibrations are excited in the actuator in order to achieve large vibration velocities of the contacting points. Piezoelectric actuator consists of two metal hollow cylinders with different cross-section area, two piezoceramic rings and a special star type waveguide that is located at the node of longitudinal vibrations of the actuator. Single channel harmonic signal is used to excite the first longitudinal mode of the actuator. The second mode of torsional vibrations is obtained by employing curvilinear radial vibrations of the star type waveguide that operates as longitudinal vibration mode converter. First longitudinal mode of the star rods is induced by transverse deformations of the cylindrical parts of the actuator. Numerical investigation of the piezoelectric actuator was performed to analyse natural frequencies, modal shapes and actuator response to the harmonic excitation. Experimental prototype of the actuator was fabricated and operating principle of the actuator was validated.

Keywords: Piezoelectric Actuator, Longitudinal - Torsional Vibration

Introduction

Piezoelectric actuators are widely used for different industrial, medical and life science applications [1, 2]. Piezoelectric actuators are capable of reaching high resolution and speed of the positioning object and possess many attractive features such as a short response time, a compact size, high force, and good controllability [3- 11]. Many design principles of the piezoelectric actuators are proposed up to date [1-6]. Summarizing it all, the following types of piezoelectric actuators can be specified: standing-wave, traveling-wave, quasi-static, and multimode vibrations actuators [6]. Different designs of standing-wave actuators are developed based on longitudinal vibrations of compound-type transducers. Usually, elliptical trajectory of the contact point is achieved by combining shifted phase vibrations of the actuators [7-8]. Multimode vibration actuators combine two different vibration modes of the actuator as for example longitudinal - bending or longitudinal – torsional. Elliptical motion of the contact point is achieved by superposing displacement of the contact point obtained from both vibration modes [8].

There are several longitudinal-torsional vibration type piezoelectric actuators developed [1-4, 11]. The main advantage of these actuators is a possibility to achieve high vibration velocity of the contacting points and the large output torque. Longitudinal-torsional type piezoelectric actuator can be divided into two main types: multi-mode type and mode conversion type [2]. Multi-mode type actuators use two separate bunches of piezoceramic elements to excite longitudinal and torsional vibrations of the contacting point independently while mode conversion type actuators use just one bunch of piezoceramic elements and only longitudinal vibration mode are excited. Torsional vibration are induced employing longitudinal vibrations and a special mode converter [1-3]. Main disadvantage of the multi-mode type actuators is complex manufacturing process of the torsional piezoceramic pieces that are used for exciting the shear vibration of the stator, using d_{15} effect of the ceramic pieces. Disadvantage of the conversion type actuators is complex design of mode converter.

Novel design of longitudinal-torsional type piezoelectric actuator is introduced in the paper. The main purpose of new actuator development was to achieve high velocities of the contacting points. Numerical modelling of the actuator was performed, and an experimental prototype was made. Results of numerical and experimental investigation are discussed.

Design and operating principle

A new ultrasonic compound type piezoelectric actuator was developed for high speed rotational type motor. Operating principle of the actuator combines both features of the longitudinal – torsional piezoelectric actuators mentioned in previous section. Proposed piezoelectric actuator consists of two metal hollow cylinders with different cross-section area, two piezoceramic rings and a special star type waveguide that is located at the node of longitudinal vibrations of the actuator between two piezoceramic rings. All parts are compacted by the fasting bolt (Fig 1).

The Investigation of Hollow Hemisphere-Shape Actuator

P. Vasiljev[1], R. Bareikis[1,2], S. Borodinas[1,2], A. Struckas[1], J. Kasperoviciene[3]
[1] Lithuanian University of Educational Sciences, Vilnius, Lithuania
[2] Vilnius Gediminas Technical University, Vilnius, Lithuania
[3] Institute of Botany, Vilnius, Lithuania

Abstract:
In this paper we are investigating two possible excitation methods of how to simultaneously excite two vibration types – longitudinal and radial. The first method – is to glue the PZT element to a specifically prepared surface area of the hemisphere. The second way is to connect the hemisphere to a Langevin type longitudinal transducer. For both cases we did modeling to find eigen frequency as well as harmonic analysis in a lower ultrasonic frequency range (20-30kHz). Impedance-frequency characteristic and mechanical vibration amplitudes are measured around resonant frequency. Comparative tests for both systems are performed using proposed actuators for algae ultra-sonication for bio-fuel production. We have determined the relation of longitudinal and radial waves that are traveling from the excitation source to a hemisphere opposite end. The prototypes of proposed systems are designed and manufactured. Comparative algae destruction results are obtained.

Keywords: Bio-Fuel, Ultrasonic Reactor, Algae

Introduction

Bio fuel made from algae is so called zero balance fuel. Because the same amount of CO_2 produced is recuperated by algae during new grow cycle. Algae are more efficient in comparison with crops. Nowadays world is facing energy crisis along with food crisis. The crops are grown on valuable farmlands that could produce food instead of soya, corn, wheat, palm, etc. In this case algae production is more efficient because it can be grown in salted or contaminated water. During past few decades when the boom of crop fuel production was at its peak the farmers started to destroy rainforests to obtain more land suitable for crop grow.

In the early 90's in the US one liter of bio fuel produced from algal oil was about 6$. Today it is about 3$, however it is still more than fossil fuels cost [1, 2]. It is necessary to take some actions in different bio fuel production stages to reduce the cost. Bio fuel made from algae cannot be counted as an alternative source of energy, but as an additional source. Energy consumption demands increasing each year so the so called alternative or renewable energy sources cannot fully replace classic energy sources, but only can slow down oil extraction volume. Today bio fuels are twice expensive comparing with fossil fuels. It is necessary to take some actions in different bio fuel production stages to make process more efficient and thus reduce the overall cost.

In this paper we are presenting an ultrasonic system for process intensification in liquids, in particular for algae disruption. Ultra sonication is not a new method [3, 4] for that purpose however the system design can be crucial in achieving such a goal [5, 6].

Design

The construction of proposed system is based on a half of hollow hemisphere. The excitation is coming from radial side and the active end is the edge of a hemisphere. The benefits of such design are largely increased surface vibration area, while the amplitude is still good for the job. The hollow hemisphere (dome) is also known in architecture as a way to distribute load. Here using resonant geometry of hemisphere we achieve a significant vibration area increment. General view of a tool is presented at Fig. 1, where longitudinal vibration is irradiated to a medium from green area, external radial from blue and internal radial from purple.

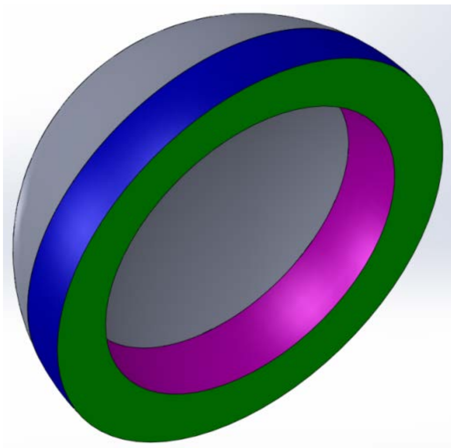

Fig. 1: *General view of proposed tool*

Piezoelectric Nonlinearity and its Temperature Dependency Under High Power Driving

S. Miyake, T. Morita
The University of Tokyo, Kashiwa-shi, Japan

Abstract:
Piezoelectric transducers are used in various devices and they are driven under high power condition. Nonlinear effects such as “jumping phenomena” in current, hysteresis of admittance curve and temperature rise of piezoelectric transducer under high power driving are well-known; however, they cannot be simulated by a traditional piezoelectric equivalent circuit because it is based on only a linear piezoelectric effect. For FEM simulation for designing piezoelectric devices, the nonlinear effect must be clarified. Our research group has already succeeded in simulating nonlinear effects without temperature rise; however, in the actual operation, temperature distribution is inevitable in the piezoelectric transducer due to mechanical dumping and dielectric loss. In this research, we measured the change of the material constants of piezoelectric transducer as a function of temperature. Based on these parameters, a transfer matrix model for piezoelectric vibration under high power driving was established.

Keywords: Piezoelectric Device, High Power Characteristic, Nonlinearity, Temperature Rise

1. Introduction

When the piezoelectric transducers are driven under high power condition, nonlinear effect such as jumping phenomena of current or/and hysteresis of admittance appears. These phenomena are problem in a design of piezoelectric devices because it is difficult to simulate them. Our research group has already formulated these phenomena under room temperature [1]. However, in the actual driving, temperature distribution is inevitable in the transducer due to mechanical and dielectric loss and material constants change due to the temperature increase. In the previous research, a LCR equivalent circuit was used and the piezoelectric vibration was calculated with a lumped parameter system. This method is simple and convenient, although, it can be valid only uniform temperature condition.

In this research, we measured the temperature dependency of the material constants including the nonlinear parameters and established transfer matrix model to consider the nonlinear vibration as a distributed parameter system. Using the transfer matrix model and considering the change of material constants due to temperature increase, we succeeded in simulating the piezoelectric vibration under high power driving.

2. Nonlinearity

The relationship between voltage V and current i in the mechanical part of piezoelectric LCR equivalent circuit is given as equation (1):

$$L\frac{di}{dt} + R_0 i + \frac{1}{C_0}\int idt = V \qquad (1)$$

where L, R_0 and C_0 are equivalent mass, equivalent dumping and equivalent elastic constant. Under high power condition, the relationship is written as equation (2) [1]:

$$L\frac{di}{dt} + R_0 i + \eta i^3 + \frac{1}{C_0}\int idt + \xi\omega^3\left(\int i\,dt\right)^3 = V \qquad (2)$$

where ω is driving angular frequency; ξ and η are nonlinear coefficients which are related to the mechanical third mode vibration excited by high stress. Nonlinear coefficient ξ and η are considered under lumped parameter system [1]. In this research, we considered the temperature distribution of the piezoelectric transducer with distributed parameter system. Accordingly, we introduce a nonlinear coefficient E_3 into the equation between stress T_1, strain $\frac{\partial u}{\partial x}$ and Young’s modulus E_1 as equation (3):

$$T_1 = E_1\frac{\partial u_x}{\partial x} + E_3\left(\frac{\partial u_x}{\partial x}\right)^3 \qquad (3)$$

where x is longitudinal position and u_x is displacement. E_1 and E_3 are complex number.

3. Temperature distribution

Heat generation due to the mechanical vibration loss per unit time is given as equation (4):

$$\dot{q}(x) = \frac{1}{2}\frac{whE_{1i}}{\omega}\left(\frac{\partial v_x}{\partial x}\right)^2 + \frac{3}{8}\frac{whE_{3i}}{\omega^3}\left(\frac{\partial v_x}{\partial x}\right)^4 \qquad (4)$$

where w, h are width, height of transducer, E_{1i}, E_{3i} are imaginary part of E_1, E_3. Large amount of heat are generated at the center of the transducer because of the largest $\frac{\partial v_x}{\partial x}$. Figure 1 is the measured temperature distribution in the piezoelectric transducer driven under high power condition.

Since the material constants change as temperature increase, we measured the material constants of piezoelectric transducer under uniformly raised temperature condition.

Barium Titanate Thick Film Deposited by Ultrasonic-Assisted Hydrothermal Method

R. Takayama, T. Morita
The University of Tokyo, Kashiwa-shi, Japan

Abstract:
In general, lead zirconate titanate ($Pb(Zr,Ti)O_3$, PZT) is practically used for the piezoelectric devices because of its excellent piezoelectric properties. However, its environmental load has become a problem since the PZT contains large amount of lead. Based on this background, a barium titanate ($BaTiO_3$, BT) was synthesized on a titanium substrate by an ultrasonic-assisted hydrothermal synthesis in this study. This method utilizes the strong ultrasonic irradiation during the hydrothermal synthesis to enhance the thickness of the thin films as reported in the case of PZT and potassium niobate. As we expected, the thickness of the barium titanate film was increased from 1.0 μm to 4.0 μm by the ultrasonic assist. In addition, the purity of barium titanate was improved with the ultrasonic irradiation. The ferroelectricity and piezoelectricity of the barium titanate thin film was confirmed by the DE hysteresis loop measurement and by the piezoelectric force microsopy (PFM) observation.

Keywords: Barium Titanate, Hydrothermal Method, Ultrasonic Assist

Introduction

The piezoelectric material has been applied to various sensors and actuators. In such piezoelectric devices, lead zirconate titanate (PZT) is mainly used because of its high piezoelectricity. However, PZT should be replaced to the environmental friendly materials because PZT contains lead. Especially, in the case of micro sensors, actuators and energy harvester devices, thick piezoelectric films are required.

Among various lead-free piezoelectric films, we examined a barium titanate thick film deposited with an ultrasonic-assisted hydrothermal method. In this method, the chemical reaction is promoted by the cavitation generated by the ultrasonic irradiation. Thus, as compared to the conventional hydrothermal synthesis method without ultrasonic assist, it was confirmed the thickness is increased to 2.7 times (in case of PZT) [1] and 5.2 times (in case of potassium niobate) [2]. However, the reaction temperature is relatively high, 240 degrees for potassium niobate, which is severe for a Langevin type transducer for applying ultrasonic irradiation.

Hydrothermal Synthesis

The hydrothermal method is a simple method, just putting a substrate into a chemical solution in a pressure vessel as shown in Fig. 1, and keeping the reaction temperature. One of the advantages is its low reaction temperature below 250 degrees, while other methods, such as sol gel method and sputtering method, require the crystallization process above 600 degrees. Especially, in the case of the barium titanate deposition, the hydrothermal reaction temperature can be reduced to be only 90 degrees Celsius as reported in [3]. The other advantage is a high-quality of the film because of little contamination from outside. The film thickness is a few micrometers, that is much larger than that deposited with conventional methods.

However, such thickness is insufficient and more than 10 μm is required for the practical devices. A. T. Chien reported that the barium titanate thickness was only 200nm for 30 hours reaction time in the previous studies [3]. In this study, we examined to increase this thickness by applying high-power ultrasonics.

Fig. 1*: The pressure vessel for hydrothermal method*

Ultrasonic-assisted Hydrothermal Synthesis

In this study, a barium titanate film was deposited by the ultrasonic-assisted hydrothermal synthesis [1, 2, 4, 5] to increase the film thickness. For the ultrasonic irradiation, the Langevin transducer as

Full Characterisation of PZT Actuators in Quasi-Static, Large Signal Operation at Elevated Temperature

C. Mangeot, B. Andersen
Noliac A/S, Kvistgaard, Denmark

Abstract:
Optimising a piezo-based application over a wide temperature range can be challenging. Currently the main obstacle is that multilayer actuators are not sufficiently characterised in temperature. To some extent, this is due to the lack of practical standards in this field. In this paper, a method is proposed to characterise the operating envelope of actuators over temperature. The approach is based on a series of simple measurements: dimensions, free displacement, stiffness and electrical measurements. The method was applied on multilayer actuators made of two different materials: one hard-doped PZT ceramic (NCE46) and one soft-doped (NCE51). Experimental results are presented, highlighting how the specification of a product evolves with temperature and providing a powerful tool for designers to verify and optimise their application.

Keywords: Piezoelectric, Multilayer, Actuator, Temperature

Introduction

Quasi-static multilayer piezoelectric actuators are finding more and more applications, for example in the field of aerospace [1], however their properties are still not fully characterised, in particular at high temperature.

The present work is performed within the project AeroPZT, specifically funded under the Clean Sky Joint Technology Initiative (EU FP7). The project partners, TWI Ltd. (UK), Cedrat Technologies (France), Noliac (Denmark) and Politecnico di Torino (Italy) are targeting the development of materials and processes for the application of piezoelectric materials in aero engine controls, which implies harsh environmental conditions, particularly elevated temperature.

Some literature is available on large signal stress-strain behaviour [2-5], however these studies are often incomplete and difficult for end-users to exploit. This is in part due to the lack of standards in the field.

Available standards

Currently available international standards focus mostly on material properties and small-signal measurements. Standards addressing large signals such as [6] still focus on transducers, not actuators, so both the parameters and methods of measurement are difficult to transpose.

[7] introduces the effect of temperature as a single slope coefficient as illustrated on Fig. 1. The standard recognises the presence of a sort of thermal hysteresis which makes the characterisation more difficult.

[8] introduces a series of linear coefficients, as defined in Eq. (1). $T^{(n)}$ is defined as the n^th^-order temperature coefficient of the quantity q at the reference temperature θ_0.

$$T^{(n)}(q) = \frac{1}{q_0 n!}\left(\frac{\partial^n q}{\partial \theta^n}\right)_{\theta=\theta_0} \tag{1}$$

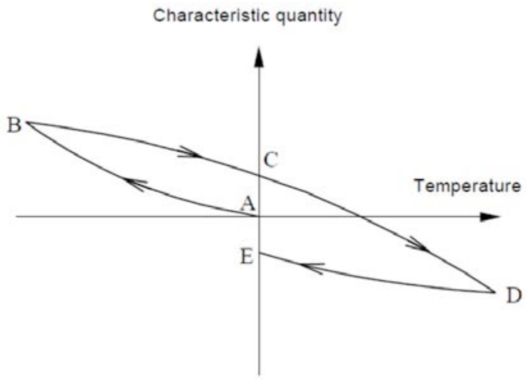

Fig. 1: Temperature dependency of a characteristic quantity according to [7]

Although these two approaches can be relevant for transducers, they are not practical for quasi-static actuators. Furthermore, standards focus mostly on material properties, while these do not necessarily reflect the behaviour of multilayer actuators for several reasons:

- Multilayer actuators are operated under high electrical field, causing significant non-linearity, while material properties are usually measured under low field excitation.
- The end-user is often unaware of the internal construction of multilayer actuators, i.e. number and thickness of the active ceramic layers.

Reliability Enhancement Through the Use of Fusing Technique

C. Mangeot, Noliac A/S, Kvistgaard, Denmark

Abstract:
Fusing is sometimes used for Multilayer Ceramic Capacitors in order to improve their tolerance to cracking, particularly under external stress. The approach can be applied to stacked “chip” multilayer actuators, where a fuse effectively allows further operation after one or more individual failures. Statistical analysis indicates that the probability of failure is greatly reduced. Experimentation confirmed the enhanced lifetime and independence of the failures with limited impact on the operational envelope of the actuators.

Keywords: Piezoelectric, Multilayer, Actuator, Fuse, Reliability

Introduction

Multilayer piezoelectric actuators are massively parallel capacitive devices, containing thousands of layers. If a short circuit occurs at any point through a layer, the whole device will not be able to hold an electrical field, therefore it will not be usable. Being mostly capacitive, multilayer piezo actuators share some similarities with multilayer ceramic capacitors (MLCC). In MLCC, a major reliability concern is crack propagation due to stress induced by deformation of the PCB substrate [1]. On standard MLCC, a crack will reduce the dielectric strength of the device, leading to internal arcing and ultimately failure in short-circuit. More advanced designs address this issue through different methods: increase of the electrode margins in order to locate the crack in inactive material (Open Mode Design); floating electrodes, i.e. effectively putting several capacitors in series; compliant termination in order to reduce the induced stress [2]; fusing [3].
Unfortunately, many of the usual approaches used in MLCC are not applicable to piezo actuators, for which they would cause a drop in performance or an increase of the required voltage. The fusing technique has however been proposed for piezoelectric actuators in the past [4], but without any known commercial application.

Analysis of failure modes

Manufacturers usually consider two different operating conditions for PZT multilayer actuators: DC and AC.
In DC operation, the actuator is submitted to a constant electrical field, leading to electro-chemical degradation. The most likely failure mode in this case is a loss of dielectric insulation, leading to short-circuit. This phenomenon is accelerated by the presence of humidity or contaminants [5].
In AC operation, the electro-chemical effects are greatly reduced. On the other hand, the structure is submitted to mechanical fatigue. In these conditions, several publications reported crack propagation at the interface between ceramic and internal electrodes [6, 7]. When this problem is avoided, it is common to see the first failure appear at the electrical interconnect, typically at the interface between the ceramic and the interconnection system (see Fig. 1). This type of failure is usually not detected, so operation of the actuator continues in degraded conditions. The intermittent contact and sparking under high voltage leads to dynamic loading and further degradation, such that the usual way the failure is observed is through short-circuit.

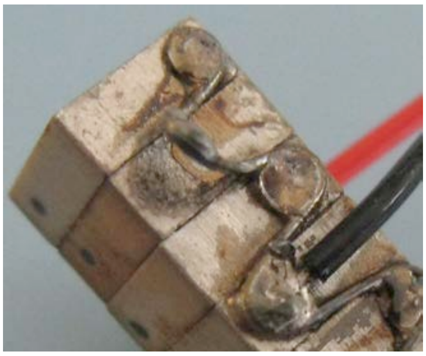

Fig. 1: *Loss of contact after 10^9 cycles at 150°C (contact lifted from surface to highlight the defect)*

In any case, the amplitude of the electrical field and temperature are major factors defining the reliability of piezoelectric devices [8, 9].
In addition to these failure modes, experience shows that external factors play a major role in the reliability of piezoelectric actuators. Uneven loading, dynamic stresses and contamination are some possible root causes. Although these causes are different from the ones observed on MLCC, in general for all those cases, the failure will manifest itself as an electrical short.

Resonance Frequency Tracking for Piezoelectric Devices

S. Safour, Y. Bernard
GeePs, UMR CNRS 8507, CentraleSupélec, Université Paris Sud, Université Paris-Saclay, Sorbonne Universités, UPMC Université Paris 06, Gif-sur-Yvette, France

Abstract:
This paper presents experimental and numerical study of the effect of the environment on the frequency response of a piezoelectric device. The intent is to highlight the key elements to be taken into consideration when selecting or designing a resonance frequency tracking system. The studied specimen is a ring shaped PZT based material. Measurements in free vibration conditions using a frequency response analyser are done to investigate the effect of the applied voltage amplitude (DC and AC) and the material temperature on its frequency response. The material is then placed within a structure made of steel and polytetrafluoroethylene (PTFE) parts. Mechanical stress is applied using a compression machine to the structure, and its effect on the frequency response is measured. A finite element based model is introduced in order to explain the observed stress-effect. At the end a resonance frequency tracking system based on the zero phase angle control is discussed.

Keywords: Piezoelectric Device, Frequency Response, Resonance, Temperature, Mechanical Stress, Voltage Amplitude.

I. Introduction

Piezoelectric devices are widely used in actuation, Ultrasonic motors, Langevin transducers or dental instruments are good examples. Polycrystalline piezoelectric materials are the most used in such devices; they have good piezoelectric characteristics and could be easily modelled to any shape. The device is excited at frequency corresponding to a vibration mode that has the required deformation shape for the application. Such devices operate at the mechanical resonance frequency or near it in order to achieve the maximum performance [1, 2]. As will be shown in the next section, the frequency response of such devices is strongly environment dependent, therefore a variation of the mechanical stress, the temperature or the electrical field might lead to their resonance frequency variation. The device wear might also have an effect on the resonance frequency. When the piezoelectric device is supplied with a fixed frequency voltage its performance decreases under the effect of those environment factors.
In order to keep the system operating at their maximum performance point, methods for tracking the resonance frequency are proposed [3, 4, 5, 6], the oscillator and the phase-locked loop circuits have been the most utilized. The effectiveness of such methods is highly dependent on the environment on which the device will operates (e.g. controlled temperature, shielded environment)

II. Environment effect on piezoelectric device

Measurement setup

The studied specimen is made of polycrystalline hard PZT material (NCE 41) from Noliac with a ring shape (see Fig. 1).

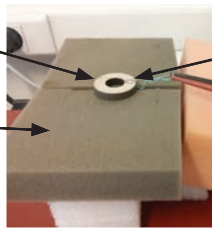

Fig. 1: *Piezoelectric specimen (OD : 35mm, ID : 15, TH : 6.35 mm)*

Wires were soldered on the top-electrodes. The formed soldering spot may introduce spurious vibration modes. The specimen is placed on foam to simulate a free vibration conditions.

Fig. 2: *Measurement setup*

Nanometric Linear Piezo-Actuator with Integrated Strain Gages for High Stability Positioning

T. Porchez, F. Barillot, C. Belly
Cedrat Technologies SA, Meylan, France

Abstract:
Many applications require a mechanism capable of nanometric resolution position tuning, and with the ability to maintain perfectly this position for a long time (more than several days). For those applications, piezo-actuators are a perfect fit since they easily provide nanometric resolution. However, they require the use of a position sensor to be able to maintain stable position over time. Until now, the long-term stability of strain gages (SG) for position measurement was questionable. Using its extensive know-how of strain gages integration and new instrumentation equipment, Cedrat Technologies has managed to demonstrate the ability of a piezo-mechanism with integrated strain gages sensors to achieve nanometric position stability. This technology opens new possibilities for industrial, aeronautical, and space applications.

Keywords: Piezo, Strain Gages, Nanometer, Stability, Space

Introduction

In most applications, compactness and cost are important issues. This is even truer for space applications. Piezo-mechanisms offer a compact solution, with high resolution, long lifetime, and high reliability. The major drawback is that those actuators suffer non linearities, such as hysteresis and creep effect, requiring closed-loop control with position sensor. Cedrat Technologies has experience with integrated Strain Gages (SG) sensors to linearise the position of its piezo-mechanisms, in order to obtain fine precision and stability. The SG technology has space heritage, since it is already used in Rosetta [2] and selected for other space programs [1]. Contactless sensors such as capacitive or eddy current position sensors are well known as accurate sensors, but their volume and cost are major drawbacks, especially for multi-axis systems.

This paper presents a new space compliant PPA40M-SG-based push-pull mechanism (see Fig. 1), called “NLA” for Nanometric Linear Actuator. This actuator is equipped with strain-gages that allow high precision position sensing and closed loop control. This mechanism has been tested to demonstrate that it is possible to achieve nanometric precision and long term stability.

Space compliant piezo-mechanism with integrated SG sensors

The mechanism is based on PPA40M actuators mounted in a push-pull configuration (Fig. 1). The push-pull configuration consists in two actuators moving simultaneously in opposite directions, when one is pulling, the other one is pushing. The two actuators are integrated in a mechanism whose kinematics takes advantage of this opposite motion. This mechanical topology has the advantage to reduce some parasitic effects and to sum the stroke of both actuators. This mechanism was designed for a space application requiring a high precision and long-term stability. The design was made in compliance with the ECSS. Redundancy of the actuation is achieved by using two independent ceramics per actuator, resulting in a primary and a secondary actuation channel. This means that the mechanism features four ceramics to cope with redundancy. The total stroke of the mechanism with both channels activated is around 80µm, giving 40µm of stroke in cold redundancy. The mechanism was modeled and simulated to justify that it can withstand the environmental constraints (vibrations and shocks), since a space application is targeted.

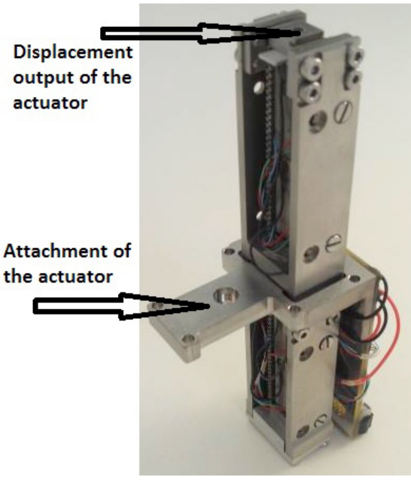

Fig. 1: *View of NLA.*

From the electrical point of view, the push-pull configuration requires a specific electrical configuration for driving the ceramics. The ceramics are connected in serial, so that there are three

Design and Optimization of a Piezo-Actuated Flapping Wing Mechanism for Micro Air Vehicles

Y. Peng, J. Cao, L. Liu
National University of Singapore, Singapore
J. Wang, Zhejiang University, Hangzhou, China
H. Yu, National University of Singapore, Singapore

Abstract:
This paper presents a novel a piezo-actuated flapping wing mechanism for micro air vehicles (MAVs). The flapping wing mechanism is composed of a piezo-actuated linear actuator and a crank-slider mechanism. The linear actuator, which consists of a piezoelectric element and a permanent magnet, is connected to the crank-slider mechanism and serves as a slider of the mechanism. Based on the principle of impact friction drive, the linear actuator can move a reciprocating linear motion with a long travel range, which can be directly converted to a flapping motion via the crank-slider mechanism. Compared with conventional flapping wing micro air vehicles driven by a rotary motor, no gearbox is needed in our design. Therefore, the proposed flapping wing mechanism can be made with small volume and light weight. The experimental results confirm that the designed flapping wing mechanism can obtain a continuous flapping motion by moving the linear actuator reciprocatingly.

Keywords: Piezoelectric, Linear Actuator, Impact Friction Drive, Flapping Wing, Micro Air Vehicle

Introduction

A flapping wing MAV (FWMAV) is a centimeter scale flying robot that mimics natural birds and insects [1-3]. FWMAVs can provide real-time intelligence, surveillance and reconnaissance (ISR) in confined spaces such as urban canyons, caves and indoors. To achieve such tasks, FWMAVs must be optimized for minimal weight and maximal lift.

The components most responsible for size and weight of FWMAVs are the actuators and related components [2, 3]. Actuators for FWMAVs currently fall into two major categories, rotary and linear [3]. The most popular rotary actuators used in FWMAVs to date are DC electric motors. However, FWMAVs of this type require gearboxes to reduce the motor speed to an appropriate level, which limits further reduction in scale for FWMAVs. On the other hand, linear actuators are thought to be a good choice for small-sized FWMAVs owing to no gearbox and simple construction. Electroactive polymers (EAP) can be made on the micro-scale however they require large voltages (over 1000 V) and the power electronics for generating such a large voltage from a 5 V battery are large and heavy. Shape memory alloy (SMA) is another choice for this type but their low bandwidth makes them a less than ideal choice. Piezoelectric ceramics (PZTs) are one of the most efficient and energy dense actuation methods available, but still have the demerits of the stroke limitation.

The paper introduces a novel flapping wing mechanism driven by a piezo-actuated linear actuator. Based on the principle of impact drive mechanism (IDM) [4-6], the linear actuator can move a reciprocating linear motion with a long travel range, which can be directly converted to a flapping motion via the crank-slider mechanism. Due to optimized geometry dimensions and the structure of the flapping wing mechanism, MAV can be made with small volume as well as a relatively large flapping frequency.

Design and optimization of the MAV flapping wing mechanism

Figure 1 shows a simplified model of the insect flight mechanism. The mechanism can be likened to a simple four-bar linkage. FWMAVs driven by rotary actuator always use a crank-rocker mechanism to transform the rotary motion into a reciprocating flapping motion. However, additional gearboxes are required to reduce the speed of the rotary actuator, which increases the volume and weight of the system. On the other hand, linear actuators are thought to be a better choice for small-sized FWMAVs owing to no gearbox and simple construction. The linear actuator is employed as a slider to generate reciprocating linear motion, which mimics the contraction and relaxation of insect muscles. In this case, a crank-slider mechanism is employed to mimic wing rotation at the wing hinge of the insect.

Figure 2 shows the schematic design of the flapping wing mechanism with a crank-slider mechanism. A linear actuator can be employed as the slider to move a reciprocating linear motion, which can be converted to a flapping motion via the crank-slider mechanism. To improve the performance of the flapping wing mechanism, the flapping frequency should be high and the driving force of linear actuator should be large. Therefore, optimization of the mechanism was carried

Effective Vibration Mode of Ultrasonic Transducers for Low Flow Rate Spraying

S. Ofuji, S. Tsuyuki, T. Kanda, S. Miyake
Okayama University, Okayama, Japan
S. Kawasaki, National Institute of Advanced Industrial Science and Technology, Sendai-shi, Japan

Abstract:
In this study, we have fabricated ultrasonic transducers for low flow rate spraying and evaluated an effect of a vibration to atomization using the Weber number. Three types of transducers which have different vibrational mode have been compared. Those vibrational modes are flexural, torsional, and longitudinal modes. A surface tension which is one of parameters of the Weber number was changed by the ultrasonic vibration. To evaluate the performance of the spraying device, we observed the spray angle and the atomization state. When a water was sprayed, the spray angle of the flexural transducer was the largest. In addition, the flexural vibration was also effective for the spraying of ethylene glycol. As a result, the flexural vibration is suitable for low flow rate spraying.

Keywords: Low Flow Rate Spray, Transducer, Piezoelectric Element, Atomization

Introduction

In various industrial fields, a spraying of coating materials at a low flow rate is required. It is expected to improve the coating quality and to reduce the emission of volatile organic compounds [1-2].
When the flow rate is low, the pressure applied to coating materials should be low. Therefore, it is difficult to spray coating materials at a low flow rate using air pressure spraying device. An ultrasonic vibration is effective to atomize materials when the flow rate is low.
In general, the atomization state is dominated by the Weber number. The Weber number is represented by the ratio of the inertial force to the surface tension. The surface tension is changed by a vibration of the nozzle. Therefore we can change the Weber number using the ultrasonic vibration and control the atomization state of the liquid [3].
The aim of this research is to realize the ultrasonic transducer which can spray coating materials at a low flow rate. In this paper, we have evaluated the relationship between the surface tension and the ultrasonic vibration. Moreover, we have fabricated a flexural, a torsional, and a longitudinal transducers to evaluate the atomization. The spray angle and the atomization state have been observed in order to evaluate the performance of transducers. The results have shown that the flexural vibration is suitable for the low flow rate spraying.

Principle of low flow rate spraying

The atomization state is dominated by the Weber number [4]. The Weber number is represented by the ratio of the inrtia of the surface tension force. The Weber number is given by

$$We = \frac{\rho L V^2}{\sigma}, \qquad (1)$$

where *We*, ρ, *L*, *V* and σ indicate the Weber number, the density of a liquid, the flow path of diameter, the flow rate and the surface tension, respectively.
The relationship between the atomization state and the Weber number is shown in Fig. 1 [3]. When the Weber number is much larger than 1, the liquid will not be atomized. The primary breakup starts and the droplets begin to be generated when the Weber number is in the order of 1. When the Weber number is much smaller than 1, the secondary breakup starts and the smaller droplets are generated [4].

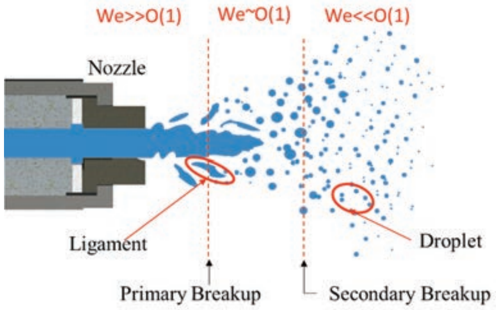

Fig. 1: *Relationship between the atomization state and the Weber number*

The principle of the atomization by the ultrasonic vibration is as follows. The free vibration state of the droplet by the surface tension is expressed as

$$\omega^2 = n(n-1)(n-2)\frac{8\sigma}{\rho d^2}, \qquad (2)$$

where ω, ρ, *d*, *n* and σ indicate the angular frequency of free vibration, the density of droplet, the flow rate, degree of number and the surface tension, respectively [5]. When an external force acts on liquid, the droplet vibrates unstable and the surface tension of the droplet increase. In consequence, the droplet

Acoustic Boosting of Battery Charging

S. Tietze, G. Lindner
Hochschule Coburg, Coburg, Germany

Abstract:
The kinetics of the charge transport across the solid-liquid interface between the electrode and the electrolyte is controlled by a diffusion boundary layer, which is responsible for the time needed for charging the battery. Therefore a removal of this boundary layer by acoustic streaming induced by surface acoustic waves propagating on the electrodes was considered to be promising approach for a reduction of the charging time. Previous electropolishing experiments have shown that Scholte waves were particularly effective in that respect. This concept has been transferred to a model electrode system representing the core of a lead acid battery, where significant reductions of the charging time and corresponding increases of the charging currents resulting from surface acoustic wave sonication have been observed.

Keywords: Surface Acoustic Wave, Battery, Charge Transport Kinetics

Introduction

Fluctuations of the energy supply from renewable energy sources such as solar radiation or wind demand for effective storage technologies for electric energy including electrochemical storage systems. In general, however, their time response is rather slow and not compatible with the rapidly changing supply e.g. from solar radiation. This slowness results from the diffusion boundary layer at the solid-liquid interface of the electrodes in an electrochemical system, which controls the kinetics of the charge transport [1], [2]. Our approach towards an acceleration of this charge transport is based on mixing of this diffusion layer by acoustic streaming, which is induced by surface acoustic waves propagating along the solid-liquid interface. By the mixing of the diffusion layer a corresponding strong increase in the current across the electrodes have recently been observed in electropolishing experiments [3], [4].

Therefore this approach has been transferred to an electrochemical system representing the core of a lead acid battery.

Methodology

Among various modes of surface acoustic waves (SAW) Scholte waves, which propagate along the interface with the velocity of the liquid, have proven to be particularly effective in this respect; an almost complete removal of the diffusion boundary layer due to acoustic streaming. The effects caused by Scholte waves near the electrode are shown in Fig. 1.

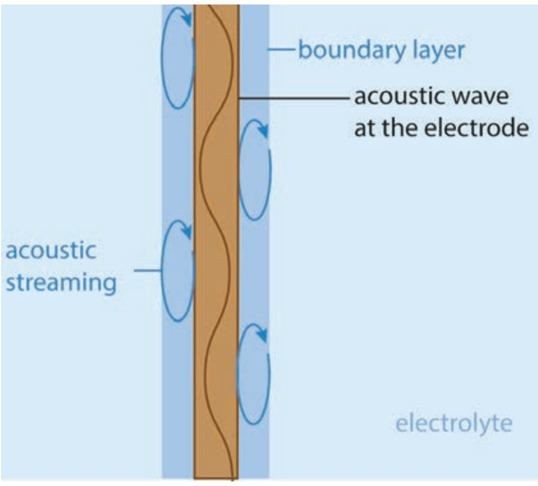

Fig. 1: *Schematic drawing of the effects caused by acoustic waves near the electrode.*

This concept was applied to two different configurations at a lead acid battery. The difference of the two systems are that the first system consists of a three-electrode-system with two positive and one negative electrode. The negative electrode was sonicated by a piezoelectric transducer mounted in PP and operated with a frequency of 1 MHz and a voltage amplitude of 200 Vpp. A schematic drawing of the experimental setup is shown in Fig. 2.
The other system consists of eight positive and seven negative electrodes, Fig. 3. The piezoelectrical transducer is glued at the top of the contact point of the positives electrodes. The operation conditions for the piezoelectrical transducers are again a frequency of 1 MHz and a voltage amplitude of 200 Vpp.

Design Optimization of Ultrasonic Motors Based on Power Flow Analysis

T. Yuan, Shanghai University, Shanghai, China, and
The Pennsylvania State University, University Park, USA
K. Uchino, The Pennsylvania State University, University Park, USA
C.D. Li, Shanghai University, Shanghai, China

Abstract:
A novel design optimization method based on the power flow analysis for a π-shape ultrasonic linear motor is presented in this paper. Power flow in the motor body was calculated and optimized to obtain the best parameters that ensure maximum energy to be transmitted to the drive feet. Based on the analysis of power flow, the π-shape ultrasonic linear motor was redesigned and optimized to improve its performance. The ATILA FEM simulation results demonstrated that the displacements in y-axis direction and total displacement of the drive feet were increase by factors of 3 and 4.1 times, respectively at the fourth bending mode frequency.

Keywords: Power Flow Analysis, Ultrasonic Linear Motor, ATILA FEM, Optimization

Introduction

Ultrasonic motors have been developed and used in various areas such as robotics, precision machines and MEMS owing to their attractive features such as quick response, non-electromagnetic interference, direct actuating operation without gear mechanisms [1, 2].The key principle of the motor designing is to enhance the horizontal and vertical vibration amplitudes at the contact point between the stator and the slider. Thus, the conventional design optimization principle has focused on the resonance frequency "degeneration" of these two horizontal and vertical vibration modes at the same frequency. In this frequency degeneration approach, the optimization module in the finite element method (FEM) is used, and the objective function F is:

$$\mathrm{F} = |f_1 - f_2| \qquad (1)$$

where f_1 and f_2 are the frequencies of two vibration modes respectively. Optimization result is evaluated by F when it approaches to zero. Y. Shi used this method to design an ultrasonic motor that combines first longitudinal mode and second bending mode [3]; while H. Xiaoyan designed a T shape linear motor in order to reduce the frequency difference between mode I and mode II [4]. However, vibration energy or power transmission within the motor body has not been taken into consideration in this approach. Improper designs such as a sudden change in the cross-sectional area may reduce or block the energy transmission and decrease the performance of the motor.

Power flow is an absolute measure of vibration energy. Combining both forces and velocities in a vibration system, it can analyse the energy transmission between different elements and find the optimized parts [5]. While the power flow analysis mainly focuses on the minimization of vibration level, in this paper, we applied this analysis to maximize the vibration in an ultrasonic motor.

The power flow analysis is demonstrated on a π-shape ultrasonic linear motor (see Fig.1,[6]) to study the energy transmission in a motor body to optimize the design that ensures maximum power flow to be transmitted to the drive feet.

Power flow calculation

Our π-shape linear motor combines first longitudinal mode and fourth bending mode to generate an elliptical motion locus at its drive foot tips, and the four shaded regions are PZT4 (see Fig 1). Because of the symmetrical structure, only half of the motor body is studied and the fourth bending mode is selected to discretize the body of motor into mass-spring-damper model (see Fig 2) according to its vibration nodes which are simulated by finite element analysis software ATILA (3.0.30b) (Micromechatronics Inc., State College, PA, USA).

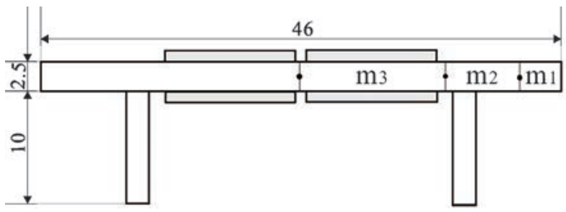

Fig. 1: *Original design of π-shape linear motor*

Parameters k_i, m_i and c_i (i =1, 2, 3) in this mass-spring-damper model are stiffness, mass and damping coefficient respectively.

Stator/Rotor Interface Analysis for Piezoelectric Motors

K. Harmouch, Y. Bernard, L. Daniel
GeePs, UMR CNRS 8507, CentraleSupélec, Université Paris Sud, Université Paris-Saclay, Sorbonne Universités, UPMC Université Paris 06, Gif-sur-Yvette, France

Abstract:
Based on a literature survey, this paper presents the implementation of analytical modeling approaches of the contact between a stator and a rotor in piezoelectric motors. These modeling approaches are validated by comparison to experimental results obtained on a specially designed piezoelectric motor. Two types of measurements are presented: the displacement of contact point, and the friction force. The second measurement is used to evaluate the friction coefficient and its dependence upon several parameters such as sliding velocity and pre-compressive force. Both the friction coefficient and the displacement of contact point are used as input in the modeling. The comparison of the predicted and measured no-load speed for different pre-compression levels shows a close agreement.

Keywords: Tribology, Sliding Speed, Pre-Compressive Force, Friction Model, Interface Reaction Forces, Universal Stator.

Introduction

Due to the growing demand of high performance motors, with minimum mass, minimum size and high service lifetime, scientists and researchers have started to investigate the potentialities of piezoelectric motors. In order to achieve optimal operation of the motor in terms of torque density, efficiency and lifetime, there is a number of key factors to address.

A literature survey shows that contact factors such as material properties, dimension of friction layer and pre-compressive force are crucial for motor performance ([1], [2], [3]).

In a first part, this paper presents the implementation of these key factors into a new model of friction drive for piezoelectric motors. In a second part, a first set of validation experiments is proposed. These experiments allow studying the tribology characteristics of contact materials in order to analyze the modeling input parameters. A comparison between modeling and experimental results is finally performed.

Friction drive model

The friction drive model of a piezoelectric motor allows predicting its operation characteristics once the vibration displacements of contact points and the properties of contact materials are known.

Note that this paper only deals with the development of friction drive models and does not address the identification of contact point displacements.

There are four basic models of friction [4] from which other models can be derived in order to simulate as accurately as possible the contact interface.

The first model (see Fig. 1.a) is the most classical dry friction model. With tangential force ***F*** applied, the contact can keep adherence (stick) until ***F*** exceeds particular value from which the contact slides (slip). In this last case, ***F*** doesn't vary with the relative velocity of contact points which is defined here as the sliding velocity.

The static/dynamic model (see Fig. 1.b) is based on the fact that the sticking forces of contact are higher than the sliding ones. This model is widely used in the modeling of traveling waves ultrasonic motors [1], [2].

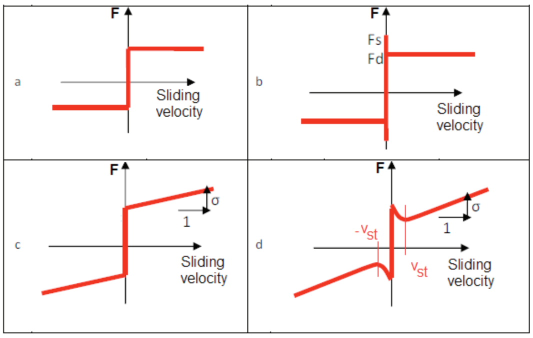

Fig. 1: *Basic friction models: a) Coulomb, b) static/dynamic, c) viscous friction, d) LuGre.*

The viscous friction model (see Fig. 1.c) differs from the previous models by the fact that ***F*** evolves linearly with the sliding velocity. This model is often used in the modeling of the lubricated contact

Force Stepping Piezo Actuator: a Motorised Solution for High Resolution Positioning and External Forces Resistance

C. Belly, F. Barillot
Cedrat Technologies SA, Meylan, France

Abstract:
Typical holding force of piezo motors is defined by friction force, required to make motor move. However, increase of friction force is not inconsequent for motor performances in terms of speed, max motion force and lifetime (tribology).
In this paper, a new motor, offering high resolution positioning and holding position when unpowered, is presented. Based on a Stepping Piezo Actuator [1] at its core, this new design decouples the outer forces from the most sensitive parts of the motor. This allows the motor to propose a high force/mass ratio and sustain even higher forces without supply. Results obtained on prototype are presented, giving the reader the benefits of proposed technology.

Keywords: Piezo, Motor, High resolution, Force, Holding position

Introduction

The paper presents state of the Art of piezo motors and interest in increasing motor stepping resolution and forces (blocked force and unpowered holding force). Innovative configuration is implemented within two different sizes prototypes, based on well established motors. Experimental results are shown. Benefits are finally listed facing several domain constrains.

Piezoelectric motor core

As it is well known, APA® shape is offering benefits within piezo motor configurations [2]. Amplification and preload are key points that lead to obtain good stepping motor characteristics. Stepping Piezo Actuators (SPA) are inertial stepper motors. They are composed of four main elements: an actuator, a shaft, a mass and a clamp. The principle of such motors is simple and relies on stick-slip effect and dissymmetrical accelerations. ***Fig. 1*** shows the two phases needed to produce one step. By repeating this operation, stroke of several millimetres can be reached. The opposite motion is done by inversing the two sequences. This motion is called “Stepping Mode”.

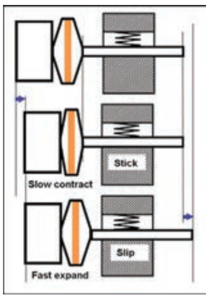

Fig. 1: *SPA motor principle*

Linear and rotating configurations have been developed, targeting camera refocusing, long stroke shutters or even medical applications [3]. However, some applications may be limited by unpowered holding force. This force is limited by axial friction force. An improvement possibility is to increase preload of the motor. This leads to higher friction force but may also have a strong impact on motor performances. Whereas there are optima for motor speed and force, it is easy to understand that if friction force is infinite, motor won’t be able to perform steps, so becomes inefficient. The proposed motor is using mechanical architecture in order to decouple external force from motor its self. This leads to compliance with extreme load facing size of motor. Moreover, high resolution and large actuation force can be achieved. Those aspects are detailed further.

Prototypes #1

Two prototypes have been developed into order to settle technology potential. First one is based on three APA40SM and presents an objective of resolution down to 100nm, actuation force above 40N and resistance of 1.8kN. It is 85mm height for 67mm in diameter (see ***Fig 2***.). External force compliance is shown using mechanical design and safety margins. Typical ECSS (European Cooperation for Space Standardization) margins [4], from space design rules are considered in this design. Moreover, according to actuation force, a 200N force is recorded facing motor while displacement still occurs, oversizing the 40N goal.

Dynamic Model of a PAD Actuator: Dynamic Operations and Pull-Off at High Speed

C. Giraud-Audine, Arts et Métiers Paris Tech, Lille, France
M. Amberg, F. Giraud
Université de Lille, Villeneuve d'Ascq, France
C. Mangeot, NOLIAC A/S, Kvistgaard, Denmark
B. Lemaire-Semail, Université de Lille, Villeneuve d'Ascq, France

Abstract:
The PAD motor has remarkable abilities for ultra-precise positioning at very low speed. Recent works have shown the possibility to extend its speed range, but some challengess remain such as pull-off. This paper proposes a model that highlights the parameters of the voltage supply that act on the torque and the contact, and can be used for control. Experimental results demonstrate the role of higher vibration modes, and show that typical signature of the imminence of pull-off can be detected thanks to some of the harmonic of the displacement of the actuators, giving some indications on means to address this problem.

Keywords: PAD Motor, Pull-Off, Dynamic Model

Introduction

PAD motors are low speed, precision motors manufactured by NOLIAC. Initially, the operations being slow, this type of motor can be considered as quasi-static motors. Recent studies have shown that the PAD could be driven at higher speed up to and beyond resonance. However, in [1] some difficulties were observed in the vicinity of resonance due the relative phase of the vibration resulting from the sudden phase rotation near the resonant frequencies of the actuators.

This paper proposes a simplified model of the PAD dynamics including the contact to address this issue. It provides some insight in the phenomena affecting the contact forces and the torque, and can describe the dynamic at higher frequencies. Furthermore, an experimental study shows that the motor can operate at frequencies higher than the free resonant frequencies of the actuators. Besides, the results indicate that the pull off resulting in the stalling of the motor is not only due the voltages applied but also to vibratory behaviour at the contact.

In the first part, the dynamic model is explained. The pull-out and the torque generation mechanism is explained in quasi static operation, and the dynamic equations are modified to yield a simplified model. In the second part, some experiments are presented. Using a frequency analysis, some insight of the vibratory behaviour of the actuators is gained, and a typical signature of the imminence of stalling is identified.

Theoretical study

Equilibrium of the crowned wheel

The PAD motor features two sets of actuators acting along two perpendicular directions, so as to generate a circular translation applied to a crown wheel (Fig. 1, top). When brought into contact with a geared shaft, this wobbling movement is converted into a rotation of the shaft. The micro gear adds a high gear ratio thus allowing ultra low speed operation and exceptional positioning capabilities. To obtain the wobbling, the actuators are driven using two sinusoidal voltages shifted by 90°.

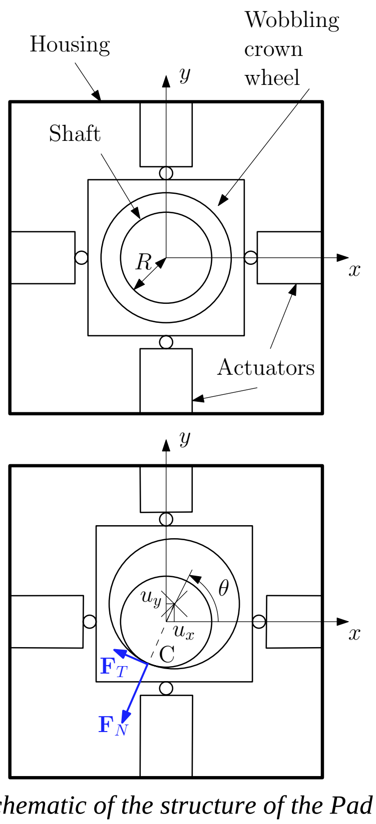

Fig. 1 : *Schematic of the structure of the Pad motor (up) and during operation (bottom)*

Excerpt only, page has been blanked!
A full pdf version in print quality is available here!

Microfluidic System for Water Sample Treatment

S. Gassmann, H. Schütte
Jade Hochschule, Wilhelmshaven, Germany
M.L. Miranda, O. Zielinski
Carl von Ossietzky-Universität Oldenburg, Wilhelmshaven, Germany

Abstract:
The control of conditions in water sample treatment can be made very efficient and precise when using small volumes. This is one of the major advantages of the microfluidic approach. A low cost micro fluidic water sample treatment system based on PCB technology is presented here. The aim is the thermal cycling of a sample containing dissolved organic matter (DOM) prior an Excitation Emission Matrix Spectroscopy (EEMS) measurement. Changes in the excitation emission matrix which are related to the thermal treatment were found. Here the design and the fabrication of the microfluidic system and material issues are described.

Keywords: PCB MEMS, Microfluidic Chip, DOM, 3D-EMM-UV, Oceanography

Introduction

The usage of microfluidic systems in the research of natural water resources is not evident. The advantages of using small sample volumes and small sized systems are not so important when it is easy to get enough sample volume. However the use of miniaturized flow systems can help to enable new and efficient ways of water sample investigation. One example, a micro fluidic system that is used for the treatment of natural water samples is presented here. With the help of this micro fluidic chip a new methodology of examining water samples was developed.
This work focuses on natural seawater samples containing among others dissolved organic matter (DOM). DOM is the largest pool of carbon in the oceans, comparable with the amount of carbon in the atmosphere [1]. It can be defined as a conglomerate of chemical compounds with a wide range of molecular weights and structures, product of biodegradation, photochemical and primary production process. Its role as light absorption controller in marine environment, carrier for several chemical compounds and source of carbon for microorganisms has been well described [2, 3]. Microfluidic thermal treatment of seawater is a novel concept in the evaluation of the prevalence and stability of some fractions of DOM in the aquatic environment.
The aim of this research is to identify and characterize changes in the fluorescence signature of DOM via ultraviolet three-dimensional Excitation Emission Matrix (UV-3D-EMM) technique, as a consequence of a sample treatment. This treatment can be thermal, UV radiation or any other condition that can be realized in the microfluidic chip. The microfluidic pretreatment is a new methodology in the investigation of DOM. It is an example of the application of microfluidics in oceanography and can be adapted to any other analyte of interest.

The usage of low cost technologies for building microfluidic systems is especially important for prototyping and for systems that will be used in lower quantities. This is the case for the application in oceanography. Here a PCB based technology was used because of its simplicity. The combination of electronics, sensors and the fluidic parts is possible at low cost using this technology. One technology for building microfluidics based on PCBs was developed by Merkel et al. [4]. A technology similar to the one used here with a transparent channel layer on top of a PCB was presented by Gassmann et al. [5] to generate a DNA chip. Other PCB based microfluidic technologies where presented by Luque [6] where SU8 is used on top of PCBs.
In the following the design and the fabrication of the chip for water sample treatment is described. At the end the result of the tests with real samples are highlighted.

Requirements description

As a first investigation the influence of temperature changes on the DOM sample should be investigated.
It should be possible to apply temperatures between 0°C and 95°C steady state as well as thermal cycling where the sample is heated and cooled sequentially. The number of cycles, the residence time and the temperature should be user definable during the runtime of the test. To reduce the overall treatment time the change between the temperatures should be finished in about 5 seconds.
These requirements are solvable by microfluidics because of the higher speed of thermal processes in the micro scale. Using normal sample volumes in the ml-range these treatments would be too slow for an effective laboratory usage. The volume that should be treated was fixed to 100µl. Since the fluorescence is a volume effect, the volume should not be selected too small to have high enough signal-noise ratio.

Fabrication of Electrostatically Actuated Microshutters Arrays

L. Oh, SGT Inc., Greenbelt, USA
M. Li, NASA Goddard Space Flight Center, Greenbelt, USA
D. Kelly, ASRC Federal Corp., Beltsville, USA
A. Kutyrev, University of Maryland, College Park, USA
S. Moseley, NASA Goddard Space Flight Center, Greenbelt, USA

Abstract:
A new fabrication process has been developed to actuate microshutter arrays (MSA) electrostatically at NASA Goddard Space Flight Center. The microshutters, made with silicon nitride membranes with a pixel size of 100 x 200 μm^2, rotate on torsion bars. The microshutters are actuated, latched, and addressed electrostatically by applying voltages on the electrodes the front and back sides of the microshutters. The atomic layer deposition (ALD) of aluminium oxide was used to insulate electrodes on the back side of walls; the insulation can withstand over 100 V. The ALD aluminium oxide is dry etched, and then the microshutters are released in vapor HF.

Keywords: Microshutters, Electrostatic, Actuation, Rotational, Fabrication, ALD, Aluminum Oxide, Breakdown Voltage, SOI

Introduction

We have developed a new fabrication process to actuate MSA electrostatically. Previously, the 175x384 microshutter arrays had been developed as multi-object aperture selectors for the James Webb Space Telescope (JWST) at NASA Goddard Space Flight Center [1, 2]. The JWST MSAs were magnetically opened and electrically latched to stay open. The magnetic operation involved moving magnets thus complicated actuation schemes and increased the payload. By eliminating the magnetic actuation and solely relying on the electrostatic actuation, the weight of the MSA assembly can be reduced. The microshutters were made with silicon nitride membranes with a pixel size of 100 x 200 μm^2 and rotate on torsion bars. Fig. 1 shows an array of the microshutters. The new electrostatic operation scheme as shown in Fig. 2 is simple, and the array scalability and operation speed are increased. In order to achieve the electrostaic actuation of the microshutters, we need to develop a new fabrication process.

Fig. 1: A front side image of a (100 x200 μm^2) microshutter array. On the microshutters, patterned alumimum electrodes and strips of molybdenum nitride are shown. .

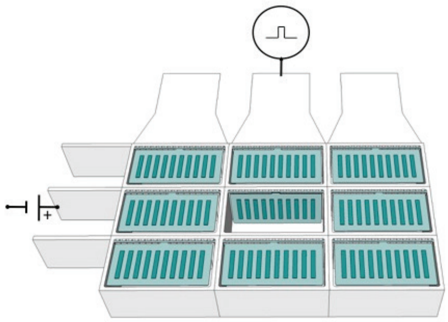

***Fig. 2:** An illustration of how the microshutters are individually actuated and addressed by applying a pulsed DC voltage to the front electrodes (top) and a DC voltage to back electrodes (left). Only the microshutters with voltages on both the front and back electrodes latch open by rotating 90° on torsion bars. The front electrodes run vertically while the back electrodes run horizontally.*

MSA Fabrication

We first grew a layer of thermal silicon oxide on a silicon-on-insulator (SOI) wafer; the buried silicon oxide, device, and handle silcon layers were 3000 Å, 100 μm, and 350 μm thick, respectively. Then, a layer of low pressure chemical vapor deposition (LPCVD) silicon nitride was deposited.

A layer of aluminum was deposited in an e-beam deposition system. Then, the aluminium was etched in an aluminum etchant for the front electrodes. The silicon nitride was etched in a reactive ion etch (RIE) system with tetrafluoromethane (CF_4) to form the microshutters. A layer of molybdenum nitride

Magnetoresistive Sensors for Angle, Position and Speed Measurement in Small- and Micro-Actuators

R. Slatter, R. Buß
SENSITEC GmbH, Lahnau, Germany

Abstract:
Magnetoresistive (MR) sensors are not only used for measuring rotational and linear motion, but also for non-contact switching applications and furthermore for highly dynamic current measurement. The increasing demand for MR sensors is largely the result of increasingly complex demands on the sensors for high performance electric drives. The sensors must not only be accurate and dynamic, but also be robust under difficult operating conditions and exhibit very high reliability. Recent market developments are generating additional demands, with respect to compact dimensions and energy efficient operation. This combination of requirements is leading to the more intensive use of magnetic sensor principles, compared to optical, inductive or capacitive principles. This paper describes the principle of operation and benefits of MR sensors. This is followed by a description of practical application examples each demonstrating the advantages of MR sensors in challenging new applications for angle, position and speed measurement.

Keywords: Magnetic Sensors, Angle Measurement, Speed Measurement, Small- And Micro-Actuators

Introduction

There is a growing demand for mechatronic motion systems in a wide range of industrial fields. Not only in the field of industrial automation, but also in the automotive and aerospace sectors, there is a sharp increase in the number of mechatronic actuators being applied. “Decentralized motion control”, “X-by-wire” or “more electric aircraft” are just some of the terms used to describe the results of this trend in different technological areas.
This development is placing new demands on the technology used for measuring rotational motion, linear motion and electrical current. Fig. 1 shows a simplified structure of a motion control system. This system typically comprises a servo controller with current sensors, a servo motor, speed and position sensors (encoders) as well as mechanical machine elements. Presently there are number of trends that are changing the technical and commercial requirements for both actuators and sensors.

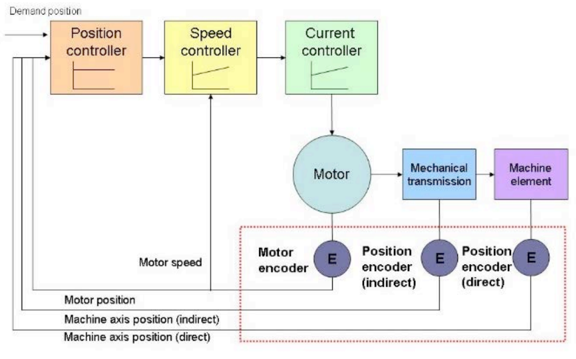

Fig. 1: *Simplified schematic of a motion control system*

The high performance and flexibility of magnetoresistive (MR) technology is playing an increasingly significant role in helping machine and actuator designers to deal with these new requirements.
The magnetoresistive effect is best known from the read heads of computer hard discs or from magnetic memory (MRAM) applications, but it is also well suited to uses in sensor technology. It has a long history, being first discovered in 1857 by Lord Kelvin. However, the MR-effect did not experience widespread use until the early 1980s, when the first MR-based read heads were implemented in hard disc drives [1], [2]. The first industrial applications for MR-based sensors followed at the beginning of the 1990s, since when the number of applications has increased dramatically. The applications are not only limited to terrestrial use – MR sensors are used to control the electric drives used on “Curiosity”, the Planetary Rover that has been exploring the surface of Mars since August 2012.

Trends in Motion Control

The market for motion control technology is characterized by a number of current trends, which are leading to new requirements for actuator and sensor technologies.
A number of these trends were already described in a paper at the same conference in 2010 [3]:

a) Higher accuracy
b) Increased power density
c) Decentralized motion control
d) Increased use of closed-loop control
e) More challenging operating environments
f) Faster time to market

New Class of Trunk-Like Robots: Structure, Control, Actuators

R. Bansevicius, Kaunas University of Technology, Kaunas, Lithuania
A. Drukteiniene, Siauliai University, Siauliai, Lithuania
V. Jurenas, Kaunas University of Technology, Kaunas, Lithuania
G. Kulvietis, Vilnius Gediminas Technical University, Vilnius, Lithuania

Abstract:
The aim of presentation is to present the results of development and investigation of the new class of multi-degree-of-freedom trunk robots, based on new concept. Classical rule of Robotics – the number of degree-of-freedom of robot should be equal to the number of applied actuators – is questioned here. This concept is realized by using kinematic pairs with alternating degree-of-freedom, controlled by a solitary force or moment, changing its direction in space. The number of degree-of-freedom of kinematic pair is controlled from 0 to 3, exploiting various methods: the dependence of friction forces upon oscillation in the contact zone of links, the control of viscosity of electro rheological (ERF) or magneto rheological fluids (MRF), when electric or magnetic fields are applied.

Keywords: Trunk Robots, Kinematic Pairs, Electro Rheological Fluids, Magneto Rheological Fluids, Piezoelectric Actuators.

The main advantages of robots, based on new idea to actuate trunk – considerably increased number of degree-of-freedom, enabling the grip to reach hardly accessible zones; highly reduced number of actuators (e.g. electric motors) - up to 1 (and it is not related to total number of degree-of-freedom of trunk robot); very simplified mechanical design and low weight (this is important for satellite applications). The trajectories of grip are realized by applying special software, controlling in real time the number of degree-of-freedom of every kinematic pair in relation to phase of external force with alternating direction (in case when the force is generated by rotating unbalance).

Applying elastic kinematic pairs (with ERF or MRF between links) the mechanical structure of trunk becomes even more simplified. Using this separation of power and control systems concept, it is feasible to realize the simpler cases, e.g. positioning systems on a plane or powerful laser deflectors in space.

The actuators with external exciting force

In this type of actuators, suggested in [1], the power and control systems are separated, resulting in simplifying the final design of the actuating systems. Thus, in 2*D* high-powered laser deflecting device (Fig.1), the positioning power is realized with the help of dynamically unbalanced rotor (a couple unbalance), mounted inside the sphere, contacting with the internal spherical component, made of active piezo ceramics. The friction between piezo ceramic component and sphere is periodically controlled (up to zero value) with the help of harmonic burst type excitation voltage (generating high frequency resonant oscillations of piezoelectric component *3*), connected to the electrodes of piezo ceramic component (Fig. 1, where ω is angular velocity of unbalanced rotor, α - angle of rotation). The burst phase in relation to rotation of unbalance is β_1.

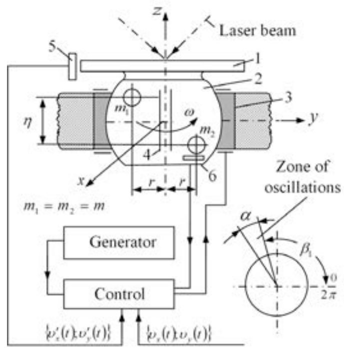

Fig. 1: *High-powered laser deflecting device: 1 – mirror; 2 – passive sphere, contacting with piezoelectric component 3; 4 – rotating coupled unbalance; 5 – 2D mirror's position sensor; 6 – rotor's position sensor*

There are two main alternatives to control friction forces between links of kinematic pair: *(a)* - using magnetic forces in the contact zone; (b) – generating resonant oscillations between links, reducing or even eliminating friction forces. Both approaches are shown in Fig.2, where exciting force is centrifugal force of rotating unbalance *m* and friction forces between passive sphere and contacting with it piezoelectric cylinder are controlled by resonant oscillations (Fig.2a), or ferromagnetic cylinder is in contact with passive

Excerpt only, page has been blanked!
A full pdf version in print quality is available here!

FlexPCB Windings, the Way Towards Very High Performance Coreless BLDC Motors

F. Baudart, B. Dehez
Université Catholique de Louvain, Louvain-la-Neuve, Belgium

Abstract:
Many high-end applications, such as in the bio robotics or aerospatial fields, requires highly performance actuators. In the fractional horse power range, the coreless, or slotless, BLDC motor established itself as the most appropriate. This paper presents a technological leap in such motors, allowing to significantly increase their performances. The improvement is made on the windings, which are realized using a flexible printed circuit board, instead of copper wires. Printing the windings on a flexible PCB opens the way to new shape and new topologies of windings, which are not realizable with wire windings, and that allows to increase the torque constant while decreasing the phase resistance. Theoretical considerations, manufacturing process and experimental results are detailed in this paper.

Keywords: Micro Actuators, Coreless BLDC Motor, Flexible PCB, Windings on PCB, Performance Increase

I - Introduction

Many applications require ever more efficient actuators, whether at the level of the dynamics, the compactness or the precision they can achieve. In the fields of fractional horse power applications, BLDC motors have emerged in recent years, and among them, coreless motors occupy a prominent place for applications requiring high quality of movement.

In comparison with classical BLDC motors, coreless BLDC motors have no teeth. As shown in Fig. 1, the windings are built as a hollowed cylinder, and are directly inserted in the airgap of the motor. The magnetic field from the magnets goes through the windings, before going in the stator yoke. The absence of teeth in the coreless motor decreases the magnetic fields, but the use of high energy rare earth magnets limits this effect, despite the greater airgap. On the counter part, without teeth, the space attributed to the windings is greater, what increases the magnetic coupling between stator and rotor. In the end, coreless BLDC motors can achieve similar or even better performances than cored BLDC motors. The absence of teeth has the benefits of supressing the cogging torque, as well as any local saturation in the teeth, which are both source of parasitic torques reducing the precision in cored motors. Finally, iron losses are smaller in coreless motors, which improve the global efficiency.

Fast growing markets such as the biorobotics, or the medical devices, require particularly high power in small volumes, which means high thermal dissipation properties, high efficiency and high power density. Despite being the best fitted motor for high precision, high power density and/or high efficiency, the coreless BLDC motor cannot always reach the requirements of these high end applications.

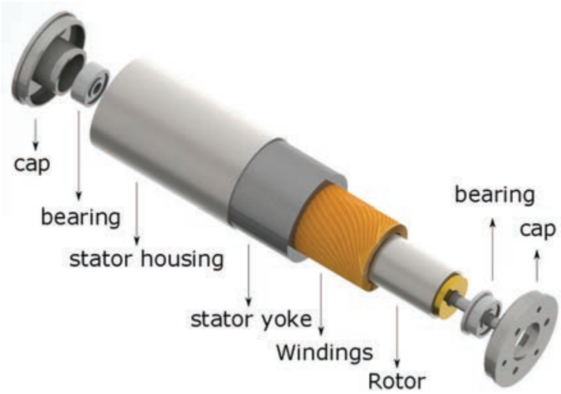

Fig. 1: *Scattered view of a corless BLDC motor*

The main limitations of the BLDC motors are their windings, because they are at the centre of the thermal and magnetic aspects of the motor. They are the main source of heat source, and strongly influence the thermal dissipations capabilities of the motor. They also fix the thermal limits, and their topology defines the magnetic coupling with the magnets, and therefore the nominal electromagnetic torque.

The windings are usually made of a copper wire, as shown in Fig. 2. Since some decades, lots of efforts have been made in the manufacturing of these windings, in order to achieve a high filling factor, which will reduce the global thermal resistance of the windings. Recently, Maxon, Portescap and Faulhaber, three well-known companies in the field of coreless motors, have filed patents about wire windings topologies and the way of manufacturing them [1-3]. The focus on the windings shows how critical they are in the achievement of high performances of the motor integrating them.

A High Precision Single Stage Compound Epicyclic Friction Speed Reducer

J.F. Schorsch, F.F.C.T. van der Helm, D.A. Abbink
Delft University of Technology, Delft, The Netherlands

Abstract:
Robotic systems, automated machine tools, and precision measurement systems often rely on electromechanical actuation systems. A common feature to many electromechanical actuators is the inclusion of a mechanical transmission to convert the output of a high speed, low torque electromotor into the low speed, high precision end joint motion that is required. The mechanical transmissions currently available are usually based on discrete gear tooth technology. This creates an inherent degree of uncertainty, as teeth load, unload, and move in and out of contact. A new type of mechanical transmission which is based on continuous rolling elements offers the potential to provide a reduced degree of uncertainty, and an increase in the degree of precision

Keywords: Speed Reducer, Gearbox, Efficiency, Compound Epicyclic

Introduction

The need for precise, high torque actuators which can enable rapid development of ever shrinking electrical, mechanical, and optical equipment is required. Precision machining, telescope positioning and alignment, and semiconductor fabrication all demand precise, repeatable, powerful actuators.[1]–[3] Current high torque speed reducer technologies based on gear tooth interaction such as precision planetary drives or strain wave gearing are typically limited to 30-60 arc-seconds of accuracy, while achieving repeatability of 4-5 arc-seconds is possible[4]. Cycloidal speed reducers often achieve accuracy of 60 arc-seconds, with a repeatability of 20-30 arc-seconds[5], [6]. These accuracy measures are often what determines the overall capability of an industrial robot, CNC machine tool, or automated inspection tool to achieve a final overall precision. A new traction[7] based configuration of compound epicyclic speed reducers[8] has recently been presented (see figure 2) which can achieve theoretical gear ratios in excess of 10.000:1 in a single stage. These speed reducers are zero backlash and can be produced using low precision (±0.1mm) standard machining techniques (turning, boring). In this work, we present measurements of a prototype single reduction compound epicyclic traction drive which achieves a gear ratio of 330:1, is rated for 10 nm of torque, and is evaluated for angular precision. The design of such speed reducer is such that the instantaneous gear ratio is a function of the set of nominal component diameters. For the low precision process used in this prototype, the maximum expected variation in gear ratio ±25%, which would correspond to an angular accuracy range of ~±170 arc-seconds. Figure 1 shows the various components of such an arrangement. The gear ratio of such a transmission is determined by the following equation.

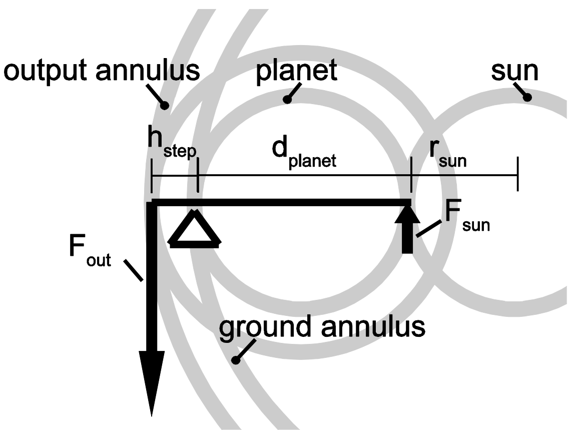

Fig. 1: Simple illustration of the arrangement and components required to determine the gear ratio of a compound epicyclic traction drive.

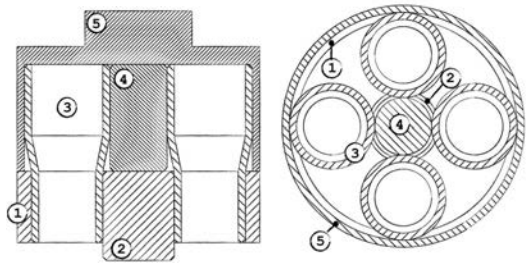

Fig. 2: *Mechanical arrangement of parts. Left, side view, right top view. (1) Ground annulus (2) Input sun wheel (3) Hollow compound planet (4) Idling sun wheel (5) Output annulus.*

$$\frac{T_{out}}{T_{sun}} = \left[\frac{d_{planet}}{h_{step}}\right] * \left[\frac{d_{planet} + r_{sun} + h_{step}}{r_{sun}}\right]$$

Compact Electrodynamic Planar Actuator for Automation

T. Bödrich, B. Rosul, M. Stock, J. Ziske, J. Lienig
Technische Universität Dresden, Dresden, Germany

Abstract:
A novel compact electrodynamic planar direct drive with a motion range of 20 x 20 mm² and a maximum rotation of the mover of ±11° is presented. It utilises four independent stator windings with iron core and permanent magnets in the mover. Peak forces are ±72 N in *x*- and *y*-direction. With an integrated planar ball guide, an integrated *x*-*y*-φ position sensor system with a resolution of 1.25 µm, embedded flatness-based position control and overall dimensions of 150 x 150 x 40 mm³, the developed planar actuator could become a very compact, cost-effective and dynamic drive module for many applications in automation and handling.

Keywords: Planar Direct Drive, 3 DOF, Moving Magnet, Embedded Position Control

Introduction

Many processes in handling, machining and assembling require planar motions in two translational directions (*x* and *y*). In some applications an additional limited rotation is needed as a third DOF, e. g. for alignment of work pieces (*x*-*y*-φ). For planar *x*-*y* motions, serial arrangements of linear stages are dominant (open kinematic chain), most often driven by lead screw motor systems. The resulting planar stages are limited in dynamics due to large masses to be moved. Parallel mechanisms or parallel robots (closed kinematic chain), e. g. delta robots for 3 DOF, are an alternative for dynamic motions. However, conventional parallel mechanisms with prismatic joint linear actuators arranged in parallel have an unfavourable small ratio of motion space to overall volume of the complete drive system.

Multi-DOF direct drives can be seen as a variant of parallel mechanisms, where the forces of different independent partial actuators act on one common mover. The desired constraint motion is achieved by proper control of the independent actuators, in most cases realised by closed-loop control of the mover position. A broad variety of electrical multi-DOF direct drives has been proposed and developed over the last decades, differing in actuation principle, motion range, forces, accuracy and intended applications [1] [2]. A well-known planar direct drive for large motion ranges is the Sawyer stepper motor, as used for example for circuit board placement. For reasons of efficiency, this long-stroke motor has an active, i. e. energised mover. For smaller motion ranges up to approx. 200 x 200 mm², the mover can be passive, avoiding the need for flexible power cords or pneumatic hoses to the mover. Typical examples of latter design intended for high resolution are presented in [3] and [4]. These drives feature three and four independent ironless two-phase windings in the stator respectively and corresponding arrays of permanent magnets in the mover. The latter is either magnetically levitated [3] or guided by air bearings [4]. Both drives feature high-resolution 6D and 3D position sensors with 5 and 20 µm resolution respectively.

A series of linear direct drives for short strokes has been developed at Technische Universität Dresden within the last years [5] [6]. These compact drives feature one or more permanent magnets in the mover and a single-phase, iron-core stator winding. This allows for particular large actuator constants, i. e. high forces at little losses. Based on that magnetic design, a novel planar direct drive for 3DOF (*x*-*y*-φ) has been developed, built and tested (Fig. 1). Design objectives have been a simple overall structure and simple subsystems, high compactness, and low manufacturing and component costs. Latter are significantly governed by the resolution of the multi-DOF position sensor and the accuracy of the guide. For that reason, simple low-cost linear encoders and a simple planar ball guide have been utilised in a first prototype. The new drive is intended for applications requiring high dynamics and compactness and a medium positioning accuracy of approx. 10 µm.

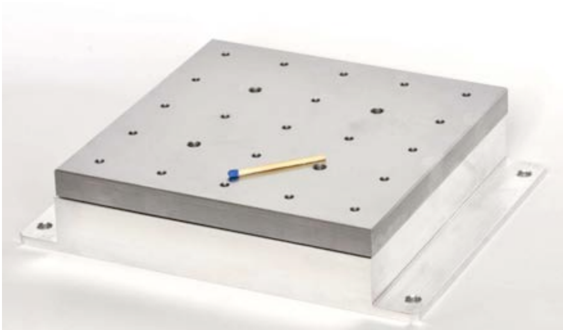

Fig. 1: *Prototype of a novel electrodynamic planar direct drive: motion range 20 x 20 mm^2, maximum rotation ±11°, peak force ±72 N in x and y direction*

Highly Integrated Linear Direct Drive for Short Strokes

J. Ziske, T. Bödrich, H.Basler, Q. Sun, J. Lienig
Technische Universität Dresden, Dresden, Germany

Abstract:
In this paper a newly developed, very compact and multifunctional single-phase linear direct drive for short strokes is presented. The innovative ball guide, the high-resolution position sensor and the motor driver as well as the motor controller are completely integrated into the actuator, resulting in an easy-to-use drive unit for various industrial applications. The moving-magnet operation principle with slotted stator winding offers 14 mm travel, high forces of up to 90 N, low response times down to 20 ms for a controlled 12 mm step in a compact overall volume of 225 cm^3. In addition to a serial interface an EtherCAT-fieldbus connection is currently integrated into the unit. The embedded flatness based position control allows fast responses without overshoot. Sensorless force measurement and control is also implemented.

Keywords: Direct Drive, Short Stroke, Single-Phase, Moving Magnet, Linear Ball Guide, EtherCAT

Introduction

Within the Priority Programme SPP 1476 of the German Research Foundation (Deutsche Forschungsgemeinschaft - DFG) small machine tools for the manufacturing of small work pieces are being developed. Tools which are optimally adapted to the size of the work pieces are more resource-friendly, while simultaneously increasing efficiency and reducing production cost considerably [1, 2].

In this context, Technische Universität Dresden develops various compact and modular uni- and multi-axial electro-dynamic feed modules. Small travel ranges (approx. 25 mm) and small maximum process forces (approx. 20 N) are sufficient for many tasks of future miniature machine tools. These changed conditions allow the use of novel drive concepts that may be better suited than actuators derived by downscaling of conventional concepts such as lead screw motor systems, piezo stages or moving-coil actuators.

Fig. 1 shows three newly developed feed units: The small linear stage LT14-6 with a tabular mover (14 mm of travel, 6 N nominal force), the cylindrical linear axis LT14-35 (14 mm of travel, 35 N nominal force), which is presented in detail in this paper, and a planar drive with *x*-, *y*- and *φ*-degree of freedom (±10 mm travel, ±11° maximum rotation, approx. 20 N nominal force). Detailed design and control of latter planar drive is described in [3] and [4], respectively. The presented drive units are still subject to further development, but the present prototypes have reached an advanced stage. All of them utilise the single-phase moving-magnet operation principle, which is well-suited for small travel ranges and process forces. Especially the high ratio of force to loss power (correlates with a high volume-based actuator constant [5]), the nearly constant force along the stroke and the relatively simple control are advantageous features. In addition, very compact, modular and easy-to-use drive units can be realized with integration of robust linear or planar guides, miniature position sensors and the complete control hard- and software (servo controllers).

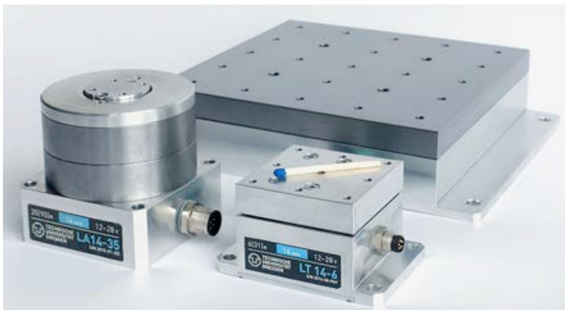

Fig. 1: *Series of novel compact moving-magnet linear and planar direct drives for short strokes*

Overall Design and Operation

Fig. 2 shows the prototype of the novel actuator LA14-35 with a travel range of 14 mm and a nominal force of approx. 35 N. It is an evolution of the actuator presented in [6]. Main improvements are reduced weight and size, an integrated optical incremental position sensor, integration of motor driver and control electronics as well as a completely reworked, smoothly running and low-cost ball guide with considerably improved stiffness. The outer dimensions are 65 x 65 x 63 mm³. The quadratic base is used for mounting and contains the motor driver, the control electronics and the interface connectors. The upper cylindrical part contains the magnetic circuit, the mover, the linear ball guide and a small PCB with the optical incremental encoder.

Development of an Artificial Muscle from Coiled Polymer Fibers for Humanoid Robotics Applications

A. Kalysheva, Z. Zhapar, K. Tulkibayeva, M. Folgheraiter
Nazarbayev University, Astana, Kazakhstan

Abstract:
Humanoid robotics aims at developing anthropomorphic robots able to move in environments and to manipulate tools that are designed specifically for human beings. The high number of DOFs required in a humanoid robot demands for compact and high power-to-weight ratio actuators. Among all the possible technologies, artificial muscles have the additional advantages to be flexible, lightweight, and to provide linear movement suitable for a human-like robotic system. Existing types of artificial muscles used in robotics and other automated systems are expensive and technically limited due to hysteresis, scalability and performance efficiency. Inspired by a recent discovery of artificial muscles made of common twisted fishing line, the goal of this study is to develop a low-cost thermally controlled actuator suitable for humanoid robotic applications. The experimental setup consists of a twisted fiber of nylon with a diameter of 1mm pre-tensioned and connected in series with a force sensor. The material is heated up thanks to a NiChrome (NiCr) wire inserted axially into the polymeric fiber. The temperature is measured and controlled thanks to a small NTC thermistor kept in contact to the NiCr wire. Different experiments were conducted in order to measure the dynamic response of the artificial muscle as well as the force-temperature characteristic in static conditions.

Keywords: Polymer Actuator, Artificial Muscle, Humanoid Robotics

I. Introduction

Artificial muscles have a wide range of possible applications. They can be used in rehabilitation and medical devices [1], in wearable exoskeletons and actuated suits [2], in the aerospace and energy industry [3], in bio-inspired robotic systems [4], in humanoid robotics [5], and in many other fields where a compact and human-like actuation system represents a good alternative to an electric motor. There are different possible technologies and materials that can be used to implement such a kind of actuation. Among of them: McKibben Pneumatic Artificial Muscle (PAM) [6], Shape Memory Alloys (SMA), Electroactive Polymers (EAPs) [7], Carbon Nanotubes (CNT), Electrorheological Fluid, and the most recent one, twisted polymeric fibers [8]. PAMs are made of an inner rubber tube covered by a braided mesh shell. The working principal is as follows: when the pressure of the gas inside the tube is increased, it causes the tube to expand radially; this creates in the shell an axial force that causes the contraction of the muscle [9]. Owing to their advantages, such as lightweight, flexibility, high power-to-weight ratio, and cheapness, PAMs are widely used in robotics. Shape memory alloys, in turn, are the class of materials, which has the ability to "memorize" some shape and return to it, when heat is applied [10]. Some problems with SMAs, such as slow response and erratic movements, are preventing their mass usage. However, some of the SMAs (for example, NiTi) have a very useful characteristic: they are biocompatible and, thus, suitable for biomedical applications. Electro-active ceramics are made of crystals endowed of piezoelectric properties. When they are exposed to a mechanical stress, they generate an electrical charge. They can also work as actuator, i.e. generating force when stimulated by an external electrical voltage [11].

Development of artificial muscles made of coiled fishing lines of different shapes and sizes is a recent discovery that can be utilized in the development of humanoid robots, prosthesis, exoskeletons and automated systems that require high load capabilities. Imitating human muscles, this kind of actuators can expand and contract generating up to 5 kilowatt of mechanical power per kilogram [12].

According to the study conducted by Haines et al. and reported in a recent number of *Science* [8], high-strength and low-cost nylon occurred to be the most appropriate material for fabrication of polymeric twisted fibers. In addition, the helical structure of coils provides contraction from 4% to 34% by rising the material temperature from 20 to 240 °C. Such systems with high range of temperature control can be used for humanoid robots to make fast and at the same time precise movements, where both, stiffness and tensile actuation, are important.

The aim of this work is to develop and study anartificial muscle suitable for humanoid robotics applications able to reach a tensile stroke up to 30% of its length. Thus, exploiting volumetric controlled thermal expansion with different fibers configurations while working in a range of temperatures between 20-80°C.

Polymer-Dispersed Liquid Crystal Elastomer Thermomechanical Actuators

A. Rešetič[1,2], J. Milavec[1,2], B. Zupančič[1], V. Domenici[3], B. Zalar[1,2]
[1] Jožef Stefan Institute, Ljubljana, Slovenia
[2] Jožef Stefan International Postgraduate School, Ljubljana, Slovenia
[3] Università degli studi di Pisa, Pisa, Italy

Abstract:
We are introducing polymer dispersed liquid crystal elastomers (PDLCEs) as a new thermomechanically functional rubber material which can be molded into any arbitrary shape and size. PDLCEs exhibit temperature driven shape memory and due to their easy and practical synthetization method and ability for custom-tailored modifications, they can be applied to a variety of actuating and other applications.

Keywords: Liquid Crystals, Elastomers, Composites, Thermomechanical Actuation, Shape-Memory Material

Introduction

Liquid crystal elastomers are thermomechanically active materials that couple together elastic properties of elastomers with orientational properties of liquid crystals, a combination through which they exert temperature driven actuation in the form of contraction along the nematic orientational director of their mesogen constituents [1]. Industrial implementation of LCEs has been largely hindered by their geometrical and size limitations, which are limited to either macro-sized thin films or to different shaped varieties of nano- or micro-sized LCEs [2,3]. To overcome this problem, we are introducing polymer dispersed liquid crystal elastomers (PDLCEs) as a new thermomechanically functional rubber material which can be molded into any arbitrary shape and size. Because of their easy synthetization procedure, they can be easily enforced into production of future applications in the fields of thermomechanical actuation and additive manufacturing [4,5].

Preparation

PDLCEs are prepared by freeze-fracturing regular oriented LCEs into microparticles and dispersing them into a polymer matrix, which is then cured under an external magnetic field to align the LCE particles in the field direction, by exploiting the diamagnetic anisotropy of mesogenic molecules. It is important that the LCEs used for preparation have a well-defined nematic or smectic ordering to produce monodomain LCE particles, which are required for successful and efficient particle alignment. Orientational order of the LCE particles is then quenched by curing the surrounding polymer matrix. The preparation diagram is depicted in Figure 1. With this method we have transferred the thermomechanical deformation of the LCE particles onto the polymer matrix, granting the bulk composite to deform.

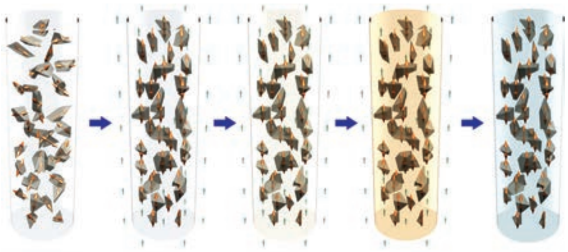

Fig. 1: *PDLCE preparation procedure.*

PDLCE morphing abilities

The degree of deformation of LCEs is not preserved completely when incorporated into the polymer matrix, i.e. it is reduced from ~45% strain exhibited by our LCEs to ~12% strain for PDLCEs; a 70% reduction. Nevertheless, by combining differently functionalized and non-functionalized PDLCE material into simple disk shaped bilayers, we can achieve different shape changes as shown in Figure 2. Upon reaching the activation temperature, the disk-shaped samples deform into the following shapes: fold (a), cup (b), saddle (c), left twist (d) and right twist (e). Blue and red lines denote the bottom and top layer nematic director orientation, respectively. We thus demonstrated that the lowered degree of strain (even though this can be altered by changing LCE particle concentration and/or using other LCE inclusions) is still high enough to achieve practical deformations. The configurations listed in Figure 2 have been specifically made to act as five basic voxels in 3D printing technology, the combination of which can produce customized morphing materials with arbitrary shape change.

Development and Experimental Characterization of a DE Membrane Actuated Valve

M. Hill, G. Rizzello, S. Seelecke
Universität des Saarlandes, Saarbrücken, Germany

Abstract:
Dielectric Elastomer (DE) membrane actuators are lightweight, high energy density systems which show promise for improving the performance of pumps and valve control units. Particularly, the use of DE's as valve control units offers advantages over traditionally used solenoid valves. Unlike solenoids which draw current continuously when activated, the DE-system draws current only during its initial motion, aside from some very small leakage currents. This means that the DE will use significantly less energy for holding a valve in position than a solenoid would performing the same action. The DE also generates very low heat and runs virtually silent. This work presents a valve which is driven by a DE-system consisting of a diaphragm, or circular, DE and a linear spring. The valve is designed for pressured air and allows a similar volume flow at various pressure drops to industrial valves. An experimental investigation of the performance of the DE valve is conducted, demonstrating an improvement with respect to a solenoid valve with similar characteristics.

Keywords: DE, DEAP, EAP, Dielectric Elastomer, Dielectric Elastomer Actuator, Valve.

Introduction

Dielectric Elastomers (DE's), also known as Dielectric Electro-Active Polymers (DEAP's), show high potential for research and industry due to their multifunctional applicability [1] . DE's can be used as actuators as well as sensors, whereby both tasks could be done simultaneous thanks to the self-sensing feature of the material, as shown, e.g., by Rizzello *et al.* in [2]. Some advantages of DE's are large deformations, high power density, high energy efficiency, low weight, fast response time, and silent operations. Promising applications of DE's include pumps and valve controls [3]-[5]. In particular, the low power consumption makes DE-controlled valves particularly attractive for industrial applications. Giousouf *et al.* [6] shown the potential of DE-stack actuators to control pneumatic valves and achieved good results in pneumatic performance and energy efficiency. Jhong *et al.* [7] used a combination of two cone DE-membrane actuators to control the airflow in a flow channel and has shown that a proportional control of the airflow is possible.
This work has a similar approach to Jhong's work, and presents a valve system driven by a DE membrane actuator. The direct comparison between a DE driven valve and a typical industrial solenoid valve is presented, and the demonstration of additional features of the DE, like proportional airflow control and lower energy consumption, is also provided.

Dielectric Elastomer Actuator Description

The basic configuration of a DE Actuator (DEA) consists of a parallel plate capacitor made of a thin dielectric elastomer foil which is sandwiched between compliant electrodes. Fig. 1 shows the structure of the DE membrane investigated in this paper, namely a circular membrane DE. The electrodes consists of graphite compound, manufactured by screen printing, and the DE-membrane is silicone polymer.

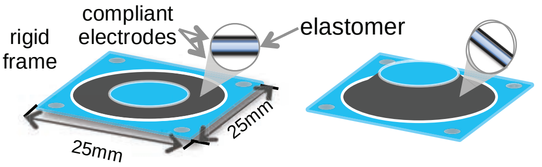

Fig. 1: *Circular membrane DE non-deflected (left) and deflected (right)*

The working principle of DE is based on an electromechanical pressure, arising as a consequence of an electric field, which squeezes the membrane, the so called Maxwell-stress (1). A voltage U applied to the electrodes results in an electric field which squeezes the DE membrane, resulting in a lateral expansion that can be used for actuation. The stress compressing the membrane, i.e., the Maxwell-stress, can be computed as follows

$$\sigma_{Maxwell} = \varepsilon_0 \varepsilon_R \left(\frac{U}{z}\right)^2, \tag{1}$$

where ε_0, ε_R are the vacuum and DE permittivity, respectively, U is the voltage, and z the thickness of the DE membrane.
The working principle of the membrane DEA requires a biasing force, such as the one provided by a mass or a spring, to generate an out-of-plane stroke. An example of biasing is shown in Fig. 2(left), where the center of the DE is pre-deflected by compression of a linear spring. The inner frame is initially deformed to a point where the DE membrane and spring reach an initial equilibrium position. The application of a voltage causes a lateral expansion of the diaphragm, which results in a decrease in the DE membrane reaction force in the out-of-plane direction. The spring extends with the inner frame of the DE, as both of them move

Design and Control Strategies for a Novel Actuator System with Dielectric Electroactive Polymer and Spring

X. Zhang, A. Verhagen
Robert Bosch GmbH, Renningen, Germany
Q. Zhu, Karlsruher Institut für Technologie, Karlsruhe, Germany
S. Hau, S. Seelecke
Universität des Saarlandes, Saarbrücken, Germany

Abstract:
A novel actuator, which is made from dielectric electroactive polymer and a spring system, has been developed and produced at the University of Saarland in cooperation with the Robert Bosch GmbH. In our research work the control concepts for this actuator are elaborated and investigated. The main problem to use such a novel actuator system is the instability, which means that the actuator cannot be stabilized at some given position. Goal of this research work is to develop and evaluate control concepts, which make the nonlinear actuator system stretch to a desired position on one side and stabilize at this given position at the other side.

At first a physical model of the whole actuator system including the dielectric elastomer (DE), linear and nonlinear spring is built within the scope of this work. The hyperelastic behavior of the DE material is approximated by the Ogden model. The model was validated with data from real measurement. The biased linear spring and nonlinear spring are described by characteristic curves which are derived from measurement data. Secondly the instability problem is investigated and solved through a nonlinear control concept which uses the gain-scheduling method and is based on the physical model developed before. With help of the gain-scheduling method different linear controller are designed and compared, e.g. the PID-controller with Ziegler-Nichols design, compensator with root locus design and robust controller with H∞-method. At the end the robustness of different controller designs are discussed and several conclusions are made.

Keywords: Electroactive Polymers, Dielectric Elastomer, Actuator, Control

Introduction

Electroactive Polymers, particularly dielectric electroactive polymers (DEAP), show a large deformation under electric actuation signal. Many research works have been conducted in the last years to investigate, how actuators with dielectric elastomer can reach a large deformation while working against an external load. In [1] the working principle of a stack actuator has been introduced to enhance the total deformation of the actuator (see Fig. 1). The total deformation of the actuator can theoretically reach N times of the single layer actuator if N layers are stacked together. In the practice the total deformation is about 70% because of the nonelastic end cap. While the stroke of such stack actuator is improved, the output force which the stack actuator can generate is limited. A novel way to maintain the large stroke under higher external loads is to add a non-linear spring to the stack actuator. In [2] such a prototype was introduced based on a circular out-of-plane DE actuator and linear as well as nonlinear springs (see Fig. 2).

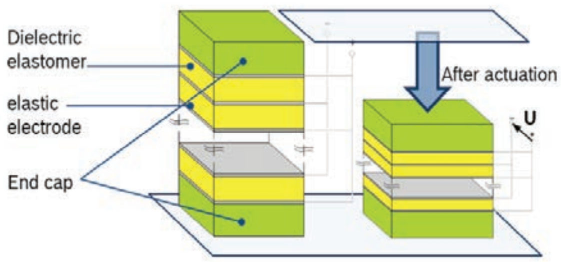

__Fig. 1:__ Actuation of a stack DE actuator

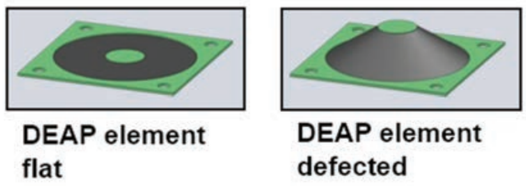

__Fig. 2:__ Actuation of a circular DE actuator with linear and nonlinear spring system

Industry 4.0 Using Shape Memory Actuators – Opportunities and Challenges

R. Theiß, A. Czechowicz, P. Dültgen
Forschungsgemeinschaft Werkzeuge und Werkstoffe e.V., Remscheid, Germany

Abstract:
Industry 4.0 is characterized by a significant increase in digitalisation and networking of products, value chains and business models. This is boosted by the use of ubiquitous sensors, data collection and sophisticated methods to analyse massive amounts of data. Therefore, the necessity for integrated sensor-actuator components and their integration into networks as so called cyber-physical systems increases. Shape Memory Alloys are multi-functional materials which allow the integration of actuator and sensor functions in a single component. Shape Memory Actuators have seen an increase in use recently but mid to long term experience especially required for product and service development is still limited. Therefore, a joint application of Industry 4.0 methods and Shape Memory Actuators is reasonable. This paper provides an overview on challenges in the use of Shape Memory Actuators in context of Industry 4.0.

Keywords: Shape Memory Actuators, Sensors, Sensor - Actuator integration, Industry 4.0

1 Introduction

The fourth industrial revolution is characterized by a significant increase of digitalization and networking of products, value chains and business models. Advances in information- and sensor-technology lead to the ubiquitous availability of computing- and sensing capabilities in every day products as well as industrial processes. So more and more information from all phases of a product life cycle is available.

On the one hand side, this information is the basis for the improvement of products and processes and in particular services. Production industry depends on fast, inexpensive but sophisticated solutions to react to new developments and competition. On the other hand, this can also be used to find visible and invisible issues in an industrial factory environment. For example, the detection of machine degradation or component wear. [1]

A new paradigm of so called cyber-physical systems (CPS) as network integrated actuators and sensors allows to connect, monitor and control a wide variety of components, products and processes. A consequence of this is the arising trend which is known today as Deep Learning in connection with Big Data and Cloud Computing. They are considered as essential models to increase productivity, quality and flexibility of manufacturing industries. [2]

Six principles can be found in the design of Industry 4.0 products and processes. [3] These principles are useful for developers and manufactures for finding Industry 4.0 applications. First to mention is interoperability between different CPS. This allows the connection and communication on basis of the Internet of Things and the Internet of Services. The second principle is virtualisation of the Industry 4.0 components by uploading real sensor data to a simulation model. As third principle decentralisation becomes relevant as the CPS receive increasing functionality and intelligence. This results in CPS with the capability to make decisions on a local scale.

Therefore, methods of self-optimization, self-configuration, self-diagnosis, cognition as well as support of well trained workers become relevant. The combination of sophisticated communication networks and intelligence CPS exhibit real time capability for the collection, analysis of data as well as for decision making.

In contrast, Industry 4.0 also has challenges which have to be overcome. In highly connected systems relaying on software IT security issues as well as reliability and stability become relevant. Especially critical machine-to-machine communication (M2M) with short latency times. Furthermore, knowledge has to be protected and measures against industrial spying has to be considered in highly connected networks.

On a more abstract level the principles of service orientation and modularity receive more attention. A characteristic trait for industrial production in an Industry 4.0 context is the advanced customization of products and services. The application of the afore mentioned principles provide the potential for sophisticated and granular service, tailored for customer needs. Modularity is a basis for using this potential and allows the adaption of CPS on changing requirements by dynamic interchanging or modification of components. Especially highly modular and dynamic industrial product service systems become more feasible with the development of the internet of things and the internet of service.

Besides the development of new algorithm for data analysis or networking it is still necessary to develop new approaches for CPS as the fundamental basis of industry 4.0. [4] An innovative approach for

Reconfigurable SMA End-Effector for Material Handling

P. Motzki[1, 2], Y. Goergen[1, 2], A. York[2], S. Seelecke[1, 2]
[1] ZeMA – Zentrum für Mechatronik und Automatisierungstechnik gGmbH, Saarbrücken, Germany
[2] Universität des Saarlandes, Saarbrücken, Germany

Abstract:
A first prototype of an SMA-based reconfigurable end-effector was already presented at the SMA network exhibition booth at the Actuator14. In this paper, the next generation of the first SMA end-effector prototype is presented. The end-effector has four independent gripping arms, which can be positioned within a 90° rotation radius. The main part of this functionality is the use of the “self-sensing” ability of the SMA wires. The resistance feedback of the SMA wires is used for position control of the gripping arms. Also, each gripping arm has a second degree of freedom, which allows it to tilt perpendicular to the rotation plane. The designs of the actuator constructions are presented and a prototype is produced via rapid-prototyping. In conclusion, different application scenarios are presented and discussed.

Keywords: SMA, Shape Memory Alloy, Reconfigurable, End-Effector, Material Handling, Assembly

Motivation

Material handling is a crucial part of manufacturing and assembly in industry. In state-of-the-art handling systems, robots use special end-effectors to grip and transport work pieces. These end-effectors contain grippers that are fitted to the special geometry of the workpiece that is to be handled in the process (Fig. 1). If the same robot is used for the handling of different shaped work pieces, the end-effector is replaced with a new end-effector that, once again, is custom fitted to the new workpiece geometry. During the exchange process, all manufacturing or assembly processes are paused. This down time can be very costly. Therefore, there is an inherent benefit to creating a reconfigurable end-effector that is able to adjust automatically to different workpiece shapes and geometries [1-3]. To make an end-effector automatically reconfigurable, a suitable actuation method is needed. The actuators in the end-effector have to be strong enough to carry the loads of the workpiece, but at the same time they have to be light-weight to avoid adding big moments of inertia in the robot or the kinematic unit. High inertial forces require bigger and stronger robot actuators and thus higher energy consumption and costs. Because of their high energy density, Shape Memory Alloys (SMA’s) are a well suited actuation method for this application [4, 5]. SMA actuator wires will contract when heated, typically via an applied current, resulting from a phase transformation between martensite (cooled wire) and austenite (heated wire) [6, 7]. The use of SMA-wires as actuators allows for the construction of very light weight and energy-efficient systems.

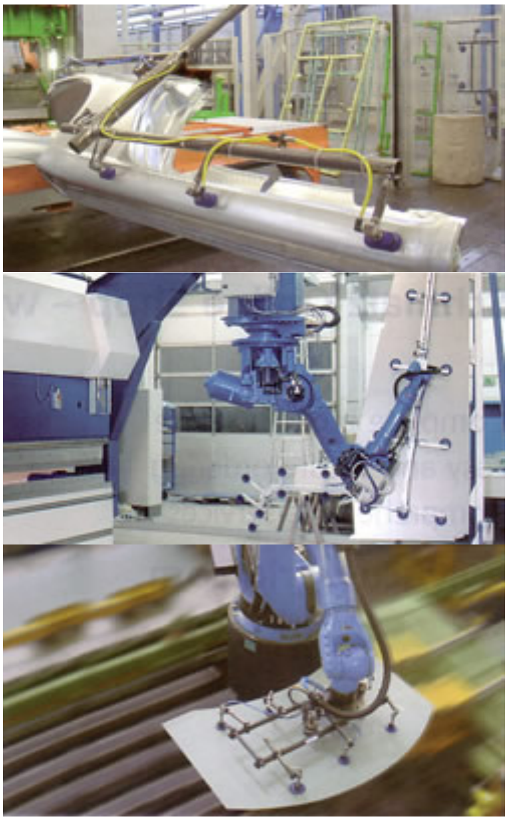

Fig. 1: *Examples of different end-effectors [8]*

Fundamentals

Shape memory alloy wires are known for their superior energy density. The most popular alloy for actuation wires is nickel-titanium (NiTi). The energy density of NiTi wires is in the range of 10^7 J/m^3 [9], the power density has a magnitude of 50 kW/kg [6].

Energy-Efficient SMA Vacuum Gripper System

P. Motzki[1,2], J. Kunze[1,2], A. York[2], S. Seelecke[1,2]
[1] ZeMA – Zentrum für Mechatronik und Automatisierungstechnik gGmbH, Saarbrücken, Germany
[2] Universität des Saarlandes, Saarbrücken, Germany

Abstract:
Shape Memory Alloy (SMA) wires are a promising actuation technology for industrial applications due to their high energy density. These wires contract when heated, typically via an applied current, as a consequence of a phase transformation between martensite (cooled wire) and austenite (heated wire). The first prototype of an SMA-actuated vacuum gripper was presented at the Actuator14 conference. The focus of this paper is on the development of a second generation prototype of an SMA-actuated vacuum gripper that does not require continuous activation during gripping. For evaluation and validation of the gripper system, a test rig is used to measure the created vacuum with a pressure sensor and the deflected membrane with a laser displacement sensor during operation. Different experiments take a look at the vacuum quality over time, lifting forces and repeatability. The paper ends with an outlook on future work and a discussion of possible application scenarios.

Keywords: Shape Memory Alloys, SMA, Vacuum Gripper, Suction Cup, Self-Sensing

Motivation

In material handling and assembly industry, vacuum grippers are widely used for the handling of plane work pieces [1]. State-of-the-art vacuum gripper systems use the Venturi effect for vacuum generation, so they need a continuous supply of energy from a central compressed air system [2]. At Actuator14, we first presented a vacuum gripper prototype actuated by SMA wires [3-5]. With this prototype we were able to demonstrate advantages of the SMA technology including lowered noise level, unaffected air quality and lowered system costs, weight and dimensions. The SMA wires in this prototype had to be constantly heated during gripping. To be more energy-efficient in processes with longer gripping phases, a new prototype is constructed with a different design scheme, in which the SMA wires are only activated with a short pulse when gripping or releasing a work piece.

Fundamentals

Thermal shape memory alloys have the highest energy density compared to other electromechanical transducers [6-8]. The most popular alloy for actuator wires is nickel-titanium (NiTi). NiTi wires can reach energy densities in the range of 10^7 J/m^3 [9] and power densities with a magnitude of 50 kW/kg [10]. A change of temperature induces a transformation of the crystalline structure in the micro-scale which can be observed as a large macro-scale deformation. For NiTi wires, this deformation is visible by a change of length of 3-4 % of its original length [11]. At low temperatures, the alloy is in a mix of two martensite phases (M_+ and M_-). Mechanical stress causes a transformation into a uniform martensite phase and quasiplastic deformation of the material. The application of heat causes a transformation to the high temperature austenite phase and a return to its original length. With a constant mechanical stress, heating and cooling of the material leads to a direct transformation between martensite (M_+) and austenite. In the case of the vacuum gripper, a mechanical spring is used for applying a constant force.

Design

The design scheme of the new vacuum gripper prototype is shown in Fig. 1. The SMA wires (1) are connected to the casing (2) and a piston (3). The coil spring (4) is compressed between the casing and the piston. The elastic membrane (5) is also connected to the casing and the piston.

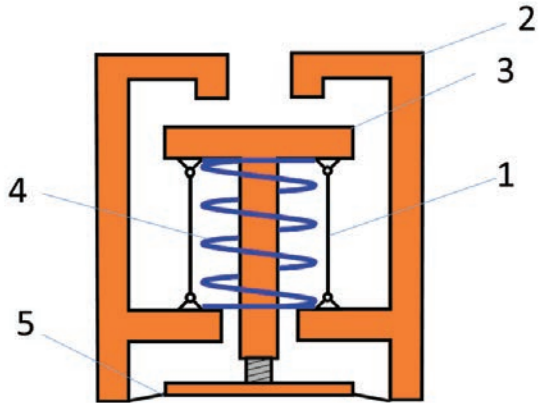

Fig. 1: *Schematic prototype design (SMA wires actived)*

In Fig. 1, the SMA wires are activated and contracted. They work against the spring force and pull the piston down. In Fig. 2 the deactivated state is shown. The SMA wires are cooled down and the

Passive Speed Control Using a Functional Clutch Driven Reversely

K. Koyanagi, Toyama Prefectural University, Imizu-shi, Japan
Y. Kimura, Osaka University Hospital, Suita-shi, Japan
M. Koyanagi, Osaka Electro-Communication University, Shijonawate-shi, Japan
A. Inoue, ER-tec Co., Minoh-shi, Japan
T. Motoyoshi, H. Masuta, T. Oshima
Toyama Prefectural University, Imizu-shi, Japan

Abstract:
In a previous study, we constructed a passive speed control system using a functional brake for systems that are driven by an external force, such as that exerted by a person, water, or wind. Such systems vary widely and are difficult to predict. The functional brake employed an electrorheological fluid, was controllable and had a quick response. However, it was difficult to reduce the vibration of the response adequately. We thus used a functional clutch instead of the brake, and attached a motor to the driving shaft. The motor rotates constantly but in the direction reverse to the driving direction of the external force. We then constructed the speed control system by controlling the functional clutch and achieved lower vibration than when using a system having a brake. The present paper finally reports on isokinetic exercise equipment for a target system, which requires a speed control function when driven by the trainee.

Keywords: Passive Control, Speed Control, Clutch, Functional Materials

Introduction

Systems that are driven by an external force, such as that exerted by a person, water or wind, vary widely and are difficult to predict. Examples of such systems are the wheel system of a car moving under the effect of an inertial force and a windmill, as shown in Fig. 1. In the case of the wheel system of a car, a resistive torque τ_b acting against the rotation of the wheel can be manipulated actively by the driver of the car applying the brake. However, the brake-assist systems of modern cars intervene in the braking process. The realization of smooth speed control via the resistive torque is expected to improve the ride quality. During the operation of an anti-lock brake system, general controllers observe the rate of slip between the tire and road and control the rotational speed of the wheel with ON/OFF braking. If proper speed control using the brake is automatically executed, it may be possible to brake more quickly or to prevent a slip. A problem affecting wind power plants is a variation in the production of electricity according to the wind power. Proper speed control with a resistive torque is thus needed for the constant production of electricity, which will reduce the cost of the electric power system and increase the efficiency of the power plant.

In previous studies, we constructed a passive speed control system using a functional brake for such systems [1][2]. The functional brake used an electrorheological (ER) fluid and was controllable and had a quick response. We presented results for isokinetic exercise equipment, which required a speed control function when it was driven by the trainee.

It was however difficult to reduce the vibration of the response adequately. We thus used a functional clutch instead of a brake, and attached the motor to the driving shaft as shown in Fig. 2. The motor rotated constantly but in reverse to the direction driven by the external force. The resistive torque was controlled by adjusting the torque transmitted from the motor with transmissibility of the functional clutch. Because this was a semi-passive system generating an active torque only in the direction opposing the motion, we expected the system had controllability better than that of a purely passive system.

In the present study, we constructed a speed control system that controls the functional ER clutch and observed vibration weaker than that in the case of the system using the brake [3]~[7].

Fig. 1: *Examples of systems driven by a disturbance force and controlled by a brake*

Noise-Robust Online Parameter Identification of BLAC Machines Using Sliding Mode Differentiator

N. König, E. Grasso, D. Merl, M. Nienhaus
Universität des Saarlandes, Saarbrücken, Germany

Abstract:
Parameter identification algorithms are needed to successfully control electrical machines, as well as for final inspection stages of motor production. Nevertheless, such algorithms make use of current sensors, which typically introduce noise. Moreover, the needed time derivative of the current measurements represents a major limitation in parameter identification. In this work a sliding mode differentiator is combined to a LMS algorithm for improving noise robustness of the parameter identification technique. Experimental results performed on a BLAC motor will be shown and discussed.

Keywords: BLAC Machine, Parameter Identification, Sliding Mode, Derivative Estimation

I. Introduction

Parameter identification algorithms are needed to successfully control electrical machines as well as for final inspection stages of motor production. In the field of electrical machine control, an online estimation of the parameters is desirable to implement adaptive control algorithms which are capable of tracking parameter changes due to temperature variation as well as to external factors.

A lot of different algorithms are used for system identification. In particular, the Least-Mean-Square (LMS), Normalized LMS (NLMS) and the Recursive Least-Squares (RLS) algorithms are among the most adopted techniques due to their simplicity of implementation [4, 5]. These algorithms have been used for parameter estimation of electrical actuators like DC-motors in [2], induction machines in [6] and unconventional dielectric polymer actuators in [1].

In reality noise is present on all sensor measurements. In particular, current sensors are usually characterized by low signal to noise ratios as well as limited bandwidth. It is well known that the time derivative of a noisy signal results into an even noisier signal. Therefore, the noise resulting in the time derivative can be so high that the signal is no longer recognizable. This leads to a bad convergence of the LMS and/or RLS algorithms and, therefore, to a wrong determination of the parameters, in particular of the inductance of the machine, which is associated to the derivative of the current. Nevertheless, the identification of the motor inductances is crucial for reaching high control performance.

In this work both NLMS and RLS algorithms are used to determine the electrical parameters of a BLAC motor such as the flux constant, the stator resistance and the inductance in the d- and q- axis. The basics about BLAC machines and parameter identification with NLMS and RLS are presented in section II. The implemented algorithms are derived from the typical mathematical model of BLAC motors. The derivatives of the currents in the d- and q-axis are obtained by means of a sliding mode differentiator, which is an established technique in control theory and differentiation estimation [3]. The sliding mode differentiator is accurately tuned based on the knowledge of the time dynamics of the motor currents. Finally, the phase shift of this differentiator has to be considered in order to get a good estimation of the parameters. The implementation will be described in section III.

These techniques have been implemented both in simulation and in an experimental set-up. In particular, the parameter identification algorithms were implemented in Matlab-Simulink where a BLAC motor and noise sources have been modeled. Persistently exciting voltages have been designed in order to optimize convergence of the algorithms. Afterwards, an electronic circuit based on an inverter stage and current sensors was designed and connected to a dSPACE DS1103 system in order to experimentally test these algorithms. Finally, this work will present and discuss the obtained results in section IV and V.

II. Basics

a) Model of a BLAC machine

The system equations for a BLAC machine in d-q-coordinates are [7]:

$$\frac{d\Psi_d}{dt} = u_d - R \cdot i_d + \omega_{el} \cdot \Psi_q, \qquad (2.1)$$

$$\frac{d\Psi_q}{dt} = u_q - R \cdot i_q - \omega_{el} \cdot \Psi_d, \qquad (2.2)$$

A Direct Flux Observer for Robust to Noise Sensorless Control of PMSMs

E. Grasso, M. Nienhaus
Universität des Saarlandes, Saarbrücken, Germany

Abstract:
Sensorless control for PMSMs represents one of the main aspects of embedded systems because it allows the removal of sensors at the advantage of dimensions' reduction and diminished maintenance. The Direct Flux Observer technique allows obtaining a measurement of the flux linkages of the motor phases, which are function of the electrical rotor position needed for motor driving, without the usage of current sensors. However, the measured signals are affected by noise. Therefore, a Sliding Mode Differentiator is used in order to perform reliable and robust to noise control of PMSMs. Simulation and experimental results are shown and discussed.

Keywords: BLAC Machine, Sliding Mode, Derivative Estimation, DFO

I. Introduction

In recent developments of low-power electromagnetic actuators there is an increasing demand of space saving solutions while preserving high quality and performance. Thus there is the need of realizing embedded motion control systems, where actuating, sensing and control capabilities are joined in one single unit. Sensorless control for PMSMs (permanent magnet synchronous motors) represents one of the main aspects of such systems because it allows the removal of sensors at the advantage of dimension reduction and diminished maintenance.

Among the techniques for sensorless control of PMSMs [1], the ones that exploit the magnetic anisotropies of the machine are capable of operating at all speed ranges, included stand still conditions. Within this category of techniques, it is important to recall the vastly adopted high frequency current injection [2] as well as INFORM [3]. Nevertheless, such techniques require current sensors in order to retrieve the rotor position of the machine. A novel technique called Direct Flux Observer (DFO) [4 – 6] has been recently introduced, which requires exclusively the measurement of the star point voltage of the machine by means of a particular PWM pattern, thus reducing further space requirement and cost. Moreover, the simplicity of this technique makes it suitable for implementation even on low performance microcontrollers.

The DFO technique allows obtaining a measurement of the machine flux linked with the motor phases, which is dependent on the electrical rotor position needed for motor driving. However, due to the presence of switching electronics, the measured signals are affected by noise. Therefore, obtaining a speed measurement suitable to control purposes can become burdensome, since the noisy position signal needs to be differentiated therefore enhancing the noise content. Using typical linear filters might result in a decrease of control performance, as the controller bandwidth will have to be reduced accordingly. Therefore, advanced filtering techniques need to be implemented.

In this work a Sliding Mode Differentiator (SMD) [7] is used in order to obtain the rotor position and speed needed for performing speed and torque control of a PMSM. SMDs are robust and exact differentiators based on sliding mode technique, and they are easily tuned based on the knowledge of the Lipschitz's constant of the signal derivative. Moreover, among other robust to noise differentiators, SMDs are characterized by a low computational effort, which is a key aspect for embedded systems, where low performance microcontrollers are typically used.

At the purpose of testing the technique, a simulation has been designed and conducted in the Matlab/Simulink environment. Simulation results have proven the capability of the SMD to significantly reduce undesirable results coming from noise flux linkage signals at the advantage of a more stable closed loop control of PMSMs.

II. Basics

a) DFC Method

Let us consider the equation of a generic phase p of a three phase motor:

$$V_p = I_p R_p + \frac{\mathrm{d}\Psi_p}{\mathrm{d}t}, \qquad (1)$$

where Ψ is the resultant flux linkage of phase p, which can also be expressed as:

$$\Psi_p = L_{\sigma p} I_p + \Psi^*, \qquad (2)$$

Semi-Passive Vibration Control Technique via Shunting of Amplified Piezoelectric Actuators

G. Mikułowski, Institute of Fundamental Technological Research, Warsaw, Poland
M. Fournier, T. Porchez, C. Belly, F. Claeyssen
Cedrat Technologies SA, Meylan, France

Abstract:
The objective of this paper is to provide results of an experimental and analytical investigation of Amplified Piezoelectric Actuators (APA) as vibrational isolator in a configuration of a mechanical Single Degree of Freedom system. The investigation is aimed at assessment of the mechanical properties modification ability via shunting techniques. The investigation consist of a phenomenological modelling of the APAs considered as generators and experimental verification of the vibrational energy dissipation ability in frequency domain.
The results obtained during this investigation reveal that it is feasible to receive more than 20 dB reduction of the displacement amplification in the resonant range. Moreover, three tested examples of APA reveal up to 9 % of resonant frequency shift due to proper adjustment of the electronic shunting circuit, which is an encouragement for further analyses towards application of the APAs in semi-passive vibration control applications.

Keywords: Vibration, Dissipation, Adaptive, Piezoelectric

Introduction

Mechanical structures dedicated to aeronautic or space applications need to be developed with regard to strict weight limitations. These requirements lead to development of slender structures with limited internal stiffness and therefore being susceptible to externally excited vibrations. These require dedicated engineering solutions. Since the beginning of 1980s, there is a technique developed with utilization of shunted piezoelectric patches adhered on the structural elements which increases the damping properties of structures in a controlled way [1]. The tested applications reveal the efficiency of that method [2] but a significant drawback of that technique is that it should be introduced on an early design stage and embedded in the structural material.

In the engineering practice, there is often a necessity of application of a vibration control treatment in an advanced phase of the design process, when each modification of the principle structure generates high costs and therefore it is difficult to introduce any embedded system. In such situations vibration energy absorbers like Tuned Mass Dampers (TMD) [3] are often utilized in order to meet the technical specification of the design.

However, the classical TMDs [4] are narrow-band devices that need to be tuned for a particular operational frequency. This is not well fitted to the requirements of the aeronautic structures where it often happens that the dominant excitation frequency changes in reference to the flight stage. The bandwidth of the passive TMD may be widen by increasing the mass of the device but this solution stays in contradiction to the weight limitations of the aeronautic or space applications.

Therefore, a solution is required which would provide an ability of adaptation of the mechanical properties of the vibration attenuation device to the recognized frequency of the vibrational excitation. There are known results of investigations dedicated to analysis of modification of the mechanical stiffness and damping of piezoelectric ceramics via shunting methods [2]. Most of them are focused on piezoelectric patches or piezoelectric stacks. However, the first group of the solutions is strictly dedicated to the applications embedded in the structural elements and the second group of materials reveals high values of stiffness which eliminates them from the prospects of practical application due to high quality factor.

The mentioned limitations drive us to an idea of utilization of Amplified Piezoelectric Actuators (APA) [5] as mechanical fuses of modifiable stiffness and damping properties by means of the shunting technique. Due to utilization of a geometric lever in the APA design, the effective stiffness of the element with the piezoelectric stack can be reduced. Therefore, the operational frequency range can be adjusted and suited to the requirements of an application in the aeronautical or space industry.

The objective of this paper is to provide results of a preliminary experimental and analytical investigation of the APAs as vibrational isolator in a configuration of a mechanical SDOF system. The investigation is aimed at analysis of the APAs mechanical properties with ability of modification via shunting techniques. The investigation consists

Potentialities of APA Composite Shell Actuators and SA75D Amplifier for New Dynamic Applications

M. Ragonet, J.-L. Petiniot, ONERA, Lille, France
M. Fournier, T. Porchez, O. Sosnicki, C. Bouchet
Cedrat Technologies SA, Meylan, France

Abstract:
The piloting of APA's composite shell by SA75D power amplifier offers new opportunities for dynamic new applications. Two in particular were received and are being studied: the design of a compact table tensile micro machine for characterizing stress-strain laws at high strain rate of wires, fibers, strands and textile samples that will usefully complete the fleet of dynamic testing machines available, the generation of synthetic jets of air pulsed also studied at ONERA. The energy capacity (displacement, force) without or with an external linear load were modeled versus the rise time using the Simulink code and experimentally measured using a very light device. Other identified improvements remain to be implemented both at the APA's actuators as the Amplifier SA75D to get some gains.

Introduction

ONERA activity on Amplified Piezo Actuators APA® from CEDRAT Technologies was initiated by the opportunity to apply them to the flap motion of active blades of helicopters. The main handicap was their weight and the idea of a composite shell came at once to the mind. Other equally interesting properties were also perceived quickly for applications in fast dynamics in other areas of activity.
Different works on the design of various other geometries [1], the manufacture [2], the optimization [3] and the repeatability of the production [4] have been done.

APA500L with Carbon/Epoxy shell

Fig. 1: *APA500L with steel shell*

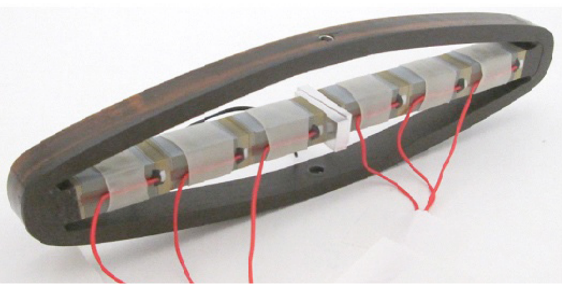

Fig. 2: *APA500L with carbon composite shell*

The two actuators (figures 1 and 2) are very similar in appropriate comparison purposes. Internal profiles are identical. The thickness more or less constant since the manufacturing method is adjusted for stiffness comparable to the steel shell. Only hooking zones differ, the dishes have not been reproduced. In the case of the composite shell, the stack supports bases are reported. They are of B_4C ceramic, EDM machinable and ensure a good transmission of forces. A specific study was conducted to optimize the geometry of these bases and increase energy capacity W = F.d and limit the risk of damage to the shell by punching.
For a shell geometry, identical stacks and a preload of 20 MPa the main properties obtained for the two actuators are shown in Table 1.

Table 1: *Comparison of the actuators properties*

Shell	Steel	Carbon/Epoxy
Number	1	Mean of 4 specimen
Interface	Plate with a ∅M3 hole	Round with a helicoil ∅M3
Short Axis (mm)	56.43	50.09
Great Axis (mm)	124.55	124.51
Thickness (mm)	20	20
Shell Mass (g)	97	28
Actuator total Mass (g)	200	131
Fr blocked-free (Hz)	462	504
Response Time blocked-free (ms)	1.09	1.01
Fr free-free (Hz)	1900	3770
Response Time	0.26	0.14
Stiffness (N/µm)	1.22	1.19
Stroke (µm)	630	630
Blocked Force (N)	769	750
Stacks Pre-stress (MPa)	20	20
Crushing for implementation (µm)	1550	1325
Thermal Coefficient CTE (µm/°C)	7	0.7
Electro-mechanical Coupling (%)	47 (45 at 70°C)	40 (42 at 70°C)
Factor of merit Q (%)	44	28

The electrical capacitance of the stacks is 34 uF. A 630 µm stroke, a blocking force of 750N and a Ky stiffness along the minor axis of 1.20 N/µm, identical for the two actuators were obtained with the advantage of the actuator to composite shell:
- A weight gain of 35%;
- A free-free resonant frequency multiplied by 2;
- A blocked-free resonant frequency multiplied by 1.1;
- A 15% lower crushing;

Embedded and Redundant Heater for Controlling of SMA-Based Rotary Actuator for Space Applications

F. Stortiero, V. Visentin, S. Gualandris
Technosprings Italia srl, Besnate, Italy

Abstract:
Embedded and redundant heater has been developed for controlling of a shape memory alloy rotary actuator for space applications. The development of the heater has been carried out to solve some issues related to the design of the Hold Down Release Mechanisms (HDRM) as power cut-off device and issues related to temperature and position control for synchronized actuation. The electrical and thermo-mechanical properties have been characterized in order to underline the self-regulating behavior useful to avoid a power cut-off device in HDRM and underline the control of the temperature and the angular position. The control of the rotary actuator either on the point of view of temperature and angular position has been exploited to demonstrate the feasibility of synchronized actuation in case of installation of multiple actuators. Some details on the application of the rotary actuator in no space fields have been illustrated and some figures of merit has been described.

Keywords: Rotaty Actuator, Position Control, SMA, HDRM

Unfortunately, the final manuscript has not been received by the printing date. Please contact the author for additional information.

Hydraulic Expansion Actuators for Ball Screws – Towards Applicable Preload Adaption

B. Denkena, P. Schreiber
Leibniz Universität Hannover, Garbsen, Germany

Abstract:

Machine tool feed drives are commonly driven by preloaded ball screws. The amount of preload is an important parameter of a ball screw drive. While the preload is required for gaining rigidity and eliminating backlash, it causes friction and heating of the ball screw. The feed drive's thermal behaviour and lifetime can be improved by adapting the preload to the required level. This work presents a novel hydraulic expansion actuator that is capable of adapting a ball screw's preload during operation. Experiments on a prototype evaluate its static and dynamic characteristics. The results provide proof for the feasibility of the novel actuator concept.

Keywords: Ball Screw, Preload Adaption, Hydraulic Actuator, Feed Drives

1 Introduction

Machine tool feed drives are subjected to demanding requirements regarding rigidity, operational life, efficiency, and cost. Preloaded ball screws satisfy these requirements to a great extent. Hence, ball screws are still the most frequently used drive of machine tool feed drives [1].

In ball screws, preload determines the rigidity and eliminates backlash. However, friction and wear also increase with higher preload. Consequently, preload is a crucial parameter of a ball screw and its value is a result of a trade-off between the said parameters. A constraint in this trade-off is the minimum preload according to DIN ISO 3408-4: The preload value is to be set at least to such extent that axial loads on the ball screw do not exceed the preload by a factor of 2.83. At this point, the balls on one side may be unloaded, which leads to undefined ball kinematics and increased wear [2].

Additionally, setting the initial preload is even more complicated by the fact that the preload value does not remain constant over a ball screw's lifetime. Initial preload has to compensate preload loss due to abrasive wear and equalizing of roughness peaks: Brecher *et al.* found a loss in ball nut rigidity of more than 20 % after 2000 km mileage [3]. Analogously, operational life calculation according to DIN ISO 3408-5 assumes an average preload of 60 % of the initial preload over a ball screw's lifetime [4].

In addition to the described slowly progressing preload loss, preload can also vary on short term depending on a number of causes such as pitch error, radial run-outs of the shaft [5], feed velocity [6], and thermal expansion of shaft and nut [7].

In practice, initial preload is often set to a level of 10 % of the ball screw's dynamic load rating [8]. This value is usually preset ex-factory and cannot be adjusted by the user, although there is one ball screw with adjustable preload commercially available [9].

In order to attenuate the described trade-off, researchers have attempted to adapt preload during operation: Pritschow *et al.* [8] present a lever mechanism that exerts a torsional moment onto one nut in a double nut arrangement, thereby adjusting preload. Verl *et al.* integrate a spring mechanism between two ball nuts in order to avoid unloading and thus allowing for lower preloads [10]. In other concepts, various actuator types are directly integrated into a double nut's force of flux: Piezo-electric actuators have been integrated by [11]. Shape memory alloys were used for compensating wear [12] as well as for compensating preload loss caused by thermal expansion [7]. In addition, a hydraulic piston actuator is shown by [13].

Those approaches were not established in practice. This is due to multiple reasons, including insufficient rigidity, cost, and practicability. In the case of hydraulic preloading, insufficient rigidity is assumed [14].

However, hydraulic actuators offer substantial advantages for ball screw preloading because of their high force density and the fact that most machine tools already have a hydraulic system. Therefore, we aim to reconsider hydraulic preload adaption with a novel actuator based on a hydraulic expansion principle.

2 Hydraulic Expansion Actuator for Ball Screw Preloading

The proposed hydraulic expansion actuator's (HEA) working principle, as shown in Fig. 1, is similar to that of hydraulic expansion chucks. The ring-shaped actuator is mounted between the two ball nuts of a double nut ball screw. The actuator comprises a cavity, which is covered by a thin diaphragm. By setting hydraulic fluid in the cavity under pressure, the actuator expands and exerts a preload force between the nuts.

A Multifunctional Pneumatic Artificial Muscle – Proof of Concept

T. Hassan, M. Cianchetti
Scuola Superiore Sant'Anna, Pontedera, Italy
B. Mazzolai, Istituto Italiano di Tecnologia, Pontedera, Italy
C. Laschi, P. Dario
Scuola Superiore Sant'Anna, Pontedera, Italy

Abstract:
This paper presents a novel multifunctional pneumatic artificial muscle (PAM) with bi-directional force and motion capabilities. PAM's are generally preferred due to their high power to weight ratio, light weight, ease of installation, hazard free use and inherent compliance To demonstrate the concept, a prototype of the bi-directional artificial muscle has been designed and developed. The prototype was characterized using a universal testing machine with an actuation pressure of 1 bar. Isometric and Isobaric experiments conducted on the prototype show good force capacity and the unique bi-directional capability.

Keywords: Double Acting Pneumatic Muscles, Mc-Kibben Actuators, Soft Actuators.

Introduction

Pneumatic artificial muscles (PAM), more commonly known as fluidic or Mc-Kibben muscles have been around for quite some time now. They are generally preferred thanks to their high power to weight ratio, light weight, ease of installation, hazard free use and inherent compliance. These properties make them an ideal choice for industrial/ robotic applications where human-machine interaction is involved. Recent and comprehensive surveys on their applications can be found in [1] [2]. PAM usually consist of a hollow cylindrical elastomeric chamber covered by an outer braided sleeve, consisting of fibers made of un-stretchable material and arranged in an anti-symmetric helical configuration. The hollow internal chamber and the braided sleeve are tightly sealed and attached to rigid end fittings, usually a passage is provided through one of these end fittings for pressurizing the elastic chamber with air or another fluid. The mechanical work done is transferred to an external system through these end fittings. When the inner elastic tube is pressurized the muscle either expands or contracts or stiffens depending on the initial angle of the braid fibers with the longitudinal axis of the muscle. The existing/traditional PAMs has a fixed initial braid fiber angle and are usually designed to produce a contractile force upon actuation, hence they are able to produce uni-directional force and motion [3]. This single acting nature of traditional PAMs poses a drawback when utilized for robotic applications, i.e. for bi-directional actuation of a robotic joint; two actuators are required in antagonistic configuration. This increases the overall size and complexity of the actuation mechanism [4].
In order to overcome this challenge previous attempts have been made to develop a bi-directional PAM. In [5] a spring over muscle (SOM) actuator is reported.

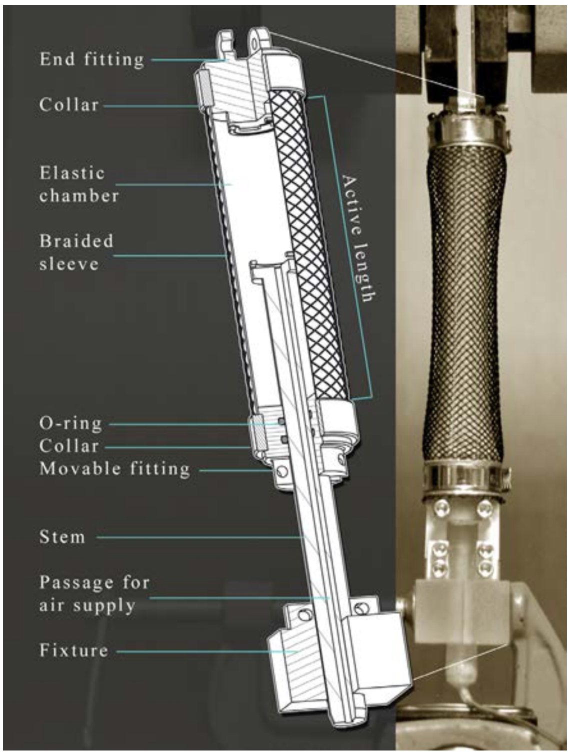

Fig. 1: *Actuator design schematics. Physical prototype and sectioned CAD rendering*.

The SOM utilizes a passive compression spring in parallel with a PAM for producing bi-directional forces. Zheng & Shen developed a double acting sleeve muscle actuator [6], which is able to produce bi-directional force and motion. The muscle incorporates a unique insert at the center, inside the hollow elastic chamber. This design results in a significant decrease in the air consumption during operation and an increase of force capacity over the

Pneumatic Actuator Using Polyimide Film for Liquid Nitrogen Temperature

D. Yamaguchi, T. Hanaki, R. Kamimura, Y. Ishino, M. Hara, M. Takasaki, T. Mizuno
Saitama University, Saitama-shi, Japan

Abstract:
A purpose of our research is development of soft robotics called Filmotics. Filmotics is a synthesized term of Film and Robotics. In this study, we introduce our soft film actuator. The actuator can be driven in liquid nitrogen temperature. The actuator is made from two different-size polyimide films. Lager film is folded in pleats, and the pleats is expanded by applying driving gas. From the expanding, the actuator generates a bending motion. We have succeeded in driving the actuator at 78 K. The generated force was 84 mN when the applied gas pressure was 26.1 kPa. However, there was a problem with a leakage from a joint between a pneumatic pipe and the actuator. Thus, we fabricated and evaluated new connecting method using heat shrink tube. From evaluation, the leakage was decreased by using new method.

Keywords: Pneumatic Actuator, Filmotics, Ultralow Temperature, Soft Actuator, Liquid Nitrogen

Introduction

Liquid nitrogen temperature provide some benefit in the fields of a medical treatment, a food industry, and an advanced scientific research [1]-[3]. For example, an ultralow temperature environment is to enable a long-term storage of organs, blood, and foods. In particular, a low-temperature environment generated by using liquid nitrogen (LN2) was called LN2 temperature environment, the temperature is about 77K. As an application example, a rapid freezing cooled by LN2 reduces a freezing damage of biological samples.

Most of material has low temperature brittleness at ultralow temperature. From this reason, previous actuators, which can be driven in LN2 temperature or lower temperature condition, were made of metallic materials. These actuators have high mechanical stiffness because of hardness from metals. However, if a handling device has high stiffness, operating a frozen sample is difficult because operation object has low temperature brittleness. From this problem, softness and flexibility is required for an actuator for ultralow temperature.

A soft actuator is a typical mechanical component for gripping brittleness objects because the actuator made of rubber materials [4]-[7]. Rubber material has low mechanical stiffness, and rubber-molding process is easy and economical. However, it is difficult to apply the previous soft actuator to low temperature environment because rubber has low temperature brittleness.

A purpose of our research is development of soft robotics called Filmotics. Filmotics is a synthesized term of Film and Robotics. In particular, we have focused on a soft operating device for LN2 temperature environment. In our previous study, we have already succeeded in a soft film actuator for LN2 temperature [8]-[9]. The actuators were made of super engineering plastics and driven by gas pressure. However, the actuator had a problem with gas leakage from connection between tube and air chamber.

In this paper, we introduce our previous film actuator and evaluation system for LN2 temperature. Additionally, to solve the problem, we evaluate new piping.

Structure of actuator

The structure of our soft actuator is shown in Fig. 1. The actuator consists of a balloon unit, a metal wire, and a tube. The tube is inserted in the balloon unit. The balloon unit and the tube are tied all round many times with the metal wire. Gas is supplied through the tube and the balloon unit is expanded.

The air chamber is composed of two different-size films. A larger film is folded in pleats. When driving gas is supplied to the chamber, the pleated film is expanded and the actuator is generated a bending motion. The diagram of the bending motion is shown in Fig. 2.

In this research, we fabricated two size actuators that have a different width according to evaluations. The width for evaluation bending angle is 10mm, and the other for evaluation force is 12mm.

As mentioned previously, typical plastics material, e.g. rubber, has low temperature brittleness. In this research, polyimide (PI) which is a kind of super engineering plastics is used as film material because PI has low temperature antibrittleness.

Furthermore, typical adhesive has low temperature brittleness. Thus, two films are heat-welded each side without adhesives, and the balloon shape is fabricated. However, welding condition of PI films

Surveying and Closed-Loop Control Study of Highly Elastic Bending Actuator for Biomimetic Gripping

J. Isermann, S. Ulrich, R. Bruns
Helmut Schmidt Universität, Hamburg, Germany

Abstract:
This paper concern with the mechanical behavior and the closed-loop control for a new elastic bending actuator. First, the behaviour of the actuator is characterized with basic preliminary experiments at different load situations. This is followed by advanced experiments to characterize the actuator behavior. Finally, the behaviour of the actuator under using a controller is presented and evaluated.

Keywords: Elastomer, Bionic Gripper, Flexible Actuator, Joint-Free Bending, Soft Gripping, Picking Cell

Introduction

In distribution logistics picking plays a crucial role. Picking aims to compile from a total amount of goods or an assortment subsets due to contracts [1].
The degree of automation in order picking process is still low compared to other areas of the company such as manufacturing. Due to economic purchasing conditions for hardware components and the technical development of sensor technology, image analysis software and corresponding algorithms, there is a wealth of new solutions for automation processes [2].
Our contribution to this problem is to provide a flexible and universal gripping system for robot-based picking for the example of drugstore products.
The gripper has no classical mechanical engineering joints. It is equipped with nine highly elastic actuators, which have a resilient joint. The other structure and the specially textured gripping surfaces are produced by 3D printing process. The gripping system is thus equally well suited for man-machine applications because of this design, the risk of injury is reduced. The constructive development process of the gripper with a focus on the development of the pneumatic drive system, and the related basic research has already been presented [3, 4]. The latest status of the engineered gripper model can be seen in the figure below:

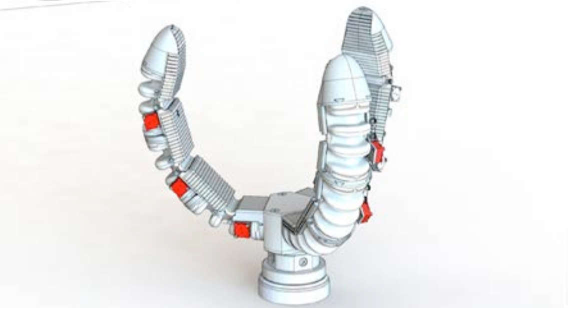

Fig. 1: *Complete CAD model of the slightly closed gripper*

In the following, the physical properties and the control of the movement of the gripper drive system are presented and evaluated.

Measuring technology tests to characterize the actuator

In preparation for the measurement a closed pneumatic measuring and control circuit was constructed. To control the inner pressure of the actuator, a proportional valve is used. The valve control characteristics for the output pressure with three different versions can be set. The optimum setting for the application has been determined in advance by evaluating hysteresis.
To measure the actuator an own test environment was developed. The test bench can be seen in below figure forming:

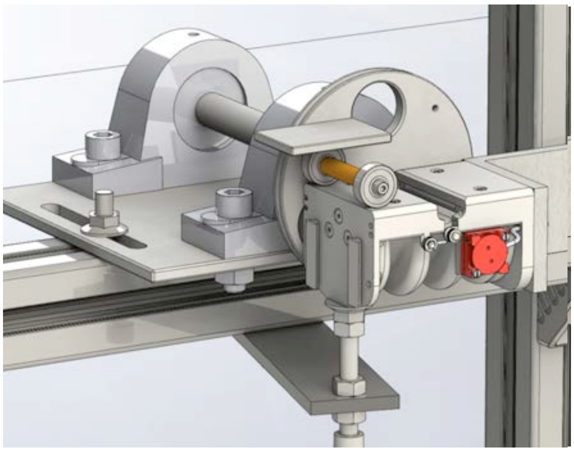

Fig. 2: *3D-CAD drawing of the actuator test bench*

In preliminary experiments it was determined that the gripping forces for the planned application with the actuator material with shore A hardness 60 presented in [3] are too low. In the following experiments, therefore, a shore hardness of A 75 was used. With the higher pressure and force level, the material has a reduced elongation at break. This amounts to only 60% of the value of the A 60 material.
The measurement of actuator angle is realized both at the test bench as well as the gripper in use by a

Dtact: A Tactile Device Which Changes How a Surface Is Perceived

F. Giraud, Université de Lille, Villeneuve d'Ascq, France
C. Giraud-Audine, Arts et Métiers Paris Tech, Lille, France
M. Amberg, B. Lemaire-Semail
Université de Lille, Villeneuve d'Ascq, France

Abstract:
Among human senses, touch is much less understood than hearing or sight. However, today, new emerging technologies are placing tactile interaction at the heart of the communication with smart devices (smartphones, tablets, …). Hence, studying the sense of touch is now very important, in order to better understand the mechanisms induced from the mechanical excitation of skin to the feeling experienced by a user. Also, being able to detect and measure tactile disabilities, and to propose rehabilitation is a challenge; otherwise, numerous people can drift away from these objects as they can't be used easily by them.
In the paper, we present Dtact, a device which stimulates the finger pulp with a calibrated stimulation. It is designed to be used during experimental studies aiming at recording nerves and brain activity of a user touching its surface. It will be used to detect tactile disabilities, and perhaps some exercises could be programmed for the purpose of rehabilitation.

Keywords: Piezoelectricity, Tactile, Power Electronics

Introduction

Among human senses, touch is much less understood than hearing or sight. However, today, new emerging technologies are placing the tactile interaction at the heart of the communication with smart devices. Tablets, smartphones are now commonly used by people all around the world, and many human to computer interfaces use flat tactile display made of glass to the detriment of knobs and buttons which produce a physical interaction much more contrasted. Hence, studying the sense of touch is now very important, in order to better understand the mechanisms induced from the mechanical excitation of skin to the feeling experienced by a user. Also, being able to detect and measure tactile disabilities[1], and to propose rehabilitation is a challenge; otherwise, numerous people can drift away from these objects as they can't be used easily by them.
One can find many examples of tactile devices in the literature. For example, Variable Friction Devices use electrostatic forces [2] or Ultrasonic Vibrations [3] to modify friction between the fingertip and the touched surface. If the fingertip's position is measured, it is possible to modulate the friction in order to create the same lateral forces as those created when the finger touches a real rough surface [4]. These devices are now widely studied, and the contact mechanisms were finely described [5]. However, the tactile stimulation is very dependant with regards to the user and some external factors like the cleanness of the surface, the property of the user's skin,...[6] If a tactile stimulation can actually be provided to the users, the stimulation is not calibrated, and this alter the reliability of the studies.
In the paper, we present Dtact, a device which stimulates the finger pulp with a calibrated stimulation. It is designed to be used during experimental studies aiming at recording nerves and brain activity of a user touching its surface. It will be used to detect tactile disabilities, and perhaps some exercises could be programmed for the purpose of rehabilitation. To be efficient, the device needs to accurately present a calibrated stimulus to the user. Hence, the paper is organized as follows: first, we present Dtact, and the principle of the tactile stimulation, then we present the system and the control achieved to obtain a same stimulation from one user to the other. A conclusion is finally given.

Presentation of the Device

When a surface vibrates, the perception of its roughness is altered by vibrations. This phenomenon was firstly introduces by [7], and has been attributed to the squeeze film effect: the air trapped between the finger and the plate compresses and depresses at high frequency according to a non-linear polytropic transformation. Friction reduction results from this process. The authors have confirmed through a psychophysical study that their surfaces made of sand paper could be perceived more or less rough as the vibration amplitude increase. The device is built up with a plate actuated by two langevin transducers at its edges. Because the plate shows nodes of vibration, the feeling is not equal all over the device. To operate, the plate has to vibrate at a frequency

Excerpt only, page has been blanked!
A full pdf version in print quality is available here!

Novel Radial Locking Actuator with Magnetoactive Polymer

H. Böse, T. Gerlach
Fraunhofer ISC, Würzburg, Germany

Abstract:
A new magnetically switchable locking actuator based on magnetoactive polymers (MAP) is introduced. It contains two MAP rings between an inner shaft and an outer housing, rotatable with respect to each other, and a coil which generates the magnetic field. In the non-activated state without magnetic field, free rotation between the inner and outer components is possible. However, when the magnetic field is activated by a current in the coil, the MAP rings expand radially and clamp the inner and outer components of the actuator to each other. A demonstrator of the radial locking device was designed, the magnetic circuit was simulated and the device was manufactured and tested. The maximum locking torque in the activated state was measured as nearly 3 Nm and the minimum torque in the non-activated state was found to be negligible. Due to the radial expansion of the MAP rings and the corresponding uniform attachment to the inner shaft of the actuator, the clamping process is very smooth.

Keywords: Magnetorheological Elastomer (MRE), Magnetoactive Polymer (MAP), Radial Locking Actuator

Introduction

In many technical systems, a rotatable shaft has to be temporarily locked and unlocked for ongoing rotation. This can be achieved by mechanical means, where a bolt is pressed against the shaft, thereby blocking its rotation. If the locking has to be electrically controlled, an actuator pushes the bolt to the shaft or to a disk connected with the shaft. Usually, an electromagnetic actuator is used for this purpose. This linear actuator is rigid and the applied force acts from one side on the shaft. For the application of balanced forces from different directions on the shaft, several actuators around the shaft are necessary or the force from one actuator has to be distributed on the shaft by a sophisticated mechanical transmission mechanism, which requires much space.

An alternative would be a radial locking mechanism, where an actuator clamps the shaft uniformly around its circumference. Such clamping mechanism can be principally achieved with magnetically driven soft materials, which are known as magnetorheological elastomers (MRE). MRE are a class of relatively soft smart materials [1]. They consist of magnetic particles which are embedded in an elastomeric matrix [2, 3]. By applying a magnetic field, the composite material reversibly changes its mechanical properties, i. e. the Young's and the shear modulus. This magnetorheological effect is reversible and occurs within milliseconds in analogy to the behaviour of magnetorheological fluids (MRF).

If the elastomer matrix of the composite is sufficiently soft and the applied magnetic field is strong enough and inhomogeneous, the MRE material shows also an actuation effect [4]. In an inhomogeneous magnetic field the material is deformed or stretched and changes its shape or geometrical dimensions. In the following, MRE composites which reveal such an actuation effect are called magnetoactive polymers (MAP). This signification is analogous to electroactive polymers (EAP) which actuate in electric fields. A MAP body can be strongly deformed in the magnetic field. It was already demonstrated that deformations of about 10 % can be achieved [4].

Like EAP, flexible magnetoactive polymers are capable to perform more complex motions in a magnetic field than it is possible with rigid bodies. In contrast to a voice coil, in which a magnetic body moves linearly with respect to the coil, driven by a magnetic force, a ring-shaped MAP body can radially be deformed by a magnetic field, which is applied between concentrically arranged inner and outer yokes.

This radial deformation of MAP materials has already been shown to be useful for various applications. In [5] a valve mechanism was introduced, where the radial deformation of a MAP ring in a magnetic field controls the flow rate of an air flow. Moreover, the clamping effect of MAP rings can be used to realize an inchworm actuator which drives a rod over a principally unlimited distance [6]

The objective of this work is to present a switchable locking device which exploits the outstanding actuation capability of MAP materials for a radial clamping mechanism. After a short explanation of the locking mechanism, the magnetic circuit with the radial magnetic field distribution is described, followed by the actuator design, the construction

Multistable Pneumatic Valve Based on Magnetic Shape Memory Alloys

T. Schiepp, L. Riccardi, R. Schnetzler, M. Laufenberg
ETO MAGNETIC GmbH, Stockach, Germany

Abstract:
Magnetic Shape Memory (MSM) actuators represent a new type of smart electromagnetic actuators where an active material elongates and contracts under the application of a magnetic field or an external stress. The MSM material has the ability to change its size or shape very fast and many million times repeatedly. Based the internal friction, recognisable from the strain-stress hysteresis, this new material technology allows the design of mono-, bi-, and multistable actuators that offer energy efficient solutions. In this paper, we present an overview of the current state of the MAGNETOSHAPE® technology and its future impact on fluidic applications.

Keywords: MSM, Magnetic Shape Memory, Smart Materials, Pneumatics, Valve, Proportional, Control, Energy Efficiency, Multistability

Introduction

Typically, the Magnetic Shape Memory (MSM) material is a monocrystalline Ni-Mn-Ga alloy, which has the ability to change its size or shape very fast [1] and many million times repeatedly [2, 3]. Some alloys are known, which are able to achieve an outstanding magnetic field induced strain (MFIS) up to 12% [4]. Actuators based on such materials can be designed as multistable actuators with near-zero current consumption in any stable position. The phase transition temperature of the MSM material between the low temperature martensite and the high temperature austenite limits the application temperature in current alloys to about 60°C, but future improvements are expected [5]. So far, MSM alloys have not been tested for the production of proportional valves within pneumatic systems, despite their potential [6,7].
In this paper we introduce a prototype valve for airflow control based on MSM alloys. The electrically controllable deformation of the alloy is used to control the aperture of the valve and the airflow.

Multistable valve for airflow control

Briefly speaking, commercially available MSM alloys can produce deformation up to 6% and stress up to 3 MPa when excited by a magnetic field perpendicular to the direction of motion [6].
Fig. 1 shows a family of typical input-output curves of a magnetic shape memory alloy under different pre-stresses. The curves are measured by increasing the magnetic field perpendicular to the strain while keeping a constant stress parallel to the strain, acting against the magnetically induced stress (MFIS). At $\sigma = 0.1$ MPa (black) the external load is not sufficient to compress the MSM element after elongation. It is visible that the deformation remains at 6% even if the field is reduced to zero. When the external load is increased (red), the MSM is compressed to the initial state. The experiments emphasise that both stress and field have to overcome some threshold in order to start contraction or elongation. This threshold is due to the inner friction of the alloy, called twinning stress, which tends to stabilise the current deformation of the MSM element. The deformation is self-supporting as long as the external load or the MFIS does not exceed the twinning stress of the material. The self-supporting leads to the multistability of the MSM element, i.e. the capability of holding any deformation without magnetic excitation.

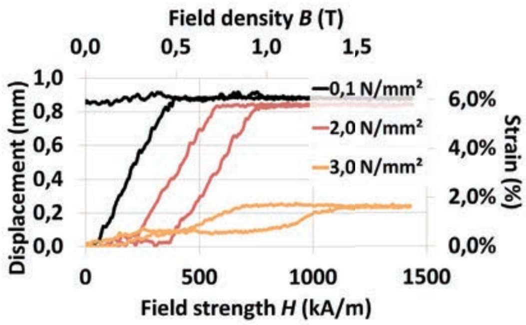

Fig. 1: Typical strain-field curves at different stress levels

An MSM-based valve that uses the multistability was designed by finite element analysis with state of the art MSM models [8]. The valve allows controlling the airflow between an inlet and an outlet. The basic idea is to exploit the elongation of the MSM element to open the valve and set the airflow, and the multistability to keep it open with low electrical power. The valve concept is sketched in Fig. 2, which shows the valve in the closed state, where the MSM element is compressed. The pressure p_L at the inlet works against the movement

Internal Stress Effects on Magnetostrictive Properties of Sputtered Giant Magnetostrictive Thin Films

S. Sakano, R. Toyoda, A.A.Y Mansi, T. Washihira, Y. Matsumura
Tokai University, Hiratsuka-shi, Japan

Abstract:
Internal stress of the Sm-Fe thin films was investigated considering ion bombardment. The Sm-Fe thin films were deposited by DC magnetron sputtering process with various substrate bias voltage. The effect of ion bombardment on internal stress of Sm-Fe thin films was estimated by the ion bombardment parameter P_i. The ion bombardment parameter P_i increased with increasing negative substrate voltage. Internal stress of Sm-Fe thin films showed a larger compressive stress with increasing amount of the ion bombardment parameter P_i. The magnetostrictive susceptibility of Sm-Fe thin films was improved by increasing compressive stress. The magnetostrictive susceptibility of the Sm-Fe thin film was dependent on the P_i.

Keywords: Sputtering, Ion Bombardment, Internal Stress, Magnetostrictive Thin Film

Introduction

Magnetostrictive properties of sputtered thin films are affected by a processing such as deposition conditions and an ion bombardment during sputter deposition. The influence of internal stress on the magnetostriction was investigated in sputtered films [1]. In previous study, Hoffman et al. reported that an impingement ratio (*i*/*a*); incident of ion and vapor particles on substrate was key factor on the internal stress of thin films [2]. On the other hand, Windischmann's reported the internal stress of a sputtered thin film depend on an ion energy [3]. In previously, we proposed an ion bombardment parameter P_i based on a magnitude of an ion momentum p_G^+ and an impingement ratio of gas ions to metal particles i_G^+/a_M. And we reported that internal stress and magnetostrictive properties of Ni thin films can be controlled with the ion bombardment parameter P_i [4, 5]. Up till now relatively few studies have been reported on effects of the internal stress caused by the ion bombardment on giant magnetostrictive thin films. In this study, effects of internal stress on magnetostrictive properties of giant magnetostrictive thin films were discussed.

Experiment

Film preparation

Sm-Fe thin films were prepared on n-type single-crystal silicon (5mm×25mm) by a dc magnetron sputtering process. The target to substrate distance was 60 mm. A chamber was evacuated below 3.0 x 10^{-4} Pa. Sputtering gases were using argon (Ar). A sputtering power was set at 60 W and the substrate temperature was kept at 373 ± 5 K. A substrate bias voltage was set at 0 to 120 V. The schematic diagram of the set-up for the Langmuir probe is shown in Fig.1.

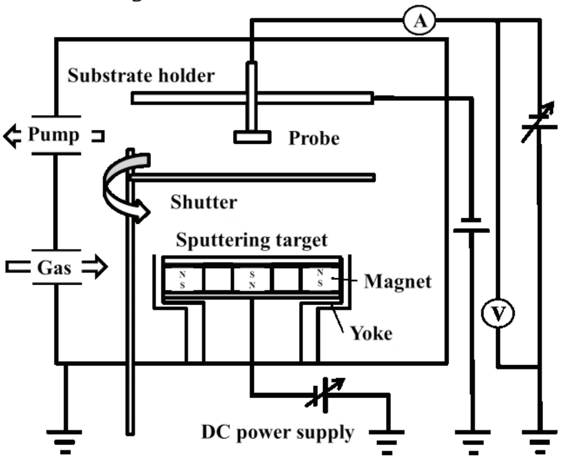

***Fig. 1**: Schematic diagram of the dc magnetron sputtering system with a single Langmuir probe.*

Sample analysis

The thickness of films was measured by stylus profilometer. Plasma diagnostics were carried out by using a single Langmuir probe during the sputtering. A plasma potential and a saturated ion current was measured by a single Langmuir probe.
The internal stress, σ was estimated by stoney's equation as follows [6].

$$\sigma = E_s t_s^2 / 3 t_f R(1 - \nu_s) \quad (1)$$

Subscript s and f mean substrate and film, E is Young's modulus, t is thickness, ν is Poisson's ratio and R is radius of the curvature.
The magnetostriction of the film sample was measured by using a cantilever method under applied magnetic fieldsand calculated by following formula. [7, 8]

Optimization of Cutting Processes for Magnetic Shape Memory Actuator Elements

A. Böhm, J. Schneider, W.-G. Drossel
Fraunhofer IWU, Dresden, Germany
E. Pagounis, M. Laufenberg
ETO MAGNETIC GmbH, Stockach, Germany

Abstract:
For the production of Ni-Mn-Ga single crystalline actuator elements dicing technology was applied. In the paper results are presented for the optimized fabrication of Ni-Mn-Ga single crystalline actuator elements using dicing temperature of 80°C. The surface of the single crystalline Ni-Mn-Ga actuator elements after the dicing process was investigated. A relation was found between processing parameters and quality of cutting edges. The results are discussed with respect to surface roughness, deformation layer and twinning behavior and will help to better understand the microstructure-property relationship of this new class of smart materials.

Keywords: Ni-Mn-Ga, Cutting, Actuator Elements, Surface Roughness, Microstructure

Introduction

The intermetallic compound Ni-Mn-Ga close to the stoichiometric composition Ni_2-Mn-Ga has drawn special attention due to the magnetic-field induced strain (MFIS) resulting from the easy twin boundary motion under the influence of a magnetic field. The magnetic shape memory alloys (MSM) are suitable for a large number of technological applications, including actuators or sensors [1-3]. Single crystalline rods can be fabricated with diameters between 20 to 60 mm and lengths of 110 to 200 mm by ETO MAGNETIC GmbH [4].
The basis for the processing sequence is the number of cutting steps for producing the actuator elements. For large cutting depths, which are typically between 20 and 60 mm, the technologies diamond wire cutting and water jet cutting were investigated [5]. The resulting roughness values have shown that generally rougher surfaces must be expected with higher cutting depths. On the other hand, dicing is suited for lower cutting depths between 1 and 5 mm [6]. Because of its high cutting speed the technology is suitable to produce very good surface qualities, but the magneto-mechanical properties are affected. Locally, a crack initiation was found along the cutting edge due to high cutting speed. The measured MFIS values are somewhat lower but of the same order of magnitude, compared to the wire electro-discharge machining (EDM) processing route [7]. EDM is the standard process to cut the single crystalline Ni-Mn-Ga material into actuator elements. Afterwards, Ni-Mn-Ga actuator elements are mechanically grinded and electro-polished. The benefit of EDM is the limited surface deformation. However, a disadvantage of this technology is the relatively low machining rate. So there is a high requirement to investigate alternative and cost-effective cutting processes for a large number of pieces.

In this paper, results will be presented for the optimized fabrication of Ni-Mn-Ga single crystalline actuator elements using flexible dicing machine at a temperature of 80°C. The results are discussed with respect to surface roughness, deformation layer and twinning behavior and will help to better understand the microstructure-property relationship of magnetic shape memory materials.

Experimental

The single crystalline Ni-Mn-Ga rods were produced using a Bridgman-type oven. The experimental details are described e.g. in [8] and [9].
The EDM technology is applied as a reference process to cut the single crystalline Ni-Mn-Ga material into actuator elements. A wire with a diameter of 250 µm was used for the tests.
A high-precision 5-axis micro machining center with small dicing-blade widths (200 µm and 600 µm) with a diameter of 58 mm was utilized for the dicing experiments. The quantitative determination of the surface roughness was performed by means of confocal microscopy.
Systematic investigations of the microstructure were carried out and the information on the twin morphology was obtained using optical microscopy. The grinding and polishing tests were realized with a system for the preparation of metallographic samples.

Results and Discussion

Dicing technology
In the first cutting step the single crystalline Ni-Mn-Ga rod is divided into appropriate slices. For the large cutting depth of 20 mm the EDM technology was used. In the second step actuator elements (sticks) are separated from the slice using dicing

Internal Stress Control for Magnetostrictive Thin Films by Substrate Bias

S. Miyata, R. Toyoda, M. Hashimoto, S. Sakano, T. Iijima, A. Tonegawa, Y. Matsumura
Tokai University, Hiratsuka-shi, Japan

Abstract:
Internal stress control is an important requirement for the magnetostrictive thin film used as thin film actuator. In this study, the ion bombardment parameter P_i was evaluated by substrate bias change during sputter deposition in order to control internal stress of the films. The P_i was determined by plasma diagnostics using Langmuir probe and ion energy analyzer. In the result, the compressive stress and magnetostrictive susceptibility of sputtered thin films were increased with the increasing of P_i. In conclusion, these results can be suggested that the evaluation of P_i could be highly advantage in designing thin film properties for actuator.

Keywords: Sputtering, Ion Bombardment, Internal Stress, Substrate Bias, Magnetostrictive, Multi Grid Electro Static Analyzer, Langmuir Probe, Argon, Plasma

Introduction

Characteristics of magnetostrictive thin films used in the thin film actuator change substantially depending on an internal stress of the films. Internal stress of films affected by deposition conditions and ion bombardment during sputter deposition. So internal stress control is an important requirement for magnetostrictive thin films used as the thin film actuator. In the existing studies, Hoffman et al. reported that the effect of ion bombardment on internal stress was influenced by the impingement ratio (*i*/*a*); incident of ion and vapor particles on substrate [1]. In addition, Windishmann reported internal stress of sputtered thin films depend on ion energy [2]. In previous research, it is clear that the internal stress of the thin film actuator could be estimate with ion bombardment parameter P_i [3]. In this study, we discuss about the ion bombardment parameter P_i which was evaluated by substrate bias change during sputter deposition in order to control internal stress and demonstrate the magnetostrictive susceptibility change in the thin films. In this study, the P_i was determined by plasma diagnostics using a Langmuir probe and an ion energy analyser. For controlling internal stress of magnetostrictive thin films, evaluating the ion bombardment parameter P_i with a substrate bias change during the sputter deposition was discussed.

Experiment

Film preparation

Thin film actuators were prepared by a D.C. magnetron sputtering process as shown in figure 1. A substrate was placed upward a sputtering target at a distance of 80 mm. The sputtering target was a Ni disc (99.9 mass%, diameter at 3”). A vacuum chamber was evacuated below 1.0 x 10^{-4} Pa. Ar gas (99.999% of purity) was introducing at 5.5x10^{-2} Pa. Substrate temperature was kept at 380 ± 15 K and the substrate bias of a ground potential had been applied for an experimental condition from −60 V to –120 V. An n-type single-crystal silicon (5mm ×25mm×0.28mm) was used as the substrate.

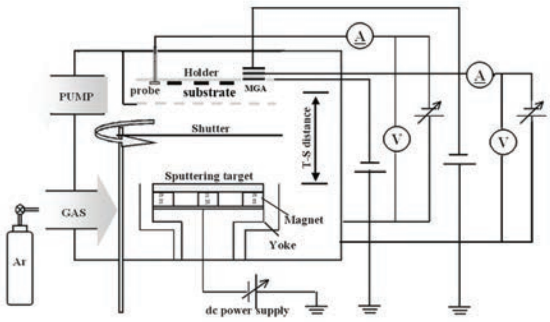

Fig.1: *Schematic diagram of the dc magnetron sputtering system.*

Sample analysis

A thickness of film samples was measured by a stylus profilometer. Internal stress of thin films and magnetostrictive characteristics of magnetostrictive thin films were measured by optical lever method with a curvature of substrate [4]. Internal stress of films were estimated by a stoney's equation [5] as tollows and was also based on results of a substrate curvature measurement.

$$\sigma = E_s t_s^{\,2} / 6(1-v_s)t_f R \qquad (1)$$

Subscript s and f represent substrate and film, *t* is thickness, *E* is Young's modulus, *v* is a Poisson's ratio and *R* is a radius of ecurvature on the film sample, where $R=l^2/2d$.

The magnetostriction of the film sample was calculated by following formula based on measurement of curvature of the film samples under applied magnetic fields by using a cantilever method[6].

$$\lambda = D t_s^{\,2} E_s (1+v_f) / 3 t_f l^2 E_f (1-v_s) \qquad (2)$$

Development of a Hand Rehabilitation Robot System for Range of Motion Exercises with Pneumatic Soft Actuators

H. Taniguchi, T. Meguro, S. Yamamoto, S. Araki, R. Kobiki
National Institute of Technology, Tsuyama-shi, Japan

Abstract:
This paper presents a hand rehabilitation robot system for range of motion (ROM) exercises. Many researchers have developed mechanical finger rehabilitation devices to improve movement disabilities. However, these devices are able to exercise only range of finger joint motion. We therefore have developed the finger rehabilitation robot system which provides not only the several ROM exercises such as flexion and extension movements but also to execute a massage therapy for the muscles of the hand and fingers. Firstly, we have developed a pneumatic soft actuator as the drive source of the device. This actuator has many advantages such as lightweight, flexibility, safety and with a high affinity for people. Basically, the finger rehabilitation is carried out for the thumb through to the little finger. Therefore, we have produced two types of hand rehabilitation robot systems for the index to little fingers and the thumb. In the experimental test, we measured the max ROM needed for finger joints. As the results, we confirmed that the robot is able to provide several ROM exercises.

Keywords: Pneumatic Soft Actuator, Rehabilitation Robot, ROM Exercises

Introduction

In Japan, there were 1.18 million patients from the cerebral vascular disease in 2014 [1]. The onset of a brain disease often causes impaired motor functions like partial paralysis. If the condition does not improve, contractures may occur in some joints and muscles. The contracture causes restricted range of motion in the joint. For example, contract around the joints of the finger makes a difficult to grip an object by oneself. Therefore, it is very important to start the rehabilitation therapy before developing the contracture. Normally, range of motion (ROM) exercise for finger joints is prescribed by an occupational therapist (OT) to prevent the joints contracture and improve the patient's symptoms. However, the patients cannot receive enough rehabilitation, because the time of therapy from the therapist is limited. In addition, the therapists will be generally less numerous than the patients; they will expect to increase workloads.

Over the past few years, many researchers have shown an interest in developing mechanical finger joints rehabilitation devices [2-5]. However, these devices are able to exercise only range of finger joint motion. In addition, they are complex in structure. Therefore, we have produced the several prototypes of hand rehabilitation robot with functions for multiple degrees of freedom ROM exercises [6,7]. Firstly, we proposed novel pneumatic soft actuator as the drive source of the robot system. This actuator has many advantages such as lightweight, flexibility, safety and with a high affinity for people. The system is more likely to be popular with users since safety is essential for them.

ROM Exercises and Muscle Stretching Exercise

The aim of this study is to propose a hand rehabilitation robot system to prevent contractures for finger joints. In general, an OT treats medically by ROM exercises. ROM exercises have several motions such as flexion, extension, abduction and adduction of the thumb and fingers. Flexion for fingers is divided into different types of motion as shown in Fig. 1[8]. “Claw” means that PIP and DIP joints are flexed and “Tabletop” means that only MP joint is flexed too. In addition, spreading fingers and arching a hand which move thumb closer to a little finger are included in ROM exercises.

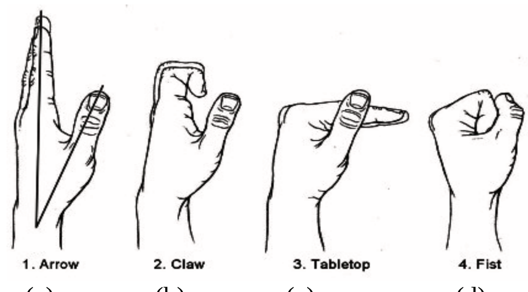

(a) (b) (c) (d)

Fig. 1: *Hand exercises which are (a) Arrow, (b) Claw, (c) Tabletop and (d) Fist motions.*

Before beginning these ROM exercises, an OT treats muscle stretching exercises such as kneading massage of the patient's muscles and compressing the hand to remove swelling. The purpose of muscle stretching is to remove patient tension and to

Design of a Balancing Device for Small High Speed Rotors

D. Pfeffer, F. Klug, H.F. Schlaak, P.P. Pott
Technische Universität Darmstadt, Darmstadt, Germany

Abstract:
An unbalance in high speed rotating machines leads to unwanted noise and vibration and thus to increased wear in bearings and higher friction losses. Therefore, it is desired to reduce the unbalance of the rotor to a well-defined amount, at which the radial forces and moments do not peril the intended life-time of the whole system. Taking an air-driven small-scale turbine as an exemplary application, a balancing device for small high speed rotors has been designed and characterized. The device is designed to allow rotational speeds up to 65 000 rpm. Based on dynamic force measurement using piezo-electric PZT stacks and digital lock-in-amplifiers, unbalance can be measured down to less than 1 mg·mm. In an iterative process, manual correction of the unbalance using a hand-operated rotary tool is verified and, if necessary, repeated. A key experiment shows, that an initial unbalance of 300 mg·mm can be reduced by a factor of more than 100, using the balancing device outlined above.

Keywords: Balancing, High Speed Rotor, Piezo-Stack, Unbalance, Lock-In-Amplifier

Introduction

A large variety of technical devices, particularly but not exclusively in medical applications, rely on high-speed rotating motors. It is desired to minimize the unbalance of the spinning rotors for the sake of efficiency and long life-time of all parts subject to wear and noise. The exemplary application of a centimetre-scale boundary layer turbine driven by pressurized air-flow was chosen as the basis for the layout of the presented balancing device.
Regarding small and fast rotating parts, that can be considered as rigid while rotating, a balancing device was set up to measure the amount of dynamic unbalance with respect to two freely definable geometric planes. The operating range is from 0 to 65 000 rpm for rotors with a maximum length of up to 50 mm and a diameter of up to 20 mm.

Methods

The following paragraphs will give a brief overview of the basics of balancing and the balancing situation of the exemplary application. Afterwards, the design of the balancing device is accurately described, followed by an operation breakdown of the balancing procedure.

Basics of Balancing Every mass element u on a radial position $\vec{r}$ on a rotor, spinning at angular velocity Ω, causes a centrifugal force $\vec{F}$ [1, 2]:

$$\vec{F} = \vec{U} \cdot \Omega^2 \quad \text{using } \vec{U} = u \cdot \vec{r} \tag{1}$$

The resultant static unbalance of the rotor is then defined as

$$\vec{U}_r = \sum_{i=1}^{n} \vec{U}_i. \tag{2}$$

When a rotor is perfectly statically balanced, $\vec{U}_r$ is equal to 0 g·mm. In case the rotor with its mass m exhibits unbalance, the centre of gravity concentricity $\vec{e}$ can be written as

$$\vec{e} = \frac{\vec{U}_r}{m}. \tag{3}$$

Besides the static unbalance, a resultant moment unbalance can occur, which can be written as a pair of unbalances $\vec{U}$ with opposite angular positions and an axial distance $\vec{l}$. Its resulting static unbalance is 0 g·mm, while the moment unbalance is

$$\vec{U}_\mathrm{m} = \vec{l} \times \vec{U}. \tag{4}$$

It causes a rotary moment

$$\vec{M}_\mathrm{u} = \vec{l} \cdot |\vec{U}| \cdot \Omega^2. \tag{5}$$

In DIN ISO 1940-1 [1] a generalized balancing quality G is defined from the related unbalance $\vec{e}_{rel}$ and the permissible residual unbalance $\vec{U}_p$:

$$G = \left|\frac{\vec{U}_p}{m}\right| \cdot \Omega = |\vec{e}_\mathrm{rel}| \cdot \Omega. \tag{6}$$

There are several balancing classes defined, regarding different applications [1]. For turbines, a class equal or lower than G2.5 is advised, meaning a trajectory velocity of the centre of gravity concentricity equal to or below 2.5 mm/s.

Analysis of the Rotor In the exemplary application, the rotating system consists of two main components, i.e. an EC13 BLDC motor/generator (Maxon Motor AG, Sachseln, CH) [3] providing a 3 mm diameter shaft and an assembled turbine rotor with a collet chuck, that attaches to the motor shaft (fig. 1).

MRI-Compatible Piezoelectric Actuator

Y. Bernard[1]*, R. Khairi[1], A. Razek[1], M. Poirier-Quinot[2], J-C. Ginefri[2], R-M. Dubuisson[2]
[1]GeePs, UMR 8507, CentraleSupelec, UPMC, Univ Paris-Sud,
11 rue Joliot-Curie, Gif Sur Yvette, France
[2]IR4M, UMR 8081, Univ Paris-Sud
Campus d'Orsay Bat 220, Orsay, France

Abstract:
The MRI employs an extreme static magnetic field (1-7 Tesla), gradient magnetic fields and electromagnetic radio frequency pulses. In this particular environment, classical electromagnetic actuators, generally based on ferromagnetic and conductor, cannot work correctly. The work is started with a numerical simulation. The MRI environment is presented using a finite element approach. Different piezoelectric materials and structures are then introduced into this environment to determine the optimal configuration. This work is completed with an experimental validation using a standard hospital MRI (static field of 1.5 T and radio frequency field of 63.9 MHz). Finally, the simulation and experiment results are used to give some recommendations in the design of MRI-compatible piezoelectric actuator.

Keywords: MRI, Piezoelectric, Actuator, Electromagnetic Compatibility.

I. Introduction

Piezoelectric devices are or will be widely used in Magnetic resonance imaging (MRI) devices. The first reason is that those piezoelectric devices can be embedded in human body [1], the second is that the piezoelectric devices are compatible with this MRI environment and can be used for surgical robots or manipulators. Hence, they can be used to perform mechatronics systems for image-guided interventions and rehabilitation [2].

In the case of using piezoelectric devices in MRI environment, many aspects have to be controlled. The device introduced in MRI equipment can be accelerated by magnetic forces, or be damaged by magnetic field but also the device can reduce the image performances.
Usually, when verifying MRI, authors compare a phantom image with and without piezomotor [3]. In this case, the information is how far has to be the motor from the field of view (FOV) that the volume observed by MRI.

In this study, we developed a finite element modelling (FEM) to predict the effect of piezo material presence in MRI environment (part. II). The model has been experimentally validated. Then, we used this model to give some recommendations on how to use such material with the lower impact on image performances (part III). Finally, validating these design orientations, we observed a new effect of piezo material that has to be taken into account.

II. MRI Environment

Principle description

The MRI equipment used for this study is a 1.5T one (fig. 1). This static field is used to align the magnetization vectors of hydrogen atoms constituting the volume that has to be observed (phantom). Once aligned, the atoms are excited by a radio frequency (RF) field to switch them from there equilibrium position. The signal measured (giving information on the homogeneity of the phantom) is the magnetic field emitted while they go back to initial position [4].

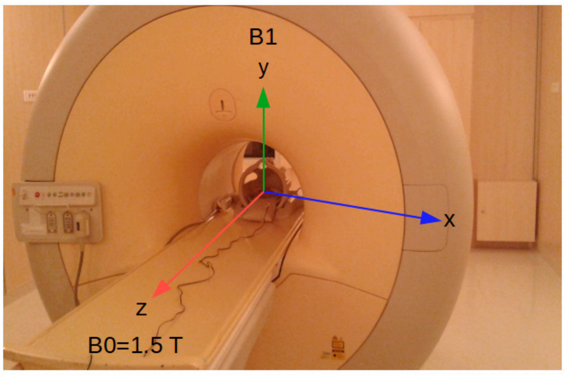

Fig. 1: *MRI device used*

As the frequencies of both magnetic fields used are far one from the other, it is possible to consider each separately from a modelling point of view.

Modelling

The simulation is realized using the commercial software Comsol Multiphysics. The static field B0 is calculated and it is verified that in a specific place (field of view) this field is homogeneous (fig. 2). Once done, the antenna used to create and to receive the RF field B1 is modelled.

List of Authors

A

Aaltio, I., Aalto University, Espoo, Finland · 124
Abbink, D.A., Delft University of Technology, Delft, The Netherlands · 491
Acosta, M., Technische Universität Darmstadt, Darmstadt, Germany · 52
Alaluf, D., Université Libre de Bruxelles, Brussels, Belgium · 232
Allevato, G., Technische Universität Darmstadt, Darmstadt, Germany · 171
Amberg, M., Université de Lille, Villeneuve d'Ascq, France · 375, 466, 569
Andersen, B., Noliac A/S, Kvistgaard, Denmark · 427
Araki, S., National Institute of Technology, Tsuyama-shi, Japan · 591
Ayvazov, K., Fraunhofer IPA, Mannheim, Germany · 163

B

Bachmaier, G., Siemens AG, München, Germany · 224
Bansal, A., The Pennsylvania State University, University Park, USA · 60
Bansevicius, R., Kaunas University of Technology, Kaunas, Lithuania · 483
Bareikis, R., Lithuanian University of Educational Sciences, Vilnius, Lithuania · 414
Barillot, F., Cedrat Technologies SA, Meylan, France · 86, 221, 439, 463
Barraja, M., Cedrat Technologies SA, Meylan, France · 221
Bartenschlager, M., Technische Universität Darmstadt, Darmstadt, Germany · 171
Basler, H., Technische Universität Dresden, Dresden, Germany · 499
Bastaits, R., Université Libre de Bruxelles, Brussels, Belgium · 232
Baudart, F., Université Catholique de Louvain, Louvain-la-Neuve, Belgium · 487
Belly, C., Cedrat Technologies SA, Meylan, France · 221, 259, 439, 463, 542
Benichou, I., Technion - Israel Institute of Technology, Haifa, Israel · 104
Bernard, Y., Génie Electrique et Electronique de Paris, Gif-sur-Yvette, France · 435
Bernard, Y., Génie Electrique et Electronique de Paris, Gif-sur-Yvette, France, and Polytech Paris Sud, Paris, France · 459
Bernard, Y., Université Paris Sud, Gif-sur-Yvette, France · 600
Berthier, Y., LaMCoS UMR 5259, Villeurbanne, France · 221
Bilz, J., Technische Universität Darmstadt, Darmstadt, Germany · 294
Binz, H., Universität Stuttgart, Stuttgart, Germany · 270
Bissal, A., ABB Corporate Research, Västerås, Sweden · 402
Bochmann, H., Hochschule Ostwestfalen-Lippe, Lemgo, Germany · 200, 278
Bödrich, T., Technische Universität Dresden, Dresden, Germany · 371, 495, 499
Böhm, A., Fraunhofer IWU, Dresden, Germany · 584
Borghesan, G., Katholieke Universiteit Leuven, Leuven, Belgium · 192
Borodinas, S., Lithuanian University of Educational Sciences, Vilnius, Lithuania · 410, 414
Böse, H., Fraunhofer ISC, Würzburg, Germany · 290, 294, 573
Bott, K., Afag GmbH, Amberg, Germany · 245
Bouchet, C., Cedrat Technologies SA, Meylan, France · 143, 259, 547
Brandt, D.R.J., Technische Universität Darmstadt, Darmstadt, Germany · 52
Bruns, R., Helmut Schmidt Universität, Hamburg, Germany · 565
Buhr, S., Technische Universität München, München, Germany · 77
Burda, I., Babes Bolyai University, Cluj-Napoca, Romania · 232
Buß, R., Sensitec GmbH, Lahnau, Germany · 479
Busse-Grawitz, M.E., maxon advanced robotics and systems, Giswil, Switzerland · 361
Butz, J., Technische Universität Darmstadt, Darmstadt, Germany · 171

C

Cao, J., National University of Singapore, Singapore, and Beijing Institute of Technology, Beijing, China · 443
Chee, S.K., Mechano Transformer Corporation, Chiyoda-ku, Japan · 255
Chida, R., Saitama University, Saitama-shi, Japan · 82
Chino, S., Saitama University, Saitama-shi, Japan · 82
Choffat, A., ONERA, Lille, France · 259
Choi, M., The Pennsylvania State University, University Park, USA · 60
Choi, S.-B., Inha University, Incheon, South Korea · 218
Christmann, M., Airbus Group Innovation, Ottobrunn, Germany · 270

Cianchetti, M., Scuola Superiore Sant'Anna, Pontedera, Italy · · · 557
Claeyssen, F., Cedrat Technologies SA, Meylan, France · · · 86, 259, 542
Coda, A., SAES Getters S.p.A., Lainate, Italy · · · 309
Comella, L.M., Fraunhofer IPA, Mannheim, Germany · · · 163
Cugat, O., Université Grenoble Alpes, Grenoble, France, and CNRS, Grenoble, France · · · 127
Cuntz, T., Fraunhofer IPA, Mannheim, Germany · · · 163
Cuschieri, A., University of Dundee, Dundee, United Kingdom · · · 167, 321
Czechowicz, A., Forschungsgemeinschaft Werkzeuge und Werkstoffe e.V., Remscheid, Germany · · · 313, 518

D

Dandois, J., ONERA, Lille, France · · · 259
Daniel, L., Génie Electrique et Electronique de Paris, Gif-sur-Yvette, France, and Université Paris Sud, Paris, France · 459
Dario, P., Scuola Superiore Sant'Anna, Pontedera, Italy · · · 557
Debray, J., Institut NEEL, Grenoble, France, and CNRS Institut Néel, Grenoble, France · · · 127
Dehez, B., Université Catholique de Louvain, Louvain-la-Neuve, Belgium · · · 487
Denkena, B., Leibniz Universität Hannover, Garbsen, Germany · · · 236, 552
Deprest, J., University Hospitals Leuven, Leuven, Belgium · · · 192
Diermeier, A., Ostbayerische Technische Hochschule Regensburg, Regensburg, Germany · · · 286
Dittrich, L., Technische Universität Ilmenau, Ilmenau, Germany · · · 327
Domenici, V., Università degli Studi di Pisa, Pisa, Italy · · · 507
Dörbaum, M., Leibniz Universität Hannover, Hannover, Germany · · · 398
Dressler, L., Technische Universität Ilmenau, Ilmenau, Germany · · · 327
Drossel, W.-G., Fraunhofer IWU, Chemnitz, Germany · · · 584
Drukteiniene, A., Siauliai University, Siauliai, Lithuania · · · 483
Dubois, F., Cedrat Technologies SA, Meylan, France, and LaMCoS UMR 5259, Villeurbanne, France · · · 221
Dubuisson, R.-M., Université Paris Sud, Orsay, France · · · 600
Dültgen, P., Forschungsgemeinschaft Werkzeuge und Werkstoffe e.V., Remscheid, Germany · · · 313, 518

E

Eck, L., CEA LIST, Gif-Sur-Yvette, France · · · 349
Ehle, F., Fraunhofer IKTS, Dresden, Germany · · · 105
Ehrlich, J., Fraunhofer ISC, Würzburg, Germany · · · 290
El Khoury, M., Technische Universität Darmstadt, Darmstadt, Germany · · · 336
Engdahl, G., KTH Royal Institute of Technology, Stockholm, Sweden · · · 402

F

Faran, E., Technion - Israel Institute of Technology, Haifa, Israel · · · 104
Fillot, F., CEA LETI, Grenoble, France, and Université Grenoble Alpes, Grenoble, France · · · 127
Folgheraiter, M., Nazarbayev University, Astana, Kazakhstan · · · 503
Fournier, M., Cedrat Technologies SA, Meylan, France · · · 259, 542, 547
Fumagalli, L., SAES Getters S.p.A., Lainate, Italy · · · 309
Furushiro, N., Kansai University, Suita-shi, Japan · · · 241

G

Gallas, Q., ONERA, Lille, France · · · 259
Gang, H.G., Kumoh National Institute of Technology, Gumi-si, South Korea · · · 188
Ganor, Y., Philips Health Systems, Andover, USA · · · 113
Gassmann, S., Jade Hochschule, Wilhelmshaven, Germany · · · 471
Ge, Y., Aalto University, Espoo, Finland · · · 124
Gebhardt, S., Fraunhofer IKTS, Dresden, Germany · · · 69
Genderjahn, R., ContiTech Vibration Control GmbH, Hannover, Germany · · · 135
Geoffroy, O., CNRS Louis Néel, Grenoble, France · · · 127
Gerlach, T., Fraunhofer ISC, Würzburg, Germany · · · 573
Gimeno, L., Université Grenoble Alpes, Grenoble, France, and CNRS, Grenoble, France · · · 127
Ginefri, J.-C., Université Paris Sud, Orsay, France · · · 600
Giraud, F., Université de Lille, Villeneuve d'Ascq, France · · · 375, 466, 569
Giraud-Audine, C., Arts et Métiers Paris Tech, Lille, France · · · 375, 466, 569
Givli, S., Technion - Israel Institute of Technology, Haifa, Israel · · · 104
Glöß, R., Physik Instrumente (PI) GmbH & Co. KG, Karlsruhe, Germany · · · 396
Goergen, Y., ZeMA gGmbH, Saarbrücken, Germany, and Universität des Saarlandes, Saarbrücken, Germany · · · 522
Goj, B., Technische Universität Ilmenau, Ilmenau, Germany · · · 327
Gołdasz, J., BWI Group, Krakow, Poland · · · 344

Grasso, E., Universität des Saarlandes, Saarbrücken, Germany · · · 534, 538
Groen, W.A., Delft University of Technology, Delft, The Netherlands,
and TNO Holst Centre, Eindhoven, The Netherlands · · · 204
Gruijthuijsen, C., Katholieke Universiteit Leuven, Leuven, Belgium · · · 192
Gualandris, S., Technosprings Italia srl, Besnate, Italy · · · 551
Gültig, M., Karlsruher Institut für Technologie, Karlsruhe, Germany · · · 340
Gurka, M., Institut für Verbundwerkstoffe GmbH, Kaiserslautern, Germany · · · 266

H

Hafez, M., CEA LIST, Gif-Sur-Yvette, France · · · 349
Hamada, Y., JAXA, Mitaka-shi, Japan · · · 255
Han, C., Inha University, Incheon, South Korea · · · 218
Hanaki, T., Saitama University, Saitama-shi, Japan · · · 561
Hanemann, T., Karlsruher Institut für Technologie, Karlsruhe, Germany · · · 340
Hannula, S.-P., Aalto University, Espoo, Finland · · · 124
Hara, M., Saitama University, Saitama-shi, Japan · · · 561
Harmouch, K., Génie Electrique et Electronique de Paris, Gif-sur-Yvette, France · · · 459
Hartmann, W., Fraunhofer ISC, Würzburg, Germany · · · 290
Hashimoto, M., Tokai University, Hiratsuka-shi, Japan · · · 588
Hassan, T., Scuola Superiore Sant'Anna, Pontedera, Italy · · · 557
Hatzfeld, C., Technische Universität Darmstadt, Darmstadt, Germany · · · 294
Hau, S., Universität des Saarlandes, Saarbrücken, Germany · · · 282, 514
Hegger, C., Hochschule Ostwestfalen-Lippe, Lemgo, Germany · · · 357
Helmer, M., ETO MAGNETIC, Stockach, Germany · · · 120
Hill, M., Universität des Saarlandes, Saarbrücken, Germany · · · 510
Hirai, T., Shinshu University, Ueda-shi, Japan · · · 299
Hirooka, D., Kansai University, Suita-shi, Japan · · · 241
Hoffmann, M., Technische Universität Ilmenau, Ilmenau, Germany · · · 327
Hoffstadt, T., Hochschule Ostwestfalen-Lippe, Lemgo, Germany · · · 278, 381
Hofmann, V., Leibniz Universität Hannover, Hannover, Germany · · · 196
Hohlfeld, K., Technische Universität Dresden, Dresden, Germany · · · 69
Horodinca, M., Technical University Gheorghe Asachi, Iasi, Romania · · · 232
Huan, Y., University of Dundee, Dundee, United Kingdom · · · 321
Huang, H., Berner Fachhochschule, Biel, Switzerland,
and Ecole Polytechnique Fédérale de Lausanne, Neuchâtel, Switzerland · · · 175
Hübler, M., Institut für Verbundwerkstoffe GmbH, Kaiserslautern, Germany · · · 266
Huimasalo, J., Elektroniikan 3K-tehdas, Savonlinna, Finland · · · 131

I

Iijima, T., Tokai University, Hiratsuka-shi, Japan · · · 588
Ille, I., Leibniz Universität Hannover, Hannover, Germany · · · 236
Inoue, A., ER-tec Co., Minoh-shi, Japan · · · 530
Isermann, J., Helmut Schmidt Universität, Hamburg, Germany · · · 565
Ishino, Y., Saitama University, Saitama-shi, Japan · · · 82, 561
Issindou, V., CEA LETI, Grenoble, France · · · 127

J

Jackel, M., Fraunhofer LBF, Darmstadt, Germany · · · 354
James, R., University of Minnesota, Minneapolis, USA · · · 113
Javaux, A., Katholieke Universiteit Leuven, Leuven, Belgium · · · 192
Jurenas, V., Kaunas University of Technology, Kaunas, Lithuania · · · 483

K

Kahrs, L.A., Leibniz Universität Hannover, Hannover, Germany · · · 159
Kalysheva, A., Nazarbayev University, Astana, Kazakhstan · · · 503
Kamimura, R., Saitama University, Saitama-shi, Japan · · · 561
Kanda, T., Okayama University, Okayama-shi, Japan · · · 241, 332, 447
Kanner, O., Yale University, New Haven, USA · · · 113
Karkosch, H.-J., ContiTech Vibration Control GmbH, Hannover, Germany · · · 135
Kasperoviciene, J., Nature Research Center, Vilnius, Lithuania · · · 414
Kawasaki, S.-I., National Institute of Advanced Industrial Science and Technology, Sendai-shi, Japan · · · 447
Kelly, D., ASRC Federal Corp., Beltsville, USA · · · 475

Kessel, R., Fraunhofer IPA, Mannheim, Germany · · · 163
Khairi, R., Université Paris Sud, Gif-sur-Yvette, France · · · 600
Khan, H., University of Dundee, Dundee, United Kingdom · · · 167, 321
Kim, W.H., Inha University, Incheon, South Korea · · · 218
Kimura, Y., Osaka University Hospital, Suita-shi, Japan · · · 530
Kintscher, M., Deutsches Zentrum für Luft- und Raumfahrt (DLR), Braunschweig, Germany · · · 249
Kloepfer, J., Fraunhofer LBF, Darmstadt, Germany · · · 354
Klug, F., Technische Universität Darmstadt, Darmstadt, Germany · · · 596
Kobiki, N., JAXA, Mitaka-shi, Japan · · · 255
Kobiki, R., National Institute of Technology, Tsuyama-shi, Japan · · · 591
Koc, B., Physik Instrumente (PI) GmbH & Co. KG, Karlsruhe, Germany · · · 214
Koch, V.M., Berner Fachhochschule, Biel, Switzerland · · · 175
Kohl, M., Karlsruher Institut für Technologie, Karlsruhe, Germany · · · 340
Köllnberger, A., Wacker Chemie AG, Burghausen, Germany · · · 274
König, N., Universität des Saarlandes, Saarbrücken, Germany · · · 534
Koruza, J., Technische Universität Darmstadt, Darmstadt, Germany · · · 52
Kotlarski, J., Leibniz Universität Hannover, Hannover, Germany · · · 398
Kovalev, S., Technische Hochschule Mittelhessen, Friedberg, Germany · · · 392
Koyanagi, K., Toyama Prefectural University, Imizu-shi, Japan · · · 530
Koyanagi, M., Osaka Electro-Communication University, Shijonawate-shi, Japan · · · 530
Kulvietis, G., Vilnius Gediminas Technical University, Vilnius, Lithuania · · · 483
Kunze, J., ZeMA gGmbH, Saarbrücken, Germany, and Universität des Saarlandes, Saarbrücken, Germany · · · 526
Kupnik, M., Technische Universität Darmstadt, Darmstadt, Germany · · · 294
Kutyrev, A., University of Maryland, College Park, USA · · · 475

L

Lahdo, M., Technische Hochschule Mittelhessen, Friedberg, Germany · · · 392
Laschi, C., Scuola Superiore Sant'Anna, Pontedera, Italy · · · 557
Laufenberg, M., ETO MAGNETIC GmbH, Stockach, Germany · · · 120, 577, 584
Lehtonen, J., Aalto University, Espoo, Finland · · · 124
Lemaire-Semail, B., Université de Lille, Villeneuve d'Ascq, France · · · 375, 466, 569
Lemke, F., Albert-Ludwigs-Universität Freiburg, Freiburg, Germany · · · 228
Leroy, E., CEA LIST, Gif-sur-Yvette, France · · · 349
Li, C.D., Shanghai University, Shanghai, China · · · 455
Li, M., NASA Goddard Space Flight Center, Greenbelt, USA · · · 475
Li, T., Berner Fachhochschule, Biel, Switzerland · · · 175
Lienig, J., Technische Universität Dresden, Dresden, Germany · · · 371, 495, 499
Lindner, G., Hochschule Coburg, Coburg, Germany · · · 451
Listmann, K.D., Listmann, ABB AG, Ladenburg, Germany · · · 364
Liu, L., National University of Singapore, Singapore · · · 443
Lötters, J.C., Bronkhorst High-Tech B.V., Ruurlo, The Netherlands,
and University of Twente, Enschede, The Netherlands · · · 326
Loussert, G., Moving Magnet Technologies SA, Besançon, France · · · 139
Lucinskis, R., Noliac A/S, Kvistgaard, Denmark · · · 73

M

Maas, J., Hochschule Ostwestfalen-Lippe, Lemgo, Germany · · · 200, 278, 357, 381
Magnusson, J., KTH Royal Institute of Technology, Stockholm, Sweden · · · 402
Maier, H., Leibniz Universität Hannover, Garbsen, Germany · · · 303
Maier, M., ETO MAGNETIC, Stockach, Germany · · · 120
Majzoubi, M., The Pennsylvania State University, University Park, USA · · · 60
Manfredi, L., University of Dundee, Dundee, United Kingdom · · · 167, 321
Mangeot, C., Noliac A/S, Kvistgaard, Denmark · · · 56, 73, 427, 431, 466
Mansi, A.A.Y , Tokai University, Hiratsuka-shi, Japan · · · 109, 581
Marienfeld, P.M., ContiTech Vibration Control GmbH, Hannover, Germany · · · 135
Martic, G., Belgian Ceramic Research Centre, Mons, Belgium · · · 232
Martin, D., maxon advanced robotics and systems, Giswil, Switzerland · · · 361
Mashimo, T., Toyohashi University of Technology, Toyohashi-shi, Japan · · · 210
Masuta, H., Toyama Prefectural University, Imizu-shi, Japan · · · 530
Matsumura, Y., Tokai University, Hiratsuka-shi, Japan · · · 109, 581, 588
Matthias, M., Fraunhofer LBF, Darmstadt, Germany · · · 354
Mazeika, D., Vilnius Gediminas Technical University, Vilnius, Lithuania · · · 410

Mazzolai, B., Istituto Italiano di Tecnologia, Pontedera, Italy · · · 557
Megnin, C., Albert-Ludwigs-Universität Freiburg, Freiburg, Germany · · · 340
Meguro, T., National Institute of Technology, Tsuyama-shi, Japan · · · 591
Meneroud, P., Cedrat Technologies SA, Meylan, France · · · 143
Meng, G., Shanghai Jiao Tong University, Shanghai, China · · · 114
Merl, D., Universität des Saarlandes, Saarbrücken, Germany · · · 534
Mešan, I., Afag GmbH, Amberg, Germany · · · 245
Michaelis, A., Technische Universität Dresden, Dresden, Germany, and Fraunhofer IKTS, Dresden, Germany · · · 69
Mikułowski, G., Institute of Fundamental Technological Research, Warsaw, Poland · · · 542
Milavec, J., Jožef Stefan Institute, Ljubljana, Slovenia · · · 507
Miranda, M.L., Carl von Ossietzky-Universität Oldenburg, Wilhelmshaven, Germany · · · 471
Misol, M., Deutsches Zentrum für Luft- und Raumfahrt (DLR), Braunschweig, Germany · · · 249
Miyake, S., Okayama University, Okayama-shi, Japan · · · 447
Miyake, S., The University of Tokyo, Kashiwa-shi, Japan · · · 419
Miyata, S., Tokai University, Hiratsuka-shi, Japan · · · 588
Mizuno, T., Saitama University, Saitama-shi, Japan · · · 82, 561
Monkman, G.J., Ostbayerische Technische Hochschule Regensburg, Regensburg, Germany · · · 286
Monner, H.P., Deutsches Zentrum für Luft- und Raumfahrt (DLR), Braunschweig, Germany · · · 148, 249
Mori, K., Okayama University, Okayama-shi, Japan · · · 332
Morita, T., The University of Tokyo, Kashiwa-shi, Japan · · · 91, 419, 423
Moseley, S., NASA Goddard Space Flight Center, Greenbelt, USA · · · 475
Motoyoshi, T., Toyama Prefectural University, Imizu-shi, Japan · · · 530
Motzki, P., ZeMA gGmbH, Saarbrücken, Germany,
and Universität des Saarlandes, Saarbrücken, Germany · · · 317, 522, 526
Müller, C., Technische Universität München, München, Germany · · · 77
Müllner, P., Boise State University, Boise, USA · · · 95
Münzing, T., Universität Stuttgart, Stuttgart, Germany · · · 270
Musiienko, D., Lappeenranta University of Technology, Savonlinna, Finland · · · 101, 131

N

Nakic, C., Technische Universität Darmstadt, Darmstadt, Germany · · · 336
Neubert, H., Fraunhofer IKTS, Dresden, Germany · · · 105
Neumeister, P., Fraunhofer IKTS, Dresden, Germany · · · 69, 105
Nienhaus, M., Universität des Saarlandes, Saarbrücken, Germany · · · 385, 534, 538
Nilsén, F., Aalto University, Espoo, Finland · · · 124
Nissle, S., Institut für Verbundwerkstoffe GmbH, Kaiserslautern, Germany · · · 266
Niu, M., Shanghai Jiao Tong University, Shanghai, China · · · 114
Niyomwaitaya, C., Tokai University, Hiratsuka-shi, Japan · · · 109

O

Ofuji, S., Okayama University, Okayama-shi, Japan · · · 447
Oh, L., SGT Inc., Greenbelt, USA · · · 475
Orefice, P.-H., CEA LIST, Gif-sur-Yvette, France · · · 349
Ortmaier, T., Leibniz Universität Hannover, Hannover, Germany · · · 398
Oshima, T., Toyama Prefectural University, Imizu-shi, Japan · · · 530
Ossmer, H., Karlsruher Institut für Technologie, Karlsruhe, Germany · · · 340
Ourselin, S., University College London, London, United Kingdom · · · 192

P

Pages, A., Cedrat Technologies SA, Meylan, France · · · 86, 143
Pagounis, E., ETO MAGNETIC GmbH, Stockach, Germany · · · 95, 584
Peng, Y., National University of Singapore, Singapore · · · 443
Perret, J., Haption, Lavalle, France · · · 192
Pertsch, P., PI Ceramic GmbH, Lederhose, Germany · · · 204
Petiniot, J.-L., ONERA, Lille, France · · · 547
Pfeffer, D., Technische Universität Darmstadt, Darmstadt, Germany · · · 596
Pittini, R., maxon motor ag, Sachseln, Switzerland · · · 361
Pohl, M., Deutsches Zentrum für Luft- und Raumfahrt (DLR), Braunschweig, Germany · · · 148
Poirier-Quinot, M., Université Paris Sud, Orsay, France · · · 600
Ponick, B., Leibniz Universität Hannover, Hannover, Germany · · · 398
Porchez, T., Cedrat Technologies SA, Meylan, France · · · 221, 439, 542, 547
Pott, P.P., Technische Universität Darmstadt, Darmstadt, Germany · · · 171, 596

Preumont, A., Université Libre de Bruxelles, Brussels, Belgium · · · 134, 232
Pruvost, M., ONERA, Lille, France · · · 259
Puchhammer, G., Karl Rejlek GmbH, Wien, Austria · · · 406

R

Rachor, B., HEMA Maschinen und Apparateschutz GmbH & Co. KG, Seligenstadt, Germany · · · 313
Ragonet, M., ONERA, Lille, France · · · 547
Razek, A., Université Paris Sud, Gif-sur-Yvette, France · · · 600
Rechel, M., Leibniz Universität Hannover, Garbsen, Germany · · · 196
Reiners, J., Leibniz Universität Hannover, Garbsen, Germany · · · 236
Rešetič, A., Jožef Stefan Institute, Ljubljana, Slovenia,
and Jožef Stefan International Postgraduate School, Ljubljana, Slovenia · · · 507
Reynaerts, D., Katholieke Universiteit Leuven, Leuven, Belgium · · · 192
Riccardi, L., ETO MAGNETIC, Stockach, Germany · · · 120, 577
Riemenschneider, J., Deutsches Zentrum für Luft- und Raumfahrt (DLR), Braunschweig, Germany · · · 249
Rizzello, G., Universität des Saarlandes, Saarbrücken, Germany · · · 510
Rödel, J., Technische Universität Darmstadt, Darmstadt, Germany · · · 52
Rojas, V., Technische Universität Darmstadt, Darmstadt, Germany · · · 52
Rosul, B., Technische Universität Dresden, Dresden, Germany · · · 495
Rowe, S., Cedrat Technologies SA, Meylan, France · · · 86

S

Safour, S., Génie Electrique et Electronique de Paris, Gif-sur-Yvette, France · · · 435
Saitoh, K., JAXA, Mitaka-shi, Japan · · · 255
Sakai, A., Tokai University, Hiratsuka-shi, Japan · · · 109
Sakano, S., Tokai University, Hiratsuka-shi, Japan · · · 581, 588
Saren, A., Lappeenranta University of Technology, Savonlinna, Finland · · · 101, 131
Saulot, A., LaMCoS UMR 5259, Villeurbanne, France · · · 221
Schiepp, T., ETO MAGNETIC, Stockach, Germany · · · 120, 577
Schlaak, H.F., Technische Universität Darmstadt, Darmstadt, Germany · · · 171, 274, 336, 596
Schmid, R., ETO MAGNETIC, Stockach, Germany · · · 120
Schmidt, D., Deutsches Zentrum für Luft- und Raumfahrt (DLR), Braunschweig, Germany · · · 249
Schmitt, P., Technische Universität Darmstadt, Darmstadt, Germany · · · 171
Schneider, J., Fraunhofer IWU, Chemnitz, Germany · · · 584
Schnetzler, R., ETO MAGNETIC, Stockach, Germany · · · 577
Schorsch, J.F., Delft University of Technology, Delft, The Netherlands · · · 491
Schreiber, P., Leibniz Universität Hannover, Garbsen, Germany · · · 552
Schütte, H., Jade Hochschule, Wilhelmshaven, Germany · · · 471
Schwesinger, N., Technische Universität München, München, Germany · · · 77
Seelecke, S., Universität des Saarlandes, Saarbrücken, Germany · · · 282, 510, 514
Seelecke, S., ZeMA gGmbH, Saarbrücken, Germany,
and Universität des Saarlandes, Saarbrücken, Germany · · · 317, 522, 526
Seemann, S., Airbus Group Innovation, Ottobrunn, Germany · · · 270
Seyfert, L., Technische Universität München, München, Germany · · · 77
Shekhani, H., The Pennsylvania State University, University Park, USA · · · 60
Sheng, J., University of Minnesota, Minneapolis, USA · · · 113
Shi, W., Harbin Institute of Technology, Harbin, China · · · 60
Shilo, D., Technion - Israel Institute of Technology, Haifa, Israel · · · 104, 113
Sindersberger, D., Ostbayerische Technische Hochschule Regensburg, Regensburg, Germany · · · 286
Slatter, R., Sensitec GmbH, Lahnau, Germany · · · 479
Sohn, J.W., Kumoh National Institute of Technology, Gumi-si, South Korea · · · 188
Sosnicki, O., Cedrat Technologies SA, Meylan, France · · · 547
Sparr, M., KTH Royal Institute of Technology, Stockholm, Sweden · · · 402
Stock, M., Technische Universität Dresden, Dresden, Germany · · · 371, 495
Stortiero, F., Technosprings Italia srl, Besnate, Italy · · · 551
Stoyanov, D., University College London, London, United Kingdom · · · 192
Ströhla, T., Technische Universität Ilmenau, Ilmenau, Germany · · · 392
Struckas, A., Lithuanian University of Educational Sciences, Vilnius, Lithuania · · · 414
Stürmer, M., Albert-Ludwigs-Universität Freiburg, Freiburg, Germany · · · 65, 228
Sun, Q., Technische Universität Dresden, Dresden, Germany · · · 499
Suzumori, K., Tokyo Institute of Technology, Tokyo, Japan · · · 241, 332

T

Takasaki, M., Saitama University, Saitama-shi, Japan · · · 82, 561
Takayama, R., The University of Tokyo, Kashiwa-shi, Japan · · · 423
Taniguchi, H., National Institute of Technology, Tsuyama-shi, Japan · · · 591
Tappe, S., Leibniz Universität Hannover, Hannover, Germany · · · 398
Tellinen, J., Lappeenranta University of Technology, Savonlinna, Finland · · · 101, 131
Ternoy, F., ONERA, Lille, France · · · 259
Theiß, R., Forschungsgemeinschaft Werkzeuge und Werkstoffe e.V., Remscheid, Germany · · · 518
Thiebaud, V., Cedrat Technologies SA, Meylan, France · · · 221
Tietze, S., Hochschule Coburg, Coburg, Germany · · · 451
Tonegawa, A., Tokai University, Hiratsuka-shi, Japan · · · 588
Toro, S., Umbra Cuscinetti S.p.A., Foligno, Italy · · · 270
Toyoda, R., Tokai University, Hiratsuka-shi, Japan · · · 581, 588
Tsuyuki, S., Okayama University, Okayama-shi, Japan · · · 447
Tulkibayeva, K., Nazarbayev University, Astana, Kazakhstan · · · 503
Twiefel, J., Leibniz Universität Hannover, Hannover, Germany · · · 91, 196, 236, 245

U

Uchino, K., The Pennsylvania State University, University Park, USA · · · 35, 60, 455
Ullakko, K., Lappeenranta University of Technology, Savonlinna, Finland · · · 101, 131
Ulrich, S., Helmut Schmidt Universität, Hamburg, Germany · · · 565

V

Vagapov, A., Leibniz Universität Hannover, Hannover, Germany · · · 245
van der Helm, F.F.C.T., Delft University of Technology, Delft, The Netherlands · · · 491
van Poelgeest, A., Fraunhofer IPA, Mannheim, Germany · · · 163
Vander Poorten, E., Katholieke Universiteit Leuven, Leuven, Belgium · · · 192
Vasiljev, P., Lithuanian University of Educational Sciences, Vilnius, Lithuania · · · 410, 414
Velsink, F.L., University of Dundee, Dundee, United Kingdom · · · 167, 321
Vercauteren, T., University College London, London, United Kingdom · · · 192
Verhagen, A., Robert Bosch GmbH, Renningen, Germany · · · 514
Viala, B., CEA LETI, Grenoble, France · · · 127
Visentin, V., Technosprings Italia srl, Besnate, Italy · · · 551
Vittorias, I., Siemens AG, München, Germany · · · 224
von Heckel, B., Hochschule Ostwestfalen-Lippe, Lemgo, Germany · · · 278

W

Wahrburg, A., ABB AG, Ladenburg, Germany · · · 364
Waldvogel, R., maxon advanced robotics and systems, Giswil, Switzerland · · · 361
Wallaschek, J., Leibniz Universität Hannover, Hannover, Germany · · · 236
Wallrabe, U., Albert-Ludwigs-Universität Freiburg, Freiburg, Germany · · · 65, 228
Wang, J., Zhejiang University, Hangzhou, China · · · 443
Wang, K., Université Libre de Bruxelles, Brussels, Belgium · · · 232
Wang, X., Shanghai Jiao Tong University, Shanghai, China · · · 152
Wapler, M.C., Albert-Ludwigs-Universität Freiburg, Freiburg, Germany · · · 65, 228
Washihira, T., Tokai University, Hiratsuka-shi, Japan · · · 109, 581
Wassenaar, J., DG Flugzeugbau GmbH, Bruchsal, Germany · · · 266
Webber, K.G., Friedrich-Alexander-Universität Erlangen-Nürnberg, Erlangen, Germany · · · 52
Weinstein, M., Leibniz Universität Hannover, Hannover, Germany · · · 91
Werhahn, M., ContiTech Vibration Control GmbH, Hannover, Germany · · · 135
Wielert, T., Leibniz Universität Hannover, Hannover, Germany · · · 245
Wiertlewski, M., Aix-Marseille Université, Marseille, France · · · 181
Winkel, T., Leibniz Universität Hannover, Hannover, Germany · · · 398
Winterstein, T., Technische Universität Darmstadt, Darmstadt, Germany · · · 336
Wurz, M., Leibniz Universität Hannover, Garbsen, Germany · · · 196

Y

Yamada, T., Okayama University, Okayama-shi, Japan · · · 332
Yamaguchi, D., Saitama University, Saitama-shi, Japan · · · 561
Yamaguchi, T., Kansai University, Suita-shi, Japan · · · 241
Yamamoto, S., National Institute of Technology, Tsuyama-shi, Japan · · · 591

Yang, B., Shanghai Jiao Tong University, Shanghai, China · · · 114, 152
Yang, Y., Nanjing University of Aeronautics and Astronautics, Nanjing, China · · · 410
Yano, A., Mechano Transformer Corporation, Chiyoda-ku, Japan · · · 255
Yano, T., Mechano Transformer Corporation, Chiyoda-ku, Japan · · · 255
Yokozawa, H., The University of Tokyo, Kashiwa-shi, Japan · · · 91
York, A., Parker Hannifin Corporaton, Sunnyvale, USA · · · 282
York, A., Universität des Saarlandes, Saarbrücken, Germany · · · 522, 526
Yu, H., National University of Singapore, Singapore · · · 443
Yuan, T., The Pennsylvania State University, University Park, USA, and Shanghai University, Shanghai, China · · · 455

Z

Zähringer, S., Technische Universität München, München, Germany · · · 77
Zalar, B., Jožef Stefan Institute, Ljubljana, Slovenia,
and Jožef Stefan International Postgraduate School, Ljubljana, Slovenia · · · 507
Zhang, X., Robert Bosch GmbH, Renningen, Germany · · · 514
Zhapar, Z., Nazarbayev University, Astana, Kazakhstan · · · 503
Zhu, Q., Karlsruher Institut für Technologie, Karlsruhe, Germany · · · 514
Zielinski, O., Carl von Ossietzky-Universität Oldenburg, Wilhelmshaven, Germany · · · 471
Ziske, J., Technische Universität Dresden, Dresden, Germany · · · 495, 499
Zoels, W., Siemens AG, München, Germany · · · 224
Zreihan, N., Technion - Israel Institute of Technology, Haifa, Israel · · · 104
Zsurzsan, T.-G., Technical University of Denmark, Lyngby, Denmark · · · 56
Zupančič, B., Jožef Stefan Institute, Ljubljana, Slovenia · · · 507
Zwinscher, I., Forschungsgemeinschaft Werkzeuge und Werkstoffe e.V., Remscheid, Germany · · · 313

List of Exhibitors

attocube systems AG
Königinstraße 11A, 80539 München, Germany
Tel.: +49 (0)89 2877809 - 0 Fax: +49 (0)89 2877809 - 19
www.attocube.com info@attocube.com

attocube is a leading supplier for nano precise motion and highly accurate interferometric sensor solutions. The portfolio includes linear, goniometric and rotational piezo stages, hexapods, and ultrasonic drives, all working with nanometer accuracy. The positioners are available for various environmental conditions, always optimized for the specific field of application. The fiber-based displacement sensor is the product of choice for challenging OEM and synchrotron applications. It offers sub-nanometer resolution and can be applied for highest precision measurements, vibration analysis and displacement detection.

CEDRAT TECHNOLOGIES SA
59, Chemin du Vieux Chêne, 38246 Meylan Cedex, France
Tel.: +33 (0)456 58 04 00 Fax: +33 (0)456 58 04 01
www.cedrat-technologies.com actuator@cedrat-tec.com

Cedrat Technologies is an internationally recognized mechatronics specialist and manufacturer of piezo and magnetic actuators offering a wide range of standard products: amplified (APA®), pre-stressed piezo actuators, XY piezo stages, stepping motors, shutters, magnetic actuators, the associated electronics and also customised products. The company has a strong experience in developing compact, precise and dynamic solutions for demanding applications (air & space, optronics, biomed, instrumentation, production machine...).

CeramTec GmbH
Multifunctional Ceramics Division
Luitpoldstraße 15, 91207 Lauf, Germany
Tel.: +49 (0)9123 77 - 0
Fax: +49 (0)9123 77 - 515
www.ceramtec.com/actuators
multifunctional_ceramics@ceramtec.de

CeramTec GmbH is one of the largest international manufacturers of ceramics for technically demanding applications and amongst others also a specialist in piezoceramics. Piezoceramic actuators utilize the piezoelectric effect: A piezoceramic PZT material expands in the direction of the electrical field when voltage is applied to it. Thus, the piezoceramic actuator provides precise movement up to about 200µm, while exerting high forces for applications such as valve control and micro-positioning.

ETO MAGNETIC GMBH
Hardtring 8, 78333 Stockach, Germany
Tel.: +49 (0)7771 809 - 0 Fax: +49 (0)7771 809 - 100
www.etogroup.com magnetoshape@etogroup.com

The ETO GRUPPE with its more than 1.800 employees at 8 locations in Europe, America, and Asia develops and produces customer specific electromagnetic actuators and sensors in highest quality for fluidic and mechanical applications in the automotive and machine building industry.
As a highlight, we present our MAGNETOSHAPE® technology with actuator solutions based on proprietary magnetic shape memory materials. These are single crystalline alloys of Nickel, Manganese and Gallium, which are able to produce 6% strain under more than 2 N/mm² external load with moderate magnetic fields.

FGL-Netzwerk

Nöthnitzer Straße 44, 01187 Dresden, Germany
Andrea Böhm
Tel.: +49 (0)351 4772 - 2320 Fax: +49 (0)351 4772-2303
www.fgl-netzwerk.de andrea.boehm@iwu.fraunhofer.de

Today shape memory alloys (SMAs) are not that well established in technical applications as for instance conventional structural materials. Therefore the network -Efficient added value in the manufacturing and application of shape memory alloys- was founded. Experts for material production, research and development as well as users of the SMA technology participate. Thus the network establishes a platform for companies which apply SMAs or are generally interested in this technology. Hence the main objective is the spacious establishment of the multi-functional material SMA with its outstanding properties and benefits. It is further aimed to connect the currently separated process steps in manufacturing, processing and adapting SMA-components. The network offers innovative proceedings, consulting services and new products using SMA to interested users of all sectors.

Fraunhofer-Allianz Adaptronik (FAA)
Marketing

Bartningstraße 47, 64289 Darmstadt, Germany
Anika Seifert
Tel.: +49 (0)6151 705 - 236 Fax: +49 (0)6151 705 - 308
www.adaptronik.fraunhofer.de info@adaptronik.fraunhofer.de

6 Fraunhofer institutes, being engaged in complementary research areas, cooperate within the Fraunhofer Adaptronics Alliance.
These partners work together in scientific as well as in industrial research projects, according to demand. Thus, interdisciplinary solutions can be found from one source. The partners' competencies cover the following areas:
- Materials and components
- Experimental system analysis
- Numerical and experimental simulation
- Electronics and control engineering
- Production and processing
- System design, evaluation and application

hivolt.de GmbH & Co. KG

Oehleckerring 40, 22419 Hamburg, Germany
Tel.: +49 (0)40 537122 - 0 Fax: +49 (0)40 537122 - 99
www.hivolt.de info@hivolt.de

hivolt.de is an internationally operating specialist for professional High Voltage Components: HV-Power Supplies, HV-Amplifiers, HV-Cables & Connectors and customized solutions. Products which are delivered by hivolt.de are being used in a variety of applications, both in industry as well as in research. Due to our inhouse design capabilities and our close co-operation with several leading manufacturers we are able to offer custom-made HV-Products, that match our customer's specific applications, including variations of standard products or full custom designs.

Johnson Matthey Catalysts (Germany) GmbH
Piezoproducts

Bahnhofstraße 43, 96257 Redwitz, Germany
Tel.: +49 (0)9574 81 - 466 Fax: +49 (0)9574 81 - 98466
www.piezoproducts.com piezoproducts@matthey.com

Johnson Matthey Piezo Products is a specialist for piezo bending actuators. We focus on development, production and sales of piezoceramic actuators, sensors, energy harvesting generators and ultrasonic atomizers as well as engineered piezoelectric systems and modules with electronics and mechanics for industry applications, textile machines, medical devices, automotive and other markets.

Sensor Magazin/ Laser Magazin
c/o Magazin Verlag Hightech Publications KG
Winklerstraße 4, 31542 Bad Nenndorf, Germany
Tel.: +49 (0)5723 5534 Fax: +49 (0)5723 76212
www.magazin-verlag.de kontakt@magazin-verlag.de

SENSOR MAGAZIN provides information to engineers and scientists who develop, manufacture and use sensors and actuators. The trade journal reports on the application of sensor and actuator technology in all branches of industry as well as in institutes and laboratories. The industry`s latest technological developments are highlighted in the MAIN TOPIC of each issue. The journal focuses on practice-oriented articles under the headings of Practice, Market and Trade Fair Reports as well as Products. Future trends are reflected under the headings of Research, Innovations, Patents and Micro-Nano Integration. Exclusive interviews with key people from research and industry round off the spectrum of articles. The content, design and service meet the high requirements placed on a high-tech journal worth reading and promoting sales. www.sensormagazin.de

Mechatronik / I.G.T. Informationsgesellschaft Technik GmbH
Oskar-Maria-Graf-Ring 23, 81737 München, Germany
Tel.: +49 (0) 89 673697 - 0 Fax: +49 (0)89 673697 - 19
www.mechatronik.info mechatronik@igt-verlag.d

MECHATRONIK is an intersectoral journal for development processes and system integration. MECHATRONIK is concerned with the synergy of mechanics, electronics and software/information technology. Technical and application-related contributions, news, product trends, interviews and opinions relating to current research guide the readers from product idea to system integration via development and systems engineering. Engineering trends are discussed in detail, new research is presented in step with actual practice and new products are introduced in an appealing way.
MECHATRONIK is linked to the web portal www.mechatronik.info.
MECHATRONIK is published 8 times a year.

Mikroproduktion / MIKROvent GmbH
Salvatorberg 2, 84048 Mainburg, Germany
Tel.: +49 (0)8441 797611 - 0 Fax: +49 (0)8441 79711-4
www.mikroproduktion.de info@mikroproduktion.de

Mikroproduktion is the German speaking special interest magazine for applied micro technology such as lithography, micro milling, micro laser processing, micro injection moulding, EDM, micro assembly and micro robotics, Nanotechnology, clean room technology and micro metrology. Mikroproduktion describes the whole process chain for the manufacturing of micro components, functional micro structures and micro systems. Main application fields can be found in micro optics, micro sensors and MEMS, micro fluidics and micro mechanics.

MSM Net
c/o ETO MAGNETIC GMBH
Hardtring 8, 78333 Stockach, Germany
Tel.: +49 (0)7771 809 - 452
www.themsmnet.net

Magnetic Shape Memory (MSM) alloys are ferromagnetic materials that produce motion and force under moderate magnetic fields. The MSM Net is an international R&D alliance whose goal is to strengthen relationships between the partners and to promote and divulge the magnetic shape memory technology in the scientific and in the industrial realm and to enable its commercialization. The network currently consists of 7 members from Germany, Finland, and the US, including 2 companies and 5 research institutions.

Noliac A/S

Hejreskovvej 18, 3490 Kvistgaard, Denmark
Tel.: +45 (0)49 12 50 30 Fax: +45 (0)49 12 50 31
www.noliac.com info@noliac.com

Noliac presents a unique proficiency in the field of piezoelectric technology. We design, develop and manufacture the total range of piezoelectric products from powders to mono- and multilayer components and all the way to finished plug-and-play applications.
At Actuator 2016, we will present two new piezoelectric actuators: Fuse actuator stacks and high temperature actuator stacks. The fuse actuator stacks are a unique solution for critical applications. The high temperature actuator stacks are ideal for high temperature applications, where you also need a high operating frequency.

Physik Instrumente (PI) GmbH & Co. KG

Auf der Roemerstrasse 1, 76228 Karlsruhe, Germany
Tel.: +49 (0)721 4846 - 0 Fax: +49 (0)721 4846 - 1409
www.pi.ws info@pi.ws

Well-known for the high quality of its products, PI (Physik Instrumente) is one of the leading players in the global market for precision positioning technology for many years. PI has been developing and manufacturing standard and OEM products with piezo or motor drives for 40 years. In addition to four locations in Germany, the PI Group is represented internationally by fifteen sales and service subsidiaries.

PI Ceramic GmbH

Lindenstrasse, 07589 Lederhose, Germany
Tel.: +49 (0)36604 882 - 0 Fax: +49 (0)36604 882 - 4109
www.piceramic.de info@piceramic.de

PI Ceramic is one of the global leaders for actuator and sensor piezo products. A broad range of expertise in the complex development and manufacturing process of functional ceramic components combined with state-of-the-art equipment ensure high quality, flexibility and adherence to supply deadlines. The company supplies piezoceramic solutions for all important high-tech markets from industrial automation and the semiconductor industry, medical engineering, mechanical engineering and high-precision engineering through to the aeronautics industry and the automotive sector.

G.Rau Gmbh & Co. KG

Kaiser-Friedrich-Straße 7, 75172 Pforzheim, Germany
Tel.: +49 (0)7231 208 - 0 Fax: +49 (0)7231 208 - 7599
www.g-rau.de info@g-rau.de

METALS ARE OUR WORLD
G.RAU is a globally active supplier of metal engineering and has become an established preferred supplier to several distinguished enterprises of automotive supply, electrical engineering, measurement and control technology and medical engineering. Founded in 1877, today G.RAU is an expert in manufacturing strips, tubes and wires made of precision metals, special alloys and composite materials. Furthermore G.RAU also uses these prematerials to manufacture precision parts and complex assemblies. G.RAU has three production sites in Germany, one in Costa Rica and a subsidiary in the USA.

SmarAct GmbH

Schütte-Lanz-Straße 9, 26135 Oldenburg, Germany
Tel.: +49 (0)441 800879 - 0 Fax: +49 (0)441 800879 - 21
www.smaract.de info@smaract.de

SmarAct develops, produces and distributes piezo-based micro- and nanopositioners, advanced control systems and tools for the nanoworld. In addition, SmarAct offers complete micro- and nanomanipulation systems, ranging from XY tables to multi-manipulator systems. The compact positioning systems combine sub-nm resolution with a high stiffness and cm-sized travels. They can be applied in normal pressure as well as in vacuum conditions.
SmarAct also presents PicoScale - an interferometer-based displacement sensor. It features three channels and extremely miniaturized opto-mechanical sensor heads.

The Smart Actuator Company

2 Assarts Lane, WR14 4JR Malvern, United Kingdom
Tel.: +44 (0)1684 565709 Fax: +44 (0)1684 560977
www.smartact.co.uk tony@smartact.co.uk

The Smart Actuator Company (SACO) was formed in 2011 to develop a new electric valve actuator by incorporating up to date computer and electronics technology in to the designs.
The first medium size actuator, delivering 40 to 100 Nm of programmable torque output was launched at the British Valve & Actuator Association (BVAA) Spring Conference in May 2014 and cost approximately £1 Million to Research, Develop, and Test. It incorporated many of the features only previously seen in actuators costing thousands of pounds more; such as failsafe, modulation and speed control.
In 2015 SACO won a €2.4 Million Horizon 2020 European Union Grant for a project to develop smaller and larger versions of the first medium product. They will deliver 0-40 Nm and 100-400 Nm of programmable torque output respectively. The large product will also be available as a ‘Subsea’ version which has already been tested down to 80 metres depth.

Thorlabs GmbH

Hans-Böckler-Str. 6, 85221 Dachau / München, Germany
Tel.: +49 (0)8131 5956 - 0 Fax: +49 (0)8131 5956 - 99
www.thorlabs.com/actuators europe@thorlabs.com

Thorlabs, a vertically integrated photonics products manufacturer, was founded in 1989 to serve the laser and electro-optics research market. As that market has spawned a multitude of technical innovations, Thorlabs has extended its core competencies in an effort to play an ever increasing role serving the Photonics Industry at the research end, as well as the industrial, life science, medical, and defense segments. The organization’s highly integrated and diverse manufacturing assets include semiconductor fabrication of Fabry-Perot, DFB, and VCSEL lasers, fiber towers for drawing glass optical fibers (silica and fluoride), MBE/MOCVD epitaxial wafer growth reactors, extensive glass and metal fabrication facilities, advanced thin film deposition capabilities, and optomechanical and optoelectronic shops.

Xeryon bvba

Interleuvenlaan 62, 3001 Leuven, Belgium
Tel.: +32 (0)16 394824 Fax: +32 (0)16 394701
www.xeryon.be steven.cappa@xeryon.be

Xeryon is specialised in the design, development and manufacture of piezo-electric actuation solutions. Our piezo motors are tailor-made to the needs of our clients who face the toughest challenges in precision applications. Xeryon’s miniature XRT rotary stages position small samples with sub-micrometre error motion and very fine angular resolution. Our unique MultiDrive piezo motor technology combines the speed and unlimited stroke of a resonant motor with the extreme accuracy of a direct stroke actuator. Both modes of operation are simultaneously realised in a single motor, enabling coarse-fine positioning with one motor.

15th International Conference on New Actuators
&
9th International Exhibition on
Smart Actuators and Drive Systems

The Crew

Hubert Borgmann
Ole Bast
Christina Laue
Sabrina Schramme
Jann-Michael Dornseiff
Alexander Fritsche
Malte Heitmüller
Christina Lolk
Chris Janina Neumann
Vanessa Ullmann

all with

MESSE BREMEN
WFB Wirtschaftsförderung Bremen GmbH

Welcome to

ACTUATOR 18

16th International Conference on New Actuators
&
10th International Exhibition
on Smart Actuators and Drive Systems

25–27 June 2018
Bremen, Germany

ACTUATOR 18

Tentative Time Schedule

8 September 2017	Mailing of Announcement / Call for Papers / Call for Exhibitors
30 November 2017	Deadline for receipt of abstracts
January 2018	Evaluation of abstracts / Compilation of conference programme
31 January 2018	Information of authors about evaluation results
15 March 2018	Mailing of Conference Programmes
27 March 2018	Deadline for receipt of manuscript files
17 April 2018	Deadline for registration for exhibition
25–27 June 2018	**ACTUATOR 2018**